South-West Monsoon Rainfall of Kerala and its Variability

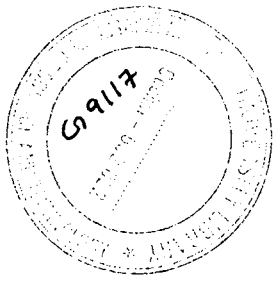

Thesis submitted to the

COCHIN UNIVERSITY OF SCIENCE AND TECHNOLOGY

in partial fulfilment of the requirement for the Degree of

DOCTOR OF PHILOSOPHY

in

ATMOSPHERIC SCIENCES

By

Aype Thomas P.

Department of Atmospheric Sciences
COCHIN UNIVERSITY OF SCIENCE AND TECHNOLOGY
LAKE SIDE CAMPUS, COCHIN 682 016

December 2005

CERTIFICATE

This is to certify that the thesis entitled ***"SOUTH-WEST MONSOON RAINFALL OF KERALA AND ITS VARIABILITY"*** is a bonafide record of research work done by **Mr. Aype Thomas P** in the Department of Atmospheric Sciences, Cochin University of Science and Technology. He carried out the study reported in this thesis, independently under my supervision. I also certify that the subject matter of the thesis has not formed the basis for the award of any Degree or Diploma of any University or Institution.

Certified that **Mr. Aype Thomas P.** has passed the Ph.D qualifying examination conducted by the Cochin University of Science and Technology in May 2005.

Kochi-16
December 8, 2005

C.K.Rajan
(Supervising Teacher)

Dr. C. RAJAN
Professor
Dept. of Atmospheric Sciences
Cochin University of
Science and Technology
Kochi-682 016

PREFACE

Nature has bestowed Kerala with abundant rainfall. The average annual rainfall of the State is about 300 cm. Despite its small size, Kerala supports about 4% of the population of India and has the highest population density among the Indian states. Kerala has large temporal and spatial variations in rainfall. It will be of great socio-economic importance if we learn to use the rainfall bounty to our greatest advantage and learn to cope with the rainfall variations.

This study focuses on the aspects of south-west monsoon rainfall over Kerala and its variability both on the spatial and temporal scales. The thesis contains eight chapters. In the first chapter a very detailed literature review pertaining to the topic of research is presented. The chapter also includes the physiography of the state and general climatology with special emphasis on the rainfall climatology. Chapter-2 gives a detailed description of the data sets and the method of analysis used in the study. A detailed description of the MM5 model is also given in this chapter.

Chapter- 3-is the study on the Intra Seasonal Variability of south-west monsoon rainfall. This is an important topic studied in the thesis. Intra Seasonal Oscillations of rainfall (ISO) for south Kerala, north Kerala and whole India is studied using the Wavelet Analysis and the statistical significance of the periods at levels 90%, 95% and 99% were determined. The results on the south Kerala rainfall series have been published in *Proc. of Indian Academy of Sciences-Earth and Planetary Sciences* (Vol. 113, No. 2, June 2004).

The interannual variability of Kerala summer monsoon rainfall and that of south and north Kerala rainfall is discussed in chapter-4. It is seen that Kerala's monsoon rainfall has large interannual variability like Indian Summer Monsoon Rainfall (ISMR). However, Kerala rainfall has no epochal variation unlike ISMR. South Kerala rainfall has a strong decreasing trend that is particularly

prominent in the hill areas of central Kerala around Peermade where there is a decreasing trend close to 25% in 100 years.

The relationship between antecedent global circulation parameters with monsoon rainfall of Kerala is studied in chapter-5 and an attempt has been made to develop a statistical model for long-range forecast of monsoon rainfall for the state. Four factors have been identified that have strong and significant linear correlation with Kerala summer monsoon rainfall. The multiple correlation coefficient of these factors with KSMR is 0.72 for the period 1977-2003 and the estimated rainfall using this equation has a standard error of estimate of 22.9cm which is about 64% of the standard deviation of KSMR

In chapter-6 we have studied the diurnal variation of south-west monsoon rainfall using data of 33 stations mostly in central and north Kerala. It is found that the first (diurnal) and second harmonics (semi-diurnal) of 24-hour rainfall are found to be prominent. Combination of these harmonics give afternoon maxima to some stations, morning maxima for another group of stations and a flat rainfall diurnal curve for the remaining stations.

In chapter-7 we have used Mesoscale Model MM5 to simulate the convective monsoon rainfall to understand the controls on the rainfall. Two factors control the rainfall of Kerala. One is a dynamic control by the Low Level Jet stream. The other is the orographic control. Using a mesoscale model which has the orography of central Kerala hills (Anamalai and Cardamom hills) we have simulated the convective rainfall around these hills for three days with Low Level Jet axis just south of Kerala and three days with Low Level Jet axis just north of Kerala. These simulations bring out the controls by LLJ and the orography.

In the last chapter (Chapter-8), the major findings of this thesis are summarized. The scope for future studies is also discussed.

CONTENTS

Chapter-1

Introduction

1.1 General

Nature has bestowed Kerala with abundant rainfall. The average annual rainfall of the State, situated in the southwestern corner of the Indian peninsula is about 300 cm, which is about three times the average for the whole of India. Kerala is one of the smallest states of India and has an area only a little more than 1% of the country as a whole. The adjoining state of Tamil Nadu to the east is three times the size of Kerala, while Karnataka to the north is nearly 5 times bigger. However, Kerala receives annual rainfall, which is three times greater than that of Tamil Nadu and twice greater than that of Karnataka. Despite its small size, Kerala supports about 4% of the population of India (31.82 million as per 2001 census) and has the highest population density among the Indian states.

The annual rainfall pattern of the state displays large north-south and east-west gradients. There are two pockets of large rainfall exceeding 400cm in the high lands. The Western Ghats act like a long wall up to a height of 1-2 km obstructing the low-level monsoon current. The southwest monsoon current, which brings in moisture for rainfall, gets a forced ascent at the Ghats and the windward slopes experiences heavy rainfall. The northern pocket of large rainfall is to the north-east of Kozhikode where the hill station Vaithiri gets annual rainfall of over 450cm and the southern pocket is to the east of Kottayam with Peermade getting more than 400cm of annual rainfall. However, rainfall is not uniformly distributed on the windward slopes and there are regions of very large rainfall and relatively less rainfall.

The peculiar geographic orientation of Kerala with Arabian Sea as the western boundary makes the weather pattern very unique in this part of the Indian subcontinent. Along the coast of Kerala, rainfall increases from about 150cm in the extreme south to more than 350cm in the extreme north. Rainfall decreases to the west with the Lakshadweep islands receiving only 150cm of annual rainfall. The Arabian Sea becomes the center of the oceanic warm pool in May with Sea Surface temperature (SST) reaching 30 to 31 degrees Celsius

(Joseph,1990). Soon after the monsoon onset over Kerala, the SST of the Arabian Sea cools rapidly. The southwest monsoon current as it approaches west coast of India, turns clockwise and becomes northwesterly. The northerly alongshore component of the surface wind produces upwelling in the coastal waters of Kerala and it has important consequences in relation to the meteorology of the region.

Even though the state does not suffer large interannual variations in annual or seasonal rainfall, there is large spatial variation in the rainfall distribution. It will be of great socio-economic importance if we learn to use our rainfall bounty to our greatest advantage and learn to cope with the year-to-year and decade-to-decade rainfall fluctuations, which are not large percentages of the mean annual rainfall. A thorough investigation on the rainfall characteristics both on the spatial and temporal scales with emphasis on the influence of orography is needed. The results of such a study will help engineers and hydrologists to manage our rainfall resource in a proper manner.

1.2 Objectives of the study

This study focuses on the aspects of southwest monsoon rainfall over Kerala and its variability both on the spatial and temporal scales. The objectives of this work are to study: (i) the Intra Seasonal Variability during south-west monsoon season (ii) the interannual, long-term and decadal variabilities in monsoon rainfall (iii) the relationship between antecedent global circulation parameters with Kerala rainfall. An attempt has been made to develop a statistical model for long-range forecast for south-west monsoon rainfall (iv) the diurnal variability using data of a large number of stations in Kerala and (v) the spatial distribution of rainfall under two large scale synoptic settings and the strong influence of the orography of Western Ghats.

1.3 Physiographic Features of Kerala

Kerala is a small-elongated coastal state in the south-west tip of peninsular India with Western Ghats to the east and Arabian Sea to the west.

Located within latitudes 8^0 15' N and 12^0 50' N and longitudes 74^0 50'E and 77^0 30' E, it has an area of 38863 sq. m (1.18 % of the area of India) with length (north-south) 590 km, a coast line of nearly 500km and an average width (east-west) of 66 km (varies from 35 to 120 km).

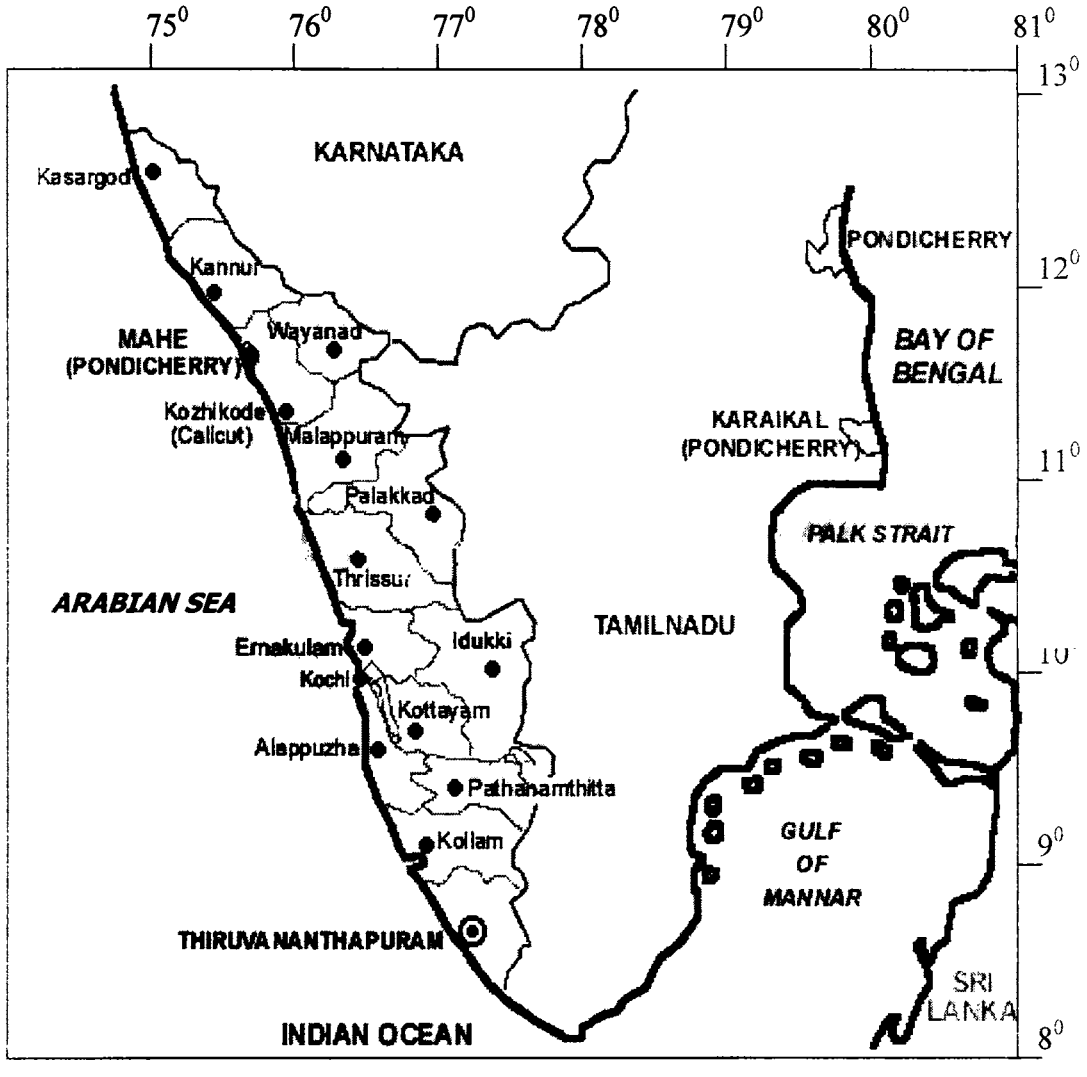

Fig. 1.1: Political map of Kerala

Kerala is surrounded by Dakshin Kanad (South Kanara), Mercara and Mysore districts of Karnataka state in the north. Nilgiri, Coimbatore, Madurai, Ramanadhapuram, Thirunlveli and Kanyakumari districts of Tamilnadu in the east, Arabian Sea to the west and North Indian Ocean to the south.

For administrative purposes the State is divided into fourteen districts (fig.1.1). The State capital is Thiruvanthapuram. These districts and their respective areas are given in Table 1.1.

Table 1.1: Districts of Kerala and their respective area in sq. km

District	*Area km^2*
Thiruvananthapuram	2,197
Kollam	2,579
Alappuzha	1,414
Idukki	5,019
Pathanamthitta	2,731
Kottayam	2,203
Ernakulam	2,362
Thrissur	3,032
Palakkad	4,480
Malappuram	3,550
Kozhikode	2,206
Wayanad	2,132
Kannur	2,997
Kasargod	1,961

The terrain of Kerala as derived by satellite data is given in fig.1.2. The land may be broadly divided into 3 natural divisions:

1. Lowlands
2. Midlands
3. Highlands.

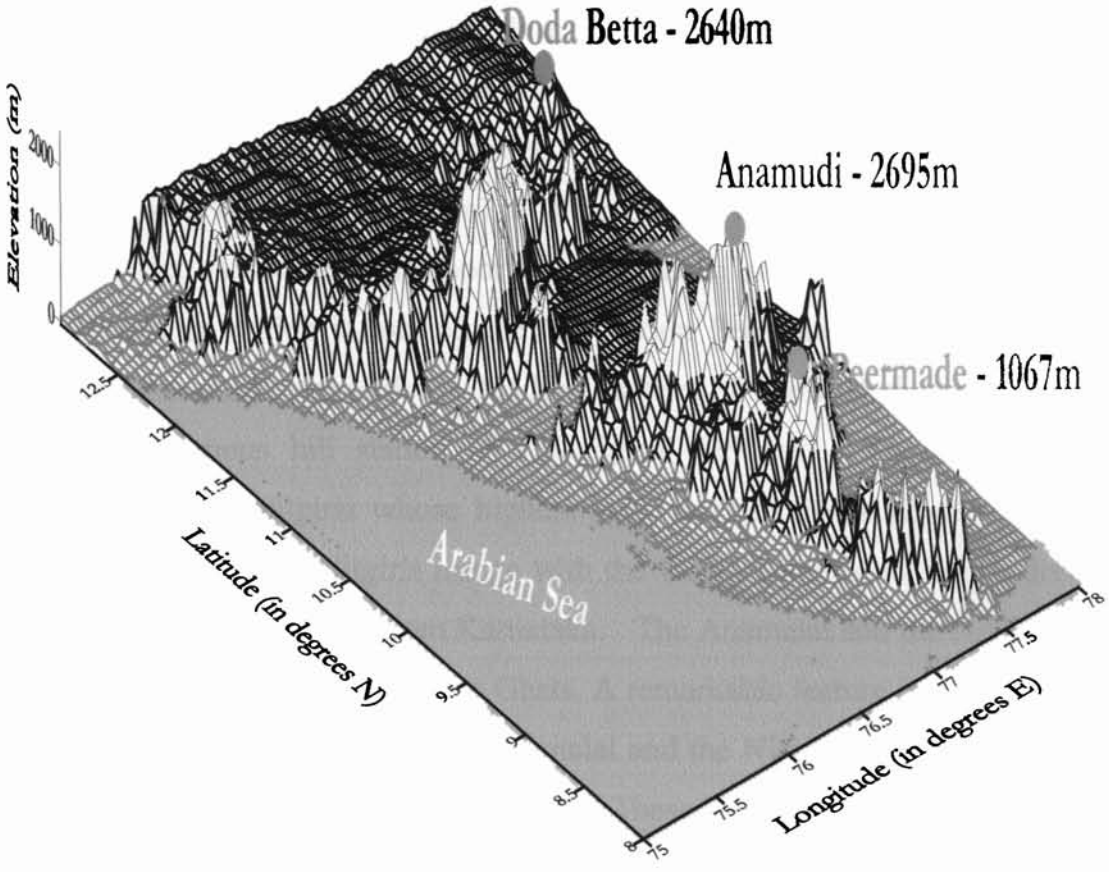

Fig. 1.2: Terrain of Kerala as taken from satellite data

Orographic features profoundly influence the meteorology of Kerala. The Western Ghats comprise the mountain range that runs along the western coast of India, from Vindhya-Satpura ranges in north to the southern tip of India. This mountain range, which forms a natural wall separating Kerala from adjoining states has an average elevation of about 1 km with peaks rising over 2 km. The highest peak is Anamudi (2695km) at the crest of Anamalai (elephant hill) in Idukki district. A southern off shoot from Anamalai is the Cardamom Hills of south Kerala on which is located the hill station Peermade. Eastwards from Anamalai, run the Palani Hills (in Madurai district of Tamil Nadu) on which is located the famous hill station of Kodaikanal (2506m). To the north of Anamalai are the Nilgiris whose highest peak is Doda Betta (2640m) in the Ootacamund area. The Nilgiris merge with the Coorg Mountains, which divide the northern parts of Kerala from Karnataka. The Anamalai and the Nilgiris are the tallest mountains in the Western Ghats. A remarkable feature is the Palakkad Gap of about 25km width between Anamalai and the Nilgiris, which is the only marked break in the Ghat mountain wall. These descriptions are taken from Ananthakrishnan et al (1979b).

The western slopes of Western Ghats receive copious rainfall during the south-west monsoon months June to September and form the watershed for a number of rivers. There are 41 west-flowing rivers in the state in addition to three east flowing ones, which are the tributaries of the Kaveri. The 41 west flowing rivers along with their tributaries cut across the state to join the Arabian Sea or one of the numerous backwaters. The longest river in Kerala is the Periyar with a length of 229 Km. The rich traditions of the state are associated with these rivers. Kaladi on the banks of Periyar was the birthplace of the great philosopher Sri. Sankaracharaya. Mamamkam, a festival of great pomp and fervour used to be held once in 12 years at Tirunavai on the banks of Bharatapuzha under the patronage of the Zamorin of Calicut till the latter half of the 18th century. Today many rivers have been harnessed for irrigation and power and are making great contributions to the economic progress of the state.

In addition Kerala has a continuous chain of lagoons and backwaters. The backwaters, rivers and the canal system form a navigable inland waterway of about 1960 kms, which is more than one fifth of the total length of India's inland waterways.

The midlands lying between the mountains and the lowlands are made up of undulating hills. This is an area of intensive cultivation where coconuts, arecanuts, tapioca, banana, rice, ginger, pepper, sugarcane and a large variety of vegetables are grown. The lowlands or the coastal area, which is made up of the river deltas, backwaters and the shore of the Arabian Sea, is essentially a land of dense coconut palms and verdant rice fields. Fisheries and coir making are major industries in this area. Backwaters form an especially attractive and economically valuable feature of Kerala. They include lakes and ocean inlets, which stretch irregularly along the coast. The biggest backwater is the Vembanad Lake, which is around 200 sq. km in area, and opens out into the Arabian Sea at the Cochin Port. Six Major rivers – the Periyar, Pamba, Manimala, Achenkovil, Meenachil and Muvattupuzha discharge into this lake.

The legend of the sea giving birth to the state -thanks to Parasurama - is widely accepted and the oceans have helped in moulding the history of Kerala. There was peaceful interaction with far-flung lands through trade and commerce for more than two millennia before the incursions from modern Europe with the landing of Vasco Da Gama at Calicut in 1498. It changed the temper of the contact., loaded it with conflicts and created a turbulent phase of history which ended only with India's independence in 1947.

There is a great variety of vegetation all along the Ghats: scrub jungles, grassland along the lower altitudes, dry and moist deciduous forests, and semi-evergreen and evergreen forests. There are two main centres of bio-diversity, the Agasthyamalai and the Silent Valley. The complex topography and the heavy rainfall have made certain areas inaccessible and have helped the region retain its diversity. Richness of soil, heavy rainfall and damp climate has given rise to a

flora and fauna of great variety. A few of the indigenous and exotic tree and plant species in the Western Ghats are the teak, jamun, cashew, hog plum, coral tree, jasmine, and crossandra. There is an equal diversity of animal and bird life. Elephants, black leopards, tigers, sloth bears, giant squirrels, bisons, a variety of deer, the charming little honey sucker, the golden beaked wood pecker and the Malabar whistling thrush are seen in the forests of Western Ghats. The famous Periyar national park in Kerala is home to a large number of elephants, gaur, sambhar, and lion-tailed macaque and a variety of birds.

The distinctive characteristic of the agricultural sector in Kerala deserves special emphasis. The high pressure of population on land has rendered a large part of the rural population traditionally dependent on agriculture. In Kerala only about 56% of the total area of the state is available for cultivation, the rest being forests and uncultivable lands. The cultivation of cash crops is better organized in Kerala than anywhere else in the country. In the country as a whole about 70% of the cropped area is under food grains, but in Kerala only about 30% is under food grains. On the other hand more than 50% of the cultivable area is under commercial crops like tea, rubber, coconut, cardamom etc. This cropping pattern has its own advantages and disadvantages. It earns valuable foreign exchange for the country by the export of commercial crops but at the same it also creates a huge deficit in food grains that sustains the population. Only about 55% of Kerala's rice requirements are produced within the state. For the balance, the state has to depend on supplies from outside.

1.4 Climatology of Kerala

The climate of India and that of Kerala in particular is dominated by the monsoon circulation. During one half of the year the wind blows from the oceans to the south of the Asian land mass, while during the other half there is a seasonal wind blowing from the Asian landmass to the oceans to the south. There is a spectacular reversal of pressure and wind patterns between these two six-month periods. The gradual rise in temperature through spring to summer

does not happen, due to the onset of the south-west monsoon. Temperatures drop sharply in June. The usual classification into spring, summer, autumn and winter is therefore not adopted in the state. January and February is winter season, March to May is the pre-monsoon season, June to September is the south-west monsoon season and October to November is the post-monsoon season.

1.4.1 Seasonal Variation of Pressure

There is an annual variation of atmospheric pressure over the state with maximum pressure during January and minimum during May, with an annual range of only 3-3.5 hPa. The monthly variation of sea-level pressure for selected stations in Kerala is given in fig.1.3. The pressure gradient over the state generally remains weak except during late summer and in the monsoon season. The diurnal range of pressure increases from the coast to inland regions and this is also within about 5 hPa (Kumar, 1994). The maximum range in the diurnal cycle is observed during February when clouding is almost minimum. However, during June and July the range in the observed diurnal pressure variation is large in the state. This is also the period of maximum clouding and precipitation. In all seasons pressure gradient over the state is in the east-west direction. The pressure decreases from west to east except during the period from about middle of October to the beginning of March when the reverse gradient prevails.

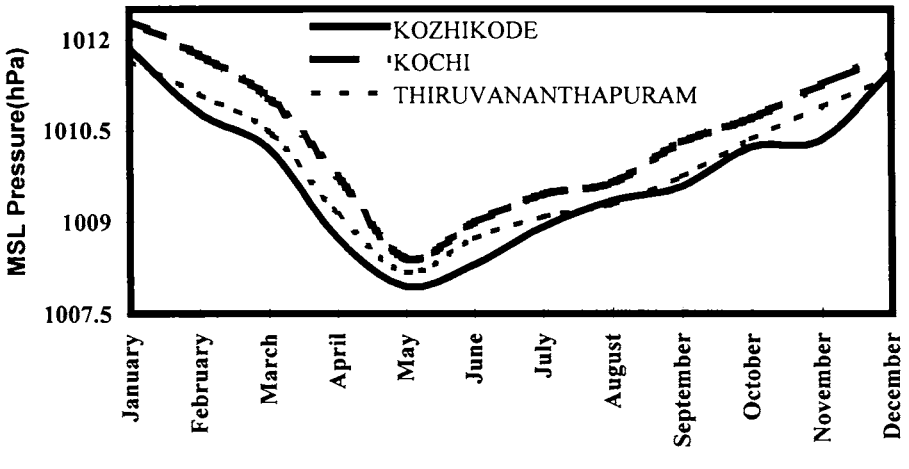

Fig.1.3: Monthly variation of mean sea level pressure in Kerala

1.4.2 Seasonal Variation of Temperature

The main factors, which affect the mean surface temperature of the air at any place, are latitude, elevation, distance from the sea, type of prevailing air mass, which in turn determines the pattern of cloudiness and weather. The annual changes in the thermal pattern would naturally show the highest temperature in summer and the lowest in winter. However, due to the onset of summer monsoon which gives rise to extensive cloudiness and rainfall temperature pattern is modified. Because of its low-latitude location the annual range of temperature over Kerala is small compared to other parts in north and central India. At coastal stations in the state, the highest maximum temperature of about 33^0 C occurs in April and the lowest minimum temperature of about 22^0 C occurs in August. However, in coastal stations in other parts of the country the maximum temperature is attained in April/May but the lowest minimum is in December/January (Ananthakrishnan, 1979a). At Palakkad, an interior station the maximum temperature during the hot weather season reaches up to about 37^0 C while the minimum temperature is more or less the same as at the coastal stations. Fig. 1.4 shows the monthly variation of mean temperature ((maximum + minimum/2)) at few stations in Kerala. The temperature at various pressure levels (1000hPa to 10hPa) for 3 selected stations in Kerala: Thiruvananthapuram, Kozhikode and Mangalore (representative station for north Kerala) for the month of July is given in fig. 1.5. During July (south-west monsoon) the surface temperature is around 25^0c for all the stations and the tropopause is at around 100hPa with a temperature of around -77^0c. The details are given in Table 1.2.

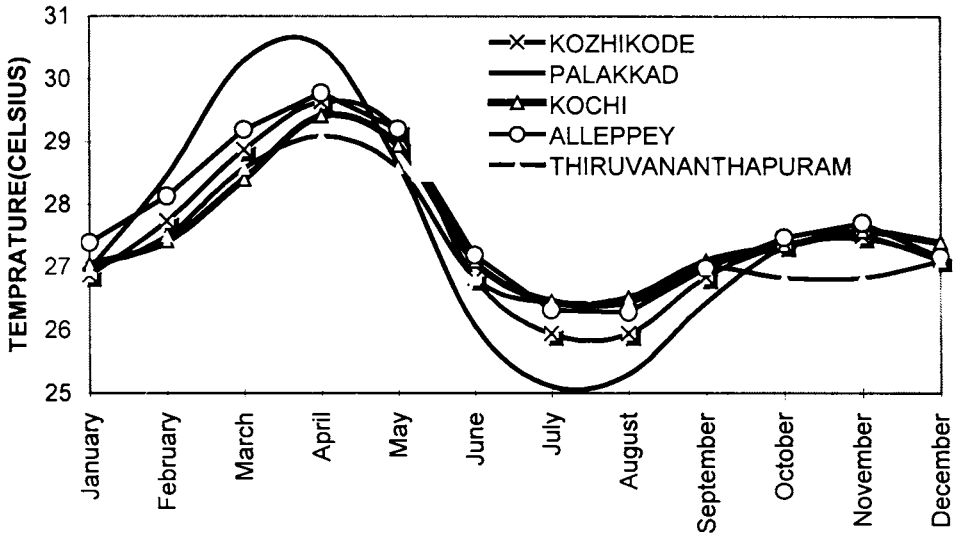

Fig.1.4: Monthly variation of mean temperature in Kerala

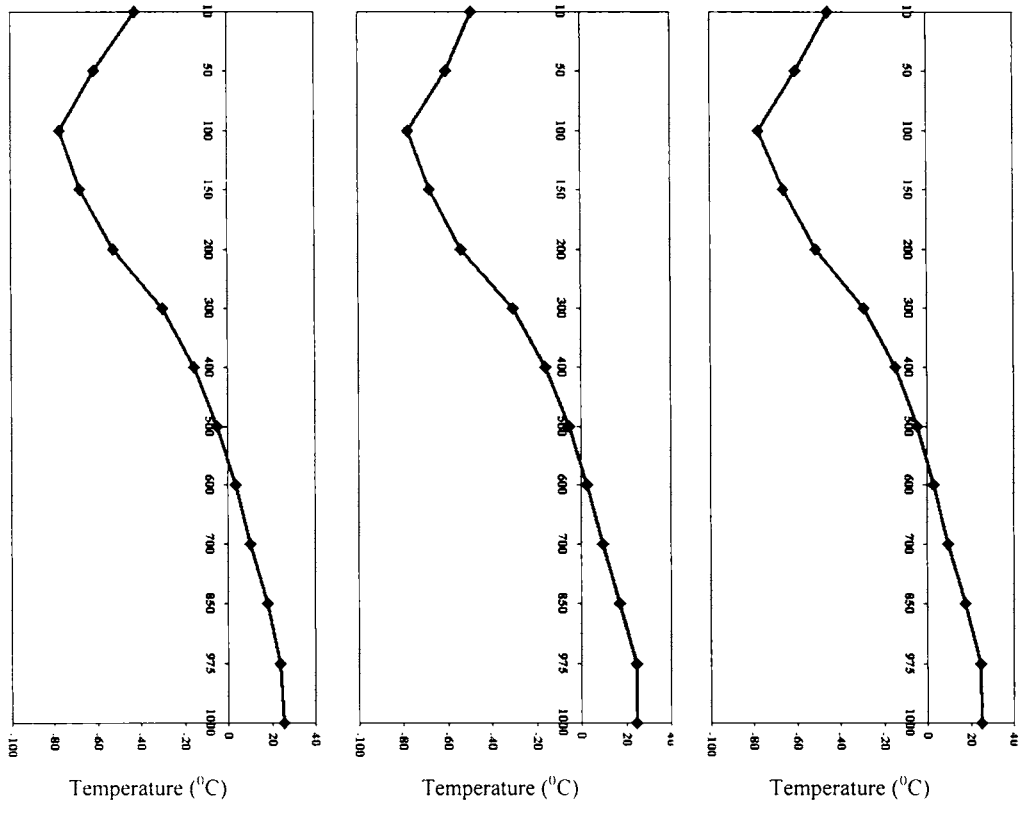

(a) (b) (c)

Fig.1.5: Temperature at various pressure levels in mb (marked on y-axis) for July for (a) Thiruvananthapuram, (b) Kozhikode and (c) Mangalore

1.4.3 Seasonal Variation of Wind

The winds are predominantly from east during October to May in the state and become westerly during the southwest monsoon season of June to September. Fig. 1.6 gives the u-component of wind for the month of July for the three selected stations. As seen from the figure, the westerlies prevail from 1000hPa to 400hPa during the southwest monsoon season, with strength of the order of 25knots at 850hPa. In the upper troposphere during July the easterlies are well established and the strengths are highest of the order of 68knots at Thiruvananthapuram. The details are given in Table 1.2. The diurnal variation in winds show that in general surface winds are strong during afternoon when the thermal circulation is well-developed and weak during night (Kumar, 1994).

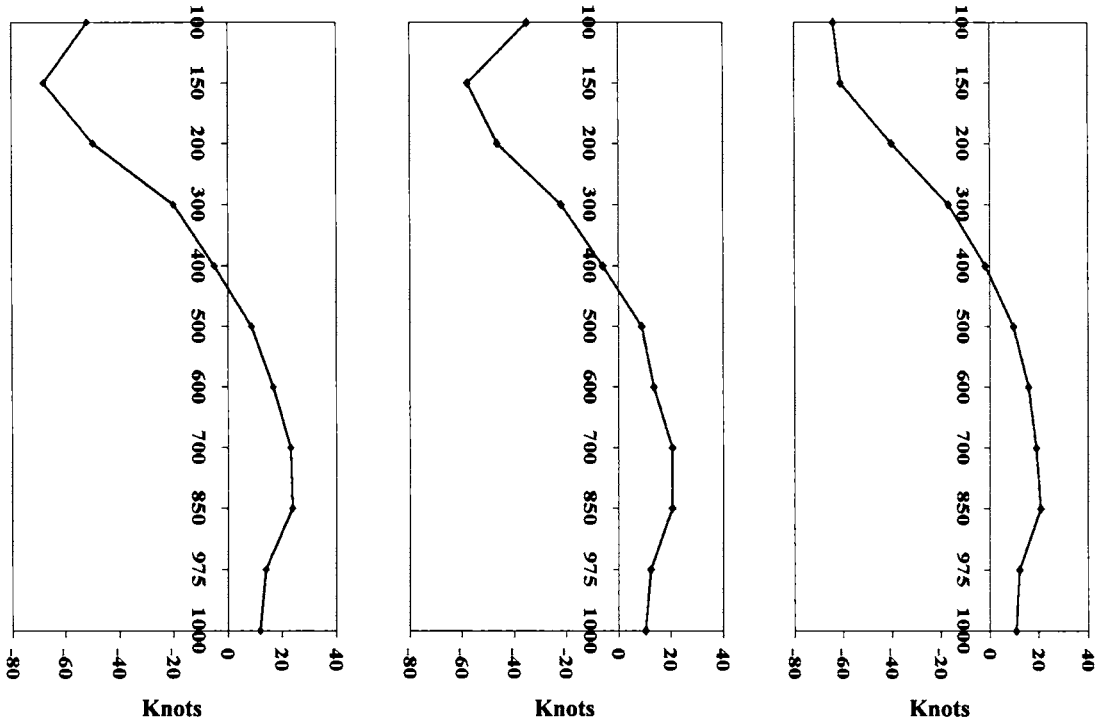

Fig.1.6: U-wind at various pressure levels for July for (a) Thiruvananthapuram, (b) Kozhikode and (c) Mangalore

1.4.4 Humidity

Over the entire subcontinent the moisture content of the atmosphere is minimum during December to February and maximum during monsoon months.

Annual variations over Kerala are less than over north India. At the coastal stations of Kerala monthly mean relative humidity at the surface is of the order of 75% in the morning during winter months and increases to about 90% in the monsoon months. The relative humidity and hence the moisture content, decreases rapidly from coastal to highlands during December to February. During monsoon periods, spatial variation in the moisture content is less. During the period from January to March, afternoon humidities reduce varying from 35% in the interior to 71% in the coastal area. Diurnal variation in relative humidity during the period is maximum and ranges from 4 to 16% depending upon the proximity of the sea. Humidity in the monsoon period rises to about 90% for the state as a whole and diurnal variation in this period is minimum and ranges from 2 to 12%.

Table 1.2 Temperature, Dew point temperature, wind speed and direction for July for three selected stations.

Thiruvanthapuram													
Pressure (hPa)	**1000**	**975**	**850**	**700**	**600**	**500**	**400**	**300**	**200**	**150**	**100**	**50**	**10**
Temperature	25.3	23.7	17.8	10.0	3.3	-4.9	-15.3	-30.2	-52.6	-68.0	-77.0	-61.4	-42.3
Dew Point temperature	22.6	20.5	14.0	1.7	-4.7	-13.3	-24.2	-39.3	-59.1	-56.0	-58.3	-	-
Wind direction	300.6	311.4	301.9	281.0	252.1	224.0	153.7	99.4	85.2	85.7	91.5	-	-
Wind Speed	13.9	18.7	28.0	23.5	17.4	12.3	11.5	20.4	50.1	68.3	51.9	-	-
Kochi													
Temperature	24.5	24.4	17.0	9.4	2.6	-5.5	-16.0	-30.6	-53.9	-67.9	-77.6	-60.6	-49.1
Dew Point temperature	21.6	21.1	13.8	3.2	-4.3	-12.4	-23.4	-38.1	-59.0	-56.7	-72.0	-	-
Wind direction	300.0	309.0	305.0	281.0	249.0	220.0	110.6	108.0	99.1	85.0	90.0	-	-
Wind Speed	12.0	16.0	25.0	21.0	14.4	14.0	6.4	23.0	47.0	58.0	35.0	-	-
Mangalore													
Temperature	25.2	24.5	17.5	9.5	2.8	-4.7	-14.6	-28.9	-51.3	-66.3	-77.4	-60.5	-45.3
Dew Point temperature	23.2	22.0	14.9	3.7	-3.8	-12.0	-22.3	-36.7	-56.3	-61.5	-61.3	-	-
Wind direction	252.9	258.6	287.2	275.4	255.4	227.7	171.2	109.5	105.0	107.2	95.0	-	-
Wind Speed	11.1	12.4	21.7	19.1	16.3	13.1	12.1	18.0	41.7	63.8	64.2	-	-

1.5 Rainfall Climatology of Kerala – Temporal and spatial

The principal rain-giving seasons in Kerala are south-west monsoon (June-September) and post monsoon (October-November). The pre-monsoon months (March-May) account for the major thunderstorm activity in the state and the winter months (December-February) are characterized by minimum clouding and rainfall.

Kerala's annual average rainfall (for the period 1901-2003) of 286 cm is received primarily during the southwest monsoon season of June to September (Table 1.3). Pattern of the spatial distribution of annual rainfall amount brings out the effect of orography on rainfall. Isohyets run more or less parallel to Western Ghats. However, orography does not have a direct relationship with rainfall (Anu Simon and Mohankumar, 2004). Rainfall increases eastwards from Arabian Sea islands as the coastline is reached. Air stream undergoes ascent and uplift progressively as it reaches the coast and then blows nearly perpendicular to the mountains. This forced ascent results in intense clouding and precipitation. Moving east from Arabian Sea there is increased rainfall on the windward slopes of Ghats and there is sharp decrease further eastwards. Steepest gradients of rainfall are seen in Idukky and Kozhikode districts. Rainfall is comparatively less in Palghat district where the presence of the Palghat gap reduces uplift.

Table 1.3: Distribution of Rainfall over Kerala

Season	*Rainfall*	
	Amount (cm)	*% of Annual*
June to Sep	193.3	67.5
Oct & Nov	46.3	16.2
Mar to May	39.5	13.7
Dec to Feb	7.2	2.1
Annual	**286.2**	**100**

The annual rainfall distribution for the 14 districts in Kerala is given in fig. 1.7. District wise, annual rainfall increases from the minimum value of 181cm for Thiruvanthapuram in the south to 329cm for Ernakulam in central Kerala. There is a slight drop for Thrissur district followed by a steep decrease for Palghat where the annual rainfall is only 236cm. The rainfall again increases to the north in Malappuram district followed by a maximum of 376 cm for Kozhikode and 343 cm over Kannur district. The districts on the high ranges also receive good rainfall.

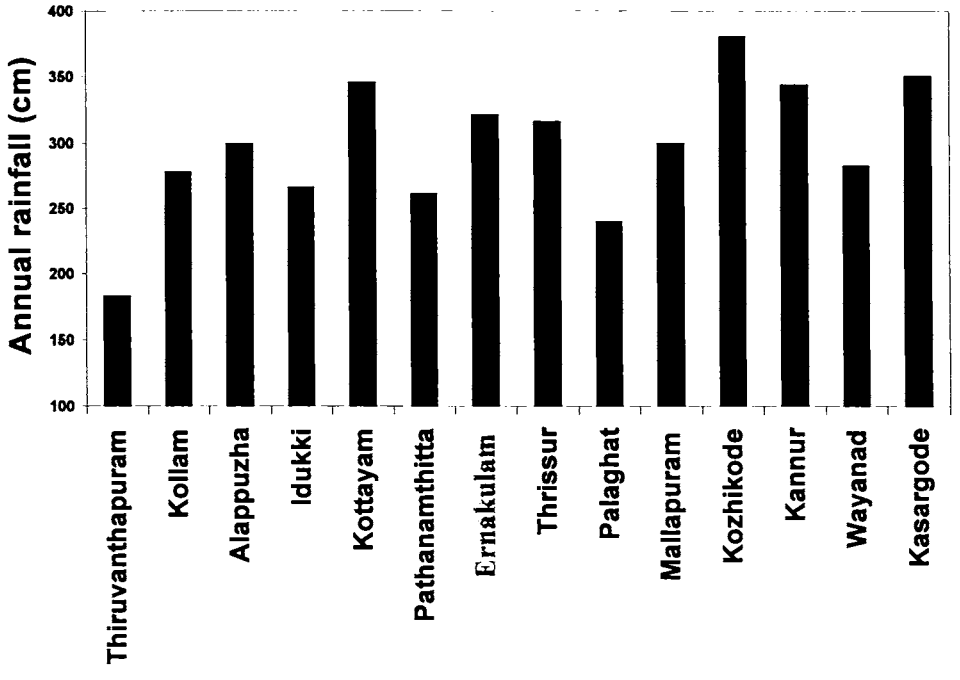

Fig.1.7: District-wise distribution of Annual Rainfall

The normal pentad rainfall reveals finer details of rainfall variations in space and time of individual stations, which may be regarded as spectra of rainfall under high dispersion compared to low dispersion spectra of monthly rainfall (Ananthakrishnan et al. 1971).Fig. 1.8(a-i) gives the pentad rainfall of some selected stations as given in Ananthakrishnan et al. (1971). It can be seen that for Trivandrum (Thiruvanthapuram)(fig. 1.8a), there is a rainfall maximum

around pentad 32 (in the month of June) and a secondary increase near pentad 58, in October. The annual rainfall for the station is 1812 mm. Similarly, Allepey (Alappuzha) (fig, 1.8b) has one maximum around pentad 32 and a small secondary maximum during pentads 54-55. The monthly rainfall distribution of this station shows that the station receives maximum rainfall in June during the south-west monsoon season (June to September) and there is an increase in rainfall during the month of October (north-east monsoon). The station also receives good rainfall during the pre-monsoon month of May. For Cochin (Kochi), shown in fig. 1.8c the pentad rainfall distribution shows a steady increase from pentad 24 (end of April), attaining a maximum at the 32nd pentad and then decreases steadily. There is a secondary maximum in pentad rainfall at pentad 58. The monthly distribution of rainfall for this station shows that the station receives maximum rainfall in June during the south-west monsoon season and in October during the north-east monsoon. Fig. 1.8d gives the pentad rainfall pattern of Palghat. It can be seen that there are two rainfall maxima (around pentad 37 and 58), although the second maximum is not very well pronounced. It should be noted that this station, which lies in the gap of the Western Ghats, receives 2040mm of annual rainfall. The pentad rainfall analysis for Kozhikode (fig.1.8e), a station in north Kerala shows that the pentad rainfall is maximum around pentad 38 (2nd week of July). The secondary maximum seen in Trivandrum, Alleppey and Cochin is not very pronounced in Kozhikode. In Manglore (fig.1.8f) a representative station just north Kerala there is one broad maximum near 34-40th pentad and then rainfall decreases gradually having no peak in October. The pentad rainfall analysis for Mercara a high altitude station east of Kozhikode is given in fig.1.8g. The station receives maximum rainfall in the month of July, as evident in the pentad and monthly rainfall pattern. For both the island stations Amini and Minicoy, (fig. 1.8h&i) the rainfall increases in the pentad near 32 and then falls steadily.

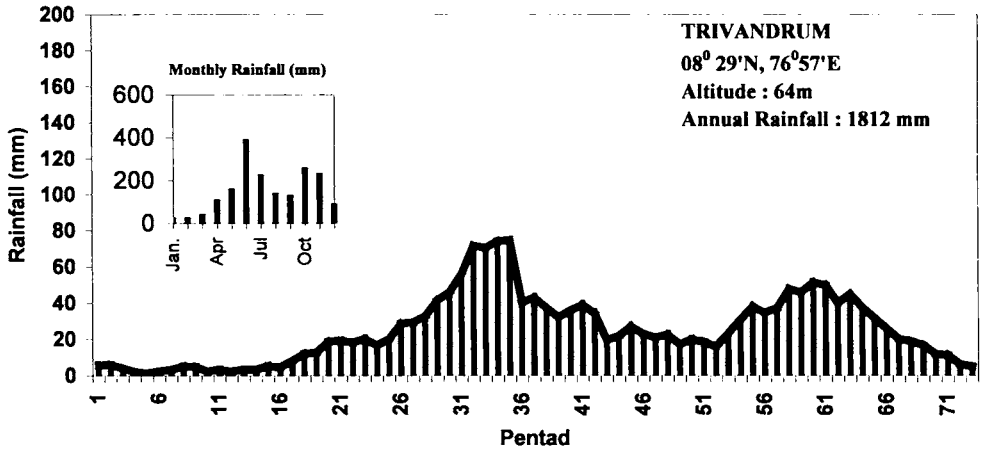

Fig. 1.8a : Pentad Rainfall for Trivandrum as given in Ananthakrishnan et al. (1971)

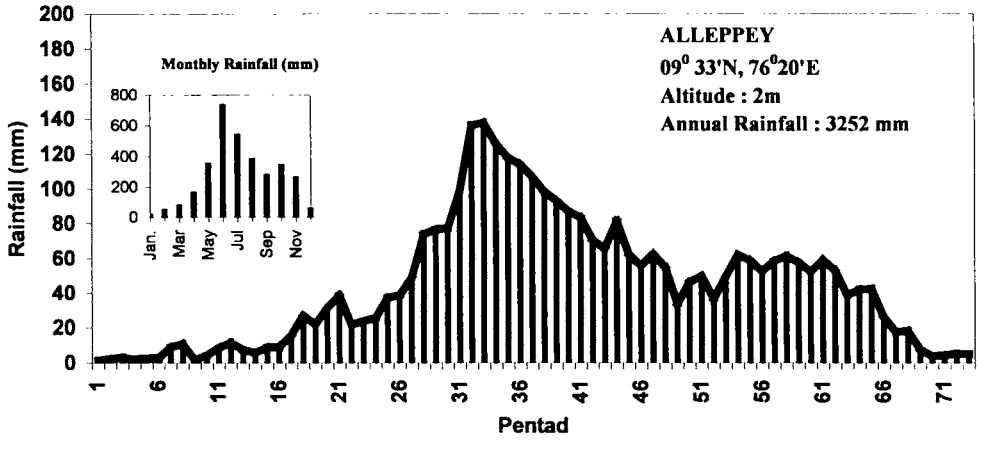

Fig. 1.8b: Pentad Rainfall for Allepey as given in Ananthakrishnan et al. (1971)

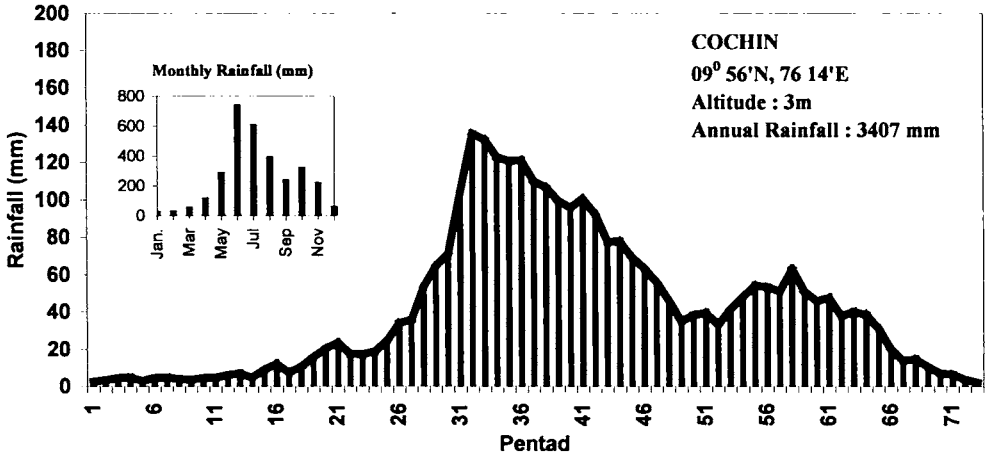

Fig. 1.8c : Pentad Rainfall for Cochin as given in Ananthakrishnan et al. (1971)

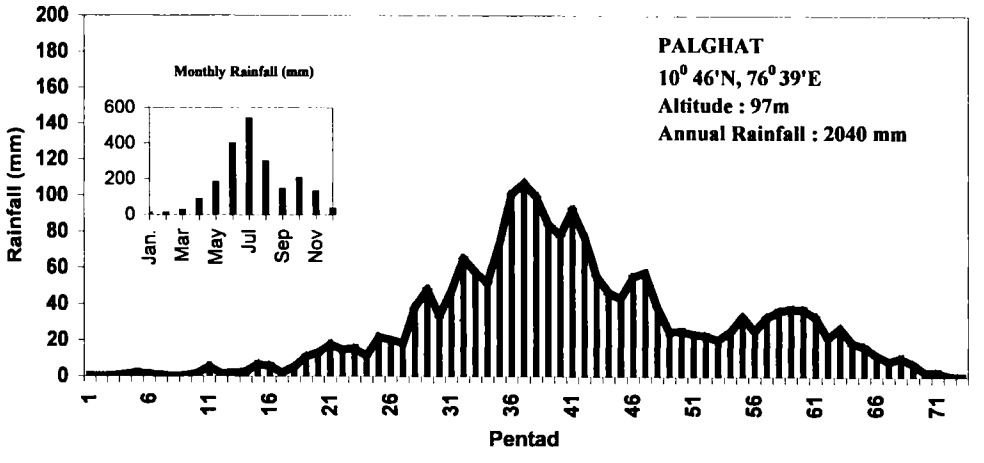

Fig. 1.8d : Pentad Rainfall for Palghat as given in Ananthakrishnan et al. (1971)

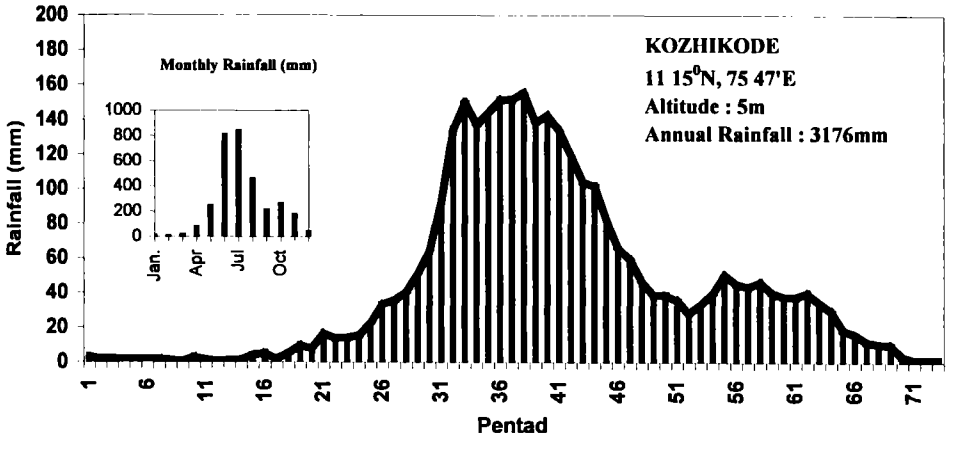

Fig. 1.8e : Pentad Rainfall for Kozhikode as given in Ananthakrishnan et al. (1971)

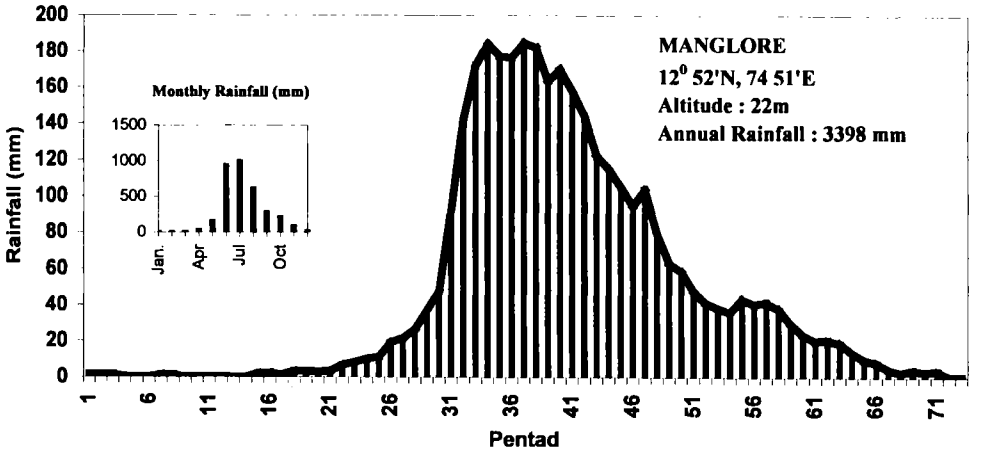

Fig. 1.8f: Pentad Rainfall for Manglore as given in Ananthakrishnan et al. (1971)

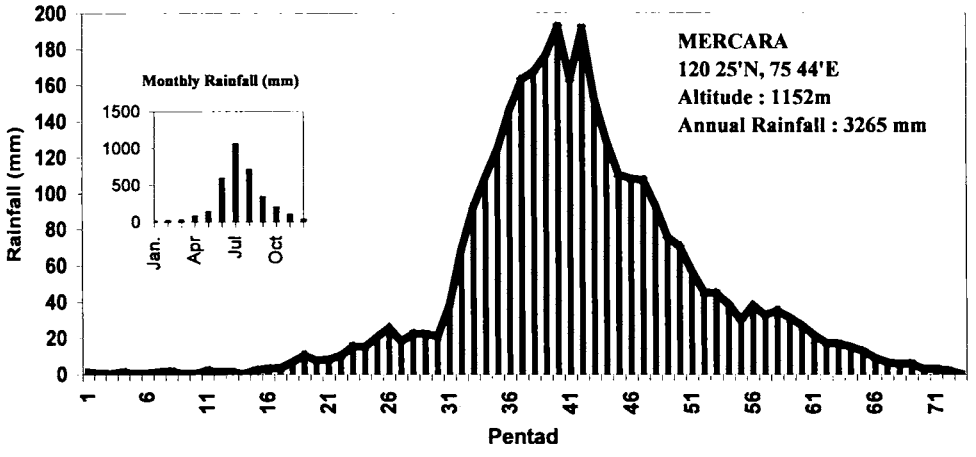

Fig. 1.8g: Pentad Rainfall for Mercara as given in Ananthakrishnan et al. (1971)

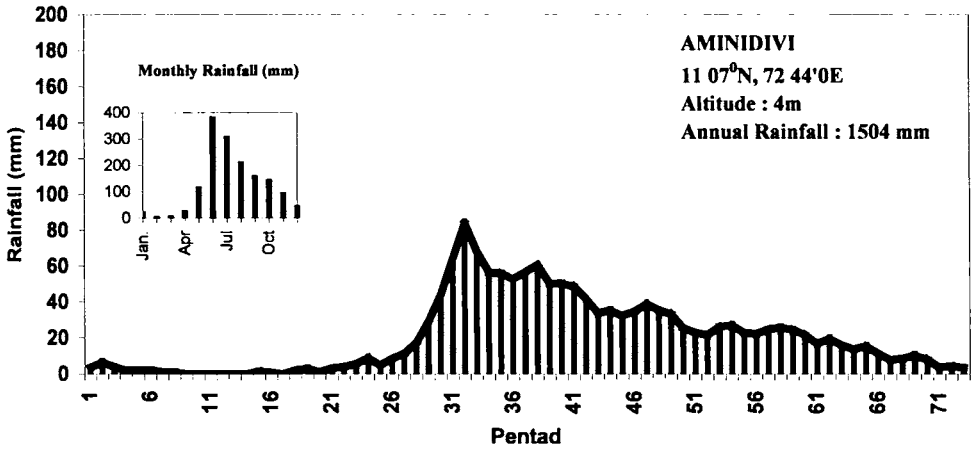

Fig. 1.8h: Pentad Rainfall for Aminidivi as given in Ananthakrishnan et al. (1971)

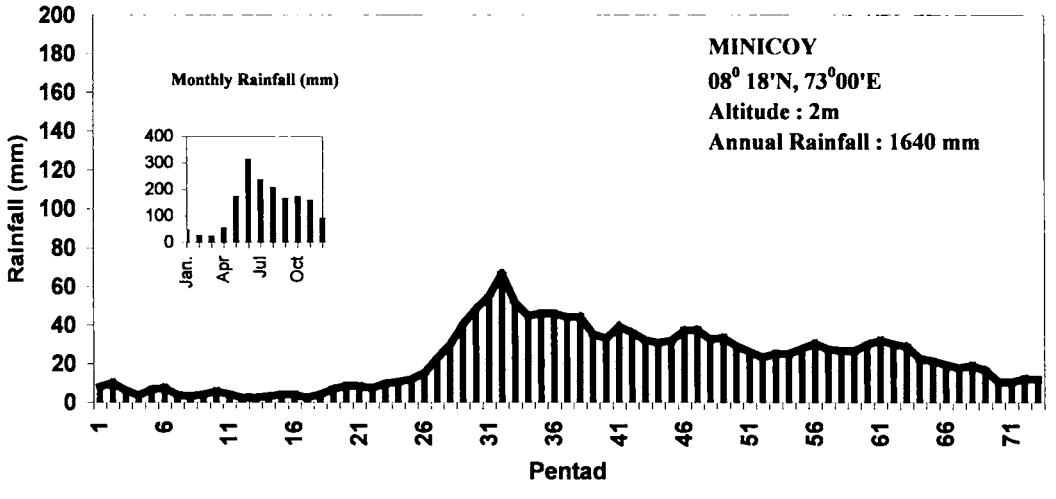

Fig. 1.8i: Pentad Rainfall for Minicoy as given in Ananthakrishnan et al. (1971)

1.5.1 South-west Monsoon (June-September)

The climate of India and that of Kerala in particular is dominated by the south-west (SW) monsoon known as Kalavarsham. The winds are south-westerly (meaning from the south-west) to westerly during six months (mid-April to mid-October) of the year and north-easterly to easterly during the remaining six months. An east-west band of tall rain-bearing cumulo-nimbus clouds form over the north Indian ocean (Arabian sea and Bay of Bengal) and further east, towards the end of May or early June. The latent heat released by the conversion of water vapour into water in these raining clouds heats the atmosphere and lowers the atmospheric pressure below the cloud band and pulls across the equator a deep current of air which accompanies the onset of monsoon. Kerala is the gateway of SW monsoon to India. After SW monsoon sets in over Kerala, the monsoon current and the monsoon rains move northwards to cover the whole of India. The four-month period 01 June to 30 September is designated as the SW monsoon season. In Kerala it is also called Edavapathy (since it commences in the middle of the Malayalam month Edavam).

The spatial distribution pattern of rainfall during this season is similar to annual pattern. Coastal rainfall of Kerala increases northwards from 70 cm in the extreme south to 290 cm in the extreme north. The increase, however, is not uniform. Rainfall increases from west to east to the ranges, the sharpest rise occurring over the high ranges, concentrated over certain areas. In the southern half of the state there are two high rain pockets. One is centered around Peermade (377 cm) in Idukki district and the other in Neriamangalam (383 cm) in the adjoining Ernakulam district. There is another high rain pocket in the north in Kozhikode district with peak rainfall at Vythiri (353 cm) and Kuttiyadi (336 cm). This pocket extends northwards into the adjoining Karnataka region with highest rainfall of 516 cm at Bhagamandla. Palghat gap area and portion of Malapuram district extending to the west from the gap between the two high rain areas of the south and north get comparatively less rainfall. The isohyets

generally run north-south. Concentration of the isolines near the heavy rain pockets may be seen from fig. 12(c) in Ananthakrishnan et al (1979). Isohyets to the east of the Western Ghats show a steep gradient indicating rapid and sharp decrease of rainfall towards the leeward side in Tamilnadu. Rainfall in this rainshadow region is less than 50 cm during this period.(Spatial distribution of rainfall during a typical monsoon month of July is given in figure 7.5a)

Kerala's average rainfall during this season is 192 cm. South Kerala (stations south of about 10N) receive around 176 cm and north Kerala (stations north of about 10N) receives 224 cm during this period. An examination of the monthly pattern shows that rainfall is highest in June in south Kerala while north Kerala experiences the highest rainfall in July (fig.1.9). With each surge in the monsoon current, amount of rainfall is more in north-Kerala than in south and the frequency of surges is higher in July than in June. Rainfall decreases in August and September in the state.

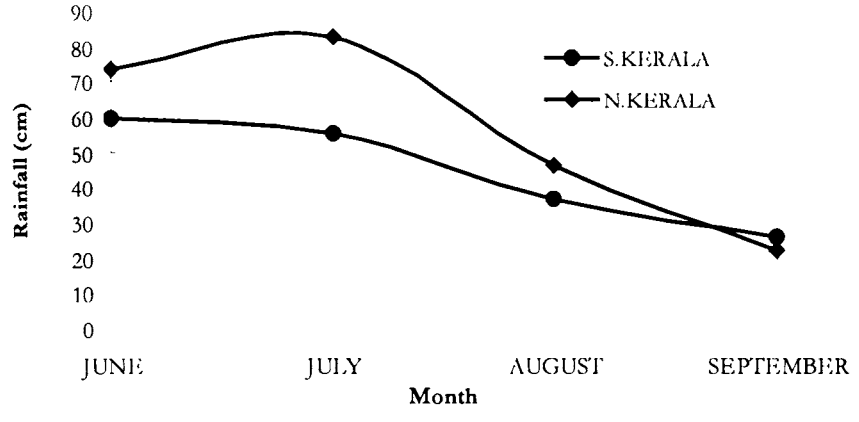

Fig.1.9 :- Month-wise distribution of rainfall during south-west monsoon season for north and south Kerala

The date of onset of south-west monsoon over Kerala has varied from as early as 11 May (in 1918) to as late as 18 June (in 1972). The long-term mean date of monsoon onset over Kerala is close to 01 June. Fig.1.10 gives the dates of monsoon onset over Kerala as declared by the India Meteorological Department over the last more than hundred years from 1901 to 2004. The date

of monsoon onset has large inter-annual variability and also prominent decadal scale variability. On the inter-annual scale, delays in monsoon onset over Kerala are associated with El Nino (Joseph et al, 1994). In the early decades of the twentieth century monsoon onset over Kerala was mostly in the first or second week of June. During the decades 1950s and 1960s monsoon onset occurred early, many times in the second and third week of May.

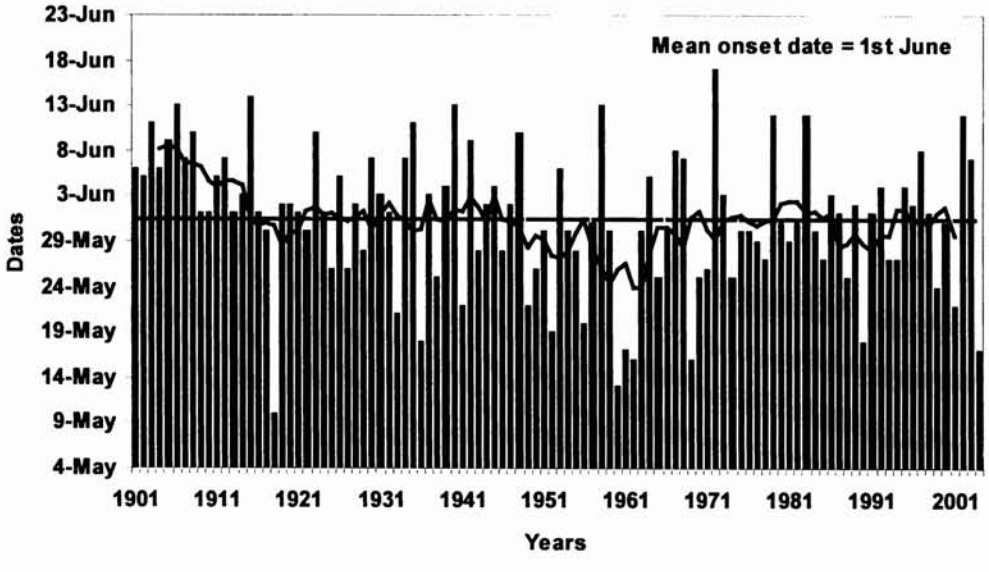

Fig.1.10 : Dates of Monsoon Onset over Kerala and the 7-year moving average

1.5.2 Retreating Monsoon (October-November)

Rainfall abates considerably in September but spurts again in October and decreases further in November. This spurt takes place in association with the retreat of south-west monsoon from north India and the consequent southward movement of ITCZ across Kerala. This period comprising October and November is the phase constituting the withdrawal of the southwest monsoon. Kerala gets ~ 50 cm of rainfall during this season. During this period rainfall decreases from south to north. Eastern side of the Ghats receives its main rainfall during this period. During the earlier part of October rainfall is confined to the interior, mostly in the afternoon, evening or early night. As season advances, rainfall incidence shifts to south and the coastal region. Time

of occurrence also shifts in the later part of the season to the early morning hours. During this season heavy falls and long spells are experienced under the influence of cyclones and depressions. In such cases rain persists throughout the day and there is no preferred time of incidence. Mostly precipitation in this season is from convective clouds (thunder cloud). Thunderstorms of the season are violent, particularly over and near the hills.

1.5.3 Pre- Monsoon (March-May)

Precipitation during pre-monsoon is mainly from thundershowers and there is an increased thunderstorm activity in the southern tip of Kerala state from March onwards increasing progressively with the advance of the season. During pre-monsoon the thunderstorm activity progresses from March to May but in the post-monsoon season thunderstorm activity decreases from October to December. South Kerala experiences more number of thunderstorms during both pre and post- monsoon seasons than north Kerala.

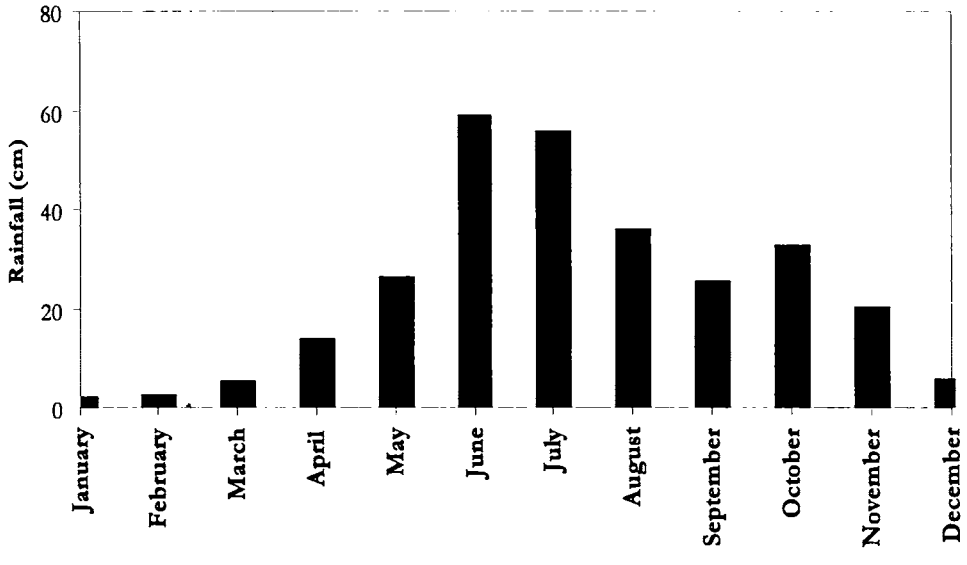

Fig.1.11a :- Monthly rainfall distribution for south Kerala

The monthly distribution shows that the rainfall for the state is bimodal with two maxima corresponding to the advancing and retreat of the Inter

Tropical Convergence Zone (ITCZ). The highest rainfall peak for all the districts is associated with the northward advance of ITCZ accompanying the onset of the southwest monsoon. This occurs in the month of June for most of the stations south of 10^0N (south Kerala) and in July for stations north of 10^0N

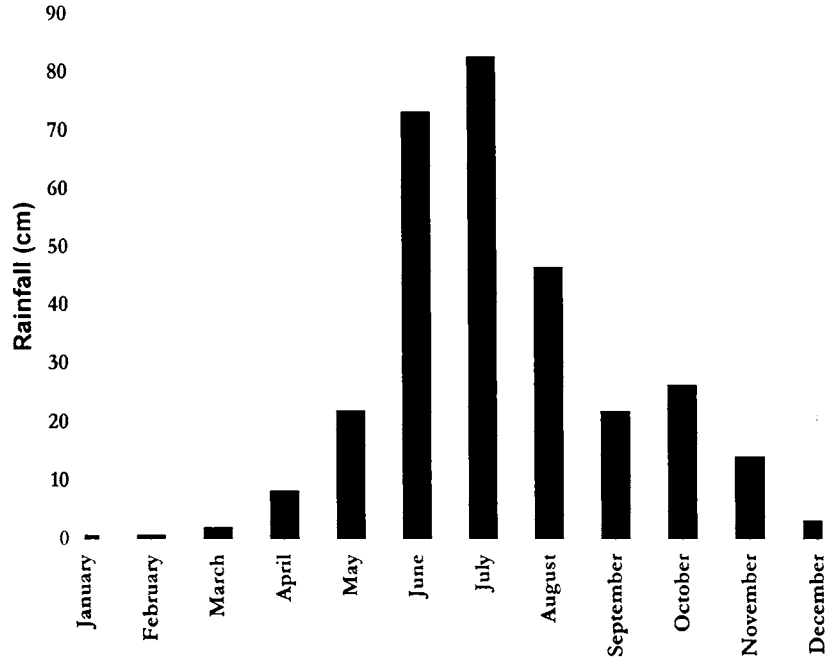

Fig.1.11b :- Monthly rainfall distribution for north Kerala

(north Kerala) (fig.1.11a&b). The second rainfall peak occurs during the receding phase of the ITCZ associated with the retreat of the south-west monsoon, which occurs in the month of October in almost all districts of Kerala. It is also interesting to note that the southern districts of the state receive 25-30% of the annual rainfall during the pre-monsoon and north-east monsoon season and only 50% during the southwest monsoon, whereas the northern districts receive almost 65-75% of the annual rainfall during the southwest monsoon season.

1.5.4 Interannual variability of monsoon rainfall over Kerala

Monsoon rainfall of India has strong interannual variability. This interannual variability affects not only local processes like agriculture but also influences the global climate. The monsoon rainfall is considered to be normal if it is within 1 standard deviation of the long-term mean and WET/DRY if it is above/below 1 standard deviation of the long-term mean.

An investigation of rainfall for 96 years (1901-1996) show that the mean monsoon rainfall for south Kerala is 176.2cm with a standard deviation of 36.1 cm and 223.6cm for north Kerala with a standard deviation of 44.8cm. The mean monsoon rainfall for the state as a whole is 192cm with a standard deviation of 40 cm. A comparative study of the monsoon rainfall over Kerala and the Indian summer monsoon rainfall (ISMR) show that while ISMR was normal in 69 years, Kerala experienced normal rainfall in 72 years. ISMR was above normal (WET) during 11 years and the subcontinent had 20 DRY years during the study period. However, Kerala experienced drought only during 17 years.

1.6 Rain Causing Mechanisms

1.6.1 Southwest *monsoon*

Seasonal variation of the atmospheric circulation and precipitation is the most distinguishing feature of the monsoonal regions of the world. Since Halley (1686), monsoon has been viewed as a gigantic land–sea breeze and the land-sea temperature contrast is considered to be one of the most important factors in generating monsoon circulation. The term '*monsoon*' is traced to an Arabic word meaning '*season*'. *Ramage* (1971) formulated four criteria to delineate a monsoon area:

1. the prevailing wind direction shifts by at least 120^0 between January and July;

2. the average frequency of prevailing wind directions in January and July exceeds 40%.

3. the mean resultant winds in at least one of the months exceed 3 ms^{-1}.

4. fewer than one cyclone-anticyclone-alternation occurs every two years in either month in a 5^0 latitude-longitude rectangle. This monsoon region which includes parts of the African continent; South Asia and North Australia is shown in fig.1.12.

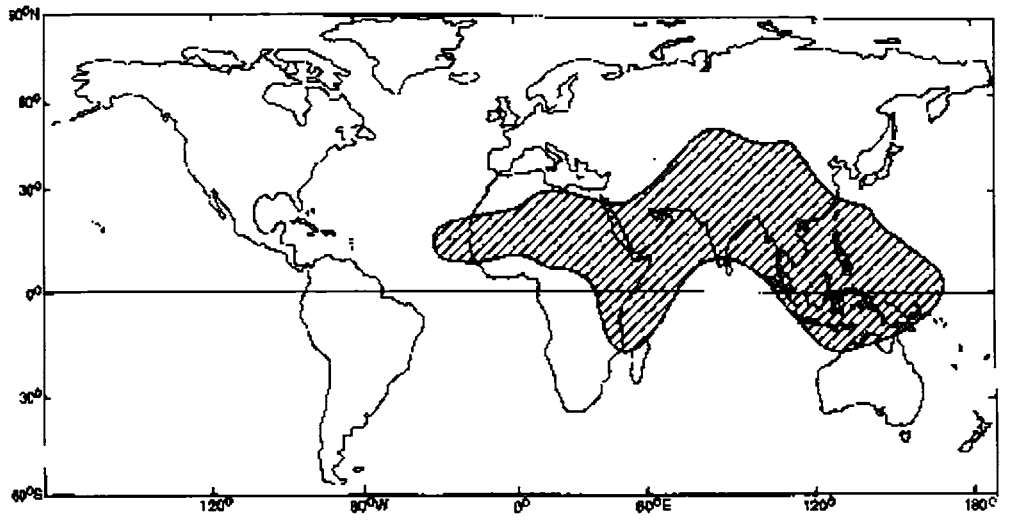

Fig.1.12: Areas with monsoon circulation according to *Ramage*, 1971

The planetary scale monsoon can be viewed as a manifestation of the seasonal migration of the equatorial trough, the near equatorial trough or the Inter Tropical Convergence Zone (ITCZ) and the associated seasonal reversal of winds. In the transitional months between southern and northern hemisphere summers, Inter Tropical Convergence Zone (ITCZ) is located in the equatorial regions making it the maximum heat zone. As sun moves northward through March to June the land is heated more intensely producing stronger vertical motion. The moisture content of the troposphere over the land slowly increases, as the surface wind turns onshore. At this time, organised precipitation zones associated with the ITCZ have moved well north of the equator, signaling the onset of the summer [redacted] monsoon. Seasonal contrasts in land surface temperature produces atmospheric pressure changes, which produce seasonal

reversal of pressure gradients. As a result there are major seasonal wind reversals (fig.1.13a and fig.1.13b).

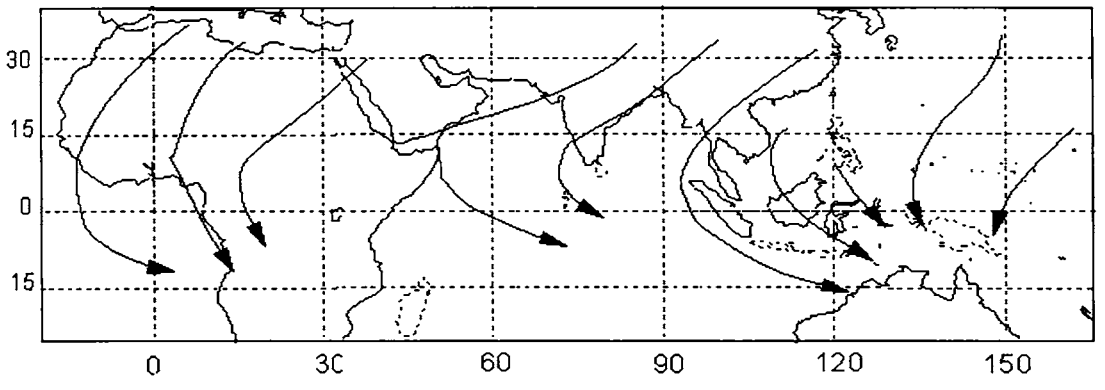

Fig.1.13a: Surface winds during northern hemispheric winter monsoon (*Webster*, 1987)

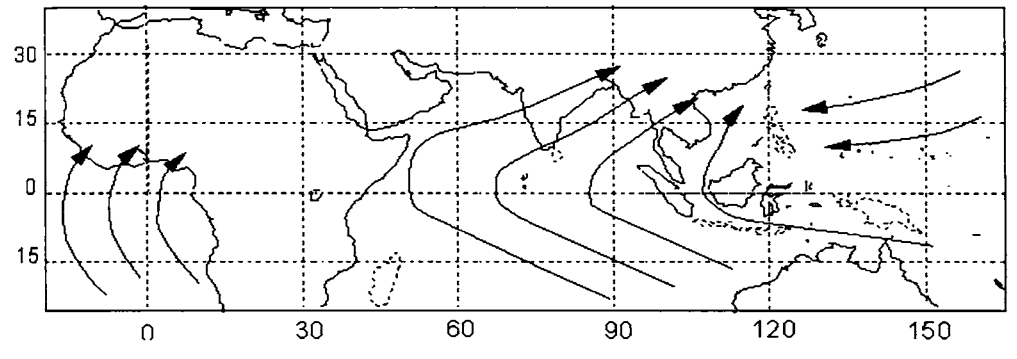

Fig.1.13b: Surface winds during northern hemispheric summer monsoon (*Webster*, 1987)

The basic trigger for the Asian monsoon is the contrast between the temperature of the Asian continent and that of the surrounding ocean (Randall, 2004). This thermal anomaly in the middle troposphere is enhanced by the elevated topography of the Tibetan plateau, which extends upward to about 500hPa. The Tibetan plateau is at about 3000m above the surrounding area and hence much of the surface heating actually occurs in the middle troposphere. After the non-permanent snow on the plateau has melted in late spring and early summer, the surface and the air above it are heated to a temperature higher than that of the surrounding atmosphere. Rising motion balances this heating and this forces convergence in the lower and middle troposphere and corresponding

divergence aloft. As the seasonal heating builds, a trough forms over southern India in late May and subsequently moves north. Cloudiness and precipitation begin to increase at the southern tip of India and by end of June the entire country receives more precipitation.

Studies of daily satellite imagery have shown that the prominent cloud band (maximum cloudiness zone) over the Indian region on a typical monsoon day bears a striking resemblance to that associated with the ITCZ over the other regions of the tropics. Sikka and Gadgil (1980) showed that over the Indian longitudes during the summer monsoon, the maximum cloudiness zone coincides with the trough zone at 700 hPa and is associated with large cyclonic vorticity above the boundary layer, strong low-level convergence and intense moist convection. The associated trough is seen from 850 hPa to 500 hPa. The temperature and specific humidity profiles over the eastern part of the trough is similar to that for the ITCZ. Thus the trough has the dynamical and thermodynamical properties of the ITCZ. Over the Indian longitudes, during summer, the belt of the low OLR extends over about 30-40° latitude which is larger by a factor 3 to 4 than the latitudinal extent over the rest of the tropics in this season and in the northern hemispheric winter, suggesting that, the ITCZ over the Indian ocean changes its character drastically from winter to summer.

An intense continental ITCZ characterises active phase of monsoon. Large-scale monsoon rainfall over the Indian region during summer is associated with ITCZ over the heated Indian subcontinent. On the seasonal scale also, convergence zone is characterized by high transport of mass, moisture and energy. Thus the variations of monsoon rainfall are associated with intra-seasonal and inter-annual time scales and are related to space-time variations of the continental ITCZ.

In meridional plane, circulation comprises of the Hadley cell with continental ITCZ as its ascending limp. Planetary circulation, in the boreal summer, is dominated by wave number 1 and 2 with subtropical highs of upper

troposphere over Tibet and Mexico regions flanked by the mid-oceanic troughs over north Atlantic and Pacific. Air ascending over large-scale heat sources over the Asian and Central American longitudes flow in a zonal direction to the mid-oceanic troughs constituting the east-west walker circulation.

The parameters of broad scale monsoon (*Krishnamurti and Balme*, 1976) are schematically shown in fig. 1.14. The main components of the monsoon circulation are the following:

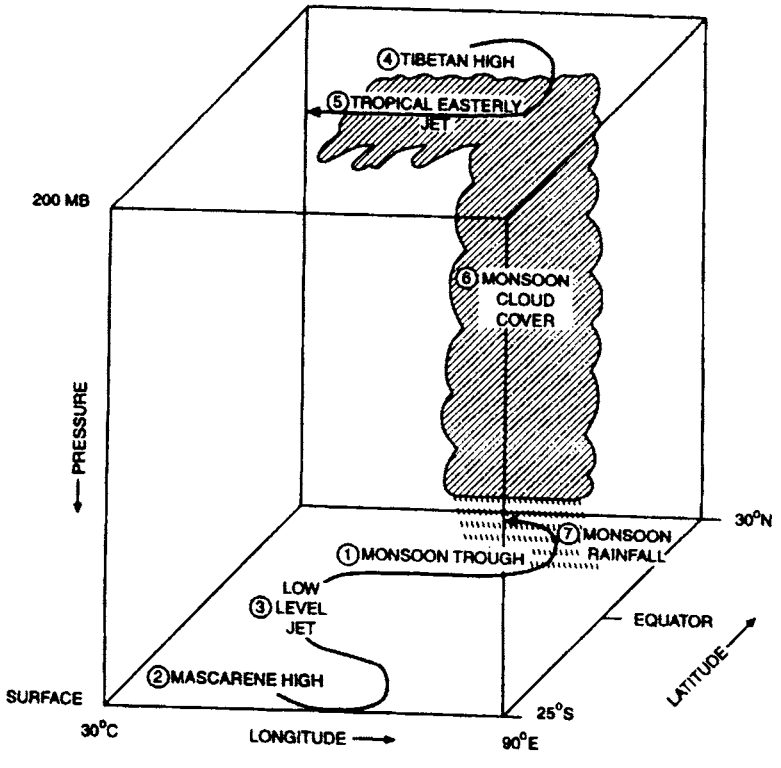

Fig.1.14: Schematic diagram of the elements of the monsoon system (*Krishnamurti and Balme*,1976)

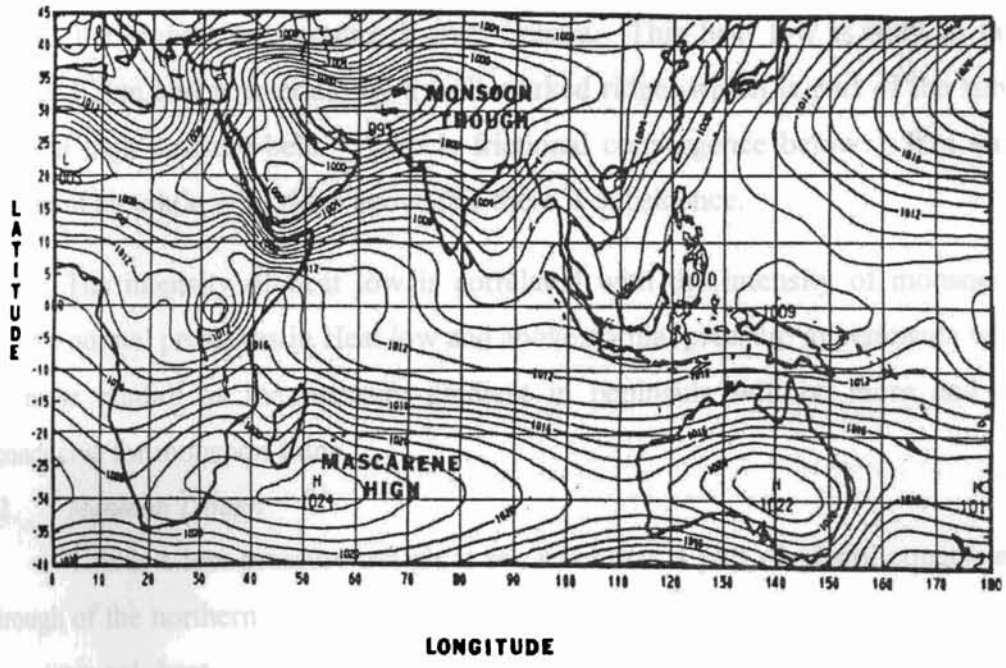

Fig 1.15: Mean sea-level pressure for July (*Krishnamurti and Bhalme*,1976)

1. Heat Low

The progressive development of a heat low over the sub-continent and its location over the central parts of Pakistan in July is the most important causative factor of the monsoon. This heat low is part of the low-pressure belt extending from Africa to central Asia through Arabia, Iran, Afghanistan, Pakistan and the northwest India with offshoots of troughs in various directions. The centres of low are at different locations over land at various months. In April it is over East Madhya Pradesh – May over Punjab and June-July over Pakistan. The centers of low are located at places near to areas of maximum heating away from maritime air. The tapering shape of the Peninsula, the Himalayan mountain ranges and the Assam Hills in the north-east which make the maritime air mass pervade over most of India displace the center of the heat low to the extreme north-west of the country. Blocking of cold air incursion from the north by the Himalayas in the lower-troposphere make the Heat low of sub-continent more intense. Lowest pressure belt for the whole belt from Africa to Asia is over

Pakistan and its neighbourhood. This is not the place of highest temperatures. In fact the highest temperature is over Sahara. This heat low is only in the lowest 1.5km and is overlain by a well-marked ridge, which is part of the sub-tropical high-pressure-belt. There is frictional convergence below 1.5km and ascent of air while with ridge above this there is subsidence.

The intensity of heat low is correlated with the intensity of monsoon. Below normal pressures in Heat low and above normal pressure in peninsula will increase rainfall as the pressure gradient in peninsula will be more and is conducive for monsoon rains. .

2. *Monsoon Trough*

This is a low-pressure trough at sea level that is part of global equatorial trough of the northern hemisphere seen during summer season (Fig1.15). From the seasonal heat low over Pakistan and neighbourhood, a trough extends southeastwards to Gangetic West Bengal. The trough line runs at surface from Ganganagar to Calcutta through Allahabad, with west southwesterly winds to south and easterly wind to the north of trough line. This trough is seen in the upper air up to about 500hPa, the trough line sloping southwards with height. At 700hPa, it runs from Bombay to Sambalpur. In the western sector the trough rapidly shifts southwards with height in the lower troposphere but the slope becomes less marked in mid-troposphere. In the eastern sector, the southward slope is less in the lower troposphere and increase appreciably in mid-troposphere.

Monsoon trough is regarded as the equatorial trough of northern summer, in the Indian longitudes. In this season, a weaker trough persists within 5 degrees south of the equator. The latitudinal position of the monsoon trough line varies day to day and has a vital bearing on the monsoon rains. No other semi-permanent feature has such a control on monsoon activity. This is not so much due to the up glide along the slope of the trough or convergence in it, as due to the various synoptic systems that prevail with the different positions of the trough. Position of trough line close to the foothills of Himalayas is known as

'Break monsoon' with decrease in rains over the country and increase in rainfall in NE India.. Swing of the trough to south of normal position takes place with monsoon depressions that form in the N/NW Bay and move west to west-northwest across the country.

3. *Mascarene High*

This is a high-pressure area (sub-tropical anticyclone) south of the equator (fig.1.15) centered at around 30^0S, 50^0E, from which there is a large outflow of air. Variations in the location and strength of Mascarene high are important in relation to summer monsoon circulation and accompanying rainfall over India

4. *Low-level cross-equatorial Jet*

The deep SW monsoon current has a high speed Low Level Jet Stream (LLJ) (Findlater,1969) whose maximum wind speed is at an altitude of about 1.5 Km as may be seen from fig.1.16 taken from Joseph and Raman (1966). This jet has maximum winds near 1.5 km level and occasionally it has speeds of 100 kts, particularly where the LLJ crosses the equator. It is a very narrow jet (both horizontally and vertically). The Jet runs roughly parallel to the north-south oriented east-African coast which is favourable for cross-equatorial flow from south to north during the northern summer season particularly July-August. During April this current flows across the northern tip of Malagasy. It penetrates into eastern Africa during May and swings across the equator into southwest Arabian Sea and then to west coast of India during June. During July the current flows from the ocean near Mauritius, reaches the Kenya coast near 3^oS and penetrates inland over the flat coastal strip of Kenya and low lands of Ethiopia and Somalia and emerges out into the Arabian sea near 9^oN. Here it moves over the cold upwelling waters off the Somalia coast. In a way this jet causes the upwelling here and this upwelling determines the horizontal and vertical shear of the Jet. The axis of the LLJ over India on a monsoon day can be anywhere between latitudes 5^0N and 25^0N. The variation of wind speed and wind direction

'Break monsoon' with decrease in rains over the country and increase in rainfall over the mountain belt. Swing of the trough to the central parts is with monsoon depressions that form in the North Bay and move west to west-northwest across the country.

3. *Mascarene High*

This is a high-pressure area (sub-tropical anticyclone) south of the equator (fig.1.15) centered at around 30^0S, 50^0E, from which there is a large outflow of air. Variations in the location and strength of Mascarene high are important in relation to summer monsoon circulation and accompanying rainfall over India

4. *Low-level cross-equatorial Jet*

The deep SW monsoon current has a high speed Low Level Jet Stream (LLJ) (Findlater,1969) whose maximum wind speed is at an altitude of about 1.5 Km as may be seen from fig.1.16 taken from Joseph and Raman (1966). This jet has maximum winds near 1.5 km level and occasionally it has speeds of 100 kts, particularly where the LLJ crosses the equator. It is a very narrow jet (both horizontally and vertically). The Jet runs roughly parallel to the north-south oriented east-African coast which is favourable for cross-equatorial flow from south to north during the northern summer season particularly July-August. During April this current flows across the northern tip of Malagasy. It penetrates into eastern Africa during May and swings across the equator into southwest Arabian Sea and then to west coast of India during June. During July the current flows from the ocean near Mauritius, reaches the Kenya coast near 3^oS and penetrates inland over the flat coastal strip of Kenya and low lands of Ethiopia and Somalia and emerges out into the Arabian sea near 9^oN. Here it moves over the cold upwelling waters off the Somalia coast. In a way this jet causes the upwelling here and this upwelling determines the horizontal and vertical shear of the Jet. The axis of the LLJ over India on a monsoon day can be anywhere between latitudes 5^0N and 25^0N. The variation of wind speed and wind direction

in the vertical at a point along the axis (Vishakhapatnam) of the jet-stream is also shown in figure (1.16). Strength of westerly winds increase from sea level upto an altitude of about 1.5 kilometer (5000 feet) and decrease above that. In active monsoon conditions the depth of the monsoon westerlies become more than 6 Kms. Moisture bearing monsoon winds with such a vertical profile impinges on the slopes of Western Ghats during south-west monsoon season producing copious rainfall on its wind facing slopes.

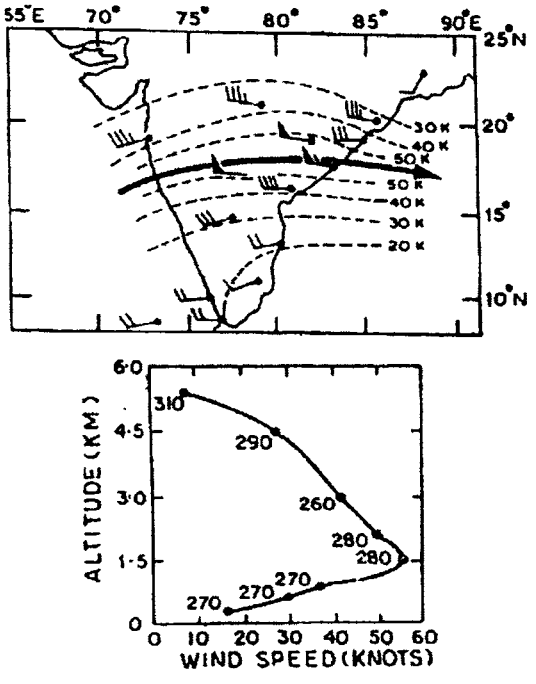

Fig 1.16: Low Level Jetstream on an active monsoon day (Joseph and Raman, 1966)

South-west monsoon of India has an Active-Break cycle. During active monsoon spells that last three to five weeks the axis of the LLJ passes through peninsular India and a major portion of India including Kerala get heavy monsoon rains. During break monsoon spells typically lasting a week, the axis of LLJ bypasses India and flows eastwards south of India. During break monsoon, most parts of India receive very little rainfall. LLJ is the channel through which the water vapour evaporated over the vast expanses of the south Indian ocean and Arabian sea is taken to the raining monsoon areas over India and south-east Asia. The raining areas mapped by satellite (Outgoing Longwave Radiation-OLR- gives a measure of the rainfall, (lower OLR indicating higher rainfall) and

the axis of LLJ during monsoon onset over Kerala and in active and break monsoon spells as average of several cases taken from Joseph and Sijikumar (2004) are shown in fig.1.17 (a-c).

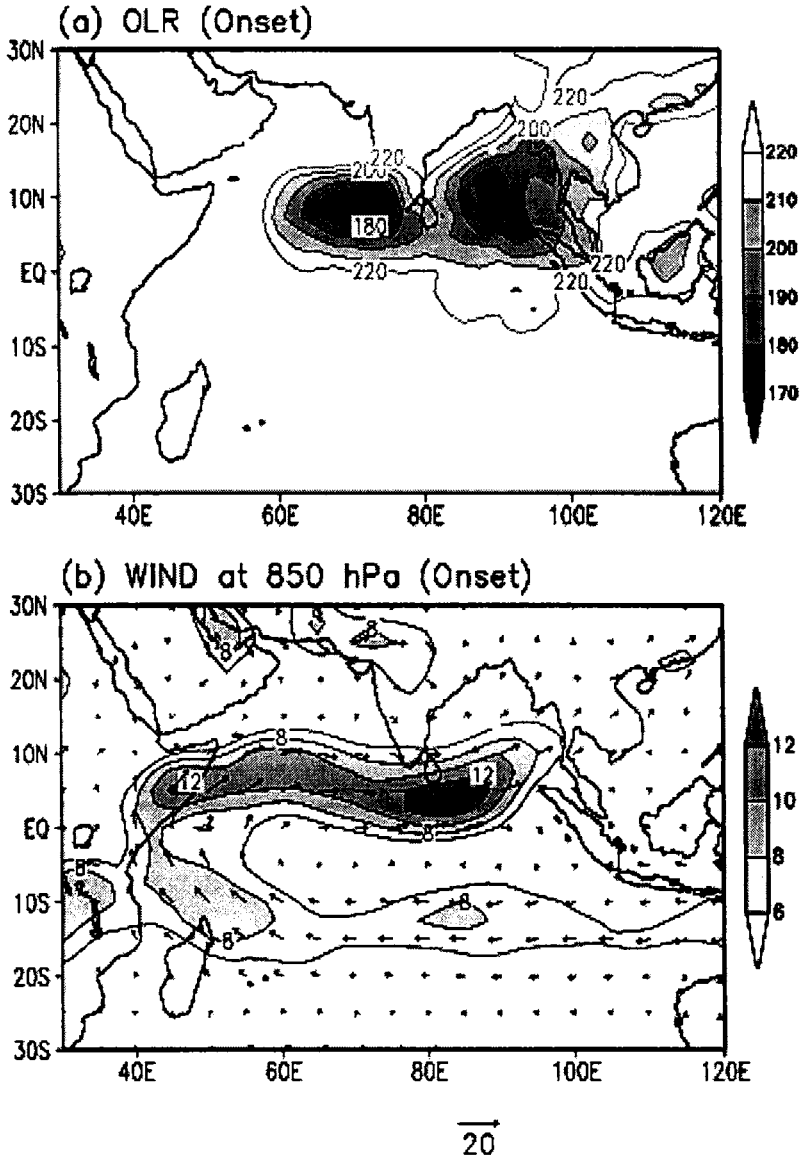

Fig. 1.17a: Axis of Low-level Jet and the associated active areas of convection (OLR in Watts/m^2) during onset as taken from Joseph and Sijikumar (2004). Wind is in ms^{-1}.

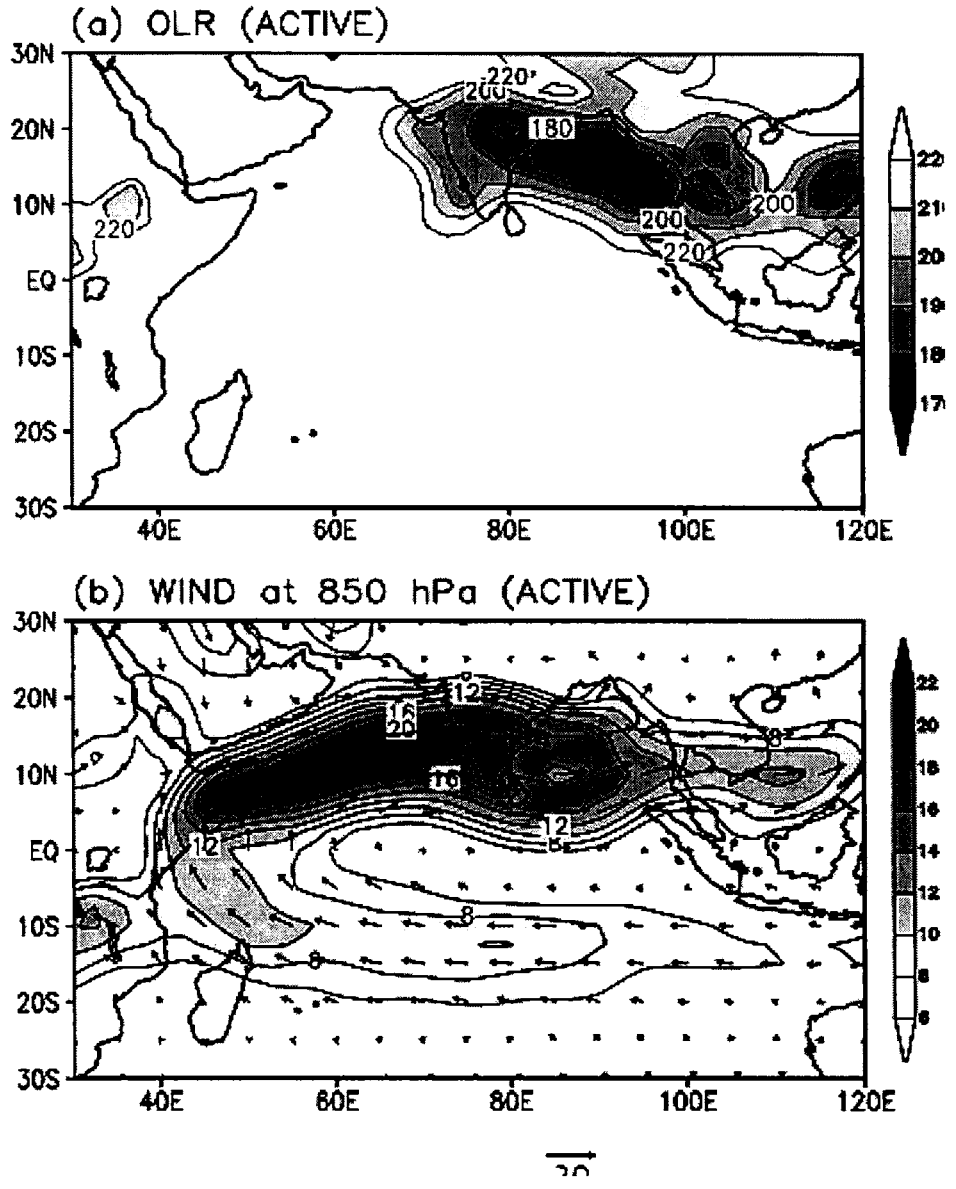

Fig. 1.17b: Axis of Low-level Jet and the associated active areas of convection (OLR in Watts/m^2) during active spells of south-west monsoon as taken from Joseph and Sijikumar (2004). Wind is in ms^{-1}.

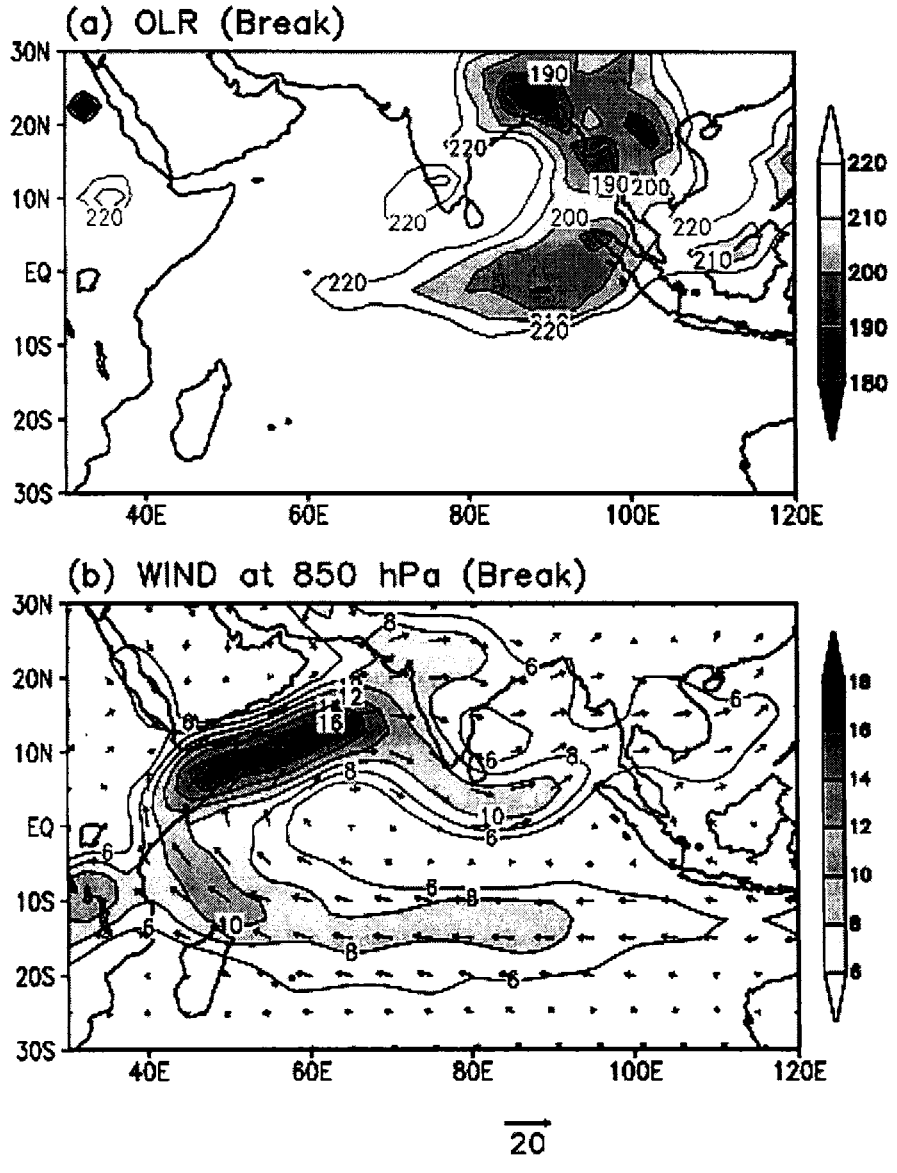

Fig. 1.17c: Axis of Low-level Jet and the associated active areas of convection (OLR in Watts/m^2) during break spells of south-west monsoon as taken from Joseph and Sijikumar (2004) Wind is in ms^{-1}.

During active monsoon conditions over India, Kerala also gets large amounts of rainfall, particularly on the wind-facing slopes of the Western Ghats, more particularly in the high ranges. On some of these days the low level westerly winds develop wave troughs and spatially small low pressure areas in them along and off the west coast of India including Kerala when the heavy

rainfall activity shifts from the high ranges to the coastal and just off-coast areas in the Arabian sea – Rao (1976).

5. *Tropical Easterly Jet*

It is seen that easterlies are well developed during northern summer over south-east Asia particularly over south India at 100hPa. Along meridian 70E – 85E, we have sea near the equator and High Himalayan plateau near 40°N. This creates intense temperature and pressure gradients between the sub-tropical and equatorial latitudes in this region, the sub-tropics having higher temperature and equatorial region having lower temperature throughout the troposphere. As a result, there is low-pressure area in the sub-tropical latitudes and high-pressure area in the near-equatorial latitudes in the lower troposphere and opposite pressure-gradient in the middle and upper troposphere. Due to the low values of Coriolis parameter in the near-equatorial latitudes, even a slight gradient of pressure can create zonal flow of considerable magnitude in these latitudes.

There is lack of observations in the tropical region and with the available data we can say that, an easterly Jet stream overlies south Asia and north Africa during northern summer (June-September.). Starting at the east coasts of southeast Asia the axis of the current accelerates and runs westwards, roughly along latitude 8^0N-12^0N attains maximum speed over south-east Arabian sea and decelerates over Africa, weakening and losing Jet intensity. Surface of maximum easterly wind is lowest (13.5km) near the equator, rising upwards towards north to a level of 16 km at 25°N. Maximum intensity of easterly wind is seen around 9°N (77kts) during this season.

6. *Tibetan High*

This is a large anticyclone that is known to have its largest amplitude near 200 hPa during the northern summer months. Upper air anticyclone first appears in April just to the north of Borneo. In May it is located over Indochina, by June it is found over northern part of Burma and thereafter it moves to Tibetan

highlands. This anticyclone moves south-south eastward in September and is found over Malaysia in November and then loses its identity. Summer heating of the Asian land mass is regarded as the principal cause of the onset of summer monsoon winds and rain. Flohn (1968) regarded the vast elevated Tibetan Plateau as the principal heat source in the mid-troposphere, which controls the monsoon circulation. Sensible heat flux from the elevated land surface is an important heat source in the monsoon system. Once the monsoon has set in very large amounts of latent heat over the monsoon region is released. Even though, the percentage contribution is not very clear, estimates say that contribution of latent heat is 80% and sensible heat is 20% for the maintenance of monsoon circulation.

1.6.2 Monsoon Depressions

Monsoon depression is one of the important synoptic scale (1000 km) tropical disturbances, which forms periodically on the quasi-stationary monsoon circulation. Prevailing over the Indian region during the south-west monsoon, its existence and pre-eminent position as a rain-producing system is well recognized. As per the current definition followed by IMD, low-pressure systems are referred to as depressions when surface winds in cyclonic circulation are between 17 to 33 kt. A depression in which the wind speed exceeds 33 kts is termed as a cyclonic storm. During active monsoon conditions these systems form in the Head Bay and move inland to Orissa and further west. These systems intensify the low level monsoon winds causing increased rainfall activity over India including in Kerala.

1.6.3 Thunderstorms

Assam and its neighbouring states and Kerala (particularly south Kerala) have the highest frequency of thunderstorms in India. In Kerala maximum frequency of thunderstorm days are in April, May and early June and in October and November. The world over one of the basic mechanisms causing rainfall,

particularly heavy rainfall is the thunderstorm. The cloud that causes a thunderstorm is the cumulonimbus. During the south-west monsoon season in Kerala, rainfall is also caused by tall cumulus clouds of height around 6 kms and by thick nimbostratus clouds. Fig. 1.18 gives the vertical structure of a typical thunderstorm (cumulonimbus) cloud growing up to altitudes of 12 to 18 kms. Strong vertical air currents (up-drafts and down-drafts) are a characteristic feature of these clouds. The down-draft air spreads on the ground causing surface wind squalls ahead of the arrival of the thunderstorm cloud overhead with its heavy showers. Kerala does not get the severe manifestations of the thunderstorm called supercell thunderstorms (frequently occurring in north India) that cause big hail and occasionally tornadoes and accompanied by surface squalls of 100 to 200 km per hour winds. However, the thunderstorms of Kerala produce heavy rain showers and strong electrical manifestations – lightning and thunder. For thunderstorms to form lower layers of the atmosphere should have large quantities of moisture and the atmosphere should be conditionally unstable. These conditions are generally available in Kerala. For severe thunderstorms to occur as in north India, the wind speed should have a large increase with height, particularly in the lowest five kilometers of the atmosphere. For triggering thunderstorms, the atmosphere should have vertical motion in the lower levels. These vertical motions are caused by atmospheric dynamics in the areas of low pressure and in areas of low-level wind speed variations (along and perpendicular to the wind direction). Stronger vertical motion is available in the high ranges when winds have a component perpendicular to the hill slopes. Heavy thunderstorm rains (cloud bursts) of a few hours duration in the high ranges can cause flash floods in our rivers and also land slides (urul pottal). The heavy rains associated with a thunderstorm cover areas only a few tens of kilometers wide.

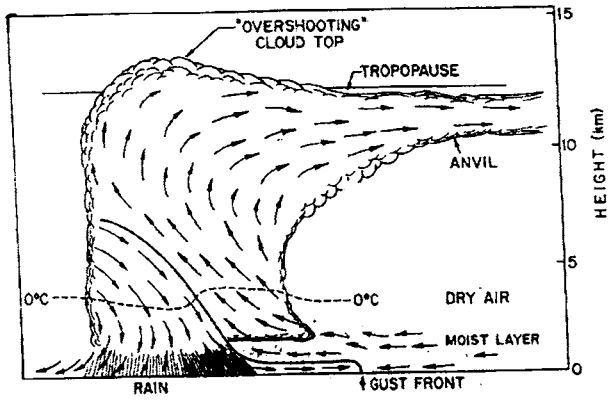

Fig. 1.18: Vertical structure of a typical thunderstorm (cumulonimbus)

1.6.4 Lows, Depressions and Cyclones

Tropical cyclones are large vortices in the atmosphere with powerful winds rotating in an anti-clockwise direction in the northern hemisphere. They develop a central eye, surrounded by an eye-wall called wall-cloud composed of thunderstorm clouds. An area extending radially upto about 100 kms from the cyclone centre causes destruction due to strong winds and heavy rain. The various stages in the intensification of a cyclone are low, depression, cyclone, severe cyclone and super cyclone depending on the speed of the low level winds in its circulation. A typical severe cyclone will have the eye, wall cloud and the spiral cloud bands of the cyclone, which occupy the inner region of the cyclone. Strong cyclonic winds without rain extend from the periphery of the spiral cloud bands up to 700 kms from the cyclone centre.

Cyclones of the Indian seas generally form between latitudes 5N and 18N during the pre-monsoon months of April, May and the early part of June and in the post monsoon period late September to December. During the south-west monsoon months only weaker systems called monsoon depressions form. The preferred motion of Indian cyclones is northward but in the month of November a high percentage of the cyclones formed in the Bay of Bengal move westwards, hit the Tamil Nadu coast and after weakening into depressions and lows move across Kerala giving plenty of rain in Kerala without causing much wind damage. Pre-monsoon cyclones of the Arabian Sea generally move northwards

and do not affect Kerala. But in May 1932 and again in May 1941, cyclones that formed in the south-east Arabian sea moved eastwards and crossed into Kerala near Kozhikode in 1932 and near Thrissur in 1941 causing widespread and heavy rainfall and considerable property damages. We have now three cyclone detection radars one each at Cochin, Chennai and Karaikal and the Indian satellites in the INSAT series to keep constant watch on cyclones likely to affect Kerala.

1.7 Rainfall and Orography of the Western Ghats

Kerala gets average annual rainfall of about 300 cms. A good part of this rainfall is caused by the orography of the Western Ghat mountain ranges. Both convective (large cumulus and thunderstorm) and non-convective (nimbostratus) rain require vertical motion in the atmosphere and the slopes of the Western Ghats generate large vertical motion fields when winds impinge on them, particularly during the south-west monsoon season with strong westerly winds. Non-convective rain is caused purely by the vertical motion present in the atmosphere where the moist air is made to move up when the water vapour in the air condenses to form rain. In convective rain the strong vertical motion in the cloud that generates the rain is caused by the conditional instability present in the atmosphere, but vertical motion in the atmosphere in its lower levels is necessary to trigger the convective clouds and make them respond to the atmospheric instability.

Vertical motion in the atmosphere outside convective clouds is caused by the following main factors:

(a) Wind speed normal to the slope of the mountain terrain

(b) Slope of the mountain terrain

(c) Mountain (lee) wave generation

(d) Land-sea and land-land contrast in friction in the atmospheric boundary layer.

(e) Cyclonic Vorticity (anti-clockwise rotation about a vertical axis in the northern hemisphere) of the air in the frictional boundary layer of the atmosphere for generating upward motion. This rotation in the air can be due to low-pressure systems like lows, depressions and cyclones (vorticity due to curvature of the flow) or due to the wind speed variation normal to the wind (vorticity due to lateral shear of the wind). Clock-wise air rotation (anti-cyclonic vorticity) in the boundary layer causes downward movement of air and suppression of rainfall.

(f) Longitudinal variations (along the wind direction) in the wind (convergence or divergence)

(g) Large scale and weak vertical downward motion field is generated in the atmosphere (subsidence) by the convective heating of the atmosphere in distant areas as when El Ninos occur.

Factors (a) and (b) (orographic control) are very important for the monsoon rainfall of Kerala. In addition the shear vorticity in the SW monsoon wind also regulates monsoon rainfall (dynamic control). Factor (e) particularly the cyclonic vorticity caused by lows, depressions and cyclonic storms is an important factor (dynamic control) in NE monsoon rainfall of Kerala. Western Ghat orography also plays an important role in this season. In the pre-monsoon season, rain is mainly due to afternoon thunderstorms where conditional instability in the atmosphere is a very important factor. Orography provides trigger mechanism to initiate the thundercloud formation.

Chapter 2
Data and Methodology

2.1 Data used in the study

2.1.1 Rainfall Data

2.1.1.1 All India Summer Monsoon Rainfall Data

The All India Summer Monsoon Rainfall for the period 1871 to 2003 is obtained from the official website of Indian Institute of Tropical Meteorology (IITM), Pune. The rainfall series is an area-weighted average for 306 rain-gauge stations in India. The network of rain-gauge stations is made in such a manner that the network provides one representative station per district having a reliable record for the longest possible period. The network selected under these constraints consists of 306 almost uniformly distributed stations for which rainfall data are available from 1871. The hilly regions consisting of four meteorological subdivisions of India which are parallel to Himalayan mountain range have not been considered in view of the meager rain-gauge network and low areal representation of a rain-gauge in a hilly area. Two island subdivisions far away from mainland have also not been included. Thus, the contiguous area having network of 306 stations over 29 meteorological subdivisions measures about 2,880,000 sq.km, which is about 90 percent of the total area of the country. The detailed description is given in Mooley et al., (1981); Parthasarthy et al., (1987, 1993,1995); Pant et al., (1997).

2.1.1.2 All India Daily June to September Rainfall Series

IITM has derived time series of the daily averaged 1June to 30September rainfall of India using data of more than 300 rain-gauge stations well distributed over the whole of India. We used this data set kindly provided by IITM to study durations of strong and weak monsoon rainfall. Daily rainfall data for India as a whole for the period 1 June to 30 September 1901-1989 were prepared from grid data (Kripalani et al., 1991) and for the period 1990- 2002 as updated by IITM from the *All India Weather Summary* prepared by the India Meteorological Department

2.1.1.3 Summer Monsoon Rainfall for South and North Kerala

The rain-gauge network of Kerala whose data for the period 1901-1980 used in this study is shown in fig. 2.1. The dividing latitude between south and north Kerala is about 10^{O}N. South Kerala has 44 rain gauge stations and north Kerala has 31 stations with long records of rainfall. Ananthakrishnan and Soman (1988) using the data of daily rainfall at these stations constructed daily rainfall series for south Kerala and north Kerala by averaging the rainfall at individual stations. This data set for 80 years (1901 to 1980) was donated to Cochin University of Science & Technology by Dr.Soman of Indian Institute of Tropical Meteorology (IITM). For the period 1981-1996, average of 39 stations in south Kerala and 24 stations in north Kerala were used. The daily data for the period (1981-1996) was obtained from the India Meteorological Department. Figure 2.2 gives the stations used for the period 1981-1996. The southwest monsoon rainfall of Kerala for the period 1901 to 1996 is calculated as an area-weighted average of south and north Kerala time series. This time series is used for studies of interannual variability, decadal variability and long-term trend of Kerala rainfall in chapter-4.

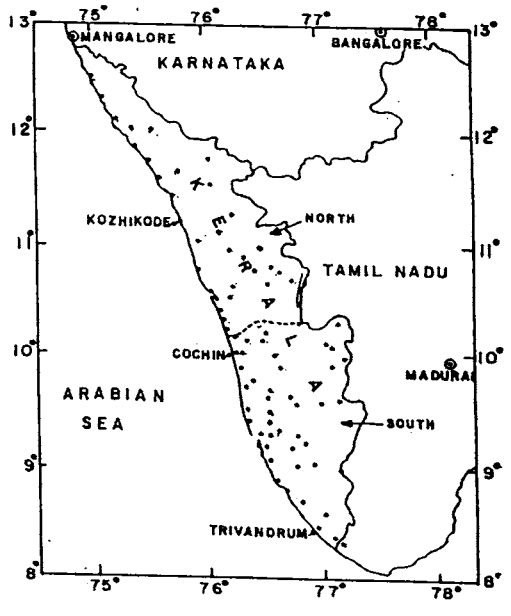

Fig. 2.1: The rain-gauge network of Kerala for the period 1901-1980.

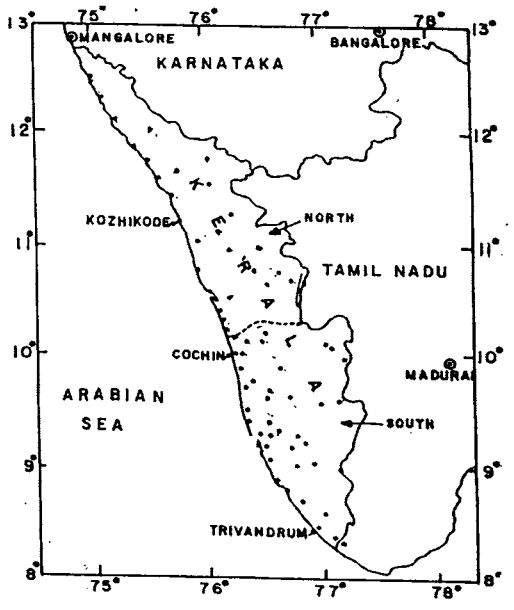

Fig. 2.2: The rain-gauge network of Kerala for the period 1981-1996

2.1.1.4 Kerala Summer Monsoon Rainfall Data

The monthly (January - December) area weighted rainfall series for each of the 29 meteorological subdivisions is available in the IITM website for the period 1901-2003. The monsoon rainfall for Kerala (June-September) is obtained from this site. The sub-divisional rainfall has been prepared by assigning the district area as the weight for each rain-gauge station in that subdivision. The data for the recent period 1991-2003 are preliminary estimates based on the sub-divisional means supplied by India Meteorological Department (IMD), which are in turn based on a variable network. However, IMD data have been rescaled to conform to the long-term means of the respective subdivisions in the IITM-IMD data set. This data set of Kerala rainfall of the monsoon season is used in chapter-5 on Long Range Forecasting.

The climatological mean (1901-1950) value for July rainfall is obtained from IMD publication Annual and Seasonal Rainfall Normals and number of rainy days – PartV

2.1.1.5 Pentad Rainfall

Normal pentad rainfall of 160 stations over India and its adjoining sea areas for the entire year comprising 73 pentads is given in Ananthakrishnan et al.

(1971). The pentad rainfall values are an average of 50 years (1901-1950). The details of the stations selected in this study are given in Table 2.1.

Table 2.1: Details of pentad rainfall as taken from Ananthakrishnan et al. (1971)

Station	Latitude	Longitude	Altitude (m)	Annual Rainfall (mm)
Trivandrum	08° 29'N	76° 57'E	64	1812
Alleppey	09° 33'N	76°20'E	2	3252
Cochin	09° 56'N	76°14'E	3	3407
Palghat	10° 46'N	76° 39'E	97	2040
Kozhikode	11°15'N	75° 47'E	5	3176
Manglore	12° 52'N	74°51'E	22	3398
Mercara	12° 25'N	75°44'E	1152	3265
Aminidivi	11 °70'N	72°44'E	4	1504
Minicoy	08° 18'N	73° 00'	2	1640

2.1.1.6 Hourly Rainfall Data

The hourly rainfall data is obtained from the International Hydrology project under the Kerala State Irrigation Department. Full Climatic Stations (FCS) under Water resources Department, established in 2000 under this project take measurements of parameters like rainfall (Siphon Rain Gauge), Pan evaporation, Maximum and Minimum Temperatures, Dry bulb Temperature, Wet bulb Temperatures, instant wind speed & daily average 2 times a day (8.30 am & 5.30 pm).

Continuous recording on graph are taken for some parameters like Sunshine duration, Temperature, Humidity and Rainfall and the graphical readings are converted into hourly values. Section offices under the department

maintain these stations, and the data is observed and validated by trained local personnel using software named SWDES. The data are validated at various levels and stored for future use in the department. We obtained the hourly rainfall for 10 stations in Kozhikode division, 14 stations in Thalassery division, 9 stations in Thrissur division and 9 stations in Chegannur division. Out of these 42 stations, we have utilized 33 stations with missing data less than 10% of the total data length. The station details are given in Chapter 6.

2.1.2 Break/Active Periods

Ramamurthy (1969) has studied the details of break period upto 1967. The main criteria used for the study is Monsoon trough running close to the foot hills of the Himalayas and absence of easterly winds to the north of monsoon trough in the lower tropospheric levels'. De et al. (1998) identified break periods from 1968 to 1997 with the help of daily weather charts of India Meteorological Department. He has used the same criteria as by Ramamurthy (1969) with some additional features. During the period studied (1968-1997) there were 193 break days in 33 break spells. Most of these occurred in July and August. Joseph and Sijikumar (2004) have taken the break spells of July and August lasting 3 days or more for the twelve years 1979-1990. These break spells are listed in Table 2.2 and we have used this for our study. An active monsoon spell is defined arbitrarily as one in which for each day of the spell the area averaged zonal wind at 850 hPa in the latitude-longitude box 10^0N-20^0N and 70^0E-80^0E in a five day period centered on that day is 15ms^{-1}or more (Joseph and Sijikumar, 2004). We have chosen Active days according to this criterion as given by them. The details are given in table 2.2.

Table 2.2 Active/Break days as given in Joseph and Sijikumar (2004)

Year	Active Monsoon	Break Monsoon
1979	23Jun-02Jul 31Jul-12Aug	17Jul-23Jul 15Aug-31Aug
1980	21Jun-07Jul 05Aug-08Aug	17Jul-20Jul 26Jul-30Jul 23Aug-27Aug
1981	05Aug -08 Aug	26July -30 Jul 23 Aug - 27 ug
1982	11Aug -16 Aug	-
1983	11Aug -15 Aug	22Aug -25Aug
1984	14Jun -18 Jun	20Jul - 24Jul
1985	-	22Aug-25Aug
1986	19Jun-27Jun 16Jul-21-Jul 06Aug- 11Aug	23Aug - 26Aug 29Aug -31Aug
1987	-	28Jul -01Aug
1988	15Jul-20Jul 31Jul-02Aug	05 Jul Œ 08 Jul 13Aug -15Aug
1989	21Jul- 26Jul	10Jul -12Jul 29Jul -31Jul
1990	22Jun-08Jul	08Jul -10 Jul 27Jul - 31Jul
Total	**113**	**84**

2.1.3 Eurasian Snow Cover Extent

The monthly values of the Eurasian Snow cover extent (SCE) are obtained from the Rutgers University from their web site http://climate.rutgers.edu/snowcover/. The data set also contains time series of monthly snow cover extent (SCE) for North America and the Northern Hemisphere from 1966 to 2005, based on snow-cover reconstruction and NOAA satellite data. The reconstruction method used *in situ* snow depth and daily climate data from the U.S., Canada, China, and the former Soviet Union (FSU) to generate a monthly snow-cover index, which was closely related to satellite-derived estimates of SCE in certain months. Details of the reconstruction are given in Brown (2000). Snow cover between 1966 and 1971 was reanalyzed at the Rutgers University Climate Lab using daily gridded composites of visible

imagery for the eastern and western hemispheres of the Northern Hemisphere. Surface resolution of the imagery is approximately 25 km. The imagery was supplemented with daily reports of snow depth at several thousand stations in the U.S., Canada, China and the former Soviet Union, gridded to 1° x 1° grid cells using all reports from within a given cell. Daily surface weather charts also provided information on cloud cover, precipitation and temperature. Infrared imagery and the above ancillary information were employed in many areas to confirm interpretations made from visible data. The weekly maps were digitized to the National Meteorological Center Limited-Area Fine Mesh grid. This is an 89 x 89 cell Cartesian grid laid over a polar stereographic projection of the Northern Hemisphere. Cell resolution ranges from 16,000 to 42,000 square kilometers (this product has also been regridded to the equal area EASE-grid in a CD rom for 1978-2001 and is distributed by the National Snow and Ice Data Center). Each grid cell in the digitized product has a binary value. Cells with at least 50% of their surface covered with snow were considered snow covered. All other cells were considered snow free. The raw NOAA gridded 89x89 data and the GSL reanalysis gridded data are both utilized in creating a unique Northern Hemisphere snow cover product. Using Perl software created at the GSL, weekly and monthly 89x89 grid cell charts are generated. In this procedure, weekly areas are calculated from digitized snow files, and monthly values are calculated by weighting the weekly areas according to the number of days of a map week falling in the given month. During this process, the raw NOAA 89x89 grid data, as well as the reanalysis gridded data, are subjected to filtering through the corrected land mask created here at the GSL. The result is an accurate grid cell product which details Northern Hemisphere snow cover data over the last 38 years.

2.1.4 Quasi-Biennial Oscillation (QBO) Zonal Wind Index

The monthly values of the QBO zonal wind index for 30hPa is obtained from the web site: http://tao.atmos.washington.edu/data_sets/ for the period January 1953 - September 2001. The index is the concatenation of values at

Canton Island (3^0S,172^0W) for Jan 1953 - Aug 1967; Gan/Maledives (1^0S, 73^0E) for Sep 1967 - Dec 1975; and Singapore (1^0N,104^0E) for Jan 1976 - Sep 2001. Naujokat (1986) documents the data, uncertainties in the early years due to the lack of daily data, the change of reference stations, and the general features of the QBO. Marquardt and Naujokat (1997) describe the update of this index.

2.1.5 Sunspot number

Daily observations of sunspot numbers started at the Zurich Observatory in 1749 and with the addition of other observatories continuous observations were obtained starting in 1849. The sunspot number is calculated by first counting the number of sunspot groups and then the number of individual sunspots. The "sunspot number" is then given by the sum of the number of individual sunspots and ten times the number of groups. Since most sunspot groups have, on average, about ten spots, this formula for counting sunspots gives reliable numbers even when the observing conditions are less than ideal and small spots are hard to see. The monthly sunspot numbers are obtained from http://science.msfc.nasa.gov/ssl/pad/solar/sunspots.htm.

2.1.6 NCEP/NCAR Reanalysis

The Global NCEP/NCAR reanalysis data set (Kalnay et al, 1996) is used in this study. Reanalysis is different from the 'traditional' data sets in two fundamental ways: (1). an atmospheric general circulation model (AGCM) is an integral component of the analysis system and (2). a wide range of observations are used. Thus, the reanalysis not only gives potentially very useful dynamical quantities that cannot be determined by subjective analysis, but may be more accurate than such traditional analyses, particularly in the data sparse regions. However, the differences in the AGCMs and the analysis methods will give rise to differences in reanalysis. Several intercomparison studies have been made to realize the magnitude and nature of this ambiguity in NCEP/NCAR reanalysis.

The NCEP/NCAR reanalysis is a joint venture between NCEP and NCAR to produce a multi-decadal record of global atmospheric analysis with unchanged data assimilation system. The assimilation system used observations from the COADS surface marine data sets, the rawinsonde network, satellite soundings (the Tiros Operational Vertical Sounder, TOVS data), aircraft data and satellite (GMS, GOES and METEOSAT) cloud drift winds. These data were subject to stringent quality control; (Kalnay et al; 1996). The NCEP/NCAR Reanalysis has three major modules (1). Data decoder and quality control (QC) preprocessor (2). Data assimilation module with an automatic monitoring system and (3). Archive module (fig. 2.3).

The preprocessor minimizes the need for reanalysis re-runs due to the many data problems that frequently appear, such as data with wrong dates, satellite data with wrong longitudes etc. The preprocessor also includes the preparation of the surface boundary conditions (SST, Sea Ice etc). For the analysis module, the Spectral Statistical Interpolation Scheme (SSI) is used, which is a three dimensional variational technique (Derber et al 1991, Parrish and Derbur 1992). An important advantage of the SSI is that the balance imposed on the analysis is valid throughout the globe, thus making unnecessary the use of nonlinear normal mode initialization. Recent enhancements such as improved error statistics and the use of full tendency of the divergence equation in the cost function (replacing the original linear balance of the increments constraint), have also been included (Derber et al 1991, Parrish and Derbur 1992). A T62/28 level global spectral model corresponding to an approximate grid point spacing of 208 km, with 28 vertical levels was used in the assimilation system. The model has 5 levels in the boundary layer and about 7 levels above 100hPa. The lowest model level is about 5hPa from the surface and the top level is at about 3hPa. The reanalysis gridded fields have been classified into four classes, depending upon the relative influences of the observational data and the model on the gridded variable (Table 2.3).

Reanalysis outputs are available in 17 standard pressure levels (hPa), 11 isentropic surfaces (K) and 28 sigma levels. The horizontal resolution is 2.5^0 longitude 2.5^0 latitude. The standard pressure levels (hPa) are 1000, 925, 850, 700, 600, 500, 400, 300, 250, 200, 150, 100, 70, 50, 30, 20 and 10.

The parameters used from NCEP/NCAR data sets are zonal (U) and Meridional (V) wind at 850hPa, 200hPa and 50hPa pressure levels, Vertically Integrated Moisture (VIM), 2-m air temperature and Sea Surface Temperature (SST). The wind data has a rating A, which means that they are strongly influenced by the observed data and the influence of the model used to derive the grid point values is minimal, whereas VIM and 2-m temperature has a rating B. SST analysis is on a nearly 1.9^0 x 1.9^0 latitude-longitude grid. The analysis is produced both daily and weekly, using 7 days of in situ data (ship and buoy) and bias-corrected satellite SST data. SST data from the UK Met office are used upto 1988 after which SST from Reynolds (CPC) are used. Since there is strong trend in SST we have calculated SST anomalies for each month removing a 11-year running mean to get a monthly data series for 1955 to 1998.

2.1.7 NOAA OLR Data

Originally the data are from the Advanced Very High Resolution Radiometer (AVHRR) aboard the NOAA Polar Orbiting Spacecraft. The data are taken from the Interpolated OLR Data provided by the NOAA-CIRES Climate Diagnostics Center, Boulder, Colorado, USA from their website (*http://www.cdc.noaa.gov*) The OLR data for a period 1974-2003 is used, with the exception of 1978. The data contains a major gap of several months during 1978 due to the failure of satellite. The data resolution are at $2.5^0 \times 2.5^0$ latitude-longitude (Gruber and Krueger, 1984). The data is in Wm^{-2}.

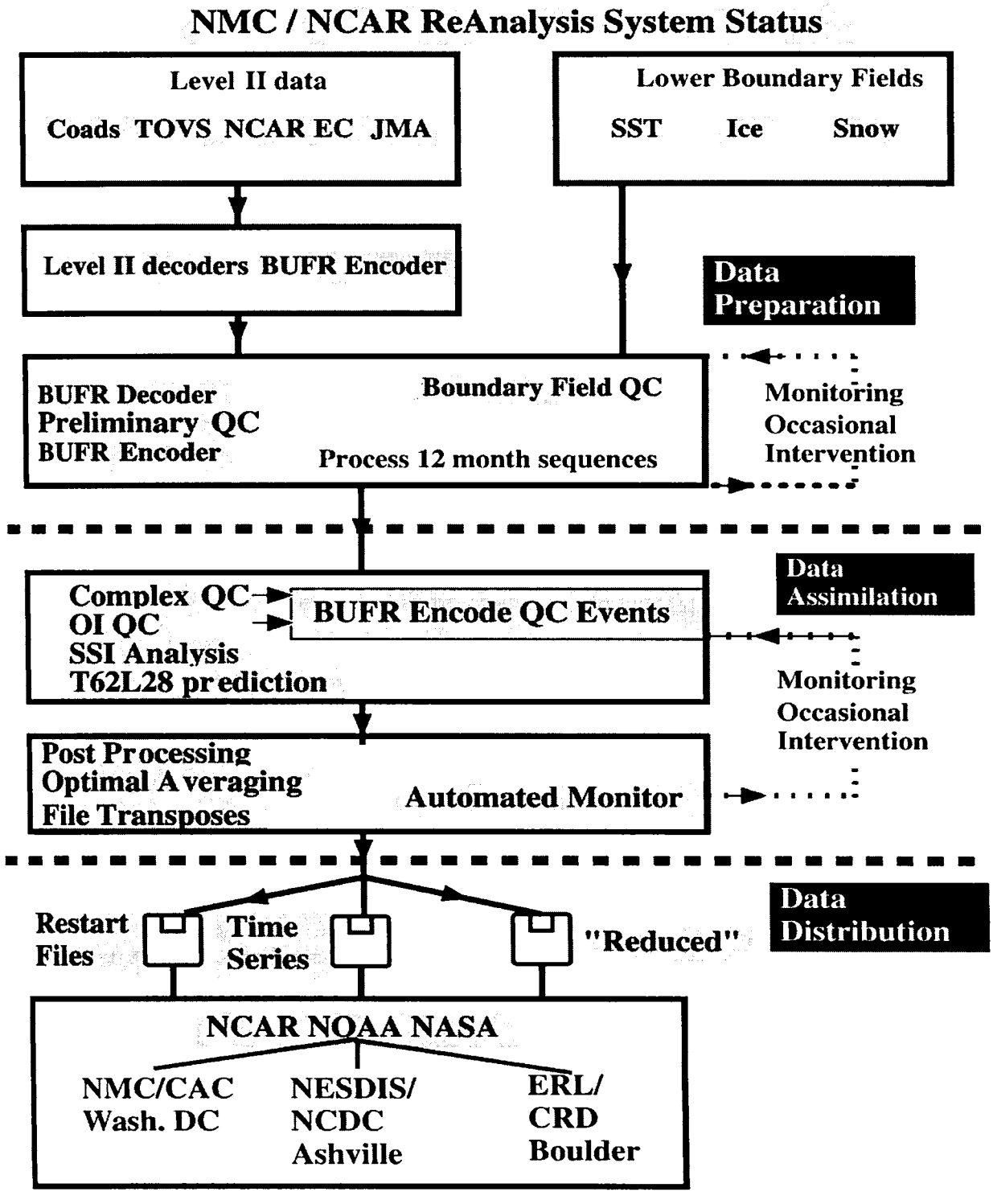

Fig.2.3: Schematic illustration of the main components of the NCEP/NCAR Reanalysis system (NMC has changed to NCEP) (Kalnay et al,1996)

Table 2.3: Classification of NCEP/NCAR reanalyzed fields.

Class	Relative influence of Observational Data and Model on Reanalysis Variable
A	Strongly influenced by observational data (most reliable) [e.g. upper air temperature and wind]
B	Model has very strong influence than observational data [e.g. humidity and surface temperature]
C	Derived solely from model fields forced by data assimilation to remain close to the atmosphere. [e.g. clouds, precipitation, and surface fluxes]
D	Obtained from climatological values and does not depend on model [e. g. plant resistance, land-sea mask]

2.1.8 Mesoscale Modeling

The Fifth-Generation NCAR/Penn State Mesoscale Model MM5 (Version 3) is used to study the orographic control on Kerala's monsoon rainfall. The MM5 is the latest in a series that developed from a mesoscale model used by Anthes at Penn State in the early '70's that was later documented by Anthes and Warner (1978). It is a three dimensional nonhydrostatic model with multiple-nest capability and a four-dimensional data assimilation capability (Dudhia, 1993).

The model is supported by several auxiliary programs, which are referred to collectively as the MM5 modeling system. A schematic diagram representing

complete modeling system is shown in figure. 2.4. Terrestrial and isobaric meteorological data are horizontally interpolated (programs TERRAIN and REGRID) from a latitude-longitude mesh to a variable high-resolution domain on either a Mercator, Lambert conformal, or polar stereographic projection. Since the interpolation does not provide mesoscale detail, the interpolated data may be enhanced (program RAWINS or little r) with observations from the standard network of surface and rawinsonde stations using either a successive-scan Cressman technique or multiquadric scheme. Program INTERPF performs the vertical interpolation from pressure levels to the sigma coordinate system of MM5. Sigma surfaces near the ground closely follow the terrain, and the higher-level sigma surfaces tend to approximate isobaric surfaces. Since the vertical and horizontal resolution and domain size are variable, the modeling package programs employ parameterized dimensions requiring a variable amount of core memory. Some peripheral storage devices are also used (PSU/NCAR MM5 User's guide, 2002).

The modeling system usually gets and analyzes its data on pressure surfaces, but these have to be interpolated to the model's vertical coordinate before being input to the model. The vertical coordinate of the MM5 model is terrain following (fig.2.5) meaning that the lower grid levels follow the terrain while the upper surface is flat. Intermediate levels progressively flatten as the pressure decreases toward the chosen top pressure.

A dimensionless quantity σ is used to define the model levels where

$$\sigma = \frac{p - pt}{ps - pt} \tag{2.1}$$

p is the pressure, p_t is a specified constant top pressure, p_s is the surface pressure.

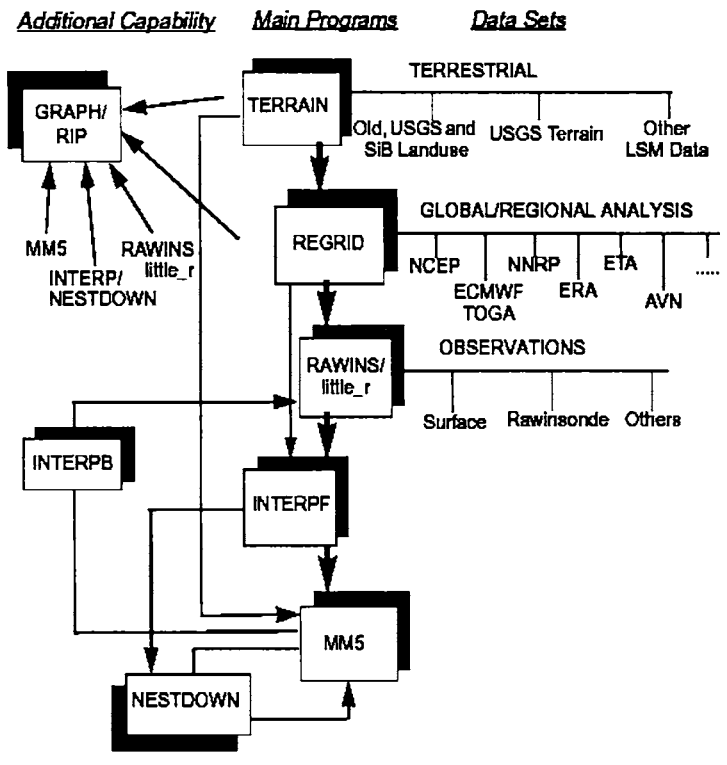

Figure 2.4: The MM5 modeling system flow chart

It can be seen from the equation and figure 2.5 that σ is zero at the top and one at the surface, and each model level is defined by a value of σ. The model vertical resolution is defined by a list of values between zero and one that do not necessarily have to be evenly spaced. Commonly the resolution in the boundary layer is much finer than above, and the number of levels may vary from ten to forty, although there is no limit in principle.

The horizontal grid has an Arakawa-Lamb B-staggering of the velocity variables with respect to the scalars. This is shown in figure 2.6 where it can be seen that the scalars (T, q etc.) are defined at the center of the grid square, while the eastward (u) and northward (v) velocity components are collocated at the corners. The center points of the grid squares will be referred to as cross points,

and the corner points are dot points. Hence horizontal velocity is defined at dot points, for example, and when data is input to the model the preprocessors do the necessary interpolations to assure consistency with the grid.

MM5 contains a capability of multiple nesting with up to nine domains running at the same time and completely interacting. The nesting ratio is always 3:1 for two-way interaction. "Two-way interaction" means that the nest's input from the coarse mesh comes via its boundaries, while the feedback to the coarser mesh occurs over the nest interior.

To run any regional numerical weather prediction model requires lateral boundary conditions. In MM5 all four boundaries have specified horizontal winds, temperature, pressure and moisture fields, and can have specified microphysical field (such as cloud) if these are available. Therefore, prior to running a simulation, boundary values have to be set in addition to initial values for these fields. The boundary values come from analysis at the future times, or a previous coarser-mesh simulation (1-way nest), or from another model's forecast (in real-time forecasts). For real-time forecasts the lateral boundaries will ultimately depend on a global-model forecast. In studies of past cases the analysis providing the boundary conditions may be enhanced by observation analysis (RAWINS or little r) in the same way as initial conditions are. Where upper-air analysis are used the boundary values may only be available 12-hourly, while for model-generated boundary conditions it may be a higher frequency like 6-hourly or even 1-hourly.

The model uses this discrete- time analysis by linearly interpolating them in time to the model time. The analysis completely specifies the behavior of the outer row and column of the model grid. In the next four rows and columns in from the boundary, the model is nudged towards the analysis, and there is also a smoothing term. The strength of this nudging decreases linearly away from the boundaries. To apply this condition, the model uses a boundary file with information for the five points nearest each of the four boundaries at each

boundary time. This is a rim of points from the future analysis described above. The interior values from these analyses are not required unless data assimilation by grid-nudging is being performed, so disk-space is saved by having the boundary file just contain the rim values for each filed. Two-way nest boundaries are similar but are updated every coarse-mesh time step and have no relaxation zone. The specified zone is two grid-points wide instead of one.

MM5 modeling system requires the following data sets to run

- Topography and land use.
- Gridded atmospheric data that have at least the variables; sea-level pressure, wind, temperature, relative humidity and geopotential height at the pressure levels: surface, 1000, 850, 700, 500, 400, 300, 250, 200, 150, 100 mb.
- Observation data that contains soundings and surface reports

Three resolutions of elevation data; 30 minute, 10 minute, and 5 minute are used for this present study. All these data are created from the 30 seconds United States Geological Surveys (USGS) data. Vegetation/land-use data are also in the same resolution of elevation data and from USGS version 2 land-cover data. Data from NCEP/NCAR Reanalysis Projects (NNRP) are used for the atmospheric variables. The NNRP data are at resolution 2.5^0 x 2.5^0 latitude-longitude.

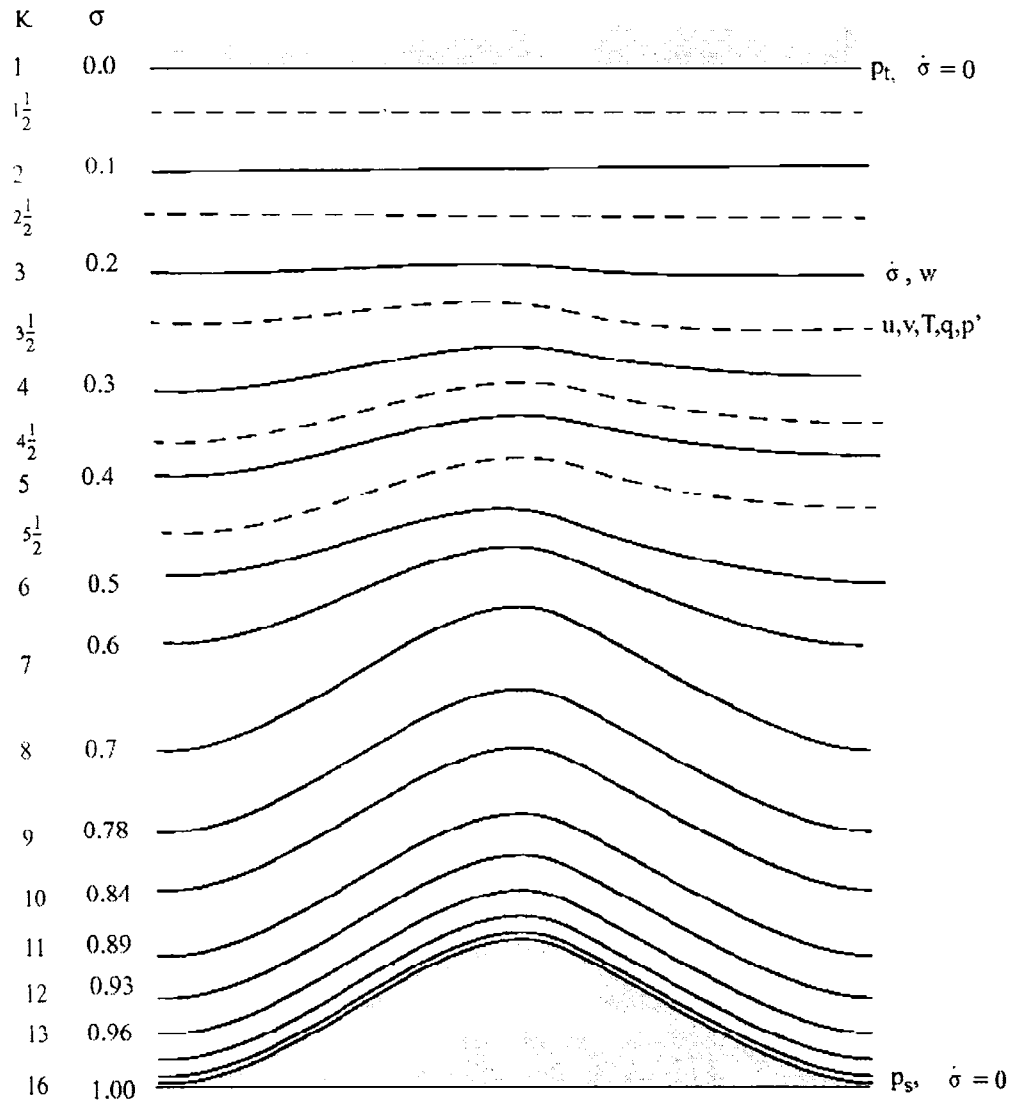

Figu
verti

Figure 2.5: Schematic representation of the vertical structure of the model.

Dashed lines denotes half-sigma levels, solid lines denote full-sigma levels

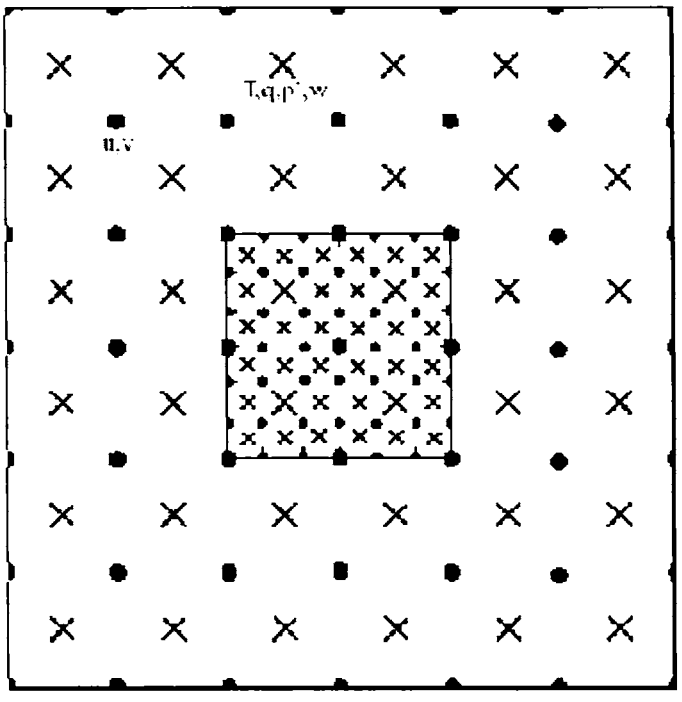

Figure 2.6: Schematic representation showing the horizontal Arakawa B-grid staggering of the dot and cross grid points. The smaller inner box is a representative mesh staggering for a 3:1 coarse-grid distance to fine-grid distance ratio

2.2 Methodology

2.2.1 Wavelet Analysis

Wavelet analysis tool is well suited to study multiscale, non-stationary processes occurring over finite spatial and temporal domain. Since its introduction by Morlet (1983), this technique has found wide application in diverse fields. Wavelet analysis gives the localised variations of power within a time scale by decomposing a time series in time- frequency space and one is able to determine both the dominant modes of variability and how those modes vary in time. Morlet wavelet is defined as the product of a complex exponent wave and a Gaussian envelope:

$$\varphi_0(\eta) = \pi^{-1/4} e^{iwo\eta} e^{-\eta 2/3} \qquad 2.2$$

where φ_0 is the wavelet value at non-dimensional time η, and w_0 is the wavenumber. The "scaled wavelet" is .

$$\varphi\left[\frac{(n'-n)\partial t}{s}\right]=\left(\frac{\partial t}{s}\right)^{1/2}\varphi_o\left[\frac{(n;-n)\partial t}{s}\right] \qquad 2.3$$

where s is the "dilation" parameter used to change the scale, and n is the translation parameter used to slide in time. The factor of $s^{-1/2}$ is a normalization to keep the total energy of the scaled wavelet constant. Details regarding the analysis procedure are given in Torrence and Compo (1998).

For the Morlet wavelet transform, where the mother wavelet is given by equation 2.2 we first choose the wavenumber w_0, which gives the number of oscillations within the wavelet itself. One condition of the wavelet transform is that the average of the wavelet itself must be zero. In practice, if we choose w_0=6, then the errors due to non-zero mean are smaller than the typical computer round-off errors (Farge 1992).

In order to adequately sample all the frequencies present in our time series, we have chosen the smallest resolvable scale, s_0, which is a multiple of our time resolution, as 2 days. The larger scales (longer periods) are chosen as power-of-two multiples of this smallest scale,

$$s_j = s_0 2^{j\partial j},\ j = 1, 1, \ldots\ldots, j$$

$$j = \partial j^{-1} \log_2 (N\partial t/s_0)$$

The choice of octave which is logarithmic with the base of 2 as a unit to divide the frequency domain allows us to include a broad range of scales, from very small to very large in an efficient way in a coordinate system with linear interval in octave while logarithmic in frequency scale. In a continuous WT

where more scale decomposition is desired, each octave may be further divided into infinite voices. For this study we have divided each octave into 4 voices.

To determine significance we choose an appropriate background spectrum as follows :

$$P_k = \frac{1-\alpha^2}{1+\alpha^2-2\alpha\cos(2\pi k/N)} \qquad 2.3$$

where k = 0 .... N/2 is the frequency index and α is the lag-1 autocorrelation. .

The null hypothesis is defined for the wavelet power spectrum as follows: It is assumed that the time series has a mean power spectrum, given by 2.3; if a peak in the wavelet power spectrum is significantly above this background spectrum, then it can be assumed to be a true feature with a certain percent confidence 90%, 95% or 99%.

2.2.2 Harmonic Analysis

Harmonic analysis consists of representing the fluctuations or variations in a time series as having arisen from the adding together a series of sine and cosine functions. These trigonometric functions are "harmonic" in the sense that they are chosen to have frequencies exhibiting integer multiples of the "fundamental" frequency determined by the sample size of the data series. A common physical analogy is the musical sound produced by a vibrating string, where the pitch is determined by the fundamental frequency, but the aesthetic quality of the sound depends also on the relative contributions of the higher harmonics.

A time series having a sinusoidal character and executing a single cycle over the course of *n* observations can be represented as :

$$y_t = y + C_1 \cos\left(\frac{2\pi t}{n}\right) \qquad 2.4$$

The equation can be written in terms of the phase angle or phase shift ϕ_1, as

$$y_t = y + C_1 \cos\left(\frac{2\pi t}{n} - \phi_1\right) \qquad 2.5$$

The trigonometric identity

$$\cos(\alpha - \phi_1) = \cos(\phi_1)\cos(\alpha) + \sin(\phi_1)\sin(\alpha) \qquad 2.6$$

used to compute C_1 and ϕ_1.

Substituting $\alpha = 2\pi t/n$ and multiplying both sides by the amplitude C_1, we obtain

$$C_1 \cos\left(\frac{2\pi t}{n} - \varphi_1\right) = C_1 \cos(\varphi_1)\cos\left(\frac{2\pi t}{n}\right) + C_1 \sin(\varphi_1)\sin\left(\frac{2\pi t}{n}\right) \qquad 2.7$$

$$= A_1 \cos\left(\frac{2\pi t}{n}\right) + B_1 \sin\left(\frac{2\pi t}{n}\right) \qquad 2.8$$

where $A_1 = C_1 \cos(\phi_1)$ 2.9

and $B_1 = C_1 \sin(\phi 1)$ 2.10

The sine and cosine trigonometric functions are periodic, effectively the same phase angle is produced by adding or subtracting a half-circle of angular measure if $A_1<0$. The alternative that produces $0<\phi_1<2\pi$ is usually selected. Equation (2.7) says that it is possible to mathematically represent a harmonic wave either as a cosine function with amplitude C_1 and phase ϕ_1 or as the sum of an unshifted cosine and unshifted sine wave with amplitudes A_1 and B_1. The amplitude C_1 is then

$$C_1 = [A^2 + B^2]^{1/2} \qquad 2.11$$

and phase ϕ_1,

$$\phi_1 = \left\{ \begin{array}{l} \tan^{-1}\dfrac{B_1}{A_1}, A_1 > 0 \\ \tan^{-1}\dfrac{B_1}{A_1} \pm \pi, or \pm 180^0, A_1 < 0 \\ \dfrac{\pi}{2}, or 90^0, A_1 = 0 \end{array} \right\} \qquad 2.12$$

Usually A_1 and B_1 are computed from the following equations

$$A_1 = \frac{2}{n}\sum_{t=1}^{n} y_t \cos\left(\frac{2\pi t}{n}\right) \qquad 2.13$$

$$B_1 = \frac{2}{n}\sum_{t=1}^{n} y_t \sin\left(\frac{2\pi t}{n}\right) \qquad 2.14$$

Chapter -3
Intra Seasonal Oscillation (ISO) of Rainfall

3.1 Introduction

Kerala being in the low latitude belt (8^0N-13^0N), equatorial eastward propagating low frequency modes like Madden Julian Oscillation can affect its rainfall throughout the year and the east-west oriented maximum cloud zones (Sikka and Gadgil, 1980) that form at 30-50 day intervals to its south and move north across it during the May to October period modulate its rainfall. It is well known that Indian summer monsoon exhibits prominent low frequency intra-seasonal oscillations of period 30-50 days (Krishnamurti, 1985) and that this oscillation is associated with variability in large scale circulation and convection features in the tropical atmosphere. The equatorial 30 to 50 day oscillation was first detected by Madden and Julian (1971,1972) in zonal wind and convection. Eastward propagating large scale features on 30 to 50 day time scale have been studied by Lorenc (1984) in velocity potential and by Weickmann (1983), Weickmann et. al (1985), Lau and Chan (1985,1986) and Murakami et al (1986) in Outgoing Longwave Radiation (OLR).

Although the Active-Break cycle of the monsoon with a periodicity in this range was known for almost a hundred years, details of the 30-50 day monsoon oscillation were captured only after weather satellite data became available for routine use. Yasunari (1979,1980,1981) and Sikka and Gadgil (1980) reported convective cloud bands moving northward across India and Southeast Asia on this time scale. Krishnamurthi and Subramanyam (1982) studied the 30 to 50 day mode in wind field anomalies at 850 hPa of the 1979 summer monsoon using MONEX data. Their study illustrated zonal troughs and ridges with 3 to 6 m/s wind anomalies propagating steadily (at ~ 0.75 deg. lat./day) from the equator to the Himalayas. The zonal extent of this anomalous area is about 60 degrees in longitude. This low frequency mode has been viewed as a see-saw in convective cloudiness between the equatorial Indian Ocean and the monsoon trough region or as a northward movement of an east-

west oriented band of convective clouds from low latitudes of Indian ocean to the Himalayas. Analysis of a 70 year (1901-70) record of daily rainfall of 3700 stations of India by Hartmann and Michelson (1989) revealed a strong spectral peak at 40-50 day time scale over India south of 23^0N. Lau and Chan (1986) showed that for the period May to October, variance of the OLR was strong in the tropical Indian and west Pacific oceans in the period range 40 to 50 days and that there was a see-saw between Indian and west Pacific oceans in OLR (convection). Wang and Rui (1990) and Rui and Wang (1990) studied cases of large scale (spatial) negative anomalies in OLR (areas of active convection) moving eastwards across the Indian and Pacific oceans in the equatorial belt. The convection anomalies develop over equatorial Africa, intensify over the Indian ocean, weaken over the maritime continent and intensify again over western Pacific and then move east. They weaken again around the date line. Northward motion was observed over the Indian and west Pacific oceans during the period May to October.

From the beginning it was clear that this oscillation hereafter called Intra Seasonal Oscillation (ISO) had a highly variable period. Madden and Julian (1994) in their review of the work done on the ISO discovered by them two decades earlier, concluded that the periods of ISO varied from year to year and ranged from 22 to 79 days and that ISO was prominent in nearly 75 % of the years. Their conclusions were however, based on studies using short periods of data.

A question of importance is whether the period of ISO during the boreal summer monsoon season has any dependence on occurrence of El Nino/La Nina, strength of Indian summer monsoon etc. Yasunari (1980) observed that the period of ISO increased to nearly 60 days during the summer of 1972 a severe drought year for India (and also a strong El Nino year). On the other hand Madden and Julian (1994) showed evidence from literature for a shift to lower periods during El Nino Southern Oscillation events. More recently Lawrence

and Webster (2001) found that the ISO activity had a strong inverse relationship with the strength of the Indian monsoon. For the 22 year period studied by them, the relationship between the Indian summer monsoon strength and the ISO activity is comparable to or even stronger than the well known relationship between ENSO and the monsoon rainfall.

We have studied the monsoon ISO in the period range 20-100 days in the daily averaged southwest monsoon rainfall of south and north Kerala for ninety-five years 1901 to 1995. This is the longest record studied so far. Singh et al (1992) had examined one degree squared average daily monsoon rainfall of India of 80 years 1901-1980 for interannual variability of the monsoon ISO. They found that these oscillations are strongest over west central India where they explain 10% (20%) of the variance of the daily (5-day) rainfall. These oscillations showed considerable interannual variability in intensity ranging from about half to double the average value. They are not well organised in every year, and about 40% of the years exhibit organised oscillations. This variability of the monsoon ISO did not show any linear relationship with the total seasonal Indian monsoonal rainfall or the phases of the El Nino-Southern Oscillation phenomenon.

Data used in this study are described in chapter-2: data. For studying the ISO in the rainfall of south and north Kerala and also of India we have used the wavelet analysis method. Since it is a relatively new technique we have given details of the method used in chapter-2. ISO of the monsoon rainfall in the period range 20 to 100 days of the 95 years 1901 to 1995 has been studied. The resolved periods correspond to 23, 27, 32, 38, 45, 54, 64, 76, and 91 days. We got two groups of periods at the level of significance of 99%, one named LONG with a period of 64 days and the other named SHORT, which comprises of periods 23,27 and 32 days. We have examined in this chapter the relation between the ISO period and some large-scale features of the atmosphere and

ocean. Case studies of three years with ISO of periods 64, 32 and 23 days in south Kerala rainfall are discussed.

3.2 ISO of South Kerala Monsoon Rainfall

For south Kerala the prominent periodicities in the monsoon season's daily rainfall were picked up from wavelet analysis for significance levels 90%, 95% and 99%. Each year of the period 1901 to 1995 had at least one period which could thus be picked up, except for the 11 years having no significant period – 1920,1929,1937,1945,1959,1968,1969,1980,1984,1985 and 1990. The periods of the ISO for each significance level (90%, 95% and 99%) are given in Table 3.1. There are many years having more than one period. The frequency distribution of the periods significant at 90%, 95% and 99% are given in Table 3.2.

There are two main clusters for the periods. One cluster has periods of 23 days, 27 days and 32 days and the other cluster is of a single period of 64 days. On either side of 64 days the periods 54 and 76days (not shown in the table) have zero and 2 cases respectively. Out of the 25 cases of 64 day period 20 are significant at 99% level. The cluster of periods 23, 27 and 32 days is called SHORT and the other cluster with a single period of 64 days is called LONG in this study. We have studied the properties of these two clusters LONG and SHORT. In Table 3.2 we see that for significance level of 99%, SHORT and LONG period ISO are found in 44 and 20 years respectively out of the 95 years 1901 to 1995.

Table 3.1: Significant period in days of south Kerala monsoon rainfall during 1901-1995, El Nino, La Nina, WET and DRY monsoon years are indicated against the years by El, LA, Dr and We.

YEAR	PERIOD			YEAR	PERIOD			YEAR	PERIOD		
1901		Dr	27** 32*	1933		We	64**23*	1965	El	Dr	64**
1902	El		64**	1934			64**	1966		Dr	27**23*
1903	La		23** 27*32 38 45	1935			64**23*	1967			23** 27
1904		Dr	27	1936			38* 32*	1968		Dr	
1905	El	Dr	27	1937	La			1969			
1906	La		32*	1938	El		23** 27**	1970	La	We	27** 32**
1907	El		23** 64**	1939			27** 32**32	1971			32**27*
1908	La		38* 45	1940	El		23	1972	El	Dr	32* 27*64
1909			45** 38*	1941	La	Dr	32* 27*	1973	La		64**
1910			27** 32*	1942	El	We		1974		Dr	23**
1911	El	Dr	38 45	1943			38** 45**	1975	La	We	27** 32*
1912			32	1944			23** 27**	1976	El		32**27*
1913			45*	1945				1977			45**38*
1914	El		27* 23*	1946			64**	1978			32
1915			32** 27*	1947		We	32**	1979		Dr	23*64
1916	La	We	45** 38*	1948	La		64**	1980			
1917		We	23**27** 32*	1949			23**45*	1981			32**27*
1918	El	Dr	64**	1950	El		45**38*	1982	El	Dr	64** 23
1919			64**	1951		Dr		1983		We	32**
1920	La	Dr		1952			64**	1984			
1921			64* 45	1953	El		23** 27**	1985		Dr	
1922			64*	1954	La		23** 27**	1986		Dr	45* 38 23
1923	El		64* 38* 45	1955			32*	1987	El	Dr	64**
1924	La		45 23 38	1956		We	64**23*	1988	La	We	23**
1925	El		23** 27*	1957	El		27**	1989			32** 27
1926			45* 38	1958			64** 27	1990			
1927	La		23** 27*	1959		We		1991	El		64**
1928			27** 23*	1960			23** 27	1992			23** 27**
1929	El			1961		We	23**27*	1993			27*
1930	La		38** 45**	1962			64** 32	1994		We	45**38*
1931	El		64**	1963			23** 27**	1995	La		23** 27**
1932			64**	1964	La		32**				

*Significance levels (by chi-square test) at 99%,95% and 90% are denoted by suffices **,* and no suffix respectively.*

Table 3.2: **Frequency distribution of period in days of south Kerala Monsoon Rainfall in the range 20-100 days at different significance levels 99%,95% and 90% during the period 1901-1995**

	Number of years at significance levels			
Period	99%	95%	90%	Total
64	20	3	2	25
54	0	0	0	0
45	7	4	6	17
38	2	8	5	15
32	10	9	7	26
27	16	12	6	34
23	18	7	4	29

3.3 ISO Period and large scale features of atmosphere/ocean

We examined the years of SHORT and LONG periods of the low frequency oscillation in south Kerala rainfall in relation to moderate /strong El Nino years and also La Nina years as obtained from Quinn and Neal (1987), Rasmusson and Carpenter (1983), Kiladis and Diaz (1989) and Trenberth (1997). The El Nino and La Nina cases are marked against the years in Table 3.1 as El and La respectively. It is seen that out of 22 El Nino years during 1901 to 1995, 8 years have LONG period (at 99% level of significance) and 6 years SHORT period at the same level of significance. Out of the 18 La Nina years during the same period 2 years have LONG and 10 years SHORT period ISO at 99% level of significance. Thus La Nina has a strong preference for SHORT period ISO. LONG periods are only slightly more probable than SHORT in El Nino years.

Out of the 19 DRY monsoon years during 1901-1995 four years each have LONG and SHORT ISO. (DRY and WET years in all India monsoon rainfall have been described in chapter-2: Data) Out of 13 WET monsoon years in the same 95 years, two years have LONG ISO and seven years have SHORT ISO (only ISO periods at the 99% level of significance have been considered.)

DRY and WET years are marked in Table 3.1 as Dr and We respectively. Thus as in the case of La Nina, WET years have a preference for SHORT ISO. It is well known that La Nina years are associated with WET Indian monsoon.

We have composited SST anomalies of the summer monsoon season June to September for two groups of years during 1965-1993. SST data used are described in Chapter-2:Data. Since there is a strong trend in SST we have calculated SST anomalies for each month removing a 11 year running mean to get a monthly data series for 1965-1993. The first group is of 5 years with LONG ISO period of 64 days for south Kerala rainfall at significance level of 99% and the second group is of 12 years with SHORT ISO of periods 23, 27 and 32 days at the same level of significance. These years and the corresponding ISO periods of south Kerala rainfall are given in Table 3.3.

Table 3.3: SHORT (23-32 days) and LONG (64 days) period ISO at significance 99% during 1965 to 1993 of south Kerala monsoon rainfall. Other ISO periods present are also marked

LONG Years	ISO Periods		SHORT Years	ISO Periods	
1965	64**		1966	27**	23*
1973	64**		1967	23**	27
1982	64**	23	1970	27**	32**
1987	64**		1971	32**	27*
1991	64**		1974	23**	
			1975	27**	32**
			1976	32**	27*
			1981	32**	27*
			1983	32**	
			1988	23**	
			1989	32**	27
			1992	23**	27**

Figures 3.1(a) and 3.1(b) give the SST anomaly composites for the LONG and SHORT period composites respectively. It is seen that for the LONG period composite there is a large area of positive SST anomaly in the equatorial central and east Pacific ocean. Weaker positive & negative anomalies are seen over the Indian ocean and western Pacific ocean respectively. The SST

anomaly signals over the Indian and Pacific oceans are similar to the composite El Nino anomaly of Ramusson and Carpenter (1982) and Tourre and White (1995, 1997). The SST anomaly composite for the SHORT periods is similar to a typical La Nina case. Thus we conclude that the low frequency mode in south Kerala rainfall are related to the large scale SST anomalies in the tropical areas of Indian and Pacific oceans in respect of the period of ISO. It is necessary to study the mechanisms that control the periods of the ISO.

3.4 Case Studies of SHORT and LONG period ISO

Study of 95 years of south-west monsoon rainfall of south Kerala has shown that its daily rainfall of the period June to September has strong and significant ISO in most of the years. Although the period of oscillation remains nearly the same throughout a season, there is pronounced interannual variability in the periods. The analysis has brought out a prominent period of 64 days, which appears in a very large number of years, either as the only period or in combination with other periods. Three case studies are presented here one for a year with LONG ISO period of 64 days (year 1987) and the other two for a case each of SHORT ISO periods of 32 days (year 1989) and 23 days (year 1961) respectively.

3.4.1 Monsoon of 1987 - a case of LONG ISO of period 64 days.

The daily rainfall average for south Kerala for each day from 01 June to 30 September 1987 is given in fig 3.2(a) along with their 7-day moving averages. From the figure it is seen that monsoon rainfall has occurred in two spells separated by about two months. There are long periods of very low rainfall. Wavelet analysis of daily rainfall show a 64 day period significant at 99% level (fig. 3.2b). Other years like 1982, 1965, 1958, 1918 etc showing significant 64 day ISO signal at the 99% level also show long dry spells in the daily rainfall of south Kerala (figures not given). Since, 64-day period is half the data length another test was performed to see whether the 64-day period is real

or not. The lag-correlation of daily KSMR for lags 1 to 80days is computed . It is seen that there is a maximum correlation of 0.36 at a lag of 65 days, which is significant according to t-test at 99% level.

Fig.3.3a gives the trend removed NCEP SST anomaly of monsoon season of 1987. Equatorial central and east Pacific ocean had large areas covered by warm SST anomalies of 1^0C-2^0C. 1987 was an El Nino year. It was a DRY year in all India monsoon rainfall also. As against the long term average ISMR of 852.4 mm, 1987 monsoon gave only 697.3 mm. (Parthasarathy et al, 1994). During this monsoon season Kerala also had drought. South Kerala received only 117.8cm rainfall during the southwest monsoon season which is less by 33% of the long-term mean of 176.2cm.

3.4.2 Monsoon of 1989 – a case of SHORT ISO of period 32 days

Fig 3.4a gives the daily rainfall of south Kerala and its seven day moving average for the year 1989. Wavelet analysis of south Kerala rainfall is shown in fig 3.4b. The ISO period here is 32 days significant at 99% level. Dry spells in south Kerala had short duration in 1989 unlike in 1987. Fig.3.3(b) gives the NCEP SST anomaly of monsoon season of 1989. Equatorial central Pacific ocean and Indian ocean had large areas covered by cold SST anomalies. The rainfall in south Kerala for 1989 is 143.3cm which is less than 19% of the long-term mean of 176.2cm.

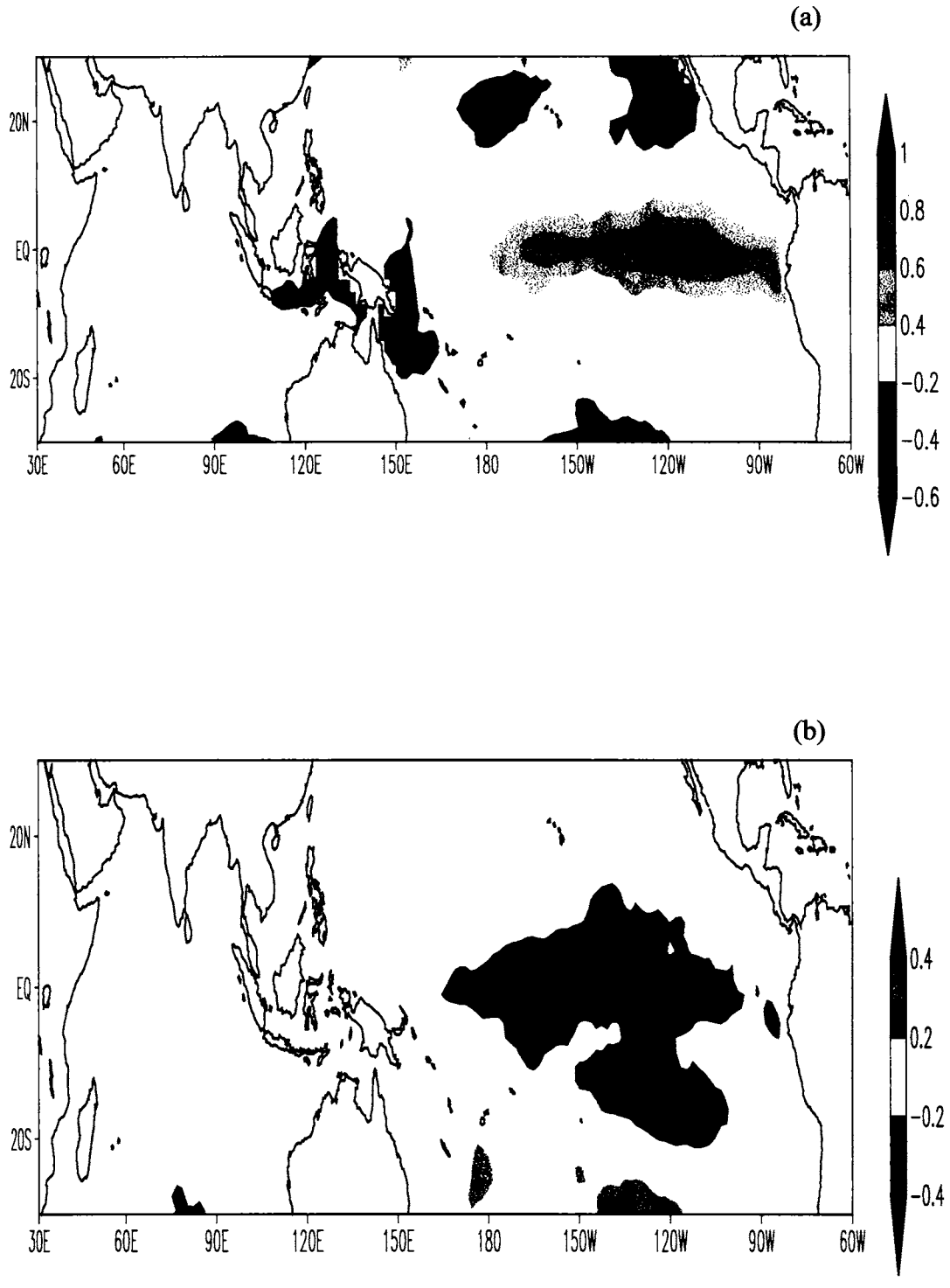

Fig. 3.1 NCEP SST anomaly composites of years during 1965-1993 with ISO periods significant at 99%. (a) Five years with LONG period (b) Twelve years with SHORT period as given in Table 3.3. Isolines are drawn at intervals of 0.2^{0}C

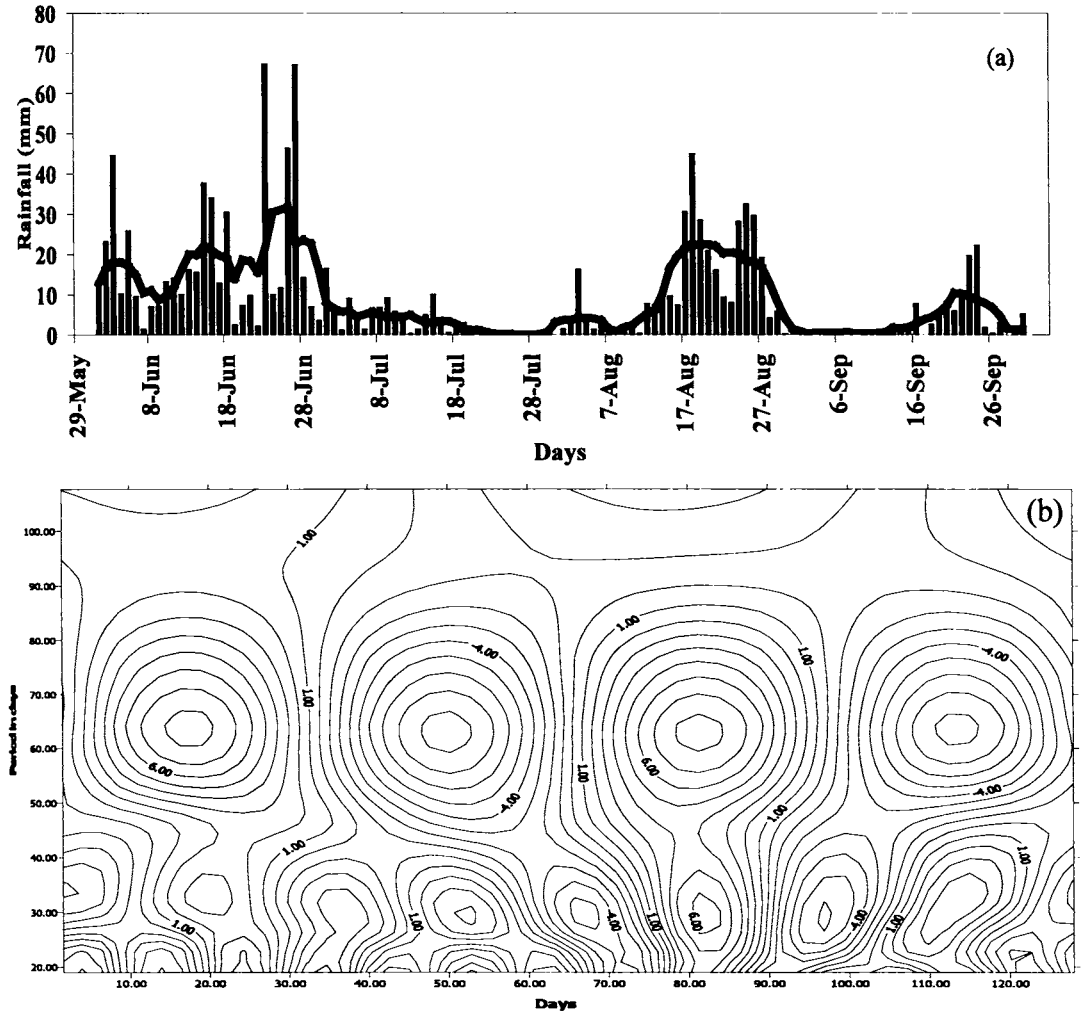

Fig. 3.2: (a) Daily average rainfall of south Kerala for 1987 along with the 7-day moving average; (b) Wavelet analysis of south Kerala rainfall for 1987.

3.4.3 Monsoon of 1961- a case of SHORT ISO of period 23 days

Fig.3.5(a) a gives the daily rainfall of south Kerala and its seven day moving average for the year 1961. Wavelet analysis of south Kerala rainfall is shown in fig.3.5(b). The ISO period here is 23 days significant at the 99% level. Dry spells in south Kerala had extremely short duration. Fig.3.3(c) gives the SST

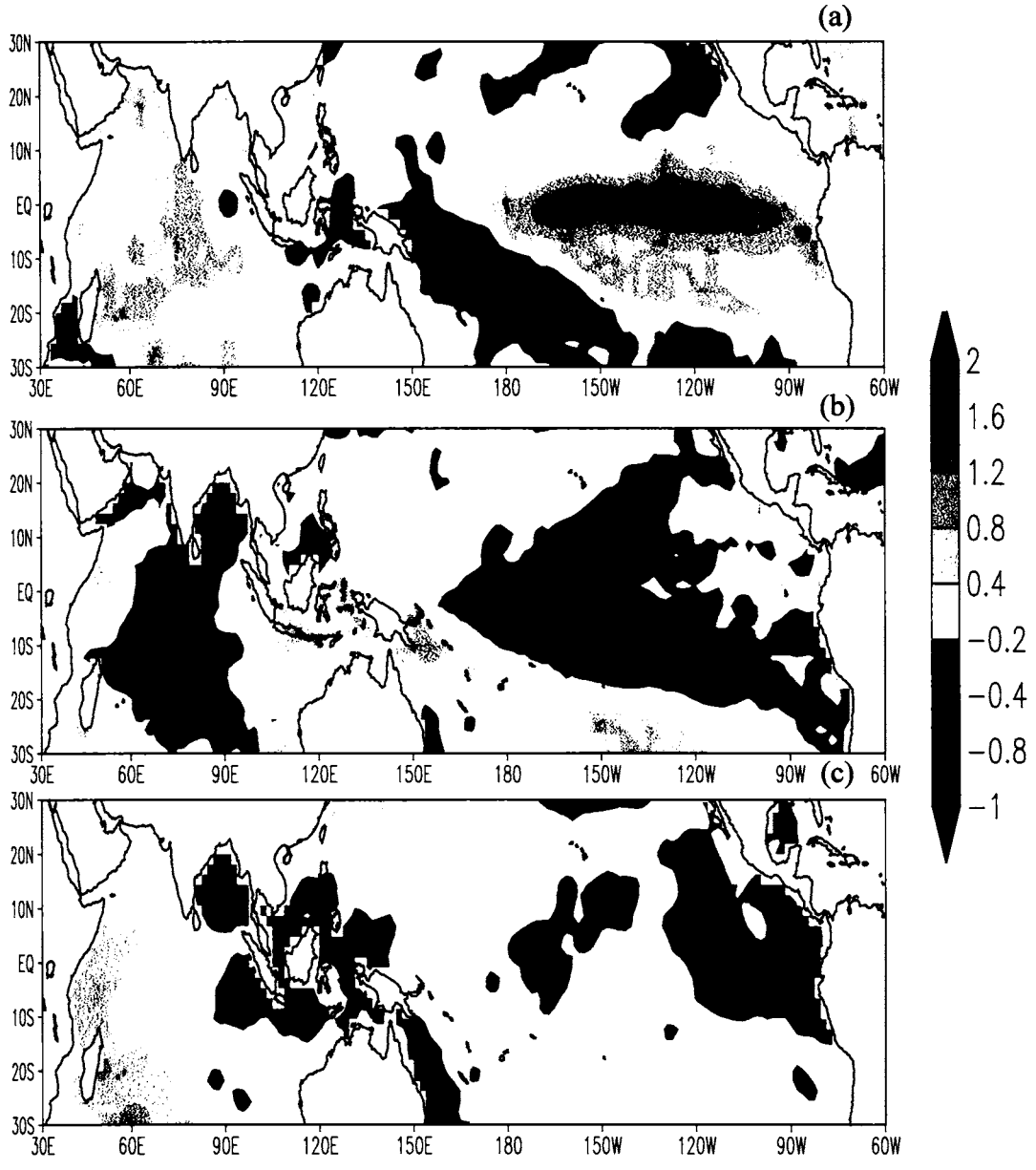

Fig.3.3: NCEP SST anomaly of the monsoon season June to September for (a) 1987 (b) 1989 (c) 1961. Isoline intervals are 0.2^{0}C.

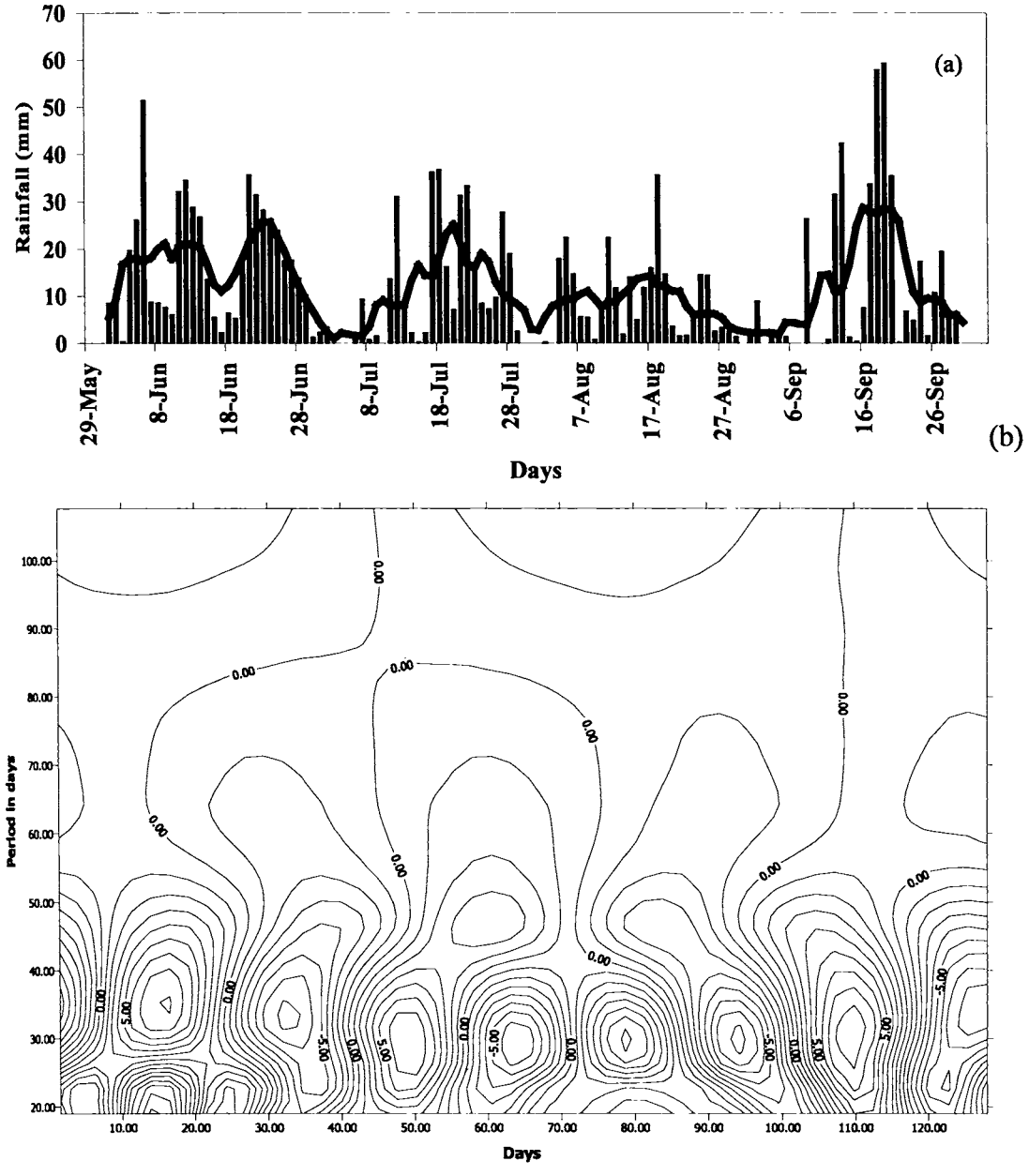

Fig. 3.4: (a) Daily average rainfall of south Kerala for 1989 along with the 7-day moving average; (b) Wavelet analysis of south Kerala rainfall for 1989.

anomaly of monsoon season of 1961. Equatorial central and east Pacific ocean had large areas covered by cold SST anomalies. South Kerala received 243.1cm in 1961 which is 38% more than the long-term mean.

3.5 ISO in North Kerala and All India Daily Monsoon Rainfall

Wavelet analysis was done for the daily north Kerala monsoon rainfall series 01 June to 30 September of each year from 1901 to 1995 as done for south Kerala. A similar analysis was done for the daily rainfall averaged over the whole of India (the Daily Indian summer monsoon rainfall series) for the period 01 June to 30 September of 1901 to 1995 as derived by IITM and described in chapter-2 : Data. For comparison the significant ISO periods obtained from wavelet analysis for south and north Kerala and for the whole of India are given in table 3.4. North Kerala has only 10 years in the period 1901-1995 with LONG period of 64 days significant at 99% level compared to the 20 years for south Kerala. For India as a whole there are 11 years with 64-day period significant at 99% level. For the SHORT periods (23, 27 and 32 days) significant at 99% level south Kerala, north Kerala and the whole of India has 44 years, 40 years and 37 years respectively. Only in the 4 years 1902, 1918, 1958 and 1987 all the three areas south and north Kerala and the whole of India have LONG (64 day) ISO significant at the 99% level during the 95 year period. The SHORT (23, 27 and 32 day) ISO at significance 99% occur together at these three areas only in the 7 years 1901, 1915, 1917, 1925, 1928, 1938 and 1970.

The daily rainfalls of south Kerala, north Kerala and the whole of India during the monsoon of 1987 are given in fig.3.6(a-c). From Table-3.4 it is seen that all the three rainfall series have ISO period of 64 days significant at 99% level and these years show long dry spells during July-August. Fig.3.7 (a) and (b) show Hovmuller diagrams of OLR and zonal wind of 850 hPa averaged over

Table 3.4: Significant period in days of south Kerala, north Kerala and All India monsoon rainfall during 1901-1995, El Nino, La Nina, WET and DRY monsoon years are indicated against the years by El, LA, Dr and We.

YEAR			PERIOD (SOUTH KERALA)	PERIOD (NORTH KERALA)	PERIOD (ALL INDIA)
1901		Dr	27** 32*	27**32*	27**
1902	El		64**	64**	64**
1903	La		23** 27*32 38 45	32	
1904		Dr	27		23** 45*38
1905	El	Dr	27	32	64**
1906	La		32*	32* 23	23**
1907	El		23** 64**		27
1908	La		38* 45		
1909			45** 38*	23**	23**
1910			27** 32*	38* 32 45	45** 38**
1911	El	Dr	38 45	32** 38	27** 32**
1912			32	32**	
1913			45*	45* 64	23**
1914	El		27* 23*		
1915			32** 27*	32** 38	32** 38
1916	La	We	45** 38*	45**38* 27	32* 27*
1917		We	23**27** 32*	32** 27*	23**
1918	El	Dr	64**	64**	64**
1919			64**	32** 27** 64	27** 23**
1920	La	Dr			
1921			64* 45	64** 23 27	45** 38**
1922			64*	64** 23	64**
1923	El		64* 38* 45		
1924	La		45 23 38	45* 38	27** 38
1925	El		23** 27*	23** 27	23**
1926			45* 38	23** 27**	
1927	La		23** 27*	64**	23**
1928			27** 23*	27** 23*	27** 23
1929	El			27	
1930	La		38** 45**	45**38*	45**38*27*
1931	El		64**	23** 64*	
1932			64**	27** 91**	32 64
1933		We	64**23*	32**	45* 23*
1934			64**	64** 32	45** 27* 23
1935			64**23*	23**	23* 64*
1936			38* 32*	32*	
1937	La				64 23
1938	El		23** 27**	23** 27*	27**32*
1939			27** 32**32	32*	64** 23*
1940	El		23		
1941	La	Dr	32* 27*	32** 27	32** 27**
1942	El	We		32** 27	
1943			38** 45**	45	27**
1944			23** 27**		
1945				32**	64*
1946			64**	64**	

Table 3.4 contd.:

YEAR			PERIOD (SOUTH KERALA	PERIOD (NORTH KERALA	PERIOD (ALL INDIA)
1947		We	32**	32**38*	23
1948	La		64**	64*	
1949			23**45*	23**32*	64**
1950	El		45**38*	45**	23** 45
1951		Dr		64**	
1952			64**		
1953	El		23** 27**	23**	
1954	La		23** 27**	32** 27**	27*
1955			32*	32** 27**	64** 23* 27*
1956		We	64**23*	23** 27**	
1957	El		27**		
1958			64** 27	64**	64**23* 27*
1959		We		32 64	64**
1960			23** 27	23** 27**	32
1961		We	23**27*	23**	64* 23
1962			64** 32	23** 27	32**
1963			23** 27**	27**32*	27* 45
1964	La		32**	32* 27*	
1965	El	Dr	64**	23*	32*
1966		Dr	27**23*	27	
1967			23** 27		32**
1968		Dr			
1969				45*	
1970	La	We	27** 32**	32** 45 64	23**
1971			32**27*	27** 32* 23*	
1972	El	Dr	32* 27*64	23** 45*27*	
1973	La		64**	27*	64** 23**
1974		Dr	23**	23** 32	
1975	La	We	27** 32*	23** 27**	
1976	El		32**27*	32	
1977			45**38*		23*
1978			32	32*	45*
1979		Dr	23*64		64**27*
1980					
1981			32**27*	32** 23*	
1982	El	Dr	64** 23	64*	
1983		We	32**	32** 27**	
1984				23** 27*	23**
1985		Dr			
1986		Dr	45* 38 23	23** 27	27*
1987	El	Dr	64**	64**	64** 27
1988	La	We	23**	23**	32 27 64
1989			32** 27	23* 32	32** 27* 23
1990					64*
1991	El		64**	23** 27**	27
1992			23** 27**	38* 45	
1993			27*	23**	23*
1994		We	45**38*	45**	23
1995	La		23** 27**	64* 32	

*Significance levels (by chi-square test) at 99%,95% and 90% are denoted by suffices **,* and no suffix respectively.*

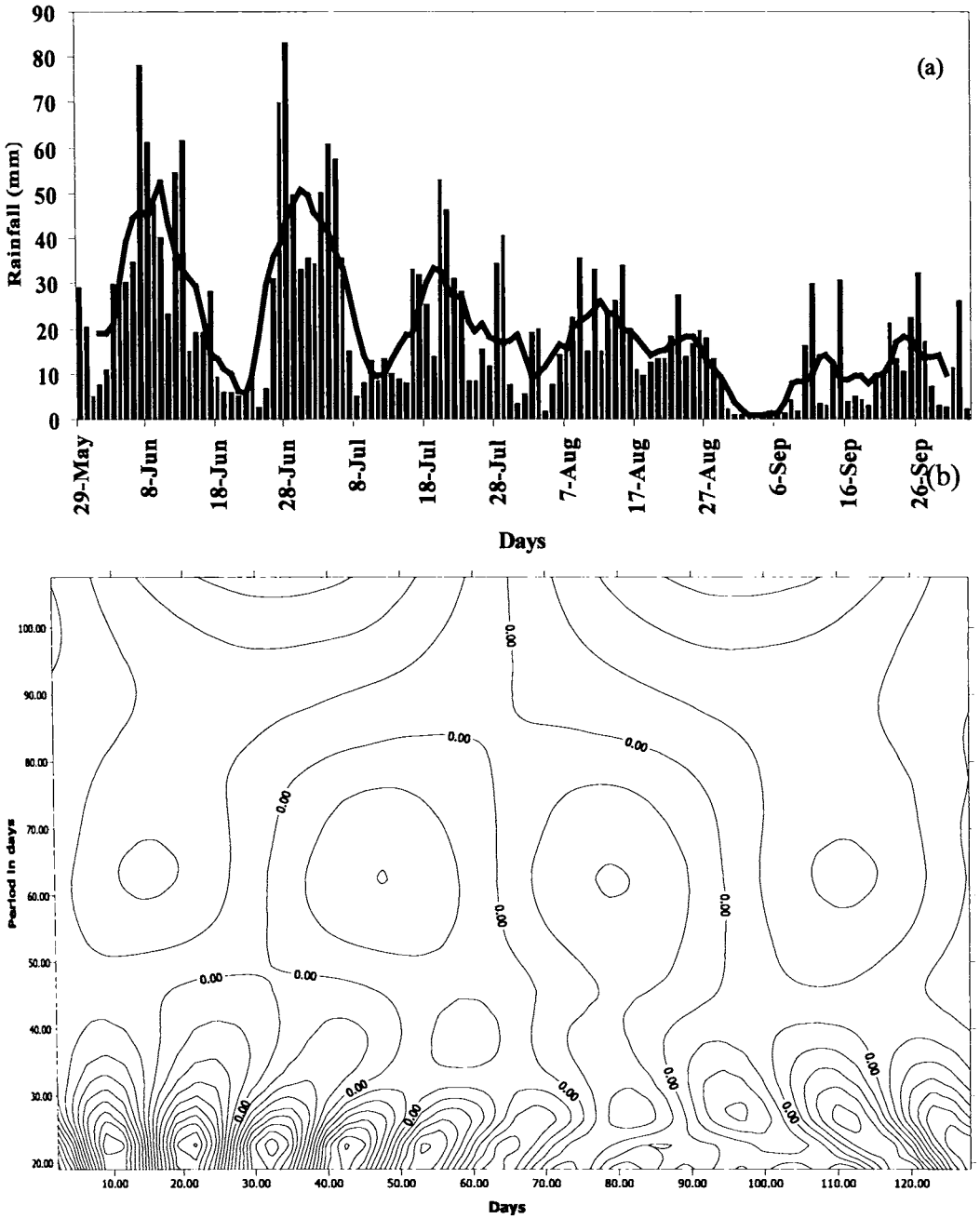

Fig. 3.5: (a) Daily average rainfall of south Kerala for 1961 along with the 7-day moving average; (b) Wavelet analysis of south Kerala rainfall for 1961.

the longitudes 70E- 80E for the monsoon season of 1987. The OLR diagram shows bands of convective clouds as in Sikka and Gadgil (1980) moving northwards from low latitudes to the Himalayas with long time periods in between. When the convective activity reached central and north Bay of Bengal

the Low Level Jetstream strengthened as in active monsoon conditions as described in Joseph and Sijikumar (2004). Thus one of the most important causes for severe monsoon rainfall deficiencies in Kerala and India during 1987 was the very long period ISO. A similar situation occurred during 2002 according to a study by Thomas et al (2003). In this year the whole of July had highly deficient rainfall both in Kerala and India as a whole. Fig.3.8 gives the Hovmuller diagram of OLR for 2002 (as for 1987). In many years such a simple picture of Sikka-Gadgil cloud bands forming in low latitudes and moving across Kerala and India and being the dominant mechanism for modulating their rainfall at Intra Seasonal scales does not occur. Only in 4 years (7 years) during 1901-1995 south Kerala, north Kerala and India as a whole have LONG (SHORT) periods significant at 99% level. The scenario is complicated by the synoptic disturbances that form during the monsoon in the 15^0N-25^0N latitude belt. Chowdhury et al (1988) showed that the variance explained by the 10-20 day ISO for central India rainfall exceeded that of the 30-60 day ISO in WET (all India monsoon rainfall more than 10% of the normal) monsoon years.

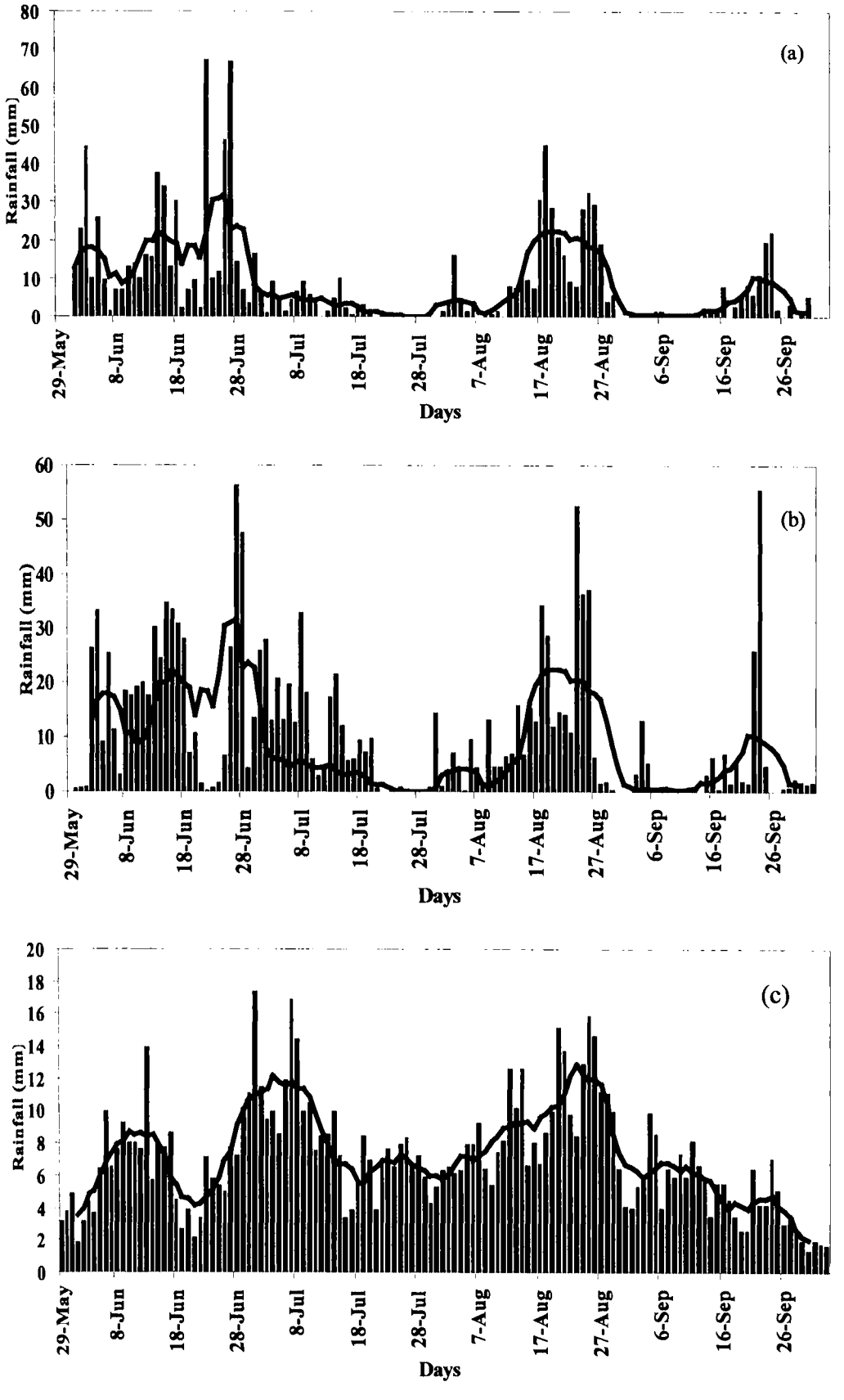

Fig. 3.6 The daily rainfalls of (a) south Kerala; (b) north Kerala ; (c) whole of India during the monsoon of 1987. The seven-day moving average is also plotted

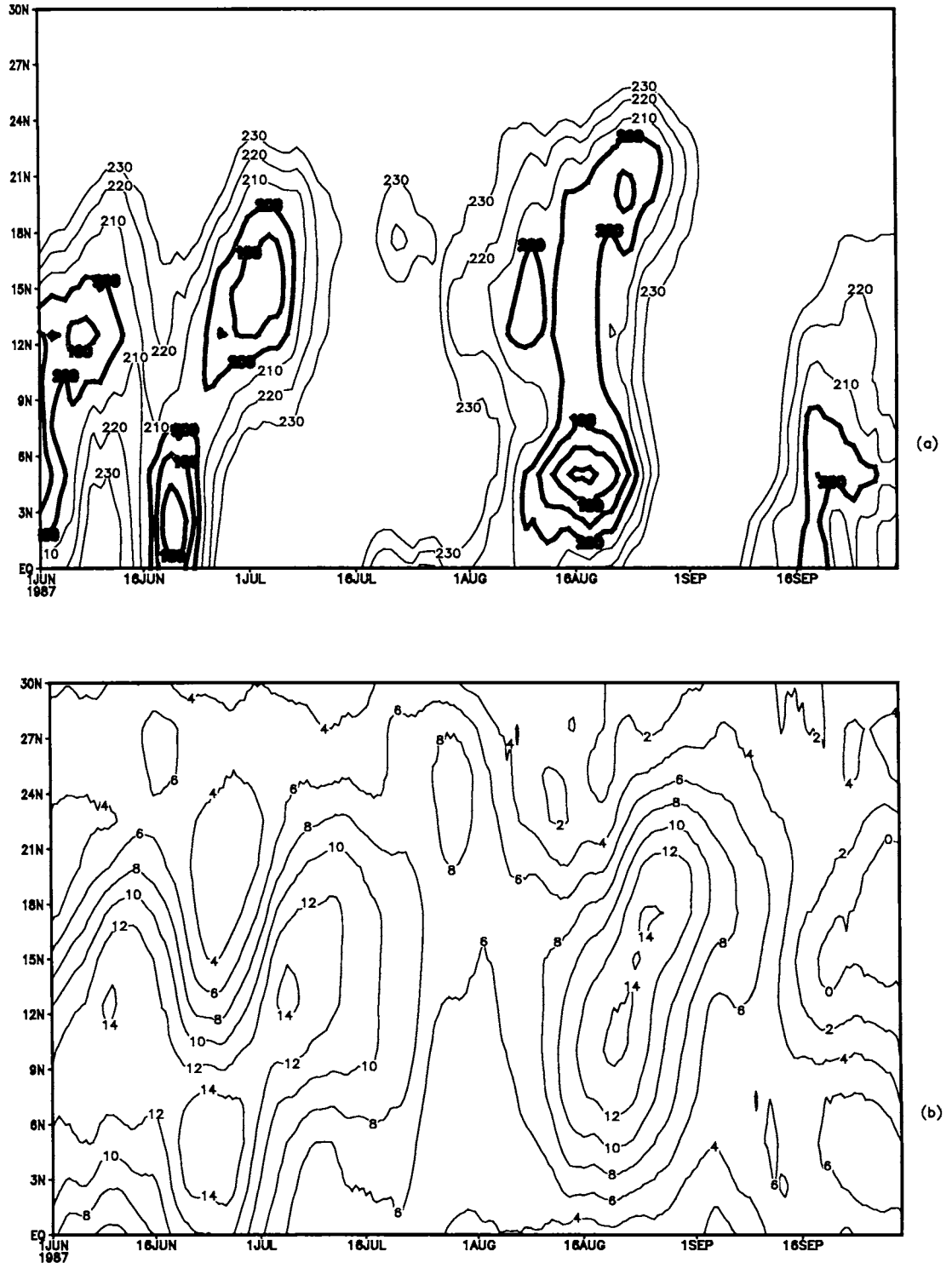

Fig.3.7 : Hovmuller diagrams of (a) OLR (b) zonal wind of 850 hPa averaged over the longitudes 70E- 80E for 1987. OLR in Watts/m^2

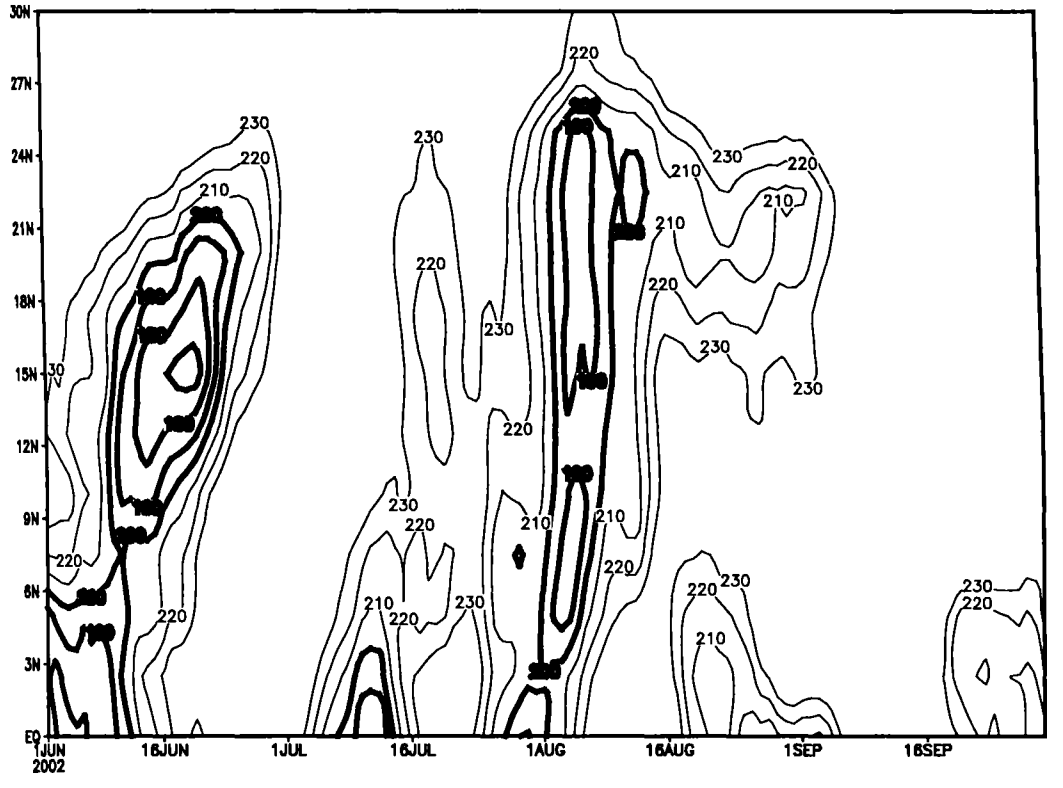

Fig.3.8 : Hovmuller diagrams of OLR over the longitudes 70E- 80E for 2002.
OLR in Watts/m^2

3.6 Conclusions

Time series of mean daily rainfall of south Kerala, north Kerala and whole India for the summer monsoon season of 95 years (1901-1995) have been analyzed to study the inter-annual variation of the period of the intra-seasonal oscillations in rainfall. Each data series has 128 days of daily rainfall data from 29th May to 3rd October. Intra Seasonal Oscillations (ISO) of periods 23,27,32,38,45,54 and 64 days were resolved using Wavelet Analysis and their statistical significance at levels 90%, 95% and 99% were determined.

It is found that for south Kerala out of the 95 years, 11 years had no significant ISO. Period-wise the remaining years clustered into two groups, the SHORT of periods 23,27 and 32 days and the LONG with a single period of 64 days. At the 99% level of significance SHORT and LONG period ISO were found in 44 and 20 years. Composites of LONG (SHORT) period ISO

significant at 99% of the years 1965 to 1993 showed that the SST anomalies are of the El Nino (La Nina) type in the tropical Pacific and Indian Oceans. It is seen that only in 4 years (7 years) during 1901-1995 south Kerala, north Kerala and India as a whole have LONG (SHORT) periods significant at 99% level. In the remaining years a simple picture of Sikka-Gadgil cloud bands forming in low latitudes and moving across Kerala and India and being the dominant mechanism for modulating their rainfall at Intra Seasonal scales does not occur. The scenario is complicated by the synoptic disturbances that form during the monsoon in the 15^0N-25^0N latitude belt.

Chapter 4
Inter-Annual and Long-Term Variability

4.1 General

Rainfall is the most important weather element for India, a tropical country. Agriculture, hydro-electric power, industry and the economy as a whole are heavily dependent on the performance of the summer monsoon which provides 75-90% of the annual rainwater over large parts of India. Even though, the summer monsoon is considered to prevail over India during the period 01 June to 30 September, there is considerable variability in the date of onset, withdrawal and the activity of the monsoon during the season. These variations are sometimes very large that they critically affect the economy of the country. The behaviour of the summer monsoon over India has been studied by Blanford (1886), Walker (1910), Rao and Jagnnathan (1963), Jagnnathan et al. (1973), Parthasarthy and Dhar (1974), Banarjee and Raman (1976), Ramasamy (1976), Mooley (1975,1976), Parthasarthy and Mooley (1978).

Summer monsoon rainfall of India has considerable interannual variability as shown by Parthasarathy et al (1994). It has a long-term (1871-1990) mean of 85.2 cm and a standard deviation of 8.5 cm. Figure 4.1 shows the rainfall of individual years for the period 1871 to 2003. The time series of rainfall is obtained from the Indian Institute of Tropical Meteorology (IITM) web site and the description of the data in detail is given in Chapter 2. This series exhibits large amplitude interannual variability. It is found that a year with large above normal rainfall is generally followed by a year with large below normal rainfall and vice versa, a type of biennial oscillation (Meehl, 1987). This biennial tendency is shown to be associated with the changes in ocean surface temperature of tropical Indian and west Pacific oceans, in a phenomenon now known as Tropical Biennial Oscillation (TBO), (Chang and Li, 2000). Examination of Indian Summer Monsoon Rainfall (ISMR) for the last hundred years has shown that there have been only three occasions when two or more consecutive drought (DRY) years have occurred. A DRY year is defined as a year in which ISMR is one standard deviation or more less than the long-period average. These are 1904 & 1905, 1965 & 1966 and 1985,86 & 87. Studies by

several authors have shown that ISMR has not exhibited significant long-term trend (Parthasarathy et al. 1990), however, ISMR is known to have DRY and WET epochs of a 30-year duration (Parthasarathy et al., 1994, Kripalani and Kulkarni 1997, Kripalani et al., 1997). Joseph (1976) had shown decadal type variability in the monsoon rainfall of India and in the direction of motion of cyclones in the Bay of Bengal. He had identified WET and DRY epochs of the monsoon rainfall. The relationship between Indian monsoon and ENSO has been studied extensively by Krishnamurthy and Goswami (2000) on a decadal time scale. In the DRY epochs decadal mean ISMR is low and there is a large standard deviation. Weaker meridional pressure gradients, larger northward seasonal shifts of the monsoon trough, larger numbers of days of breaks in the monsoon, smaller frequencies of depressions and shorter westward extents of depression tracks are the factors attributed to large-scale droughts; opposite features are observed during large-scale floods (Bhalme and Mooley, 1980). In the WET epochs the decadal mean ISMR is high and the standard deviation comparatively small and vice versa for the DRY epochs. The 30-year DRY epochs are 1901-1930 and 1961-1990. The 30-year WET epochs are 1871-1900 and 1931-1960 (Parthasarathy et al., 1994). Table 4.1 gives the DRY/WET ISMR years during each decade for the period 1871-1990. It can be seen that in the DRY epochs of 1901-1930 and 1961-1990 there are 6 and 10 DRY years respectively, while there were only 3 and 5 WET years in these epochs. However, during the WET epoch of 1871-1900 there were 6 WET years and only 3 DRY years. The WET epoch of 1931-1960 had 6 WET years and only 2 DRY years.

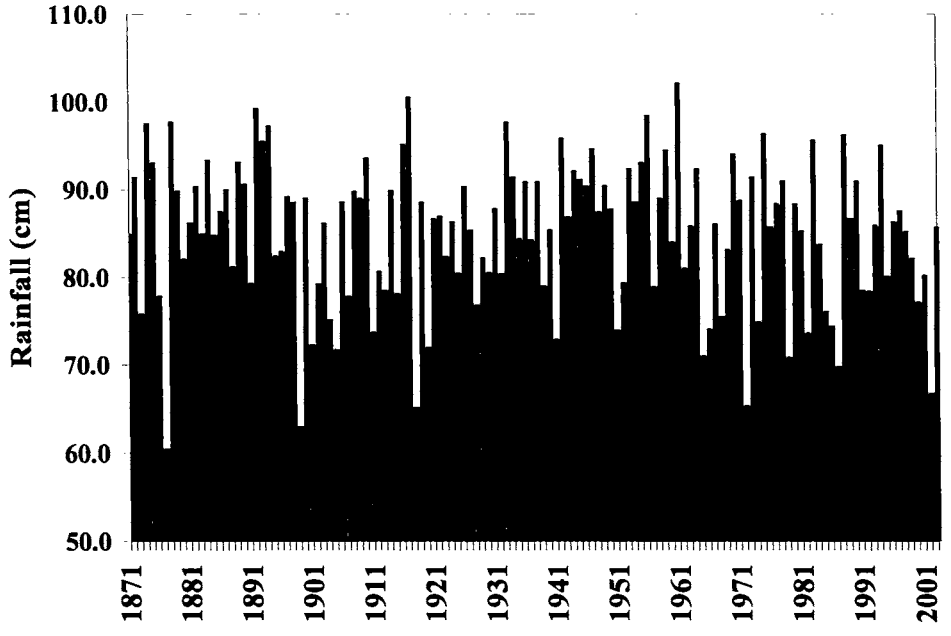

Fig. 4.1: All-India Summer Monsoon Rainfall 1871-2003

Table 4.1: Number of DRY/WET ISMR years in each decade for the period 1871-1990.

Decades	DRY Years	Number	WET years	Number
1871-1880	1873, 1877		1874,1878	
1881-1890	-	3	1884	6
1891-1900	1899		1892,1893,1894	
1901-1910	1901,1904,1905		1910	
1911-1920	1911,1918,1920	6	1916,1917	3
1921-1930	-		-	
1931-1940	-		1933	
1941-1950	1941	2	1942,1947	6
1951-1960	1951		1955,1956,1959	
1961-1970	1965,1966,1968		1961,1970	
1971-1980	1972,1974,1979	10	1975	5
1981-1990	1982,1985,1986,1987		1983,1988	

4.2 Interannual Variability of the Summer Monsoon Rainfall of Kerala

To study the Interannual variability (IAV) of Kerala Summer Monsoon Rainfall (KSMR) we have three time series: (a) Summer monsoon rainfall (01 June to 30 September) for the whole of Kerala for the time period 1901-1996 (b) Summer monsoon rainfall for south Kerala (SK) as an average of 44 stations south of latitude about 10^0N for the period 1901 to 1980 as derived by

Ananthakrishnan and Soman (1988) and for the period 1981 to 1996 as an average of 39 stations (Joseph et al., 2004). (c) Summer monsoon rainfall of north Kerala (NK) for the period 1901 to 1980 as an average of 31 stations north of latitude about 10^0N (Ananthakrishnan and Soman, 1988) and as an average of 24 stations for the period 1981 to 1996.

A study on the relationship of ISMR and KSMR show that the correlation between the two time series is very small (0.26). Comparison of data during the past 96 years show that while ISMR was normal in 63 years, Kerala experienced normal rainfall in 73 years. ISMR had 15 WET years and 18 DRY during 1901-2003. Table 4.2 shows the linear correlation coefficients between the 4 rainfall time series for the period 1901-1996.

Table 4.2: Linear Correlation Coefficients between the summer monsoon rainfall series

	ISMR	KSMR	SK Rainfall	NK Rainfall
ISMR	1	0.26	0.21	.28
KSMR		1	.96	.94
SK Rainfall			1	.79
NK Rainfall				1

4.2.1 Interannual Variability of KSMR

Figure 4.2 shows the bar diagram of KSMR (rainfall of whole Kerala) for the period 1901 to 1996 along with the linear regression line. The long-term mean is plotted as a thick straight line and the seven-year moving average is also plotted as a wavy line. Its mean and standard deviation are 195.5cm and 37.6cm respectively. It is seen that the time series exhibits considerable interannual variability. The extreme rainfall years are 1924 with the highest summer monsoon rainfall of 336.8 (72% above the long-term mean) and 1918 with the lowest rainfall of 104.5 cm (55% below the long-term mean) during this period.

Defining a DRY monsoon as a year with rainfall less than one standard deviation from the long-term mean there are 12 DRY years during the 96-year period. Two or more consecutive DRY years are 1965 & 1966 and 1986 & 1987. Similarly defining WET years as years with rainfall more than one standard deviation of the long-term mean there are 11 WET years. Two or more consecutive WET years during the period are 1923 & 1924.

During the period (1901-1996) there were 17 DRY ISMR years, out of which 6 years were also DRY years for Kerala state. These years are: 1918,1965,1966,1972,1986 and 1987. Out of the 15 WET ISMR years, 4 were WET years for Kerala; 1933,1959,1961 and 1975. However, during 1944 and 1986 both WET ISMR years, the state experienced DRY monsoon.

One standard deviation of 37.6cm is around 19% of the long-term mean of KSMR. The state depends on the summer monsoon rainfall for its economy and a departure of 10% is also considered large. Hence we have defined DRY*/WET* years as years with ½ standard deviation below/above normal of the long-term average. According to this criterion there are 28 DRY* years and 26 WET* years. Two or more consecutive DRY* years are 1934 & 1935, 1944 & 1945, 1952 & 1953, 1965 & 1966, 1972& 1973, 1976&1977, 1985,1986, 1987, 1988, 1989 & 1990. It is note worthy that there has been 6 consecutive DRY* years from 1985 to 1990. Similarly two or more consecutive WET* years are 1902,1903&1904, 1922,1923 & 1924, 1946& 1947, and 1991 & 1992. While, 10 out of the 17 DRY ISMR years are DRY* KSMR years only 6 out of the 15 Wet ISMR years are WET* for the state.

Table 4.3: Number of DRY/WET KSMR years in each decade for the period 1901-1990.

Decades	DRY Years	Number	WET years	Number
1901-1910	-		1907	
1911-1920	1918	2	-	3
1921-1930	1928		1923,1924	
1931-1940	1934		1931,1933	
1941-1950	1944	3	1946	4
1951-1960	1952		1959	
1961-1970	1965,1966		1961,1968	
1971-1980	1972,1976	7	1975	3
1981-1990	1986,1987,1990		-	

Table 4.3 gives the DRY/WET KSMR years for each decade from 1901 – 1990. It is clear from the table that unlike ISMR, the summer monsoon rainfall of Kerala does not show an epochal behaviour, the numbers of DRY/WET years are uniformly distributed. It is also seen that during the 1901-1930 DRY ISMR epoch there were only 2 DRY years for Kerala and 3 years were WET during that period. However, in the 1961-1990 ISMR DRY epoch 7 years were DRY for Kerala. During this 30-year epoch ISMR was DRY for 10 years. The linear regression fitted to this rainfall series shows a decreasing trend of 12.0 % in the 96 years for the summer monsoon rainfall of the state. It is due to this trend that in the epoch 1961-1990 there are 7 DRY KSMR years. It should be noted that ISMR does not show any significant trend but only epochal behaviour. The linear correlation between years and rainfall is –0.21. It is significant at the 95% level. The Mann-Kendall test for trend also shows a significant trend at the 95% level.

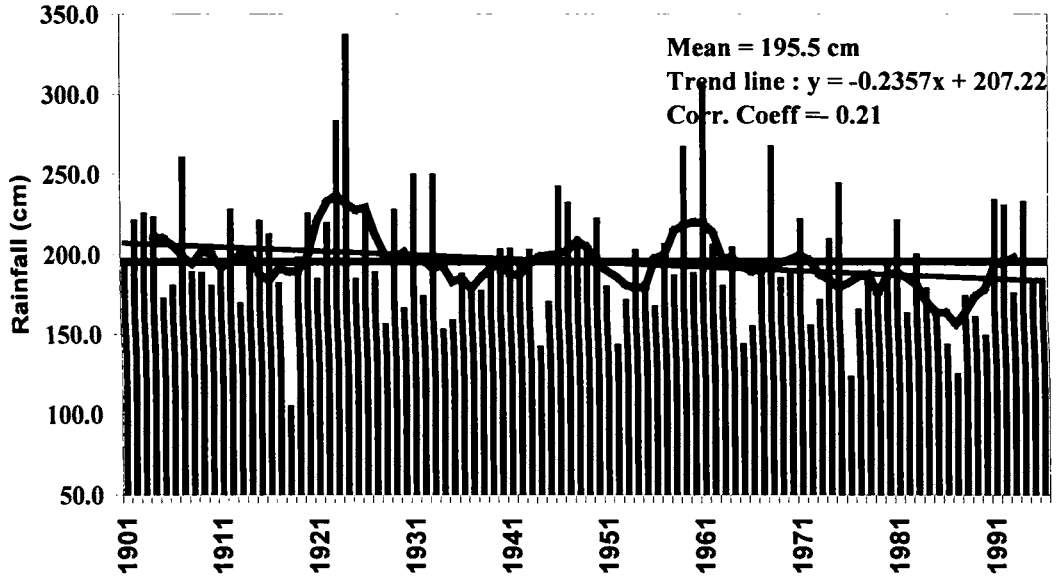

Fig.4.2: Kerala Summer Monsoon Rainfall 1901-1996

4.2.2 South Kerala Rainfall Series

Figure 4.3 shows the monsoon rainfall series of south Kerala along with the linear regression line for the period 1901 to 1996. The long-term mean (bold straight line) and the seven–year moving average (wavy line) are also marked. The mean and standard deviation of the time series are 176.2cm and 36.1cm respectively. The extreme rainfall years are 1924 with the highest summer monsoon rainfall of 310.6 (76% above the long-term mean) and 1918 with the lowest rainfall of 100 cm (43% below the long-term mean) for this period. There are 16 DRY years for south Kerala during the period 1901-1996, with rainfall less than 1 standard deviation of the long-term mean. Two or more such consecutive DRY years are 1976 & 1977 and 1985,1986 & 1987. Similarly there are 16 WET years with rainfall more than one standard deviation of the long-term. Two or more consecutive WET years during the period are 1903 & 1904, 1923 & 1924, 1946 & 1947 and 1991 & 1992. However, there are 30 DRY* years and 29 WET* years for south Kerala with rainfall below/above ½ standard deviation of the mean value. Two or more consecutive DRY* years with this criteria are 1934 & 1935, 1944 & 1945, 1952 & 1953, 1965 & 1966, 1972&

1973, 1977,1978 & 1979, 1985,1986,1987,1988,1989 & 1990. It should be noted that the clusters with below normal rainfall are increasing in the recent decades and this is reflected in the trend analysis of the summer monsoon rainfall of south Kerala. Similarly two or more consecutive WET* years are 1902,1903 & 1904, 1915 & 1916, 1919 & 1920, 1923 & 1924, 1946, 1947& 1948 and 1991 & 1992.

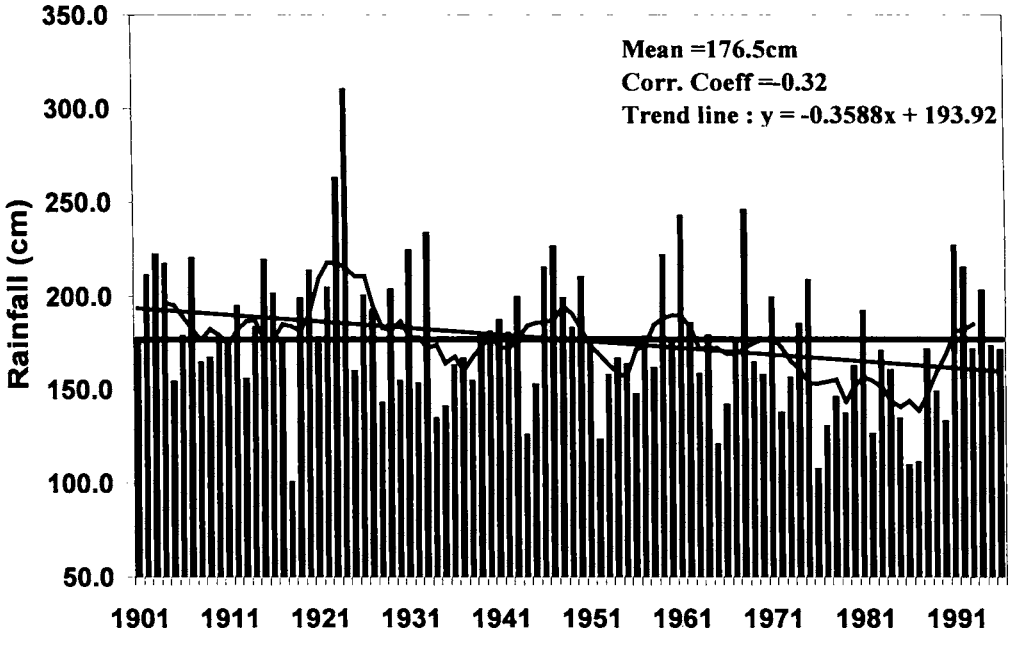

Fig.4.3: Summer Monsoon Rainfall for south Kerala 1901-1996

During the period 1976 to 1990 we had only one year with above normal rainfall. Some of the years in this period had very low rainfall, years like 1976 (107.6 cms), 1977(130.2 cms), 1979(137.0 cms), 1982(126.4 cms), 1985(134.4 cms), 1986(109.7 cms), 1987(111.1 cms) and 1990(133.1 cms). Part of this is because south Kerala's monsoon rainfall has a strong decreasing trend during the last century shown by the trend line of fig. 4.3. Rainfall decrease has been at the rate of 35.9 cms per 100 years, which is 20.3% of the long-term mean rainfall of 176.5 cms, comparable to its standard deviation of 36.0 cms. Urgent research is needed on this aspect. The negative correlation coefficient of –0.32 between rainfall and years is significant at the 99% level.

A study by Soman et al (1988) has thrown some light on this problem. They found that the decreasing trend in south Kerala's rainfall is a feature contributed mainly by the rainfall of the high ranges and it is not confined to the monsoon season alone. Annual rainfall also is affected. They studied the data of the 80 years 1901 to 1980. Figures 4.4(a & b) give the percentage decrease in the mean annual and southwest monsoon rainfall respectively from the first 40 years to the second 40 years. The area around Cardamom Hills has suffered the major decrease.

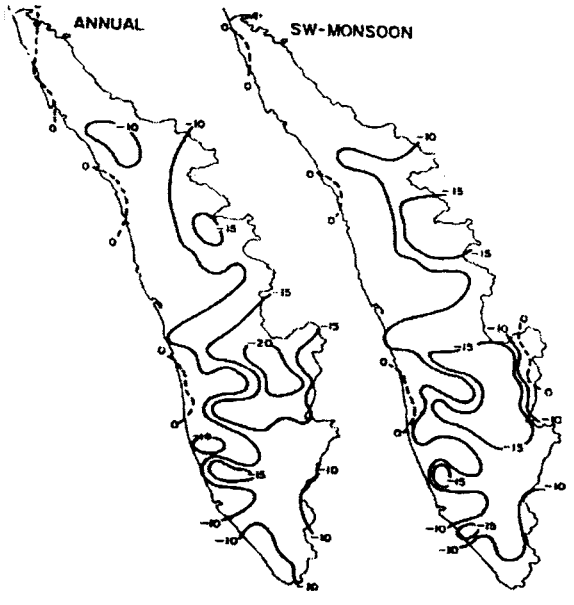

(a) (b)

Fig. 4.4 : Percentage change in rainfall from 1901-1940 to 1941-1980 from Soman et al. (1988)

The long term decrease in rainfall is particularly large in the high ranges area of south Kerala is confirmed by the examination of the long term records of annual rainfall of three stations of South Kerala, a coastal station Alappuzha ($9^0$33'N latitude, $76^0$25'E longitude, 2m above MSL), an inland station Kottayam ($9^0$35'N latitude, $76^0$32'E longitude, 30m above MSL), and a station on the windward (during the south-west monsoon season) slopes of the Western Ghats, Peermade ($9^0$34'N latitude, $76^0$59'E longitude, 950m above MSL), as

available for the period 1901 to 2003 (shown in figure 4.5(a-c)). Seven year moving averages and the linear trend lines are also marked in the figure. For the coastal station Alleppey rainfall has decreased at the rate of 31.7 cm per 88 years (1916 –2003) which is 9% of the long-term mean rainfall of 302.8 cms. The correlation coefficient of –0.18 is not significant even at the 95% level. For the inland station, Kottayam rainfall has decreased at the rate of 45.0 cm per 103 (1901 – 2003) years (minus 14.3% of the long term mean rainfall of 312.6 cms). The correlation coefficient is –0.28 significant at the 99% level. However, for a high altitude station, Peermade in the Cardamom Hills the decrease is 110.4 cms per 95 years which is minus 26.5% of the long term mean of 416.7 cms.. The correlation coefficient between the years and the annual rainfall for this station is –0.31 which is significant at the 99% level. A decrease in rainfall amount of this magnitude is certainly a reason for concern especially for the cardamom growers in that area and well focused study is needed in this regard.

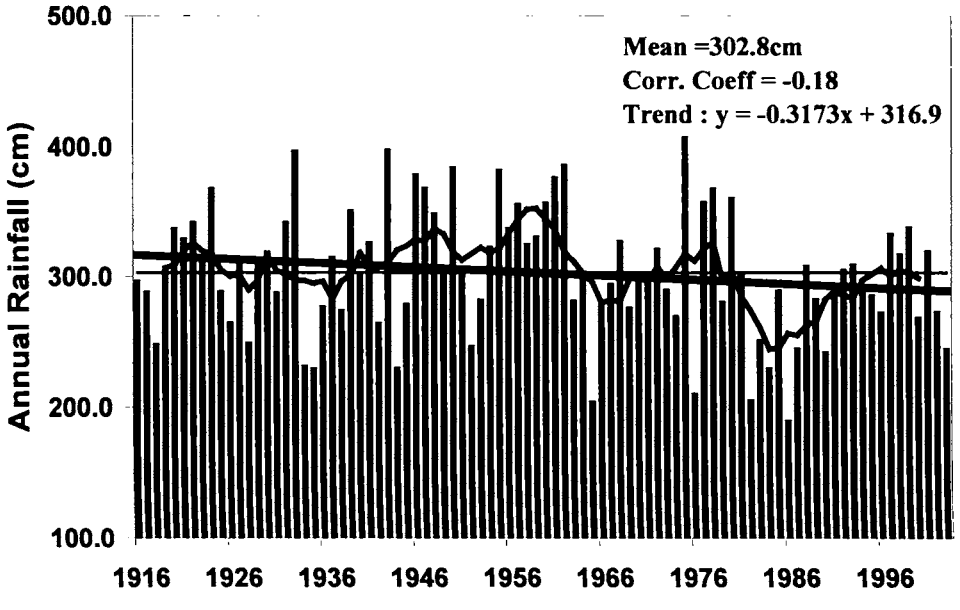

Fig.4.5(a): Annual Rainfall in cms for Alappuzha for the period 1916-2003.

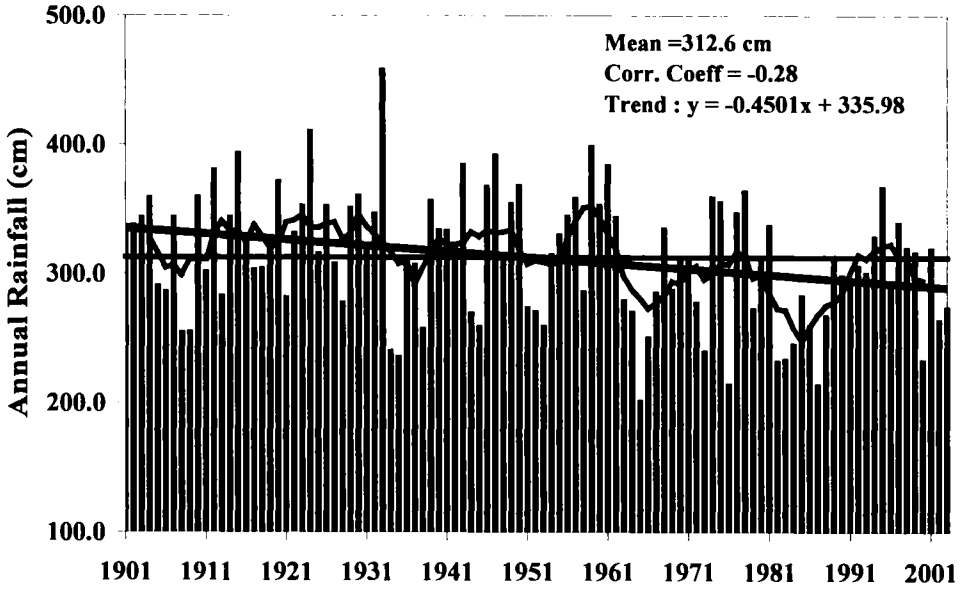

Fig.4.5(b): Annual Rainfall in cms for Kottayam for the period 1901-2003

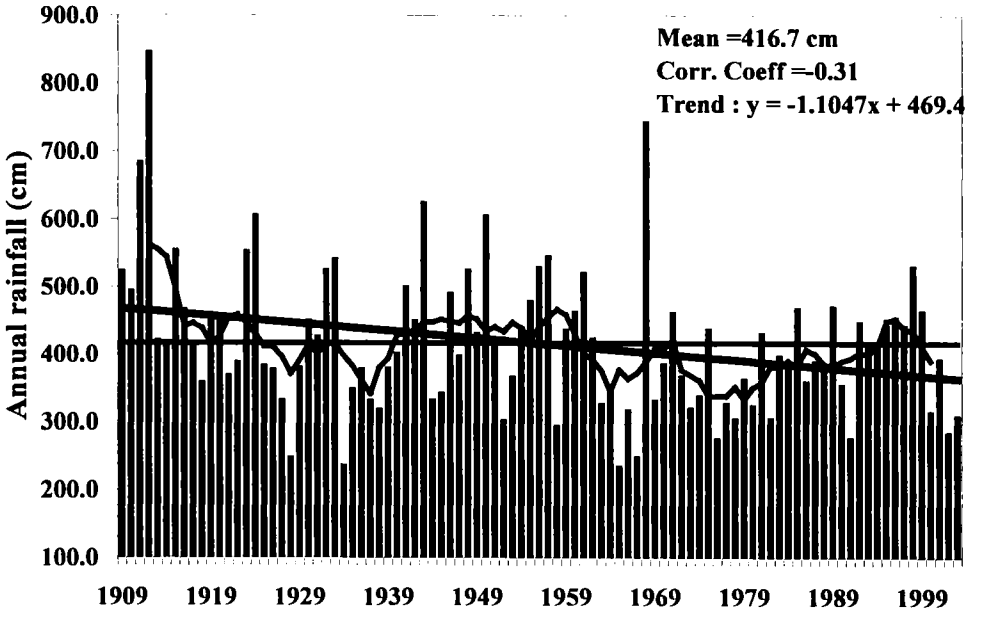

Fig.4.5(c): Annual Rainfall in cms for Peermade for the period 1901-2003

4.2.3 North Kerala Rainfall Series

The average summer monsoon rainfall of stations north of 10^0N is plotted in fig. 4.6 along with the long-term mean, linear regression line and 7-year moving average. It is clear from the figure that the series also exhibits large interannual variability. The long-term mean of the series is 223.6 cm and the

standard deviation is 44.8 cm. The extreme rainfall years are 1961 with the highest summer monsoon rainfall of 395.7 (77% above the long-term mean) and 1918 with the lowest rainfall of 110 cm (51% below the long-term mean) for this period. There are 10 DRY years for north Kerala during the period 1901-1996, with rainfall less than 1 standard deviation of the long-term mean. There is only one pair of two consecutive DRY years : 1965 & 1966. Similarly there are 13 WET years with rainfall more than one standard deviation of the long-term. Two or more consecutive WET years during the period are 1923 & 1924. However, there are 31 DRY* years and 22 WET* years for north Kerala with rainfall below/above ½ standard deviation of the mean value. Two or more consecutive DRY* years with this criteria are 1905 & 1906, 1917, 1918 & 1919, 1927 & 1928, 1934 & 1935, 1944 & 1945, 1951, 1952 & 1953, 1965 & 1966, 1972 & 1973, 1986 & 1987, 1989 & 1990, and 1995 & 1996. Similarly two or more consecutive WET* years are 1923 & 1924, 1980 & 1981, and 1991 & 1992. It is interesting to note that although the correlation between the summer monsoon rainfall between north Kerala and south Kerala is large as shown in Table 4.1 there are large differences in the individual year rainfall amounts and the number of DRY/WET years. North Kerala has not experienced any significant long-term decrease in rainfall as seen from the linear regression line analysis (fig.4.6).

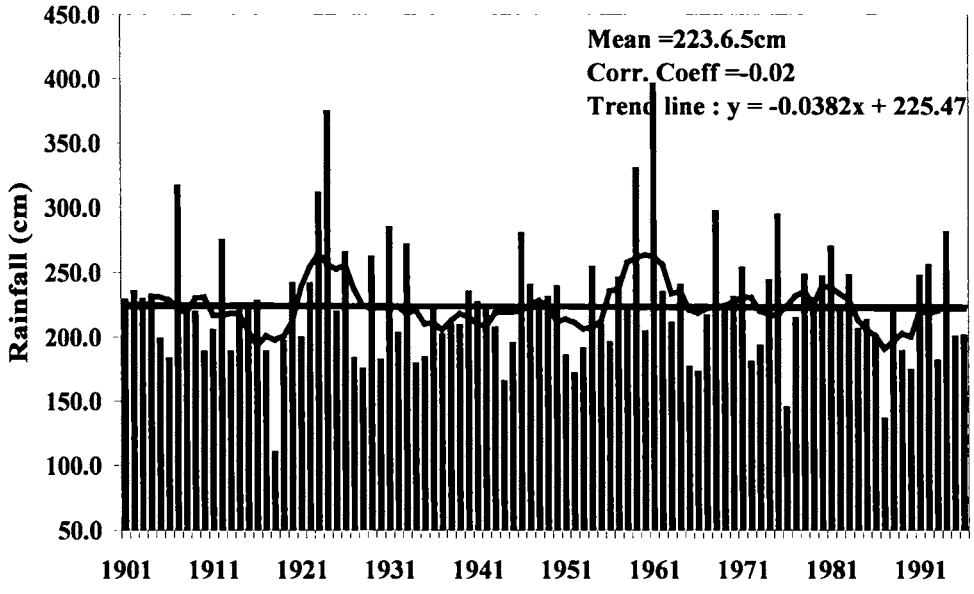

Fig.4.6: Summer Monsoon Rainfall for north Kerala 1901-1996

4.3 Duration of Strong and Weak Monsoon Periods in KSMR

The southwest monsoon current in the form of a cross-equatorial Low Level Jetstream (LLJ) with its core at an altitude of about 1.5 Kms and core wind speeds of 80-100 Km per hour is the conduit carrying the moisture generated over south Indian ocean and the Arabian sea that supports the June to September monsoon rainfall of India (Joseph and Raman, 1966; Findlater, 1969). Active spells of the summer monsoon that last for 2 to 4 weeks over the Indian region are associated with an intense monsoon trough with heavy rainfall over India. During the break monsoon condition that last 1 to 3 weeks, the monsoon trough moves northward to the Himalayas, resulting in decrease in rainfall over much of the country but enhanced rainfall in the far north and extreme southeast India (Ramanadham, 1973). Joseph and Sijikumar (2004) have shown that during active monsoon the core of LLJ passes eastward through peninsular India between latitudes 12.5^0N and 17.5^0N and in break monsoon LLJ moves southeastwards from central Arabian sea and by-passing India passes eastward between latitudes 2.5^0N and 7.5^0N.

A recent study by Joseph and Simon (2005) has shown that the mean June to September monsoon flow through India from surface to an altitude of 1.5 Kms between latitudes 12.5N and 17.5N had a significant decreasing trend and that between 2.5N and 7.5N a significant increasing trend during the recent half century from 1950 to 2003. The study also showed that the duration of break (weak) monsoon spells defined by 850hPa wind in a monsoon season has increased by about 30 percent during this period and these changes have resulted in the number of days during the monsoon season 01June to 30 September with daily average rainfall less than 8mm/day increasing in number and days with rainfall more than 12mm/day decreasing through 45.4% and 78.1% respectively during the last 53 years. It is also shown that there is a very strong and statistically significant decreasing trend of monsoon depression frequency per monsoon season during the period 1950 to 2003.

In this section, we study the relationship between the Active/Break monsoon days as defined by Joseph and Sijikumar (2004) and KSMR. The details of the dates chosen are discussed in Chapter 2. There are 113 Active and 84 Break days for the period 1979 to 1990. The average daily rainfall of south and north Kerala of the Active/Break days during the period 1979 to 1990 is given in Table 4.4. It can be seen from the table that during the Active spells in India, both south and north Kerala receive good rainfall. The average rainfall during Active spells of south and north Kerala are 18.2 and 30.6 mm per day respectively. Similarly, during the Break spells Kerala receives relatively less rainfall, the average rainfall for south and north Kerala being 7.0 and 8.3 mm per day respectively. We define a strong monsoon day in KSMR as a day with rainfall greater than or equal to 15 mm/day for south Kerala and day with more than 20 mm/day for north Kerala. Weak days are days with rainfall less than or equal to 7.5 mm/day for both south and north Kerala.

Table 4.4: The average daily rainfall (mm) of south and north Kerala of the Active/Break during the period 1979 to 1990

	Active Spells		Break Spells	
	South Kerala	North Kerala	South Kerala	North Kerala
1979	15	4.9	3.9	5.6
1980	21	37.2	10	10.3
1981	5.7	11.2	11.0	17.1
1982	16.7	34.0	-	-
1983	17.2	41.8	7.8	7.1
1984	35.4	53.4	6.7	22.0
1985	-	-	3.3	2.9
1986	20.2	32.9	0	0
1987	-	-	0.1	1.7
1988	11.8	31.5	11.0	8.6
1989	19.7	45.7	8.7	1.0
1990	19.7	23.2	14.3	14.7
Ave.	**18.2**	**30.6**	**7.0**	**8.3**
Std. Dev.	**7.6**	**15.3**	**4.7**	**7.2**

Figure 4.7(a,b) gives the number of strong monsoon spells defined according to the rainfall criteria for south and north Kerala for the period 1950 to 1996. The linear regression line fitted to the time series do not show any trend for both the time series. However, the number of weak monsoon days (fig.

4.7c,d) show an increasing trends for south and north Kerala even though these trends are not significant even at the 5 % level. It has to be noted that the increase in weak monsoon days are more prominent in south Kerala.

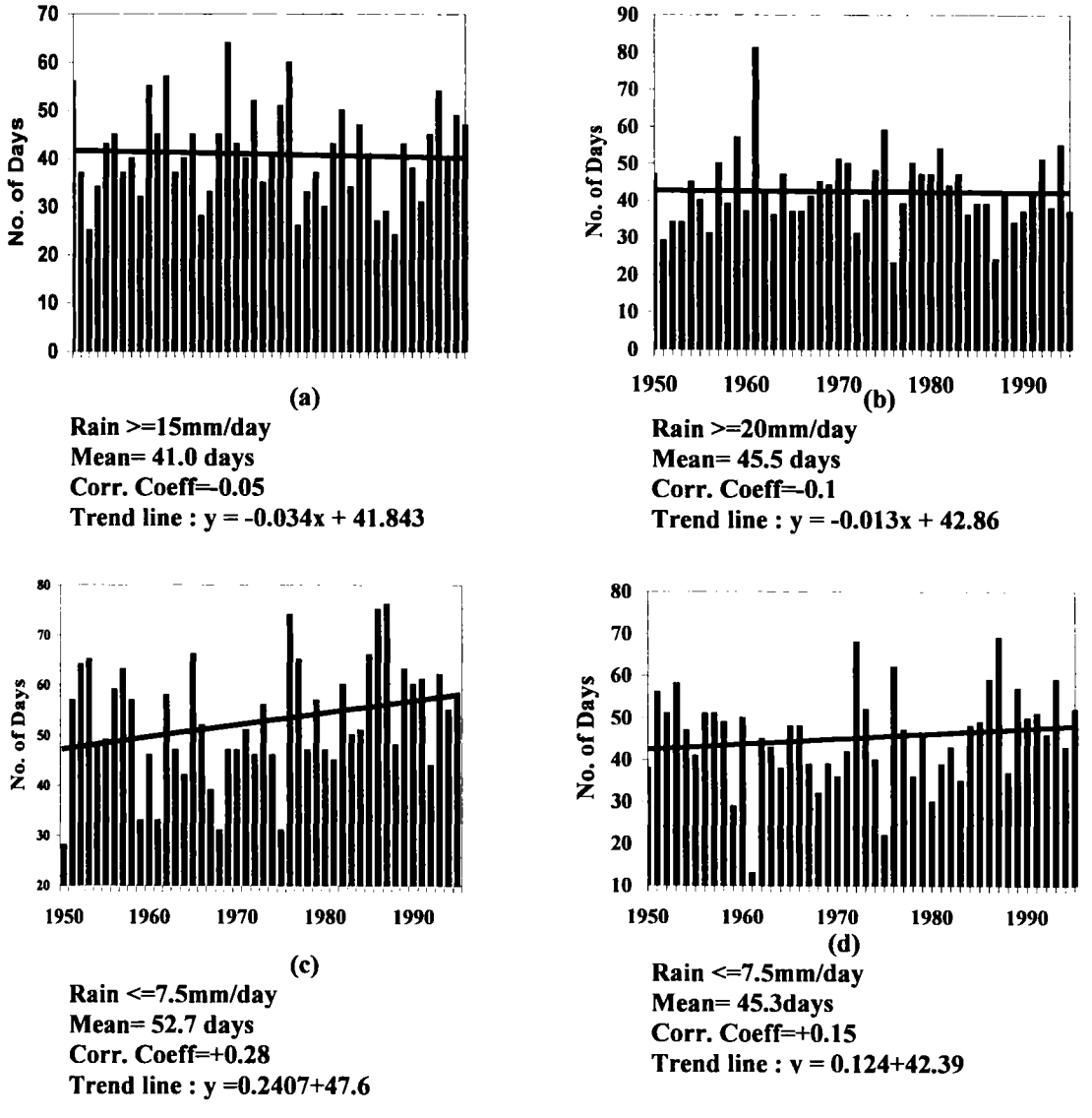

Fig. 4.7 : Number of days during monsoon season 01June to 30September with (a) daily south Kerala rainfall ≥15mm/day (b) daily north Kerala rainfall ≥20mm/day (c) daily south Kerala rainfall less than or equal to 7.5 mm/day. (d) daily north Kerala rainfall less than or equal to 7.5 mm/day Linear trend line is marked.

4.4 Conclusions

The interannual variability of Kerala summer monsoon rainfall and that of south and north Kerala rainfall is discussed in this chapter. The long-term mean of Kerala summer monsoon rainfall is 195.5 cm and standard deviation is 37.6

cm. The time series exhibits considerable interannual variability and occurrence of two or more consecutive droughts are seen in 1986,1987,1988,1989 and 1990 receiving rainfall less than ½ standard deviation of the long-term mean. The summer monsoon rainfall of Kerala shows a decreasing trend of 12.0% in 96 years, the decrease is seen more prominently in south Kerala with a decrease of 35.9 cm in 100 years which is 20.3% of the long-term mean. This decrease is comparable to the standard deviation of 36.1 cm. The long-term average monsoon rainfall of south Kerala is 176.2 cm. North Kerala receives an average rainfall of 223.6 cm and the standard deviation of the time series is 44.8 cm. Even though there is considerable interannual variability in the summer monsoon rainfall of north Kerala the series does not exhibit a trend. During Active spells of monsoon rainfall in India, both south and north Kerala receive good rainfall and during the Break spells in India the rainfall in the state is very low. While, the strong monsoon days as defined by rainfall greater than or equal to 15 mm/day in south Kerala and greater than or equal to 20 mm/day in north Kerala does not exhibit any trend, the weak monsoon spells (rainfall less than or equal to 7.5 mm/day for both south and north Kerala) exhibits an increasing trend which is more prominent for south Kerala. However, this decreasing trend is not statistically significant.

Chapter 5
Prospects for Long-Range Prediction of Monsoon Rainfall of Kerala

5.1 General

The India Meteorological Department (IMD) has been issuing long-range forecast of the south-west monsoon rainfall since 1886. It was, however the extensive and pioneering work of Gilbert Walker, who was the Director General of IMD from 1904 to 1924 that led to the development of the first objective model based on statistical correlations between monsoon rainfall and antecedent global atmosphere, land and ocean parameters. The 16-parameter power regression and parametric models developed by Gowariker et.al. (1989) were introduced operationally by IMD in 1988. The search for new predictor parameters for accurately forecasting seasonal Indian monsoon rainfall has been ongoing since then. This is because of the profound effect of the seasonal monsoon rains on agriculture production in India and their importance to the whole economy.

Long range forecast model outputs of All India rainfall from various meteorological centres in the world including India were wide off the mark in 2002. The drought of 2002 prompted the meteorological community world wide to address the short comings of the model used and look for suitable revision and improvement of the existing model.

A major criticism of the earlier model was that the mutual independence of the parameters chosen was not established and that there were too many parameters given the small data set of 37 years of monsoon on which the model was developed. Another reason for a critical revaluation of the old parameters

was the increasing evidence that over the past two decades the relationship of many of the parameters to the monsoon rainfall had been weakening and they were losing their predictive potential. Thapliyal (1997) showed that while some parameters were very stable over the years, others were unstable. Their 'correlation co-efficients (CCs)' fluctuated from year to year, rendering the current influence of some of them on rainfall forecast very weak. In that analysis, he had argued that operational models should be revised every year by replacing those parameters, which have been less stable during recent years.

Recently IMD introduced new operational models for long-range forecast of south-west monsoon rainfall for India and verified it for the year 2003 (Rajeevan et al., 2004). The models were an eight-parameter power regression model and an eight-parameter probabilistic model for an April forecast and a 10-parameter power regression model for a mid-July update. In their new models IMD omitted some predictors which lost their predictive potential and introduced new parameters.

The true challenge in monsoon forecasting is to predict the extreme events. LRF of the monsoon, rather than becoming simpler with years of modelling, is turning out to be more and more complex with even the atmospheric variables that are believed to influence the monsoon strongly becoming unstable over time. The surprising thing is that, in spite of this, the monsoon visits the subcontinent with unfailing regularity year after year. Some have even begun to take another look at the physical basis that is currently applied to study the monsoon.

The meteorological subdivision Kerala, the coastal state situated in the southwestern tip of the Indian subcontinent is the gateway of monsoon to the subcontinent. The state receives 67.5% of the annual rainfall during the south-west monsoon season (June –September) and the agriculture, power generation and the economy of this state are heavily dependent on the rainfall during this season. There is need to predict the time of arrival of the southwest monsoon

and its duration and intensity, all of which can have significant impacts on an agriculturally based society. Approximately 67% of the population depends on agriculture for livelihood (forestry and fishing included). The monsoon rains are absolutely essential for crops to grow. Indian economy has been called a "gamble on monsoon rains" because the rains from the summer monsoon fills reservoirs, tanks, rivers, and irrigation canals with water that must last until the monsoon returns the next year. Not only crop success is dependent on the monsoon, the state is increasingly dependent on hydroelectric power for its industries. Forecast of the amount of rainfall during the south-west monsoon season given a season ahead is therefore very essential for the state. Even though, IMD is giving forecasts for the country as a whole and for large homogeneous rainfall divisions, they have not been able to develop so far long-range forecasting techniques for individual states and meteorological subdivisions (Rajeevan, 2004).

Attempts to forecast monsoon rainfall over smaller areas or smaller periods such as weeks or ten day spells using statistical techniques become unsuccessful as correlations fall drastically (Rajeevan, 2004). Long-range forecasts with a higher resolution in space and time scales it is believed can be generated by dynamical models, which can handle the complex regional-scale interactions and regional rainfall variability. Even though, forecasts from global prediction centres are available they have not been able to cater to the specific need of the state as far as southwest monsoon rainfall is concerned. Hence, statistical/empirical methods for generating long-range forecast of monsoon rainfall for the state are needed. In this chapter, we try to bring the relationship between some antecedent global circulation parameters with Kerala rainfall and also try to develop a statistical model for long-range forecast of monsoon rainfall for the state.

Observational facts and physical plausibility also support the hypothesis that the interannual variability of monsoon rainfall is significantly influenced by

the slowly varying boundary conditions like snow cover, Sea Surface Temperature (SST) soil moisture etc. (Shukla, 1987). To develop a reliable long-range forecast it is very essential to identify and understand the physical forcing and associated anomalies causing the interannual variability of monsoon rainfall. For that purpose diagnostic studies examining global circulation anomalies also become very important. Such studies also help in identifying useful predictors for long-range forecasts.

Rasmusson and Carpenter (1982) made a comprehensive study of a composite El Niño based on six warm events during 1949-1976. They showed a westward migration of the equatorial Pacific SST anomaly pattern from the south American coast into the central equatorial Pacific. Maximum SST anomalies were found to occur around April-June along the south American coast and by the end of the year around 170^0W. However, in a comparative study of ENSO episodes during 1950-1992, Wang (1995) observed noticeable differences in the evolution of the SST anomalies during pre and post 1976 periods. (1) The eastern Pacific peak warming leads the central Pacific warming by about 5 months in the pre-1976 warm episodes, while it lags by about 5 months in the post-1976 warm episodes. (2) In the central Pacific, the pre-1976 episodes were preceded by a cooling during June-October of the previous year, while in the post–1976 episodes this cooling was not observed. The results indicate that there have been remarkable changes in the characteristics of the onset of the El Niño after the 1976 warm event. The changes are attributed to an abrupt interdecadal climate shift that occurred around 1976. Simon et al., 2003, have studied differences in the correlation between ISMR and SST during the pre and post 1976 period. Hence we confine our study period to 1977 to 2003.

5.2 El Niño Southern Oscillation

The tropical Pacific Ocean exhibits large-scale Sea Surface Temperature (SST) variability on both the seasonal and interannual timescales. The primary mode of tropical Pacific interannual SST variability is related to the El Niño –

Southern Oscillation (ENSO) phenomenon (Harrison and Larkin, 1998). Bjerkenes (1969) attributed this circulation to the exchange of air between the eastern and western hemispheres.

El Niño translates from Spanish as 'the boy-child'. Peruvian anchovy fishermen traditionally used the term - a reference to the Christ child - to describe the appearance, around Christmas, of a warm ocean current off the South American coast, adjacent to Ecuador and extending into Peruvian waters. El Niño affects traditional fisheries in Peru and Ecuador. In most years, colder nutrient-rich water from the deeper ocean is drawn to the surface near the coast (upwelling), producing abundant plankton, food source of the anchovy. However, when upwelling weakens in El Niño years, and warmer low-nutrient water spreads along the coast, the anchovy harvest plummets. It was ruined in the four or five most severe El Niño events this century. The South American El Niño current is caused by large-scale interactions between the ocean and atmosphere. Nowadays, the term El Niño refers to a sequence of changes in circulations across the Pacific Ocean and Indonesian archipelago when warming is particularly strong (on average once every three to eight years). Characteristic changes in the atmosphere accompany those in the ocean, resulting in altered weather patterns across the globe.

The Pacific Ocean is a huge mass of water which controls many climatic features in its region. Its equatorial expanse, far larger than the Indian or Atlantic Oceans, is critical to the development of the Southern Oscillation and El Niño.

In normal non-El Niño conditions (fig.5.1) the Humboldt current brings relatively cold water northward along the west coast of South America, an effect increased by upwelling of cold water along the Peruvian Coast. This cold water is nutrient-rich, supporting high levels of primary productivity, diverse marine ecosystems, and major fisheries. The cold water then flows westward along the equator and is heated by the tropical sun. These normal conditions make the western Pacific about 3°C to 8°C warmer than the eastern Pacific. During this

condition the trade winds blow towards the west across the tropical Pacific. These winds pile up warm surface water in the west Pacific, so that the sea surface is about 1/2 meter higher at Indonesia than at Ecuador. The rising air is associated with a region of low air pressure, towering cumulonimbus clouds and rainfall is found in rising air over the warmest water, and the east Pacific is relatively dry. High pressure and dry conditions accompany the sinking air. This circulation is called Walker circulation named after Sir. Gilbert Walker and according to his definition the Southern Oscillation implies the tendency of pressure at stations in the southeast Pacific to increase and pressure in the Indian Ocean region to decrease.

During El Niño (fig.5.2), the trade winds relax in the central and western Pacific leading to a depression of the thermocline in the eastern Pacific, and an elevation of the thermocline in the west. This reduces the efficiency of upwelling to cool the surface and cut off the supply of nutrient rich thermocline water to the euphotic zone. The result is a rise in sea surface temperature and a drastic decline in primary productivity, the latter of which adversely affects higher trophic levels of the food chain, including commercial fisheries in this region. Rainfall follows the warm water eastward, with associated flooding in Peru and drought in Indonesia and Australia. The eastward displacement of the atmospheric heat source overlaying the warmest water results in large changes in the global atmospheric circulation, which in turn force changes in weather in regions far removed from the tropical Pacific.

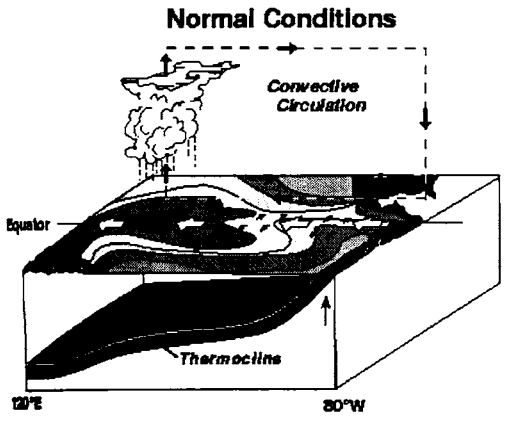

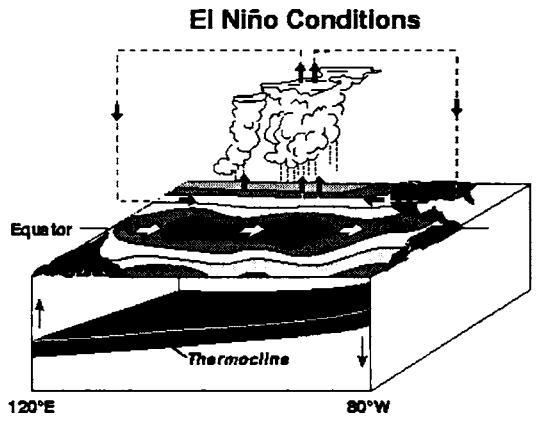

Fig. 5.1: Non- El Niño conditions

Fig.5.2: El Niño conditions

The Southern Oscillation Index (SOI) gives us a simple measure of the strength and phase of the Southern Oscillation, and indicates the status of the Walker circulation. The SOI is calculated from the monthly or seasonal fluctuations in the air pressure difference between Tahiti and Darwin. The 'typical' Walker circulation Pattern has an SOI close to zero (Southern Oscillation close to the long-term average state). When this pattern is strong the SOI is strongly ***positive*** (Southern Oscillation at one extreme of its range). When the Walker circulation enters its El Niño phase, the SOI is strongly ***negative*** (Southern Oscillation at the other extreme of its range). Positive values of the SOI are associated with stronger Pacific trade winds and warmer sea temperatures to the north of Australia. Together these give a high probability that eastern and northern Australia will be wetter than normal. During El Niño episodes, the Walker circulation weakens, seas around Australia cool, and slackened trade winds feed less moisture into the Australian/Asian region. There is then a high probability that eastern and northern Australia will be drier than normal.

One of the fundamental questions concerning the nature and prediction of El Niño-Southern Oscillation is how the turnabout from a cold to warm phase takes place. Rasmusson and Carpenter (1982) made a comprehensive description of a composite ENSO scenario based on six events during 1950-

1976. They found significant westerly anomalies occurring over the western equatorial Pacific in the onset (around the end of the year preceding El Niño) phase. These westerly anomalies occurring in the western equatorial Pacific can induce eastward propagating equatorial Kelvin waves and have been suggested as the trigger of the south American coastal warming (Wyritki 1975; Philander 1981). There has also been various speculations for the causes responsible for the initial changes in the western Pacific (Keen 1982; Lau et.al 1983; Hackert and Hasternath 1986; Lau and Chan 1986).

Many processes in the tropics relevant to ENSO have been studied in detail. Eventhough the theoretical basis for seasonal predictability of large-scale circulation in the tropics is well documented, the predictability of the meteorological variables like rainfall is not yet well established. Much work has been carried out in this direction (Matsuno,1966; Webster,1972; Gill, 1980; Charney and Shukla, 1984). An index of the ENSO is a very important input to seasonal prediction models for many tropical areas. Considerable interest in using ENSO as predictor exist in the southern hemisphere extratropics. Strong influence of ENSO are well documented throughout Australia (Nicholls, 1988; McBride and Nicholls, 1993) and New Zealand (Trenberth, 1976).

The Indian Summer Monsoon Rainfall (ISMR) is known to have large interannual variability (Parthasarathy et al, 1994). There have been many studies in the past to relate the interannual variability of ISMR and ENSO (Parthasarthy and Pant, 1984; Mooley and Shukla,1987; Ramsusson and Carpenter, 1983). The interannual fluctuations in the Southern Oscillation indices and their relation to the Indian monsoon (June – September) rainfall were examined in detail by Bhalme and Jadhav (1984). There is strong association between monsoon droughts and El Niño. More El Niño related droughts are in the decades when the Indian Monsoon is generally below normal than during the decades when it is generally above normal (Kripalani and Kulkarni, 1997). The physical link through which ENSO is related to Indian Monsoon has been

investigated by Krishnamurthy and Goswami (2000). Long-period Intra Seasonal Variability of south Kerala rainfall has been associated with El Niño type of SST variations (Joseph et al., 2004).

In the recent past, the severe droughts in 1972,1982 and 1987 were associated with El Niño events in the Pacific ocean. However, during 1997-98 the strongest El Niño of the 20th century the country received marginally above normal rainfall (Srinivasan et al., 2002). There were studies to understand the behaviour of the 1997 El Niño . Asnani (2001) studied the El Niño of 1997 and showed that while rainfall was below normal during early June, it picked up substantially from the 3rd week of June and remained rather normal through the rest of the season. Krishna Kumar et al. (1999) have argued that the association between El Niño and the Indian summer monsoon rainfall have become progressively weaker during the decade of 1990-2000.

We examined the DRY and WET years in Kerala rainfall in relation to moderate /strong El Nino years and La Nina years as obtained from Quinn and Neal (1987), Rasmusson and Carpenter (1983), Kiladis and Diaz (1989) and Trenberth (1997). Out of the 18 DRY years (less than 1 standard deviation) 7 were strong/moderate El Niño years. Details of the years and the rainfall are given in Table 5.1. These years are 1918,1932, 1965,1972, 1976, 1987 and 2002. 1928, a DRY KSMR was a La Nina year. During the 23 El Niño (Table 5.2) events 7 years experienced below normal rainfall for the state and there were two WET years. The WET years are 1907 and 1923. There are 17 WET years (more than 1 standard deviation) during the period 1901 to 2003, out of which only 4 years were La Nina years. 1907 and 1923 both WET years were however, El Niño years. Out of the 18 La Nina years 4 were WET and one year, 1928 experienced below normal rainfall.

Table 5.1 : DRY/WET KSMR years (less than 1 standard deviation) and rainfall in cm is given. The years are marked El Niño / La Nina accordingly. Only strong or moderate El Niño /La Nina years are considered.

DRY YEARS			WET years		
Year	Rainfall (cm)		Year	Rainfall (cm)	
1913	155.4		1907	259.5	El
1918	115.0	El	1912	237.7	
1928	154.3	La	1920	239.5	La
1932	157.1	El	1922	231.8	
1934	153.6		1923	266.6	El
1935	156.5		1924	311.5	La
1944	137.4		1929	230.4	
1952	143.2		1931	236.1	La
1956	152.2		1933	230.4	
1965	146.4	El	1946	244.5	
1966	140.5		1947	243.6	
1972	157.4	El	1959	234.9	
1976	126.1	El	1961	294.3	
1986	152.9		1968	260.9	
1987	145.7	El	1975	252.2	La
1990	151.7		1981	252.6	
1999	151.6		1997	230.3	
2002	129.2	El			

Table 5.2: El Niño / La Nina years and rainfall in cm of corresponding years. DRY/ WET (less than 1 standard deviation) are marked D/W accordingly.

El Niño			La Nina		
Year	Rainfall (cm)		Year	Rainfall (cm)	
1902	214.5		1903	207.43	
1905	168.7		1906	172.4	
1907	259.5	W	1908	205.0	
1911	175.2		1916	203.0	
1914	202.0		1920	239.5	W
1918	115.0	D	1924	311.5	W
1923	266.6	W	1928	154.3	D
1925	194.5		1931	236.1	W
1930	161.1		1938	176.0	
1932	157.1	D	1942	194.4	
1939	186.7		1949	206.8	
1941	186.6		1954	200.8	
1943	199.4		1964	183.9	
1951	172.8		1970	189.0	
1953	169.2		1973	172.1	
1957	205.5		1975	252.2	W

Table 5.2 contd.

El Niño			La Nina		
Year	Rainfall (cm)		Year	Rainfall (cm)	
1965	146.5	D	1988	205.1	
1972	157.4	D	1995	172.4	
1976	126.2	D			
1982	174.9				
1987	145.7	D			
1991	224.7				
2002	129.2	D			

Out of the 35 DRY* years (less than ½ standard deviation) 13 were strong/moderate El Niño years and 4 were La Nina years. During the 23 El Niño events 13 years were DRY* and 4 were WET*. There are 29 WET* years (more than ½ standard deviation) of which 4 are La Nina years and 4 El Niño. Out of the 18 La Nina years 4 were WET* and 4 years were DRY*. It is clear that although there is no close relationship between DRY/WET years and El Niño and La Nina events, the El Niño years are more likely to become DRY years than La Nina becoming WET. Details are given in Table 5.3 and 5.4. We find that El Niño/La Nina events have no potential for the LRF of KSMR.

Table 5.3: DRY/WET KSMR years (less than ½ standard deviation) and rainfall in cm is given. The years are marked El Niño / La Nina accordingly. Only strong or moderate El Niño /La Nina years are considered.

DRY YEARS			WET years		
	Rainfall (cm)		Year	Rainfall (cm)	
1905	168.7	El	1902	214.5	El
1906	172.4	La	1904	217.9	
1910	173.4		1907	259.5	El
1911	175.2	El	1912	237.7	
1913	155.4		1915	226.8	
1918	115.0	El	1920	239.5	La
1928	154.3	La	1922	231.8	
1930	161.1	El	1923	266.6	El
1932	157.1	El	1924	311.5	La
1934	153.6		1926	222.5	
1935	156.5		1927	212.9	
1944	137.4		1929	230.4	
1945	169.2		1931	236.1	La
1951	172.8	El	1933	230.4	

Table 5.3 contd.

DRY YEARS			WET years		
	Rainfall (cm)		Year	Rainfall (cm)	
1952	143.2		1940	212.9	
1953	169.2	El	1946	244.5	
1956	152.3		1947	243.6	
1958	174.4		1950	223.2	
1965	146.5	El	1959	234.9	
1966	140.5		1961	294.3	
1972	157.4	El	1968	260.9	
1973	172.1	La	1971	223.8	
1976	126.1	El	1974	221.1	
1982	174.9	El	1975	252.2	La
1984	162.2		1981	252.6	
1985	164.8		1991	224.7	El
1986	152.9		1992	215.3	
1987	145.7	El	1994	224.3	
1990	151.7		1997	230.3	
1995	172.4	La			
1999	151.6				
2000	162.0				
2001	168.7				
2002	129.2	El			
2003	158.1				

Table 5.4: DRY/WET KSMR years (less than ½ standard deviation) and rainfall in cm is given. The years are marked El Niño / La Nina accordingly. Only strong or moderate El Niño /La Nina years are considered.

El Niño			La Nina		
Year	Rainfall (cm)		Year	Rainfall (cm)	
1902	214.5	W	1903	207.4	
1905	168.7	D	1906	172.4	D
1907	259.5	W	1908	205.0	
1911	175.2	D	1916	203.0	
1914	202.0		1920	239.5	W
1918	115.0	D	1924	311.5	W
1923	266.6	W	1928	154.3	D
1925	194.5		1931	236.1	W
1930	161.1	D	1938	176.0	
1932	157.1	D	1942	194.4	
1939	186.7		1949	206.8	
1941	186.6		1954	200.8	
1943	199.4		1964	183.9	

Table 5.4 contd.

El Niño			La Nina		
Year	Rainfall (cm)		Year	Rainfall (cm)	
1951	172.8	D	1970	189.0	
1953	169.2	D	1973	172.1	D
1957	205.5		1975	252.2	W
1965	146.5	D	1988	205.1	
1972	157.4	D	1995	172.4	D
1976	126.1	D			
1982	174.9	D			
1987	145.7	D			
1991	224.7	W			
2002	129.2	D			
1939	186.7		1949	206.8	
1941	186.6		1954	200.8	
1943	199.4		1964	183.9	

5.3 Kerala Summer Monsoon Rainfall and Southern Oscillation Index (SOI)

The correlation coefficient (CC) between the Kerala Summer Monsoon Rainfall (KSMR) and the SOI of different seasons, i.e (i) preceding March-May season (Pre-MAM); (ii) preceding June-August (Pre-JJA); (iii) preceding September-November (Pre-SON); (iv) preceding December-February (Pre-DJF); (v) concurrent March-May (Con-MAM); (vi) concurrent June-August (Con-JJA); (vii) concurrent September-November (Con-SON); (viii) concurrent December-February (Con-DJF), for different periods have been calculated (Table 5.5). The correlations for the preceding September-November and concurrent March-May are negative and significant at 5% level for the period 1977-2003. Earlier study by Parthasarathy and Pant (1984) have shown that the All India south-west monsoon rainfall and the SOI for the preceding MAM, concurrent JJA and succeeding September-November are all positive for the period 1871-1974. It can be seen from the table that for the period 1950 to 1975 the correlations were positive for all the seasons and the Con-MAM was significant at the 95%level. This indicates that the correlations have not been persistent and there has been a considerable shift in the climate scenario.

Table 5.5 : Correlation table for KSMR and SOI for different seasons.

Season	1901-2003 (103yrs)	1950-1975 (26yrs)	1977-2003 (27yrs)
Pre- MAM	-0.07	+0.03	-0.25
Pre- JJA	-0.17	+0.09	-0.26
Pre- SON	-0.19	+0.16	-0.41*
Pre-DJF	-0.04	+0.20	-0.21
Con-MAM	+0.03	+0.37	-0.33*
Con-JJA	+0.17	+0.29	+0.15
Con-SON	+0.09	+0.31	-0.08
Con-DJF	+0.13	+0.30	-0.08

*significant at 95% level

Consistency of the relationship for different periods of the series is examined by calculating the variations of the CC by the sliding window method using window width of 21 years. Variation of CC between KSMR and SOI for the Pre-SON, Pre-DJF, Con-MAM, Con-JJA are shown in fig. 5.3(a-d). It is seen for the 21-year period for the Pre-SON and the Pre-DJF the CCs have been negative throughout except for a short period during 1950 – 1980. However, for Con-MAM the CCs were positive during the earlier period of the study period and then attained significant (95%) positive correlations in the pre-1976 period. However, in the later years (after 1977) the CCs are negative and significant at the 95% level.

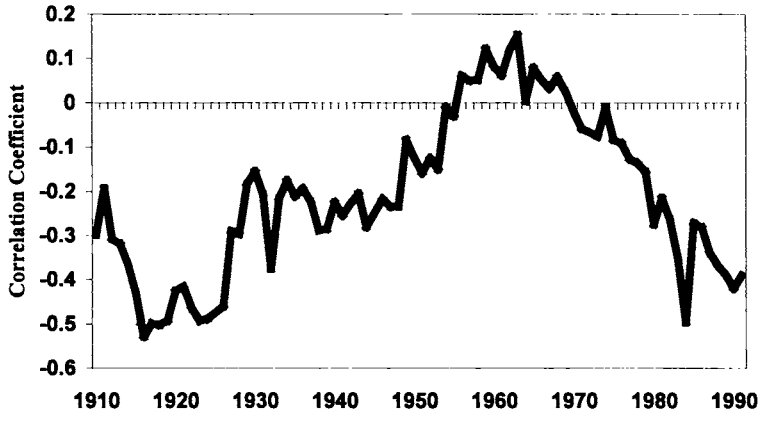

Fig. 5.3a:- 21-year sliding correlation between KSMR and SOI of Pre-SON

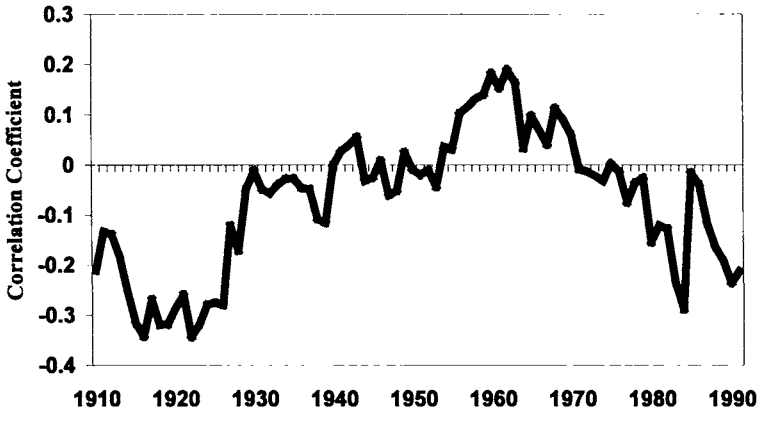

Fig. 5.3b: 21-year sliding correlation between KSMR and SOI of Pre-DJF

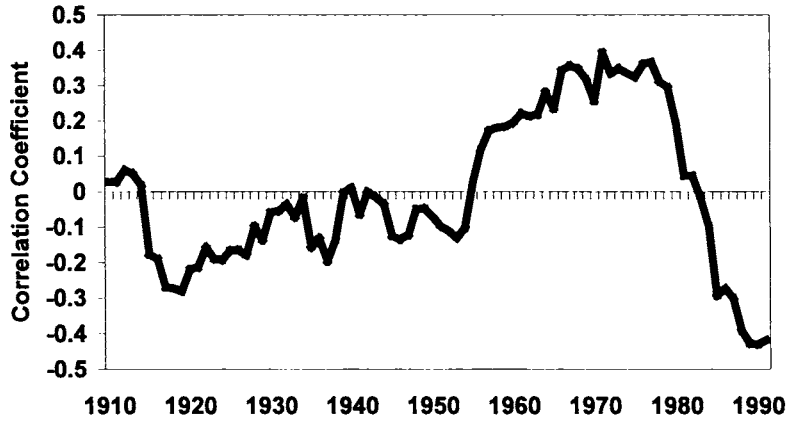

Fig. 5.3c: 21-year sliding correlation between KSMR and SOI of Con-MAM

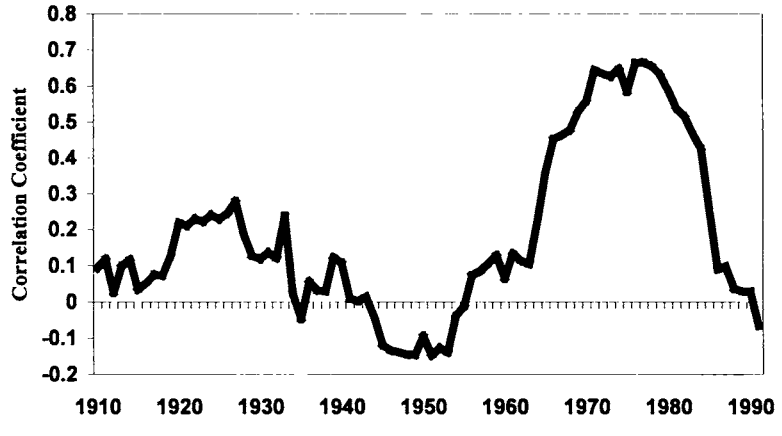

Fig. 5.3d: 21-year sliding correlation between KSMR and SOI Con-JJA

5.4 Position of the 500mb ridge and Kerala Summer Monsoon Rainfall

A mid tropospheric anticyclone over south India and its seasonal migration towards the north are a well-known feature of the climatology of the annual cycle of the atmospheric circulation. Figure 5.4 taken from (Shukla and Mooley, 1987) shows the mean location of the 500-mb ridge during the months of January, April, July and October. The axis of the ridge is located from the streamline analysis of the wind data. The 500-mb ridge along 75^0E is seen about 11.5^0N during January, 15^0N during April and 28.5^0N during July which is its northernmost location during the peak of the monsoon season. By October, the ridge position shifts southwards to 20^0N. The northward and southward displacement of this mid tropospheric anticyclonic circulation seems to be related to the seasonal march of the solar radiation and the associated diabatic heat sources.

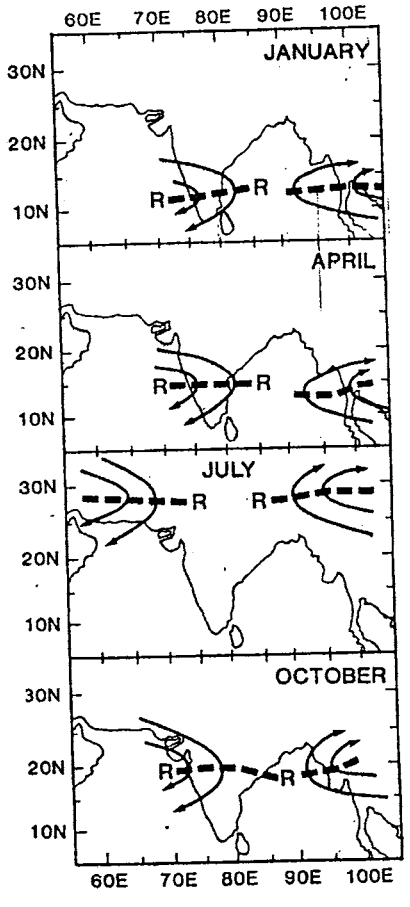

Fig. 5.4: Location of the 500-mb ridge during the months of January, April, July and October taken from (Shukla and Mooley, 1987).

Although the general character of this seasonal transition remains the same during each year, there are some differences in the latitudinal position of the ridge from one year to the other. Earlier studies (Banerjee *et al.*, 1978) have shown that if the latitudinal position of the 500 mb ridge during April is much south (north) of its normal position, rainfall over India for years with the subsequent Summer Monsoon rainfall (ISMR) is below (above) normal. Thapliyal (1982) developed empirical formulae to predict monsoon rainfall of India by utilizing the ridge position. Shukla and Mooley (1987) used the change in Darwin pressure from January to April and the latitudinal position of the April 500-mb ridge along 75^0E as two quasi-independent predictor parameters to develop a regression equation to predict summer monsoon rainfall using data of 1939 to 1984 and found that the root-mean-square error for predicted rainfall was 36mm which is less than half the standard deviation (82mm) and is only about 4% of the mean rainfall. Mooley et. al (1986) have shown that the relationship between April ridge position and monsoon rainfall over India is highly significant and stable. They showed that the latitudinal location of the mid tropospheric ridge along 75° E meridian is a measure of the influence exerted by the troughs in the westerlies on the upper tropospheric thermal conditions over North and Central India. Hence a location much south of the normal April ridge location would correspond to a much colder troposphere in April and persistence of colder than normal conditions up to June, which would delay the initiation of monsoonal heat sources thereby adversely affecting the monsoon rainfall. In a recent study Chandrasekhar and Goswami (1999) proposed one possible physical mechanism for the southward displacement of the mid tropospheric ridge. They showed that the anomalous cooling associated with the increased snow cover in Eurasia may be considered as a heat sink north of the tropical heat sources and that such a heat sink can result in significant southward displacement of the mid tropospheric ridge. The latitudinal position of the 500 mb ridge along 75° E in April has been extensively used by most of the long range forecasters to predict the Summer Monsoon rainfall of India since

it has emerged as one of the important predictors (Hasternath and Greischar, 1993).

The correlation coefficient for the position of the April 500-mb ridge and monsoon rainfall of Kerala for the period 1939 to 1984 is only +0.21 which is not significant at the 95% level. In comparison the study by Shukla and Mooley (1987) have shown that the correlation of the ridge position and Indian summer Monsoon Rainfall (ISMR) is +0.71. Table 5.6 gives the values of the correlation coefficients of the ridge position for ISMR and Kerala rainfall for the period 1939 to 1984 and also for successive 30-yr. periods. It is also seen that the correlation of the ridge position and the ISMR as well as Kerala rainfall has a similar pattern of variation and is decreasing in the recent years However, the correlation between the ridge position and KSMR is very small unlike that with ISMR. Thapliyal (1997) showed that while some parameters were very stable over the years, others were unstable and their correlation co-efficients (CCs)' fluctuated from year to year, rendering the current influence of some of them on rainfall forecast very weak. Figure 5.5(a &b) gives the sliding correlation for ISMR and KSMR respectively.

Table 5.6: Correlation coefficients of April 500mb ridge with ISMR and KSMR

Period	ISMR	Kerala Rainfall
1939-1968	0.71	0.16
1940-1969	0.68	0.15
1941-1970	0.67	0.15
1942-1971	0.62	0.16
1943-1972	0.69	0.23
1944-1973	0.69	0.21
1945-1974	0.73	0.16
1946-1975	0.74	0.21
1947-1976	0.73	0.13
1948-1977	0.70	0.08
1949-1978	0.68	0.08

Table 5.6. contd.

Period	ISMR	Kerala Rainfall
1950-1979	0.70	0.08
1951-1980	0.70	0.05
1952-1981	0.67	0.07
1953-1982	0.69	0.06
1954-1983	0.65	0.07
1955-1984	0.65	0.0
1939-1984	**0.71****	**0.21**

** significant at 99% level

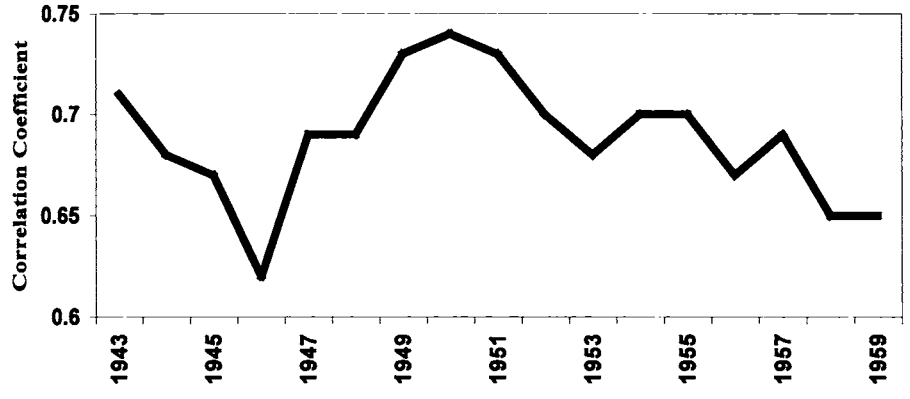

Fig. 5.5(a): 30-year sliding correlation between 500mb ridge and ISMR

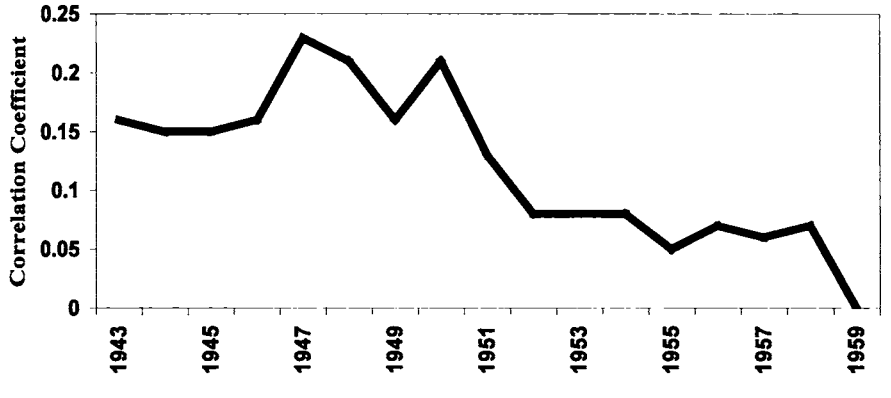

Fig. 5.5(b): 30-year sliding correlation between 500mb ridge and KSMR

5.5 Kerala Summer Monsoon Rainfall and Sunspot number

The sun-weather relationship has been an active field of study over the last 100 year and there have been many studies on the relation between rainfall and solar activity (Parthasarathy and Mooley, 1978). Parthasarathy and Dhar (1974) detected significant correlation in rainfall and solar activity for arid and semi-arid regions of Rajasthan, central parts of India and extreme south Indian peninsula. Epoch analysis of sunspot numbers and its relation to annual rainfall of India was done in detail by Ananthakrishnan and Parthasarathy (1984). They showed that excess rainfall years are during the ascending phase of the alternate cycles in sunspot activity. They also found significant correlation between sunspot number and annual rainfall of India. Detailed analysis in this thesis showed that there is no significant correlation between KSMR and sunspot numbers.

5.6 Stratospheric Tropical Quasi-Biennial Oscillation and Kerala Summer Monsoon Rainfall

The Quasi-Biennial Oscillation (QBO) in the mean zonal wind is a dominant feature of the tropical stratosphere in the height range 20-30km. The easterly and westerly wind regimes alternate regularly with a period varying from about 24 to 30 months (Ebdon and Veyard, 1961). This oscillation occurs simultaneously in both hemispheres and at all longitudes. An important feature of the oscillation is its downward phase propagation. The wind reversal first appears above 30km and propagates downward at a speed of about 1km/month (Reed and Rogers, 1962; Holton, 1968). The amplitude reaches its greatest strength at an altitude of about 24 km and diminishes rapidly as the downward moving wave approaches the tropopause (16km) where the phenomena essentially disappear.

The discovery of the QBO in tropical stratospheric winds stimulated the search for stratospheric – tropospheric links. A link between the Indian monsoon and stratospheric zonal winds were established by Rao et al. (1978); Mukherjee et al., (1979). A dominant QBO spectral peak in the Indian monsoon

rainfall and the number of monsoon storms/depressions was also reported (Bhalme, 1972; Jagnnathan and Bhalme, 1973; Bhalme and Jadhav, 1984). Mukherjee (1985) showed that there is a tendency for monsoon rainfall of India to be less during the easterly phase of the QBO.

The Quasi-Biennial Oscillation (QBO) monthly Zonal Wind Index for 30mb (24km) of the period 1953-2001 is used to find a relationship of the QBO and the KSMR. The details of the data is discussed in Chapter 2. The figure 5.6 gives the linear correlation coefficient between the QBO index for each month and KSMR. It is clear that there is no significant correlation between QBO and KSMR. Earlier Bhalme et al.(1987) had found statistically significant relationship between QBO and Indian summer monsoon rainfall for the period 1958 –1985.

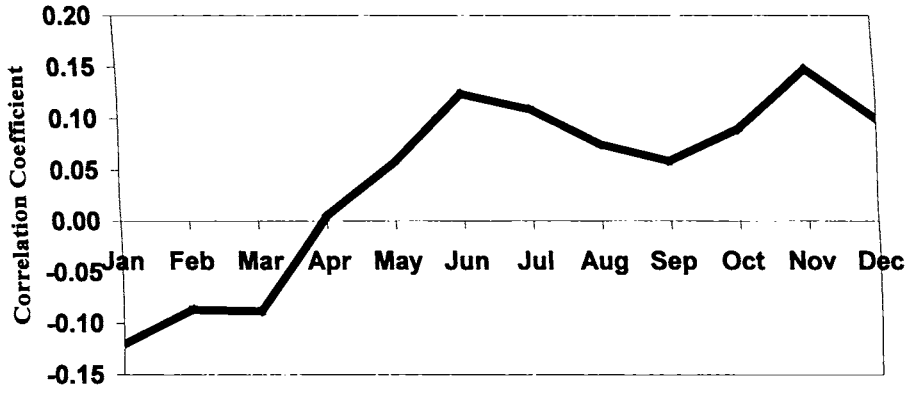

Fig. 5.6: Correlation between QBO Zonal wind index and KSMR

From the above discussions it is clear that the above parameters cannot be used as potential factors of long-range forecast of monsoon rainfall for Kerala. While, there is no close relationship between strong/moderate El Niño years and KSMR, the relationship of monsoon rainfall of Kerala and SOI have also not shown a persistent relationship during the years. The 500mb ridge position has a significant correlation with All India monsoon rainfall, but the correlation is not significant even at the 95% level for Kerala monsoon rainfall.

5.7 Possible factors for Long-Range Prediction of KSMR

5.7.1 Low Level Vorticity Factor

(a) 850hPa Zonal Wind

Figure 5.7 gives the correlation map of the 850hPa zonal wind for the month of May and the summer monsoon rainfall of Kerala. It is seen from the figure that there is an area of significant negative correlation between 5^0N and 15^0N extending from 30 to 120^0 E and an area of significant positive correlation at the equator and to its south over the Indian ocean. Positive correlation indicates that during years of good monsoon over Kerala there is strong westerly anomaly at the equator and to its south and negative correlation shows that the easterly anomalies are stronger north of the equator in the month of May. Therefore, during years of good summer monsoon rainfall in Kerala, there will be large positive (cyclonic) vorticity anomaly in the area north of the equator (0 to 15^0N, 60^0E to 100^0E) and during poor monsoon years vorticity anomaly will be negative. A measure of vorticity can be obtained by taking the velocity gradient of the zonal wind in the y-direction. . Thus the difference in the average of the 850hPa zonal wind between the boxes bounded by co-ordinates (a) 2.5^0S to 2.5^0 N, 55^0 to 75^0E and (b) 10 to 15^0 N , 55 to 75^0E is taken as a measure of vorticity. The correlation between KSMR and the vorticity factor thus measured is –0.49 (significant at 99% level) for the period 1977 to 2003.

(b) Outgoing Long-wave Radiation (OLR)

The cyclonic rotation of air (vorticity) in the atmospheric boundary layer over south Asia is a dynamic forcing for the generation of vertical upward air motion and rainfall. Thus in a DRY/WET monsoon year, we expect a –ve/+ve anomaly in convection during May in an area equatorward of Kerala. This relationship is clearly seen in the correlation map of OLR and KSMR (fig.5.8). The area of negative correlation just south of India indicates the presence of increased convection there in the month of May prior to a good monsoon season in Kerala and vice versa. The correlation of OLR in the box 5^0S to 5^0N and 75

to 95^0 E in May with the following KSMR for the period 1979 to 2003 is –0.61 which is significant at the 99% level.

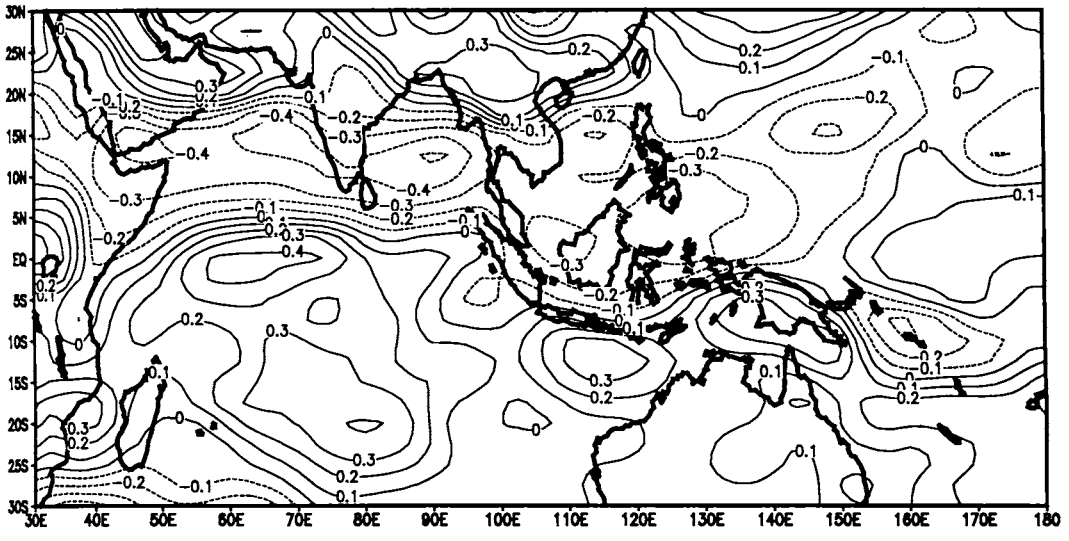

Fig. 5.7: Correlation map between 850hPa zonal wind of May and KSMR

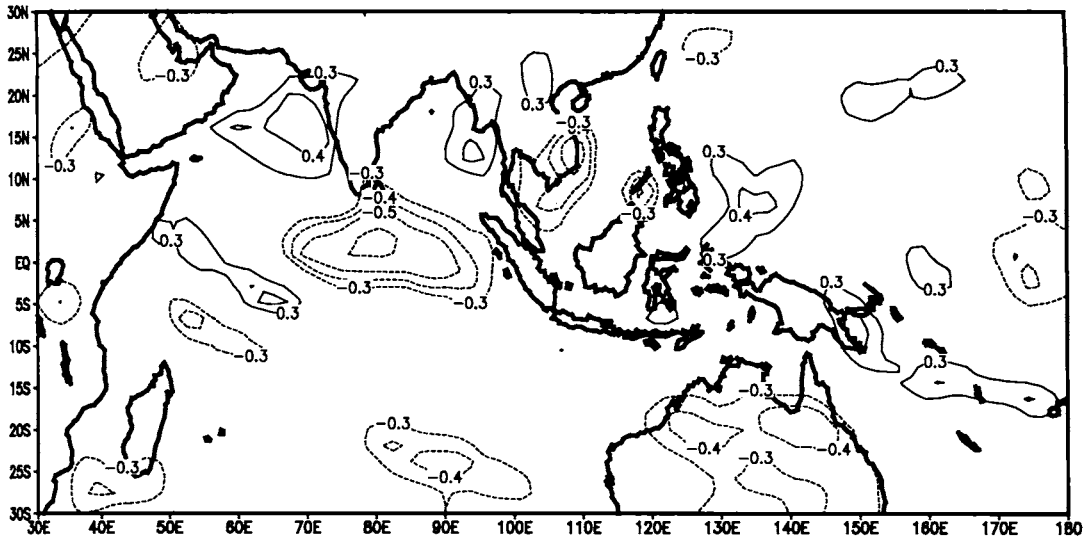

Fig. 5.8: Correlation map between Outgoing Longwave radiation (OLR) of May and KSMR

(c) Vertically Integrated Moisture (VIM)

Latent heat release, the heating of the atmosphere in a deep column and pumping of moisture upwards by the cumulonimbus towers are important consequences of the low–level convergence and the resulting moisture convergence and vertical air motion. Vertically integrated moisture in the atmosphere is largely proportional to the amount of cumulus convection and rainfall. Modelling studies (Shukla and Wallace, 1983; Stone and Chervin, 1984) have also shown that precipitation anomalies are primarily associated with anomalous low-level moisture convergence. The depth of liquid water that would result by the precipitation of the entire water vapour present in a vertical atmospheric column of unit cross section is taken as Vertically Integrated Moisture (VIM). The VIM data is taken from the NCEP/NCAR reanalysis data set and the description is given in Chapter 2. Figure 5.9 shows the correlation map of the vertically integrated moisture of May and KSMR. The significant positive correlation shows that the precipitable water in the atmosphere increases during May prior to a good monsoon. The correlation coefficient of VIM in a box 5^0S to 5^0N and 75 to 95^0E is +0.53 which is significant at the 99% level. Srinivasan (2001) developed a simple Thermodynamic model for seasonal variation of monsoon rainfall. He has shown that precipitable water (that is, the total amount of water vapour in the column) plays an important role in determining the strength of the monsoon. Based on this thermodynamic approach, he has been able to model successfully the rainfall pattern in Africa, Asia and South America over the years.

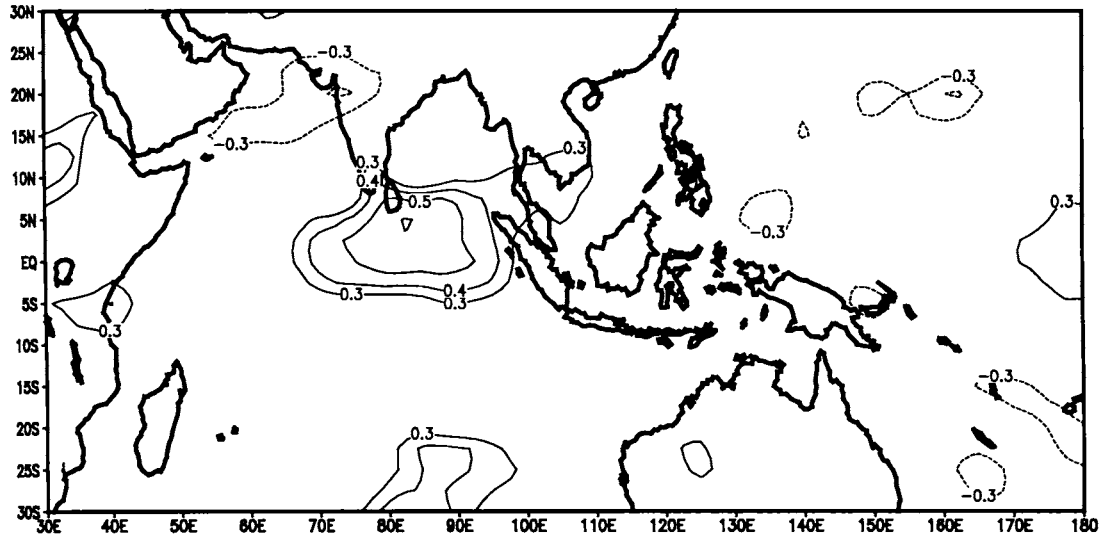

Fig. 5.9: Correlation map between Vertically Integrated Moisture (VIM) of May and KSMR

(d) Sea Surface Temperature (SST)

There is considerable observational evidence (Cornejo-Garrido and Stone, 1977; Ramage and Hori, 1981; Rasmusson and Carpenter, 1982; Horel, 1982; Liebman and Hartman, 1982) to show that the precipitation anomalies in the tropics are closely associated with the anomalies in the Sea Surface Temperature (SST). Joseph (1981) showed that there is a correlation between monsoon rainfall of India and SST anomalies in the Indian seas. A statistical model developed by A.K. Sahai (2002) at the Indian Institute of Tropical Meteorology (IITM), Pune, using only global SSTs, predicted 11-12 per cent rainfall deficit for 2002. However, the robustness of a model that is based only on SSTs of 18 regions of the world's oceans is yet to be proven.

Figure 5.10 shows the correlation maps of KSMR and SST for the 5 seasons. (a) Previous June-August (Pre. JJA) ;(b) Previous September – November (Pre. SON) ;(c) Previous December to February (Pre. DJF); (d) Concurrent March-May (Con. MAM). (e) Concurrent June-September (Con. JJA) for the period 1977-1998. The SST anomaly is used by removing the 11-

year running mean, since SST has a long-term trend. It is seen from the figure that one-year before a good monsoon rainfall in Kerala during June-August, the entire equatorial Pacific basin and the Indian ocean is warm (positive correlation). There is cold SST anomalies (negative correlation) in the western Pacific only. By September –November, the Indian ocean remains warm and there is a build up of cold temperatures in the west Pacific. The relationship remains in December to January but becomes very prominent during March-May. That is prior to a good monsoon in Kerala there is an area of positive SST anomaly in the tropical Indian ocean and negative SST anomaly in the west tropical Pacific ocean during the March-May season both north of the equator. The correlation between the SST gradient (difference in SST between (a) 0-10N,60-90E and (b) 0-10N, 140-150E) for March-May season and KSMR is +0.49 (significant at 95%). It is interesting to note that during the monsoon season the relationship weakens.

It has been pointed out by Reihl (1979), Sarchik (1985) and others that the lower troposphere over the tropical oceans can be efficiently mixed in the vertical due to buoyant convection forced by surface evaporation to about 2- 3 km. If the tropical lower troposphere is relatively well mixed there will be horizontal gradients in temperature corresponding to SST gradients. This temperature gradient in the low-levels of the atmosphere would induce pressure gradients. The temperature-induced pressure gradient between the south Indian Ocean and west Pacific (Fig.5.10d) will produce an anomalous easterly flow north of the equator in low latitudes during the March-May season just prior to a good monsoon in Kerala. This is reflected in the 850hPa zonal flow (fig.5.7).

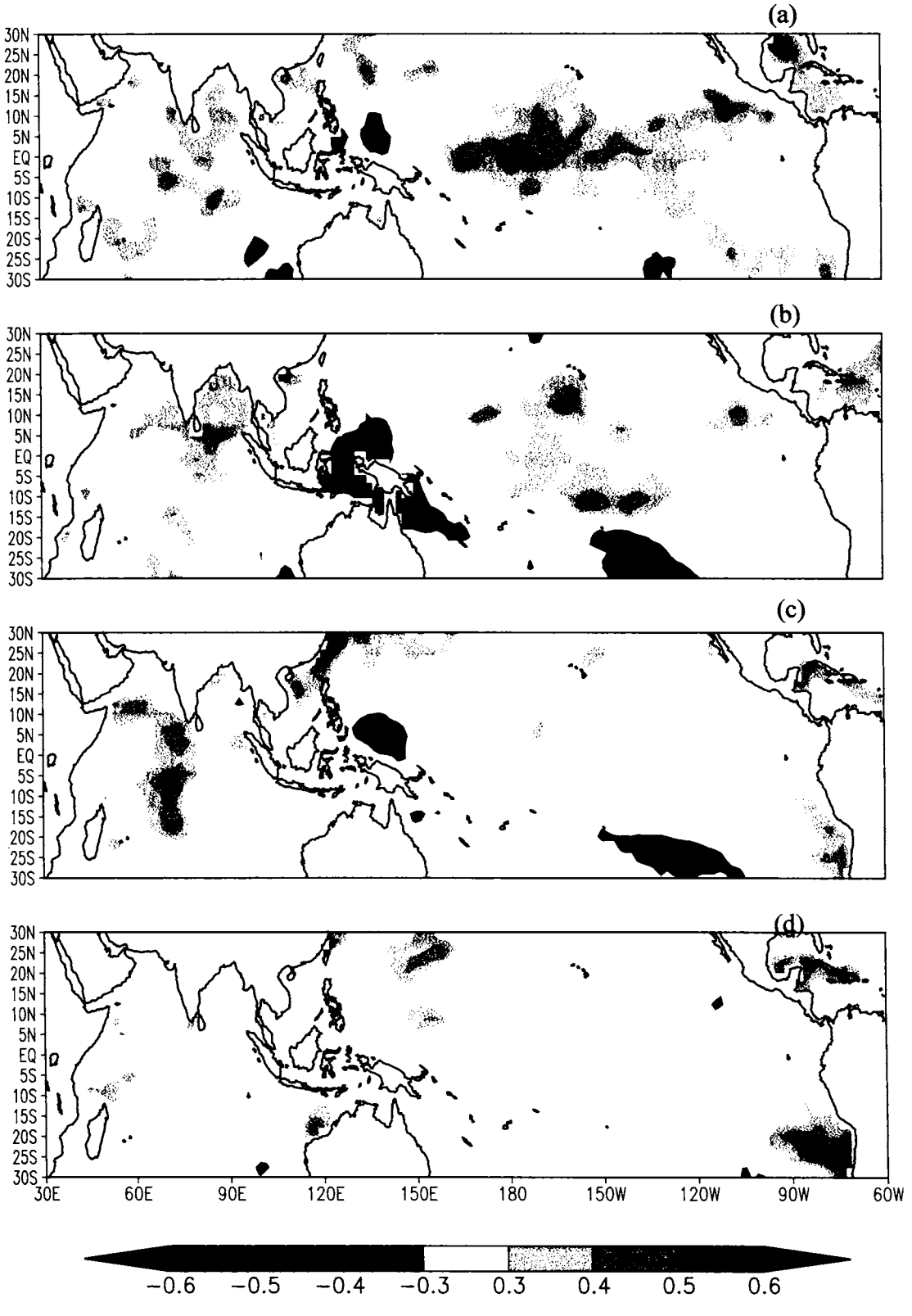

Fig. 5.10: Correlations maps of KSMR and (a) Pre.JJA; (b)Pre.SON (c)Pre. DJF; (d)Con.MAM; (e)Con.JJA.

Thus the four factors discussed in this section are related with each other. SST gradient in the east-west direction is related to the 850hPa easterly wind anomalies which create positive vorticity anomaly that generate convection (OLR) anomaly which generates VIM anomaly. One of these factors could be used for the LRF of KSMR.

Table 5.7 shows the inter-correlations between the four factors coming in this group. We find that all these correlations are significant at the 95% level except the correlation between OLR and SST gradient. However, we chose the VIM as the potential predictor from this group.

Table 5.7: Intercorrelations among the various parameters under the vorticity factor

	Vorticity	VIM	OLR	SST gradient
Vorticity	1	-0.61	0.60	0.44
VIM		1	-0.73	0.54
OLR			1	-0.25
SST gradient				1

5.7.2 Global Temperature/Eurasian Snow Cover

Monsoon is basically a thermally driven large-scale circulation and any thermal anomaly will have its influence on the monsoon. Sikka (1980) examined the All-India summer monsoon rainfall and northern hemisphere surface air temperatures during the period 1875 to 1975 and observed that the high rainfall epoch (1921-1950) was associated with higher temperatures and the low rainfall epoch (1951-1970) with lower temperatures. Verma et al., (1985) examined the relationships between Indian monsoon rainfall and northern hemisphere surface air temperatures. Their results suggest a statistically significant positive relationship with a time lag of about 6-months between monsoon rainfall and northern hemisphere surface temperature. A cooler

northern hemisphere during January/February leads to a poor monsoon. Mooley and Paolino (1988) and Krishnakumar et al. (1997) studied the relationship between pre-monsoon thermal field over India and the following summer monsoon rainfall using May minimum and maximum temperatures. Recently, Rajeevan et al., (1998) found significant differences in the composite of temperature anomaly patterns between excess and deficient monsoon years over north Europe, central Asia and north America during January to May, over north west India during May and over eastern parts of Asia during July. They suggested that during excess (deficient) monsoon years temperature gradient over Eurasian land mass from sub-tropics to higher latitudes was directed equatorwards (polewards) indicating strong (weak) zonal flow.

In the present study we have used the monthly values of 2-meter level air temperature obtained from NCEP/NCAR to find out the relationship between KSMR and the temperature anomaly. The data details are given in Chapter 2. Figure 5.11 shows the correlation map of KSMR and the 2m-temperature (mean of January & February) for the period 1950 to 2003, 1950 to1976 and 1977 to 2003. It can be seen that there is a marked difference in the spatial pattern of correlation prior to and after 1976. While there was negative correlation between temperatures in western part of the subcontinent and KSMR during the whole period 1950 to 2003, there appears to be a region between 140 to 160E which is positively correlated during 1950 to 1976. During the period from 1977 to 2003, however, the positive correlation is absent and also the region of negative correlation over northwest India has shifted to northeast India. This agrees with the earlier studies that there has been an abrupt climate shift during 1976.

A cold temperature anomaly in the region during January and February is associated with a good monsoon season for Kerala and vice versa. We have taken the temperature (mean of January & February) of the box bounded by latitudes 22.5^0N and 32.5^0N and longitudes 80 to 100^0E as a potential factor for

long-range prediction. The correlation of the temperature in this box and KSMR is –0.49 which is significant at the 99% level.

The extent of winter and spring-time snow cover over the Eurasian land mass and the latent heat released during spring have a major impact on the land-sea thermal gradient that drives the monsoons. Positive snow anomalies in winter and spring give rise to colder ground temperatures in the subsequent summer because a substantial fraction of the available solar energy during spring and early summer goes toward melting the snow and evaporating water from the wet soil rather than toward heating the ground. Excessive snowfall in the early part of winter also tends to reduce solar radiation in winter by increasing the surface albedo, resulting in persistently colder temperatures. Conversely, reduced snow cover over Eurasia strengthens the spring and summer land-sea thermal contrast and is considered favourable for the strong south-west monsoonal winds and positive rainfall anomalies over the subcontinent.

Interannual variability of snow extent over the Eurasian continent during the winter season has long been considered to have a possible impact towards the climatic conditions of the subsequent seasons. "Blanford hypothesis" suggests an inverse relationship between the winter and spring snow accumulation over the Himalayas and the subsequent monsoon rainfall over India. This relation was later supported by Hahn and Shukla (1976) where they used snow area data to show a statistically significant negative correlation with Indian summer monsoon rainfall. Extending this result to a continental scale, Bamzai and Shukla (1999) showed that the inverse correlation between the Indian monsoon rainfall exist only over the western European region during late winter, and over the western Russian plains during early spring. Observational studies have also suggested a significant correlation between monsoon rainfall and Himalayan snow cover (e.g. Dickson 1984). Fasullo (2004) showed that while the snow cover is largest in north Eurasia, its variability is more pronounced over southwestern Asia and across the northern Indian Himalayan

and Tibetan plateau regions. He also showed that correlation between Indian summer monsoon rainfall and snow cover is largely from anomalies in the northern Eurasian region during El Nino neutral years. Studies have also raised the possibility that enhanced Eurasian snow amounts may themselves be part of a remote response to the warm phase of El Niño in which there is a systematic equatorward shift in the Asian subtropical jet in the winter and spring preceding the monsoon (e.g. Webster and Yang 1992, Soman and Slingo1997).

The seasonally reversing monsoons of the Indian ocean drive one of the most energetic current systems in the world and the greatest seasonal variability observed in any ocean basin. It is the only ocean that fully reverses its circulation on a semi-annual basis, a phenomenon in which the Indian Ocean, the Eurasian continent and the Pacific Ocean play significant roles. In summer, (south-west monsoon: June-September), heating of the Eurasian land mass results in low pressure over Asia, while high pressure prevails over the Indian Ocean. The direction of the monsoon winds is then south-westerly. In winter, (north-east monsoon: November-February), cooling of the northern hemispheric land mass results in high pressure over land while lower pressure prevails over the Indian ocean, causing a reversal in the direction of the monsoon winds from southwesterly to northeasterly.

The correlation coefficient for the Eurasian Snow Cover Extent (SCE) during December and Kerala monsoon rainfall for the period 1977 to 2003 is -0.43 which is significant at the 95% level. Earlier Rajeevan et. al. (2004) found negative correlation (-0.46) between Eurasian Snow Cover for December and All India Summer Monsoon rainfall for the period 1983–2002. They have used this as a potential predictor in the new IMD operational long-range forecast model. The 21-year sliding correlation between Eurasian SCE and KSMR is given in fig. 5.12. From the figure it is clear that the correlations till the period 1990 had a steady increase and then showed a slight fall. But it is seen there is a tendency for the correlations to increase in the coming decades.

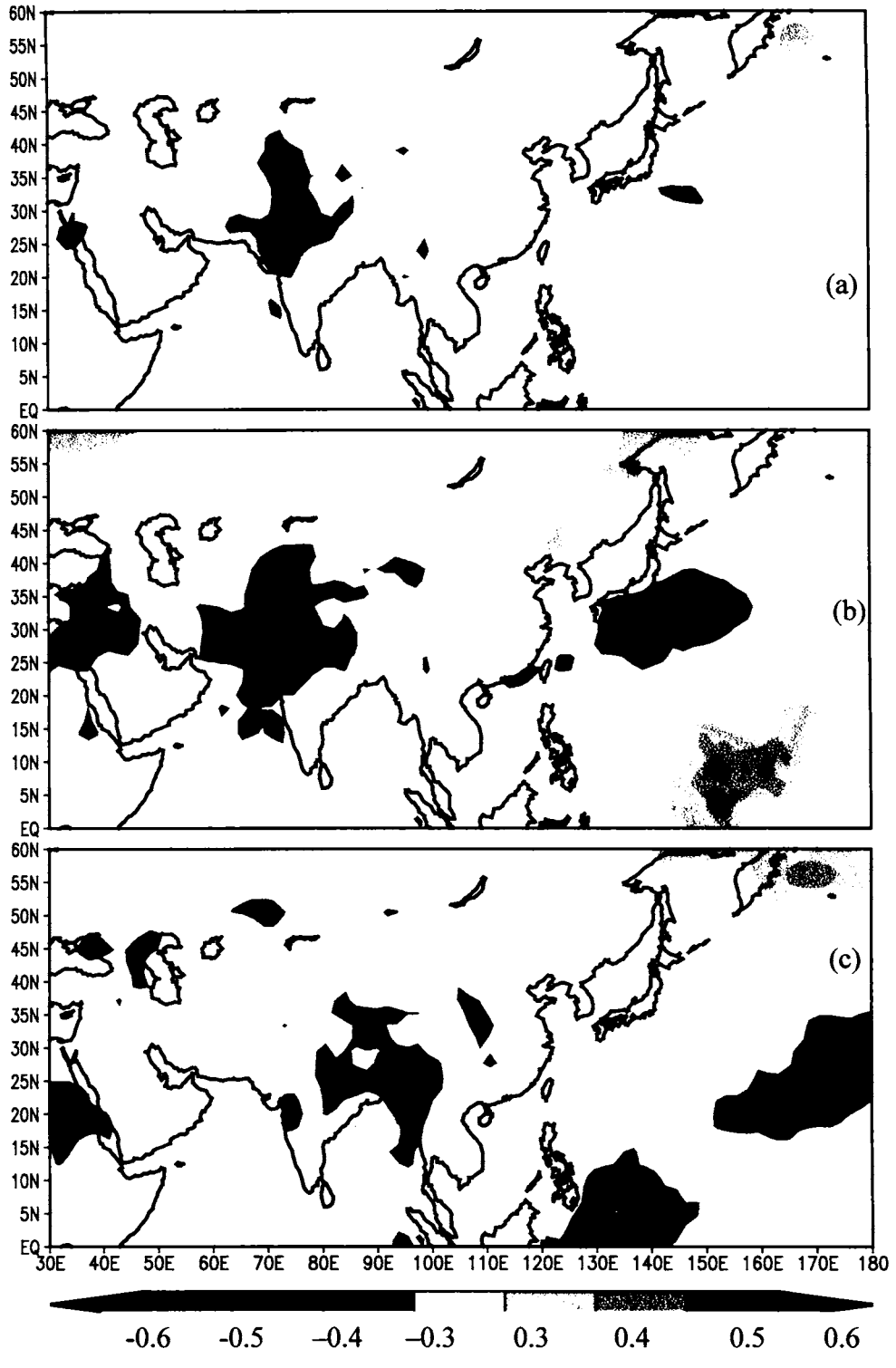

Fig. 5.11: Correlations maps of KSMR and 2m-temperature for the period (a) 1950-2003; (b)1950-1976 (c)1977-2003

In El Niño events before 1980, colder Eurasian temperature anomalies coupled with positive SST anomalies in the Pacific coincided with negative monsoon rainfall anomalies over India. The usual historical inverse relation between the monsoon and ENSO was maintained. However, in recent decades, the increased pre-monsoon surface temperatures over Eurasia due to global warming far exceeded the warming in the Indian Ocean. Thus, the stronger land-sea thermal gradient has more influence on the monsoon rainfall, apparently overriding the influence of El Niño (Kumar et al., 1999).

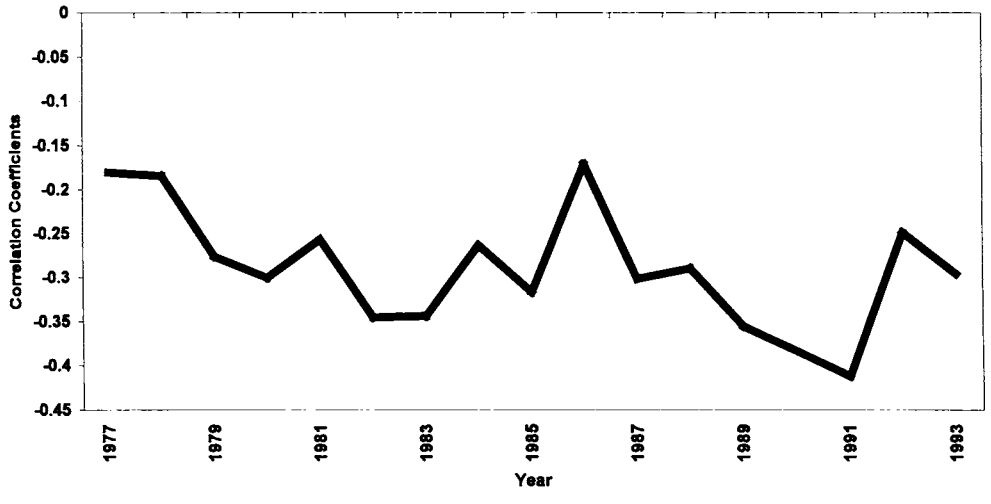

Fig. 5.12: 21-year sliding correlation between Eurasian SCE and KSMR

The correlation between 2-m temperature during January and February and Eurasian Snow Cover Extent during December for the period 1977 to 2003 is +0.43. Therefore we take one of these two factors, that is the 2-m temperature of January and February as a factor for long-range prediction of KSMR.

5.7.3 Upper Tropospheric Winds

The monsoon circulation over India involves marked changes in the upper-tropospheric wind field. There have been many studies to show that the upper-winds during their pre-monsoon transition phase can provide a useful predictor. Verma and Kamte (1980) and Joseph et al. (1978) have identified the association between Indian monsoon rainfall and the 200hPa meridional wind component for the month of May and indicated its potential for prediction of the

seasonal rainfall. Joseph et al (1981) and Parthsarthy et al., (1991) have further investigated the relationship between the meridional wind index (arithmetic average of the 200 hPa meridional wind component of wind for May at Bombay, Delhi, Madras, Nagpur and Srinagar) and Indian summer monsoon rainfall and found significant correlation between the two series.

Figure 5.13 gives the correlation map of the 200 hPa meridional wind obtained from NCEP/NCAR data set for the month of May and KSMR. The meridional wind over almost whole of India show a positive correlation with KSMR, which is particularly significant over north-west India. Almost equally strong negative correlation is seen on western side. A region of significant positive correlation is also seen around Burma and far east. Positive correlation means southerly meridional winds are stronger during years of good KSMR since southerly meridional wind is taken as positive. The physical link between this type of circulation in relation to KSMR is not well understood. Joseph et al. (1981) had shown that the southerlies during May over India particularly northwest India become stronger in poor ISMR. We take average of the meridional wind of May for the box bounded by co-ordinates $35^0 - 45^0$N, $65^0 - 75^0$E as a parameter for prediction of monsoon rainfall of Kerala. The correlation of this box-average and KSMR is +0.54 which is significant at 99% level.

5.7.4 Zonal Winds in the Stratosphere

The winds in the stratosphere during northern hemisphere winter are found to have a relation with the summer monsoon rainfall of India. Even though the physical link between this wind pattern and ISMR is not clearly understood, the 50hPa wind of winter has been used as a predictor for all India summer monsoon rainfall (Gowariker et al., 1991) and also in the IMD's new operational long-range forecast model (Rajeevan et al., 2004). We have studied

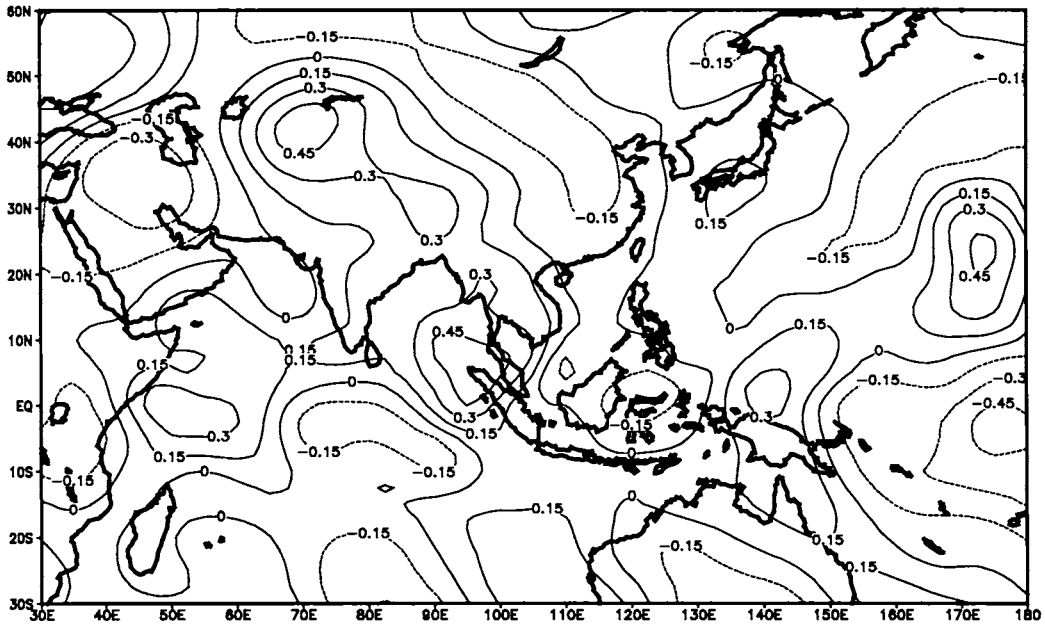

Fig. 5.13 : Correlation map between 200hPa meridional wind of May and KSMR

the relationship of the 50hPa wind during winter (mean of January & February) and KSMR. Figure 5.14 shows the correlation map of the wind and KSMR. There is a region of large negative correlation north of around 25^0N and extending between 40 and 120^0E, and positive correlation south of it. The 50hPa circulation is characterised by strong westerly Jetstream during winter over the negative correlation area, which means that when KSMR is below normal, the westerly Jetstream at 50hPA is stronger. The wind for the box (30^0 –45^0N, 80-120^0E) is taken as a possible factor for long-range prediction of KSMR. The correlation of this box average and KSMR is –0.45 (significant at 95%).

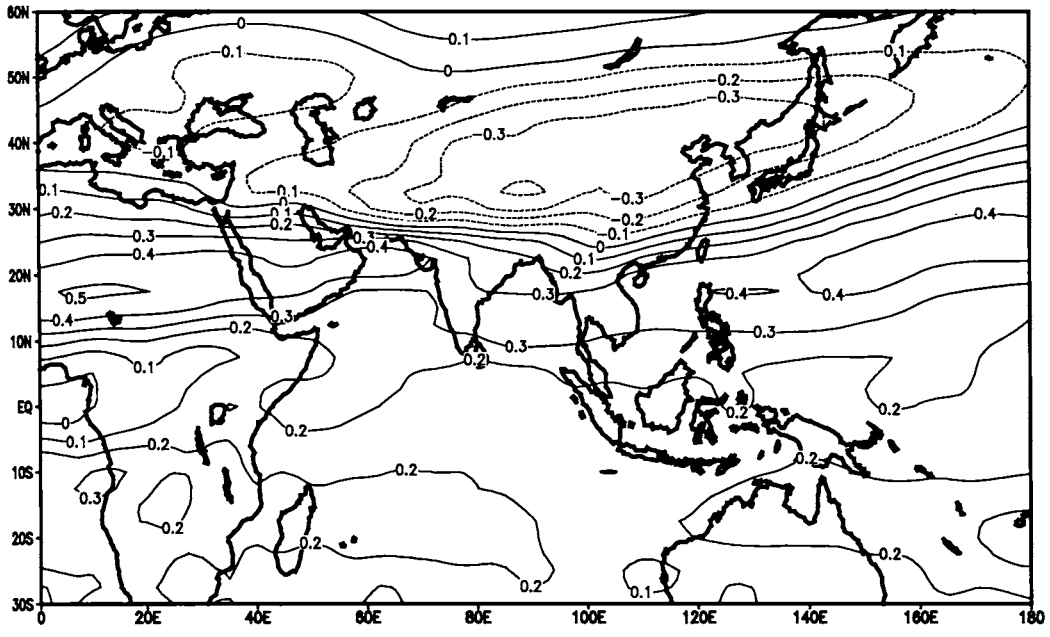

Fig. 5.14 Correlation map between 50hPa zonal wind of winter (mean of January & February) and KSMR

5.8 Multiple Regression of KSMR

Most of the studies on long-range forecast of Indian monsoon rainfall are based on empirical/ statistical techniques. Statistical models have inherent limitations (Kumar et al., 1995, Rajeevan, 2001, Thapliyal et al., 1992). Although correlation is a very useful diagnostic tool in bringing out the association between various meteorological fields/circulations, it is highly sensitive to the data window over which it is calculated, in terms of both its spatial position and length of the window in the time domain. They may also undergo epochal changes and there may be strong cross correlations between the parameters (Hasternath and Greischar, 1993, Parthasarthy et al., 1991). Dynamical atmospheric general circulation models with specified boundary conditions and varying initial conditions may eventually have better predictive skills for seasonal rainfall. However, as of today, global dynamical models do not have the required skill to simulate the mean monsoon and its variability. They are further hampered by the lack of data in ocean regions which is very important for the monsoon.

The most commonly used statistical technique for the long-range prediction of monsoon rainfall is linear regression analysis (Krishna Kumar et al., 1995). A large number of regression models (simple as well as multiple) have been proposed. The predictors for the model are either subjectively chosen as representing various important forcings on the monsoon or entered into the scheme by some objective criteria. Both approaches have their limitations (Parthasarthy et al., 1988; Hasternath et al., 1993).

In the present study the multiple regression technique is used to give a long-range forecast method for KSMR. The predictors identified in this chapter fall into four major categories. Factors in each group show significant inter-correlations among themselves as discussed earlier, hence we choose one factor from each group. The parameters chosen and their correlation (CC) with KSMR are given in Table 5.8. The presence of multicollinearity among predictors imposes the problem of redundancy (Krishna Kumar et al., 1995).

Table 5.8: Possible factors for long-range prediction of KSMR

Domain of predictor/parameter	Month/Season	Acronym	CC	Period of CC
Vorticity factor Vertically Integrated Moisture	May	VIM	+0.53**	1977-2003
Global Temperature 2-m Temperature	(Jan.+Feb)/2.	TMP	-0.49**	1977-2003
Upper Tropospheric Wind 200hPa meridional wind	May	200V	+0.54**	1977-2003
Stratospheric Wind 50hPa zonal wind	Jan.+Feb	50U	-0.45*	1977-2003

* significant at 95% ** significant at 99%

The final regression equation, which is given below shows a multiple CC of 0.72. The standard error of estimate is 22.69cm which is 63% of the standard deviation of 35.7cm.

KSMR=354.22+4.49*VIM-1.33*TMP+3.46*200V-1.75*50U

Using this equation the Kerala Summer Monsoon Rainfall is estimated. Table 5.9 gives the actual and estimated values and their percentage departure. From the figure 5.15, it can be seen that although the equation picks up the rainfall fairly well in a large number of years there are large differences in some years.

Table 5.9: Estimated values if KSMR using the regression equation

Year	Actual Rainfall (cm)	Estimated Rainfall (cm)	% Departure
1977	178.98	175.75	1.8
1978	204.78	216.54	-5.7
1979	186.84	190.12	-1.8
1980	197.54	205.73	-4.1
1981	252.64	224.25	11.2
1982	174.94	179.59	-2.7
1983	205.4	187.36	8.8
1984	162.23	181.14	-11.7
1985	164.79	189.52	-15.0
1986	152.88	183.20	-19.8
1987	145.66	140.66	3.4
1988	205.09	189.53	7.6
1989	176.33	189.07	-7.2
1990	151.73	174.53	-15.0
1991	224.71	207.79	7.5
1992	215.27	197.83	8.1
1993	175.42	188.51	-7.5
1994	224.27	188.07	16.1
1995	172.37	193.73	-12.4
1996	188.89	178.14	5.7
1997	230.33	187.37	18.6
1998	203.22	212.14	-4.4
1999	151.62	160.06	-5.6
2000	162.03	161.52	0.3
2001	168.67	131.10	22.3
2002	129.23	154.57	-19.6
2003	158.07	178.46	-12.9

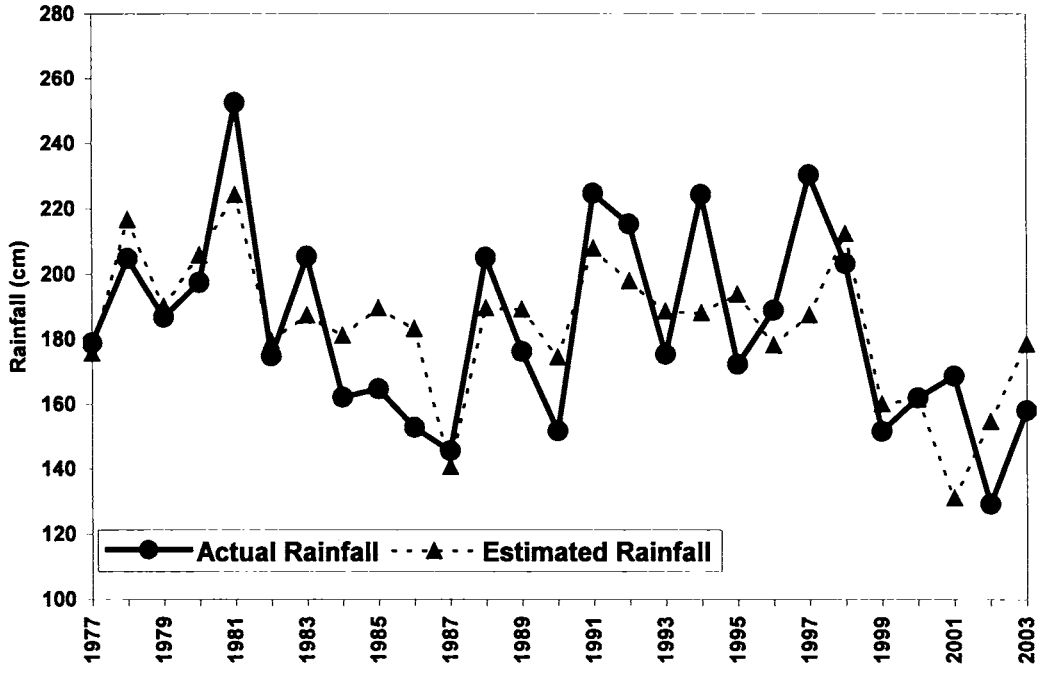

Fig. 5.15 : Actual and Estimated values of rainfall using the multiple regression equation using VIM

The Vertically Integrated Moisture as given in NCEP/NCAR data set is of class B wherein although there are observational data that directly affect the value of the variable, the model also has a very strong influence on the variable. Hence, we tried to use the measure of vorticity (VF) derived from the 850hPa zonal wind as discussed in section 4.8.1 (a) as a factor instead of VIM. The correlation value of this factor and KSMR is –0.49. The multiple regression equation using this factor is given below and has a multiple correlation coefficient of 0.70 and standard error of estimate 27.2. Table 5.10 gives the actual and estimated values and their percentage departure using this factor and is illustrated in figure(5.16).

KSMR=256.6-2.2*VF-0.21*TMP+3.72*200V-1.91*50U

Table 5.10: Estimated values of KSMR using the regression equation with zonal wind index instead of VIM

Year	Actual Rainfall (cm)	Estimated Rainfall (cm)	% Departure
1977	178.98	178.18	0.4
1978	204.78	201.13	1.8
1979	186.84	195.20	-4.5
1980	197.54	210.90	-6.8
1981	252.64	211.48	16.3
1982	174.94	179.92	-2.8
1983	205.40	178.08	13.3
1984	162.23	187.97	-15.9
1985	164.79	187.07	-13.5
1986	152.88	193.39	-26.5
1987	145.66	143.69	1.4
1988	205.09	187.48	8.6
1989	176.33	196.26	-11.3
1990	151.73	158.22	-4.3
1991	224.71	209.85	6.6
1992	215.27	198.75	7.7
1993	175.42	184.10	-4.9
1994	224.27	190.19	15.2
1995	172.37	198.76	-15.3
1996	188.89	183.28	3.0
1997	230.33	205.62	10.7
1998	203.22	200.17	1.5
1999	151.62	156.28	-3.1
2000	162.03	159.21	1.7
2001	168.67	132.82	21.3
2002	129.23	156.64	-21.2
2003	158.07	181.87	-15.1

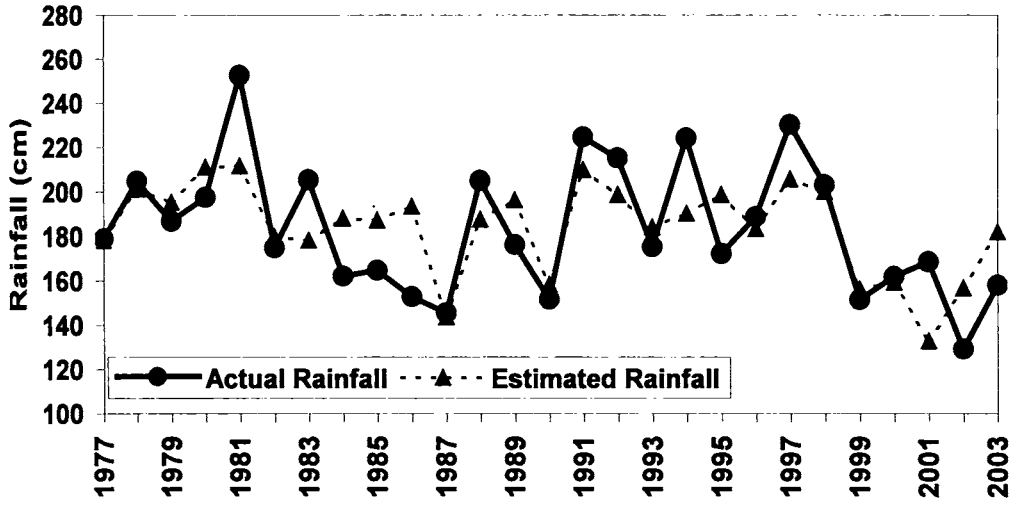

Fig. 5.16 : Actual and Estimated values of rainfall using the multiple regression equation using Vorticity factor

Positive skill in forecasting the seasonal rainfall for India as a whole and also of its three large subregions and meteorological subdivisions lying in west-central parts of the country was obtained by a multiple regression model using only three parameters (Prasad and Singh, 1991). The parameters are (i) the subtropical ridge position at 500 hPa over India in April, (ii) January–April Darwin surface pressure tendency, and (iii) January and February Northern Hemispheric surface air temperature

5.9 Conclusions

The relationship between antecedent global circulation parameters with monsoon rainfall of Kerala is studied in this chapter and an attempt has been made to develop a statistical model for long-range forecast of monsoon rainfall for the state. It is seen that although there is no close relationship between DRY/WET years and El Niño/La Nina events, the El Niño years are more likely to become DRY years than La Nina becoming WET. Southern Oscillation Index (SOI) of preceding September-November and concurrent March-May has significant negative correlations with summer monsoon rainfall of Kerala for the

period 1977-2003. However, the relationship is not persistent throughout the period and hence cannot be used as a possible factor for long-range forecast of KSMR. The 500mb ridge position, which has a significant correlation with all India monsoon rainfall, is not correlated with KSMR.

An attempt to identify possible factors of long-range forecast of summer monsoon rainfall of Kerala is made in this chapter. The factors that influence KSMR are (1) Low-level vorticity of May (2) Global temperature of winter (mean of January &February) (3) 200hPa meridional wind of May (4) 50hPa zonal wind (mean of January &February) and they have significant correlation with the monsoon rainfall of Kerala. The multiple correlation coefficients of these factors with KSMR is 0.72 for the period 1977-2003 and the estimated rainfall using this equation has a standard error of estimate of 22.9cm which is about 64% of the standard deviation of KSMR.

Chapter 6
Diurnal Variation of Monsoon Rainfall of Kerala

6.1 General

Diurnal variation is seen prominently in the surface temperature, with temperature maximum at about 1400 hrs local time and minimum soon after sunrise. It is well known that at tropical stations there is a large amplitude oscillation in the surface air pressure with maximum around 1000 and 2200 hours and minimum around 0400 and 1600 hours local time. Harmonic analysis of the pressure oscillations has shown two prominent components S_1 and S_2 with periods of 24 and 12 hrs respectively. The amplitude of higher harmonics and their contribution to the total variance is small (Ananthakrishnan, 1977).

Diurnal variation in the surface winds is exhibited prominently at stations close to land-ocean boundary in the form of sea and land breezes. When fully developed, sea breeze penetrates deep into the interior even up to 100 km from the coast. For example sea breeze from Bombay is found to reach up to and even beyond Pune. (Ramanathan,1931). During the south-west monsoon months the direction of prevailing wind along the west coast of India is same as that of the sea breeze which is now much less conspicuous because of reduced thermal contrast between land and sea due to the cloudy skies and rainfall. However, at stations like Chennai on the east coast of India where there is little clouding and rainfall, sea breeze is more pronounced during the south-west monsoon months.

Diurnal variation in surface winds also occur due to vertical exchanges of momentum in the boundary layer arising from thermal convection due to the diurnal variation in ground heating by sun. This exchange of momentum due to the turbulent convection from the ground heating leads to the increase of wind speed near the ground and decrease of speed at the top of the boundary layer.

Diurnal variation of south-west monsoon rainfall of a few coastal stations in Kerala have been studied by Ananthakrishnan et al. (1979a, b), Rajan et al. (1981) and Pathan (1994). Ananthakrishnan et al. (1979a) performed Harmonic analysis of the hourly rainfall of south-west monsoon rainfall of Trivandrum, Cochin and Mangalore (just north of Kerala). A table (Table 6.1) giving the time

of maximum and variance explained of the first four harmonics of the 24-hour rainfall at these three stations as given is given below extracted from Ananthakrishnan et al. (1979a):

Table 6.1 Harmonic Analysis of Diurnal variation of rainfall (Anathakrishnan et al. 1979a)

Station	I Harmonic		II Harmonic		III Harmonic		IV Harmonic		Variance (I+II+ III+IV)
	TX (hr.)	VR (%)	T (hr.)	VR (%)	TX (hr.)	VR (%)	TX (hr.)	VR (%)	
a. Trivandrum	0912	1.1	1518	23.7	0154	12.0	1324	5.5	42.3
b.	0606	1.3	1606	5.3	0154	4.1	0948	10.2	20.9
a. Cochin	0354	50.9	1142	4.3	1600	7.0	2042	4.6	66.8
b.	0224	21.1	1118	13.5	1618	11.0	0942	0.3	45.9
a. Mangalore	0642	35.1	1724	14.3	0518	19.3	0854	2.0	70.7
b.	0718	8.5	1635	20.1	0500	27.5	1000	0.2	56.3

a. Total rainfall **b. Rainfall ≥10mm/hr.**
TX- Time of maximum (IST) **VR – Variance (%)**

From the table it is seen that while, at Cochin and Mangalore, the 24-hour harmonic (I Harmonic) has explained 51 % and 35% respectively of the variance with maximum between 0400 and 0700 hours local solar time (LST), at Trivandrum the I Harmonic is unimportant. Maximum variance at Trivandrum is in the II Harmonic which explains of about 24% of the variance with day time maximum around 1500 hours LST. For some stations along the west-coast like Bombay, the variance explained by the I Harmonic is as high as 74% (with maximum rainfall at about 0700 hrs local time). A similar study by Pathan (1994) with a different period data has however, shown that at Cochin and Mangalore the 1st harmonic explains about 80% of the total variance. In general the results show that for coastal stations in Kerala monsoon rainfall has a

prominent 24-hour harmonic with its maximum in the early morning hours. For interior stations of Kerala there has been no study reported in literature.

For stations in the tropics outside the Indian Ocean area Gray and Jacobson (1977) found that over the tropical western Pacific, rainfall has a morning maximum (0700-1200 hours local time) compared to the evening hours (1900-2400 hours local time). They also found that the diurnal variation of rainfall is more pronounced for rain of intensity > 10mm/hour associated with cumulus convection. However, in the GATE experiment over the tropical Atlantic, intensity of rainfall was found to have an afternoon maximum (analysing cases of high intensity rainfall). The rain received during 1000-2200 hours being 3-4 times greater than during 2200-1000 hours. . According to Ananthakrishnan et al. (1979b) the behaviour of south-west monsoon rainfall at the coastal stations Cochin, Mangalore and Bombay are generally similar to that of west Pacific tropics.

Morning thunderstorm and /or heavy rainfall maxima are frequent phenomena at tropical and subtropical land stations. There are many theories to explain this diurnal rainfall variability (Atkinson, 1971, Ramage, 1971, Wallace, 1975). Atkinson (1971) showed that many tropical land stations do not show a rainfall maximum during the afternoon period associated with maximum surface heating, instead many tropical continental stations show rainfall maximum during the night-time hours. Ramage (1952) also studied the diurnal variation of rainfall at stations in east Asia during summer months of May to August. He found that the morning maximum between 0700 and 1000 LST to be prominent at tropical and subtropical coastal stations of southeastern China and southern Japan. Some coastal stations and all inland stations also showed a maximum during the afternoon so a pronounced semi diurnal rainfall variation was evident at many stations.

Rajan et al (1981), studied the hourly rain contributions by all rain spells of south-west monsoon rainfall of Cochin for each chronological hour and the

hourly rainfall contributed by the spells ≥5 mm, ≥10 mm, and ≥15 mm during the hour. The hourly variation of rainfall for the season is shown in fig.6.1. He has obtained a prominent early morning maximum.

Documentation of diurnal variability of precipitation over various regions has been done extensively in the past. Wallace (1975) reviewed the work done on the diurnal variability of precipitation for various locations in the United States. The diurnal variability of coastal and inland stations in eastern Asia have been studied by Hu and Hong 1989; Oki and Musiake 1994:and Shinoda et al.1999. The results of these studies can be summarized as follows:

- Summer precipitation and thunderstorms in inland regions tend to be more frequent during afternoons while the maximum rainfall is at night or early morning over the coastal areas.
- There are however, exceptions to this general tendency. For example, summer precipitation is most frequent from the mid-night to the early morning over central United States and around 1400-1600 local solar time (LST) over the entire Florida Peninsula (Wallace 1975:Dai et al. 1999)
- During other seasons, precipitation has much weaker diurnal cycle than in summer, with a morning maximum in winter over many land areas (Dai et al.1999)
- Precipitation intensity generally has much smaller diurnal variations than precipitation frequency (Oki and Musiake 1994)
- Although a single large peak is a dominant feature in most rain gauge records, there is a secondary peak or a week semidiurnal (12hr.) cycle of rainfall at many tropical (peak around 0300LST) and mid latitude (peak around 0600LST) stations (Oki and Musiake 1994).

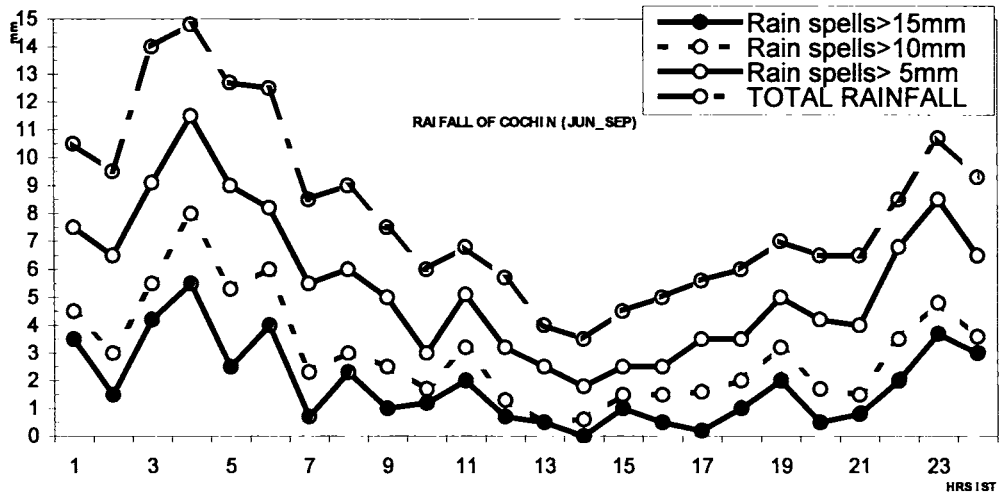

Fig. 6.1 :- The hourly variation of rainfall for the season at Cochin taken from Rajan et al. (1981)

6.2 Diurnal Variation of monsoon rainfall of Kerala

We find from the literature reviewed earlier that diurnal variation of rainfall in Kerala has been done only for a few coastal stations. In this chapter we have analysed the diurnal variability of 33 stations distributed mostly over the mid-land and high-land regions across the state. The hourly data of rainfall for the summer monsoon months (June to September) for a period 2000 to 2004 at these stations were obtained from the Hydrology Project of the State Irrigation Department. The description of data is given in Chapter 2. The details of the stations used are given in Table 6.2 and the station locations are marked in fig.6.2. It should be noted that the data distribution is more to the northern parts of the state.

Harmonic analysis of the 24-hour rainfall data sets averaged for five years has been done for all stations to study the first four harmonics (24-hr., 12-hr., 8-hr., and 6-hr. harmonics). In the tropics, it is shown that showery precipitation (due to deep cumulus convection) occurs more frequently than non- showery precipitation (Dai 2001). In the present analysis, showery precipitation days are taken as days with rainfall more than or equal to 5cm/day and harmonic analysis was done on the 24-hour rainfall data as an average of these days.

Stations which have almost the same harmonic pattern for both the rainfall sets (total rainfall days & days with rainfall ≥5cm per day) were bunched together. Stations which do not have sufficient days with rainfall ≥5cm /day are not included in the analysis. The stations can be broadly classified into (1) Stations with one rainfall peak (prominent 24-hour harmonic) (2) Stations with two rainfall maxima (prominent 12-hour harmonic).

Table 6.2: Details of the Stations used for the study

Sl. No.	Stations	Lat (deg.)	Lon (deg.)	Altitude (m)
1	Vamanapuram	8.717	76.895	41
2	Kollam	8.894	76.609	1
3	Achankovil	9.073	77.158	239
4	Konni Estate	9.204	76.873	52
5	Kanjirappily	9.563	76.776	81
6	Kottayam	9.582	76.526	15
7	Vynthala	10.264	76.300	27
8	Vettilapara	10.292	76.600	241
9	Varandrapilly	10.422	76.344	52
10	Amalanagar	10.567	76.158	44
11	Elanad	10.617	76.433	77
12	Kunnamkulam	10.646	76.067	45
13	Ottapalam	10.760	76.203	114
14	Perinthalmana	10.975	76.233	69
15	Attapadi	11.033	76.650	679
16	Parapangadi	11.048	75.863	1
17	Edakkara	11.385	76.315	66
18	Thikkodi	11.491	75.624	8
19	Kalladi	11.508	76.129	915
20	Vazhavatta	11.614	76.182	846
21	Manathavadi	11.800	76.045	731
22	Cheruvanchery	11.817	75.633	93
23	Payyavvor	11.850	75.370	1
24	Mallor	11.900	75.633	334
25	Thillenkeri	11.933	75.667	76
26	Palapuzha	11.939	75.742	66
27	Pazhassi	11.967	75.617	44
28	Kaithaprem	12.167	75.333	115
29	Kakkadvu	12.267	75.283	51
30	Pulingome	12.275	75.325	51
31	Erikkulam	12.325	75.133	40
32	Padithadukka	12.500	75.200	133
33	Paika	12.550	75.100	104

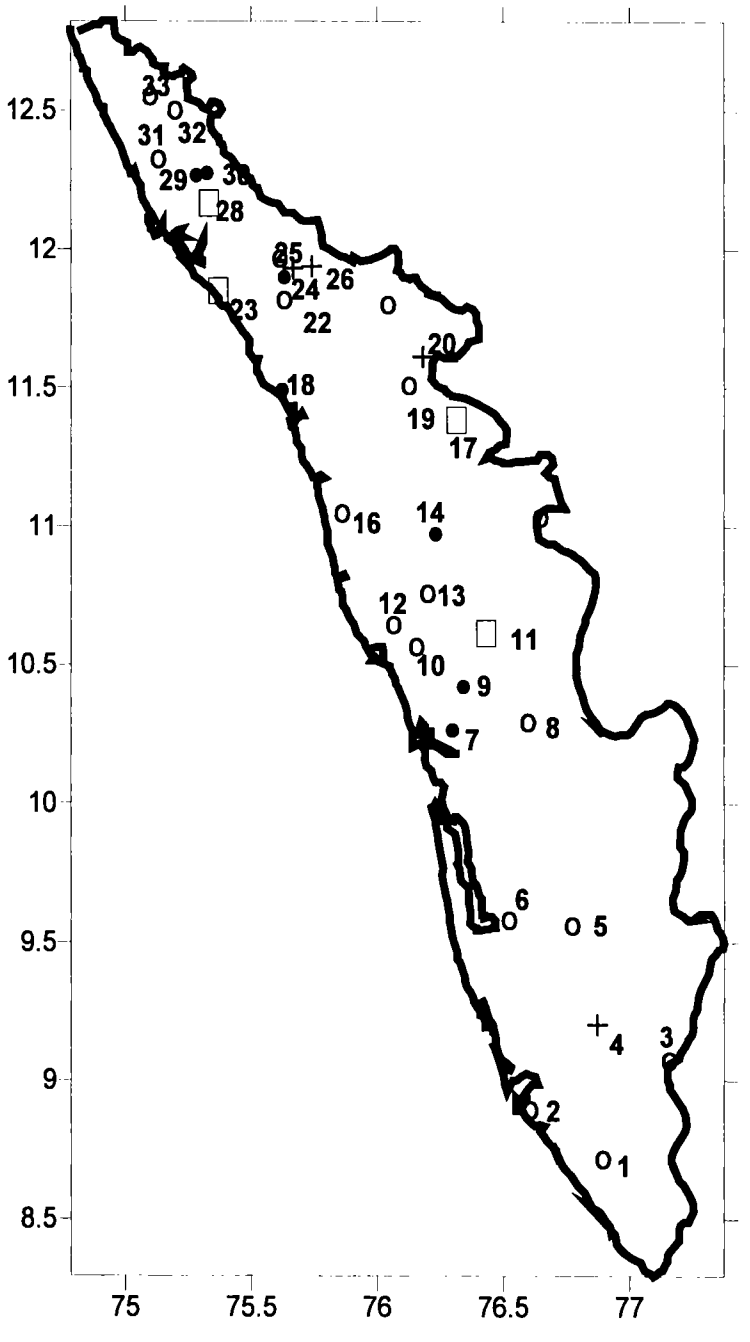

Fig.6.2 Station location used for the study. The station numbers are given as in Table 6.2

6.2.1 Stations with one rainfall peak

6.2.1.1 Stations with rainfall maximum in the afternoon-evening hours (1500 hrs to 1900hrs)

There are seven stations with a single afternoon-evening maximum as shown in Table 6.3. The stations are marked as closed circles in fig. 6.2. It can be seen that the hour of maximum rainfall peak is close to the hour of maximum of the first harmonic. The first harmonic contributes more than 45% of the total variance at most of these stations. These stations are Perinthalmana, Kakkadavu, Maloor, Vynthala, Thikkodi, Varadranpilly and Pulingome. Out of these seven stations, Thikkodi is a coastal station and all other stations lie on the slopes of the Western Ghats. Figure 6.3 give the 24-hour rainfall of 2 stations in this group along with the first harmonic, 1+2 harmonic (sum) and 1+2+3 harmonic (sum). It is noted that Perinthalmana that lies near the bell mouth of Palghat gap has both the first and second harmonic equally important unlike other stations in the group.

Table 6.3 Amplitude, Time of maximum and Variance of the first four Harmonics of stations having one rainfall maximum in the afternnon-evening

		Ist Harmonic			IInd Harmonic			IIIrd Harmonic			IVth Harmonic		
Station		Amp.	Tx	Var.(%)	Amp.	Tx	Var.(%)	Amp.	Tx	Var.(%)	Amp.	Tx	Var.(%)
Perinthalmana	TR	0.061	1528	27.4	0.061	0501	27.2	0.027	0049	5.2	0.025	0243	4.4
	5≥	0.863	1514	32.9	0.547	1841	13.2	0.251	2340	2.8	0.131	2308	0.8
Maloor	TR	0.174	1416	45.6	0.122	1826	22.5	0.016	0220	0.4	0.067	2102	6.7
	5≥	1.128	1408	56.0	0.570	1803	14.3	0.290	0038	3.7	0.508	0204	11.4
Kakkadavu	TR	0.201	1603	50.6	0.091	0308	10.5	0.030	0353	1.1	0.040	2118	2.0
	5≥	1.188	1349	32.9	0.595	0347	8.3	0.350	2027	2.9	0.715	0246	11.9
Vynthala	TR	0.126	1804	50.3	0.029	0252	2.7	0.023	0341	1.8	0.048	2201	7.3
	5≥	0.827	1532	23.5	0.516	0215	9.2	0.297	2114	3.0	0.261	2133	2.3
Thikkodi	TR	0.226	1810	77.6	0.038	2044	2.2	0.056	2217	4.8	0.060	2211	5.5
	5≥	1.255	1659	33.4	1.112	1818	26.2	0.308	2218	8.0	0.419	0217	3.7
Varadranpilly	TR	0.162	2056	34.3	0.060	2015	4.8	0.069	2100	6.3	0.013	0017	0.2
	5≥	1.454	2349	18.0	1.406	2207	16.8	0.219	0130	0.4	0.532	0152	2.4
	5≥	1.331	0931	47.5	0.860	1816	19.8	0.270	2246	2.0	0.074	2152	0.2
Pulingome	TR	0.325	1632	50.7	0.198	1953	18.8	0.215	2022	22.2	0.075	2115	2.7
	5≥	1.045	1237	52.3	0.517	1952	14.3	0.486	2005	12.6	0.318	0253	5.4

TR – Total Rainfall ; 5≥ - Rainfall greater than or equal to 5cm/day; Tx – Hour of maximum

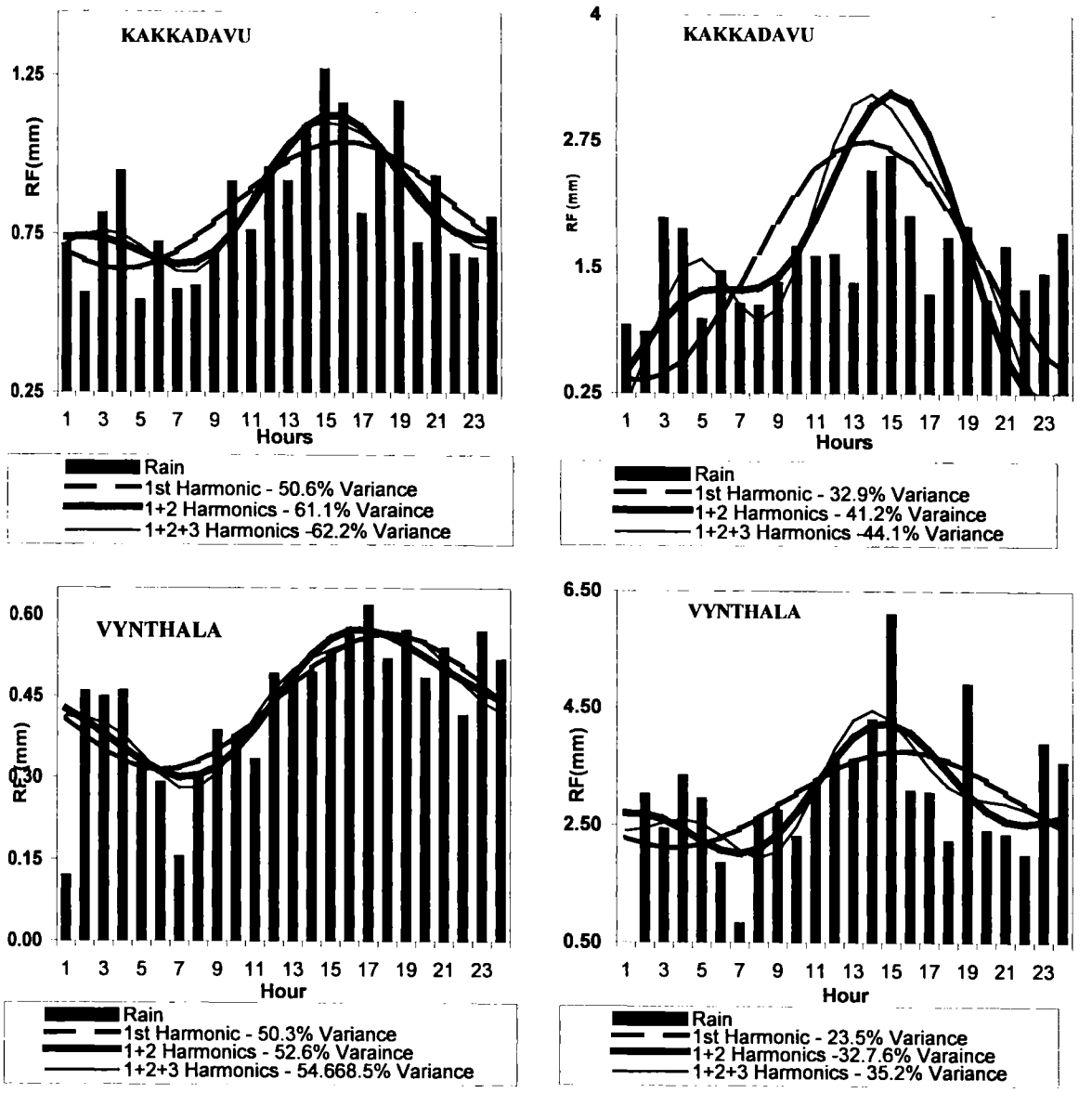

Fig. 6.3: 24-hour rainfall of Kakkadavu and Vynthala along with the first harmonic, 1+2 harmonic (sum) and 1+2+3 harmonic (sum). The left panel is for total rainfall days and right panel for days with rainfall ≥5cm per day.

Figure 6.4 gives the 24-hour rainfall along with the first harmonic, 1+2 harmonic (sum) and 1+2+3 harmonic (sum) for Thikkodi, a coastal station. It is very evident from the figure that the prominent harmonic is the 1st harmonic, which contributes about 78% of the variance for the total rainfall days (left panel of figure) and 33% for the days with rainfall more than 5cm/day (right panel of

figure). The rainfall maximum is in the evening hours (~1800 hours) for the total rainfall days and there is a rainfall minimum in the morning hours. For days with rainfall greater than 5cm per day, however, there is a maximum in the evening (~1800 hours) and there is a secondary maximum in the morning (~0700 hours). The contribution of the second harmonic is 26%. Earlier studies for coastal stations in Kerala had shown a morning maximum.

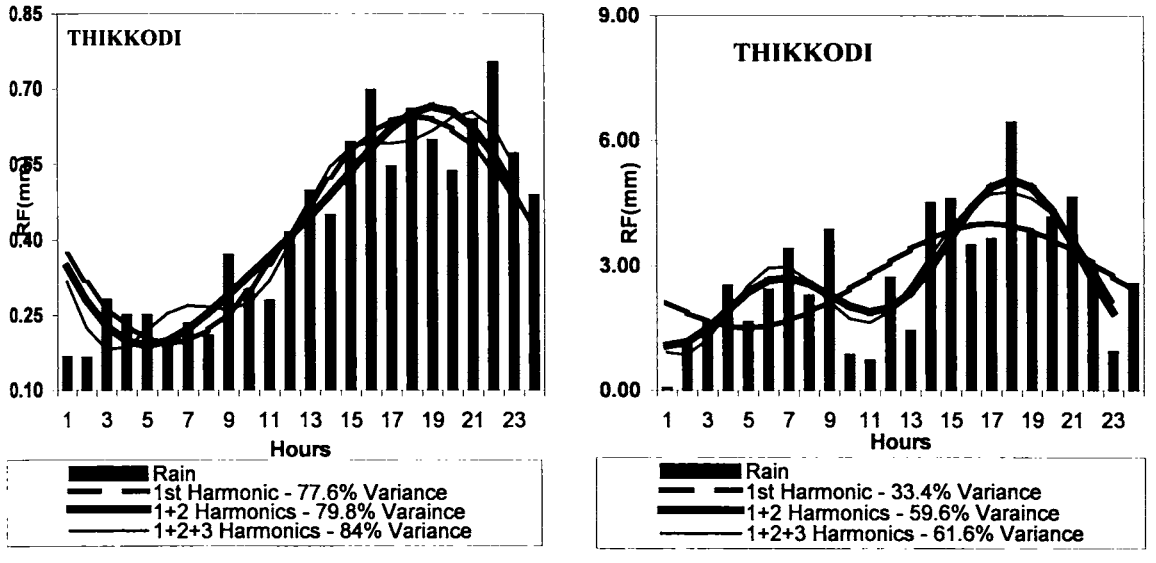

Fig. 6.4: 24-hour rainfall of Thikkodi along with the first harmonic, 1+2 harmonic (sum) and 1+2+3 harmonic (sum). The left panel is for total rainfall days and right panel for days with rainfall ≥5cm per day.

6.2.1.2 Stations with one rainfall maximum in the morning hours (0500 hrs to 1100hrs)

The four rainfall stations: Payyavoor, Kaithaprem, Elanad and Edakkara have a 24-hour rainfall maximum during morning hours. These stations are marked by open squares in fig. 6.2. The details are given in Table 6.4. Of these four stations, both Elanad and Edakkara have peculiar local topographical features. Elanad is in the Palghat Gap and Edakkara is in a valley with elevated terrain on all sides except south. A few of these stations have a second (12 hour) harmonic, which explains about 20% of the variance with an evening rainfall maximum. Figure 6.5 give the 24-hour rainfall of 2 stations in this group along with the first harmonic, 1+2 harmonic (sum) and 1+2+3 harmonic (sum).

Table 6.4 Amplitude, Time of maximum and Variance of the first four Harmonics of stations having one rainfall maximum in the morning hours

		Ist Harmonic			IInd Harmonic			IIIrd Harmonic			IVth Harmonic		
Station		Amp.	Tx	Var.(%)	Amp.	Tx	Var.(%)	Amp.	Tx	Var.(%)	Amp.	Tx	Var.(%)
Payyavoor	TR	0.458	0907	16.6	0.276	1842	22.0	0.069	2244	1.4	0.079	2109	1.8
	5≥	1.331	0932	47.5	0.860	1816	19.8	0.270	2246	2.0	0.074	2152	0.2
Kaithaprem	TR	0.125	0955	30.5	0.111	1808	24.3	0.046	2035	4.2	0.410	2215	3.3
	5≥	1.409	1031	42.7	0.874	0432	16.5	0.202	0209	0.9	0.407	0128	3.6
Elanad	TR	0.084	0823	38.4	0.061	1807	20.4	0.031	2202	5.4	0.004	2215	0.1
	5≥	0.860	0922	19.9	0.842	0543	19.0	0.751	2259	15.2	0.547	0259	8.1
Edakkara	TR	0.116	1105	61.5	0.050	0538	11.3	0.013	0352	0.8	0.022	2137	2.3
	5≥	0.359	1214	4.5	0.629	0404	30.7	0.210	0458	1.5	0.540	2128	10.5

TR – Total Rainfall; 5≥ - Rainfall greater than or equal to 5cm/day; Tx – Hour of maximum

6.2.2 Stations with two prominent rainfall peaks

There are four stations in this group: Palapuzha, Vazhavatta, Thillenkeri and Konni. Table 6.5 gives amplitude, time of maximum and variance of the first four harmonics of these stations. The stations are marked by crosses in Fig. 6.2. All these stations have one peak in rainfall during evening and another rainfall peak in the morning hours. Fig. 6.6 gives the 24-hour rainfall of two stations of this group, Palapuzha and Vazhavatta, along with the harmonic analysis.

Table 6.5: Amplitude, Time of maximum and Variance of the first four Harmonics of stations having two rainfall maximum

		Ist Harmonic			IInd Harmonic			IIIrd Harmonic			IVth Harmonic		
Station		Amp.	Tx	Var.(%)	Amp.	Tx	Var.(%)	Amp.	Tx	Var.(%)	Amp.	Tx	Var.(%)
Palapuzha	TR	0.126	0659	11.4	0.182	1892	23.8	0.148	0239	15.7	0.061	2178	2.7
	5≥	0.227	0662	10.5	0.339	1892	23.5	0.281	0247	16.2	0.118	2183	2.9
Vazhavatta	TR	0.055	0973	16.2	0.092	1856	44.8	0.010	0149	0.6	0.027	0117	3.9
	5≥	1.580	1588	32.1	1.400	1889	25.6	0.858	0201	10.0	0.725	0059	7.1
Thilenkeri	TR	0.126	0656	24.8	0.110	0531	18.8	0.025	0107	1.0	0.028	0159	1.3
	5≥	0.897	0435	4.8	1.353	0450	10.8	0.850	0141	4.3	0.907	0053	4.9
Konni	TR	0.107	0901	36.8	0.076	0536	18.8	0.063	2043	12.9	0.029	0133	2.7
	5≥	0.084	0556	6.8	1.976	1842	33.9	1.243	2141	13.1	0.871	2253	6.4

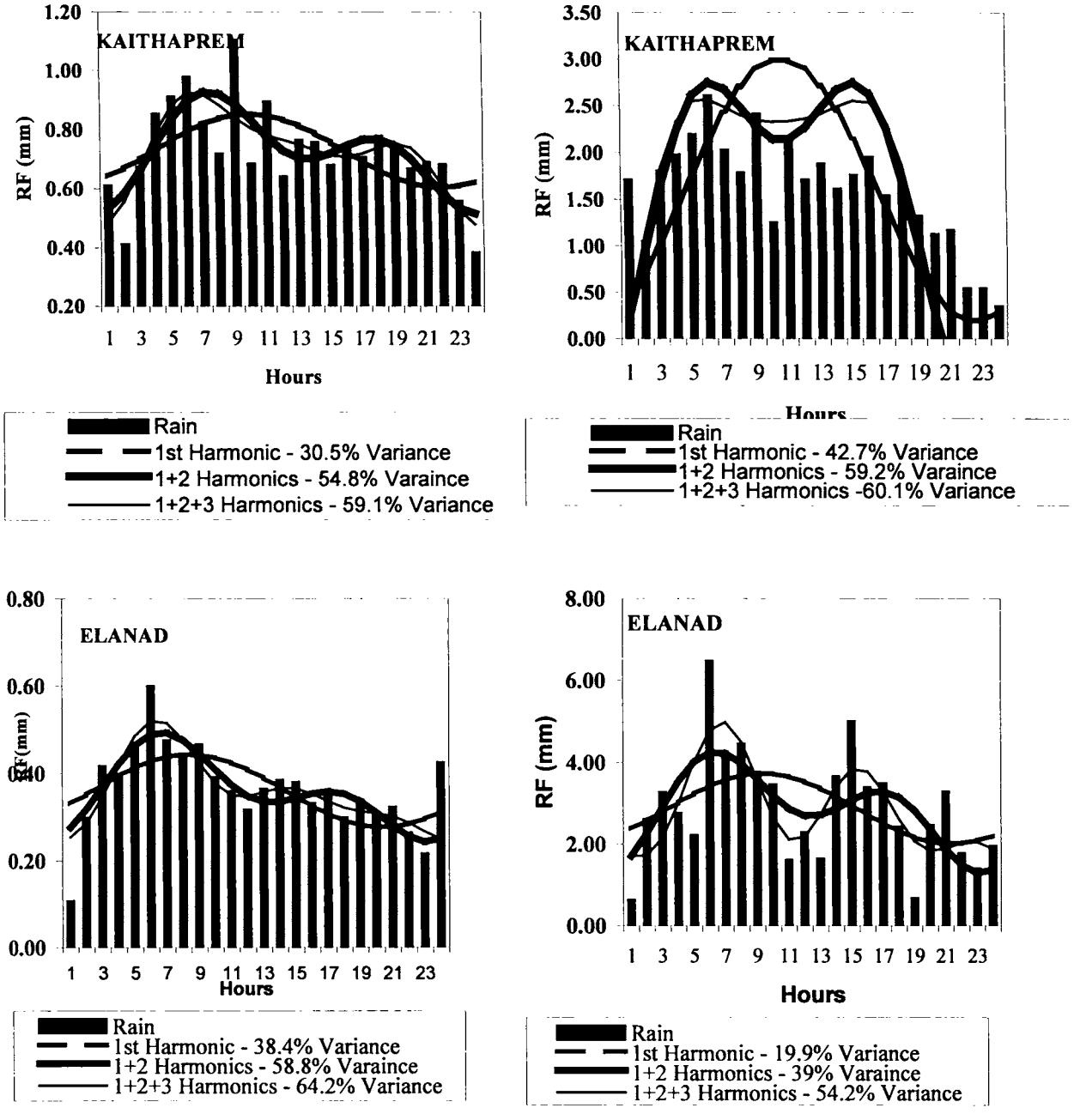

Fig. 6.5: 24-hour rainfall Kaithprem and Elanad with the first harmonic, 1+2 harmonic (sum) and 1+2+3 harmonic (sum). The left panel is for total rainfall days and right panel for days with rainfall ≥5cm per day.

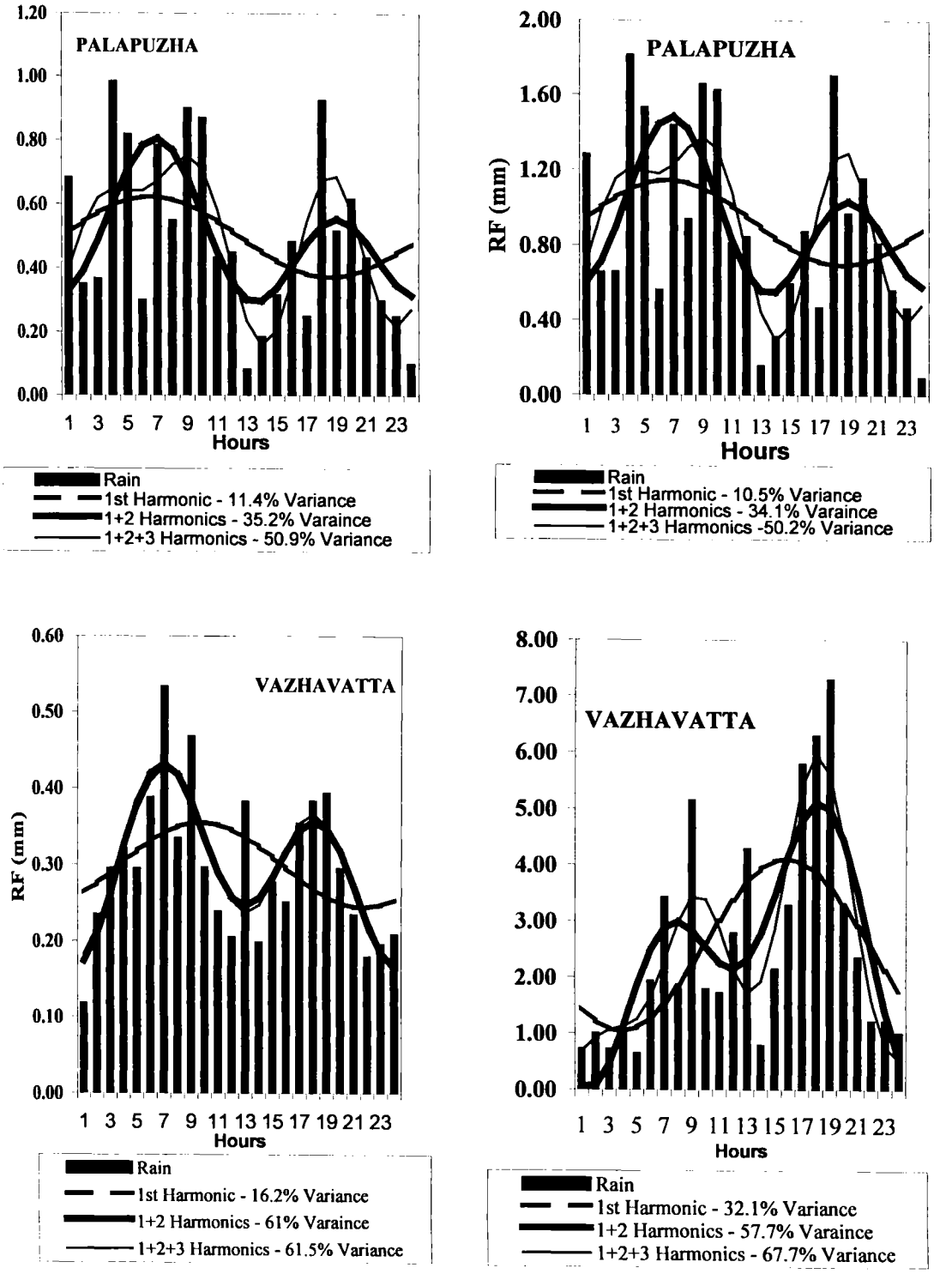

Fig. 6.6: 24-hour rainfall Palapuzha and Vazhavatta with the first harmonic, 1+2 harmonic (sum) and 1+2+3 harmonic (sum). The left panel is for total rainfall days and right panel for days with rainfall ≥5cm per day.

6.2.3 Stations with a flat diurnal curve

It is seen that some stations do not show prominent peaks in the 24-hour rainfall and they have a flat diurnal curve. Table 6.6 gives amplitude, time of maximum and variance of the first four harmonics of these stations. They are marked in fig. 6.2 as open circles. In most of such stations the amplitude for the first harmonics are low and hence the hourly rainfall tends to have a more flat profile. Fig. 6.7 shows the harmonic analysis of the 24-hour rainfall for Cheruvanchery for the total rainfall days. In Cheruvanchery the first harmonic has a percentage variance of 27.7% but the rainfall does not show a single maximum.

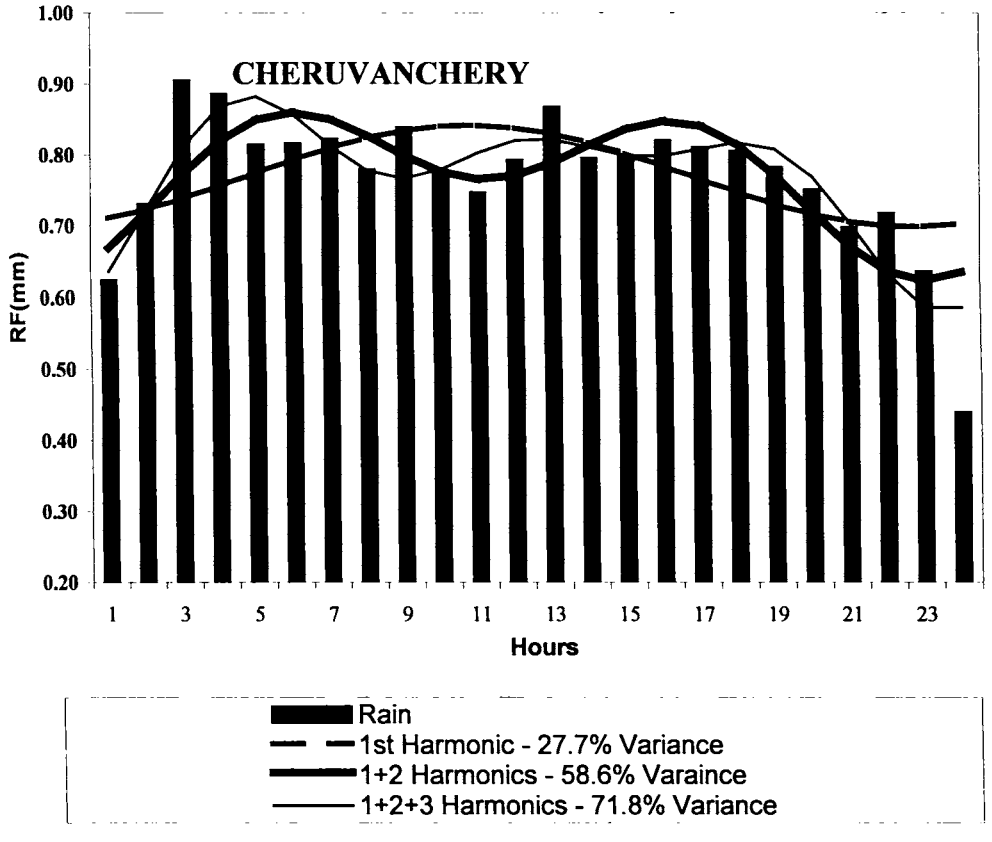

Fig. 6.7: 24-hour rainfall of Cheruvanchery with the first harmonic, 1+2 harmonic (sum) and 1+2+3 harmonic (sum) for total rainfall days.

Table 6.6: Amplitude, Time of maximum and Variance of the first four Harmonics of stations having a flat diurnal curve

		Ist Harmonic			IInd Harmonic			IIIrd Harmonic			IVth Harmonic		
Station		Amp.	Tx	Var.(%)	Amp.	Tx	Var.(%)	Amp.	Tx	Var.(%)	Amp.	Tx	Var.(%)
Vamanapuram	TR	0.056	1612	28.9	0.036	1824	12.0	0.047	2036	20.8	0.006	0130	0.3
	≥5	0.017	1624	27.3	0.099	1824	9.3	0.160	1042	24.1	0.036	0136	1.3
Kollam	TR	0.300	1703	30.0	0.251	1728	20.9	0.101	2136	3.9	0.181	0230	10.9
	≥5	0.751	1650	32.6	0.570	1925	18.7	0.237	2130	3.3	0.439	0219	11.1
Achenkovil	TR	0.130	0827	30.8	0.097	2049	16.9	0.014	0051	0.3	0.048	2128	4.2
	≥5	0.658	0526	2.9	1.223	0048	10.1	0.926	2351	5.8	0.493	2257	1.7
Kanjirappily	TR	0.064	0715	19.2	0.067	1804	20.7	0.004	0024	0.1	0.082	0135	31.4
	≥5	0.176	0742	13.9	0.022	1810	21.8	0.015	0017	0.1	0.254	0133	29.0
Kottayam	TR	0.029	2815	1.2	0.043	2119	2.7	0.066	2046	6.3	0.060	2340	5.1
	≥5	0.894	0600	6.8	1.976	1841	33.0	1.243	2126	13.1	0.871	2251	6.4
Vettilapara	TR	0.080	0843	14.4	0.051	1910	5.9	0.036	2125	2.3	0.077	2121	13.4
	≥5	0.495	0652	5.7	0.155	1833	0.6	0.617	2226	8.9	0.430	2208	4.3
Amalanagar	TR	0.146	1515	19.7	0.160	2250	23.7	0.040	2243	1.5	0.093	0120	8.1
	≥5	0.797	1003	11.4	1.301	2118	30.3	0.240	0125	1.0	1.021	0124	18.7
Kunnamkulam	TR	0.094	2205	37.1	0.025	0213	2.6	0.033	2142	4.6	0.034	2213	5.0
	≥5	0.403	0412	3.6	0.902	2330	17.9	0.807	2226	14.4	0.624	2147	8.6
Ottaplam	TR	0.050	0761	7.3	0.074	0350	16.4	0.052	2045	8.0	0.051	2206	7.7
	≥5	1.061	0425	18.8	1.197	0336	24.0	0.915	2119	14.0	0.240	2238	1.0
Attapadi	TR	0.018	0840	18.6	0.011	2254	6.6	0.009	0107	4.6	0.017	0204	18.1
	≥5	0.226	0825	18.9	0.151	2304	8.4	0.086	0142	2.7	0.226	0156	18.9
Parapangadi	TR	0.086	1414	64.3	0.021	2019	3.6	0.017	2055	2.5	0.014	0103	1.8
	≥5	0.324	1406	58.1	0.117	2025	7.5	0.057	2104	1.8	0.076	0006	3.2
Kalladi	TR	0.360	1007	67.7	0.134	1902	9.4	0.120	2024	7.6	0.018	0005	0.2
	≥5	1.575	1218	50.9	0.644	1918	8.5	0.863	2008	15.3	0.287	2355	1.7
Manathavady	TR	0.023	0904	50.5	0.010	0538	8.9	0.002	2045	0.3	0.004	2327	1.7
	≥5	0.065	1055	10.9	0.101	0412	26.6	0.025	2112	1.6	0.068	2312	12.0
Cheruvanchery	TR	0.072	1042	27.7	0.075	0503	30.9	0.049	0354	13.2	0.039	2106	8.1
	≥5	0.614	0845	25.4	0.612	0324	8.7	0.358	2045	0.5	0.087	2307	6.3
Pazhassi	TR	0.051	1719	5.8	0.082	0306	14.8	0.131	0224	38.1	0.027	0214	1.6
	≥5	0.780	1545	25.4	0.834	0350	29.0	0.596	0250	14.9	0.246	0214	2.5
Erikkulam	TR	0.158	0102	36.4	0.050	0232	3.7	0.119	0240	20.7	0.073	0216	7.8
	≥5	1.783	0114	42.6	0.565	0308	4.3	0.732	0143	7.2	0.500	0214	3.4
Padithuaduka	TR	0.108	1225	16.6	0.119	0232	20.4	0.125	2037	22.5	0.069	2126	6.9
	≥5	0.880	1306	31.5	0.537	0225	11.7	0.597	2162	14.5	0.266	0204	2.9
Paika	TR	0.067	1125	27.4	0.021	0338	2.7	0.063	2156	24.8	0.020	2137	2.5
	≥5	0.397	1006	4.4	0.301	0537	2.5	1.132	2149	35.8	0.308	0203	2.7

6.3 Discussion

Wallace (1975) grouped the possible mechanisms for diurnal variation of rainfall under three main categories: (1) those based on thermodynamic process, that affect the static stability, (2) those based on thermodynamic process that influence mass convergence within the planetary boundary layer (3) those process based on the semidiurnal pressure wave or S_2 oscillation.

The first explanation is primarily on the assumption of enhanced Infra Red (IR) cooling off the tops of clouds at night and a consequent increase of conditional instability or CAPE. The top of the clouds cool more at night than the cloud bases. The resulting instability produces more vertical overturning. The process continues through out the night. During the day solar radiation warms the cloud tops and stabilizes them. It also reduces the liquid water content of the clouds. This acts to reduce precipitation (Kraus, 1963).

The second of the proposed basic processes for the diurnal convection cycle has to do with day and night radiation differences within the planetary boundary layer over land. Wallace (1975) lists these as (i) the familiar land breeze and sea breeze circulation in coastal areas;(ii) a uniform diurnal heating cycle in regions of slopping terrain.(Holton ,1968; Lettau,1967);and (iii) changes in frictional drag associated with the Diurnal variation in static stability within the planetary boundary layer.(Blackdar , 1957).

The atmospheric response to inhomogeneous lower boundary conditions, especially in coastal regions, is a classic topic in mesoscale meteorology. The most familiar of coastal boundary layer circulations is the sea breeze. As sunlight warms land in day time hours, sensible heat fluxes transfer this energy to a well-mixed planetary boundary layer typically hundreds of meters deep. The resulting density gradient between atmospheric columns over land and sea drives a solenoidal circulation with rising motion over land. Non-linearity quickly becomes important, as the horizontal branch of this circulation advects the temperature gradient. Flow convergence can collapse the gradient down to a

sharp sea-breeze front. At night, the situation is not simply opposite. Radiative cooling of land may cause it to become cooler than the water offshore, and the overlying cool boundary layer may participate in dynamics similar to those discussed above, yielding a thermal land breeze (Holton,1968).

Another argument for the diurnal cycle in convection is the semidiurnal pressure wave or S_2 oscillation. This explanation holds good for the early morning late afternoon maximum of convection often observed on large islands and at a number of other stations. The physical explanation (Bier and Simpson, 1969) is that during each day there occurs two successive patterns of divergence and convergence caused by sun's heating on one side of the globe and lack of heating on the other. This solar tide produces maximum pressure peaks near 1000 and 2200 LST with minima near 0400 and 1600 LST. According to this hypothesis, maximum pressure rise and convergence is around 0700 and 1900 LST. This significantly enhances the cumulus cloud activity.

Diurnal radiational hypothesis by Gray et al. (1977) is based on differences between organized mesoscale cloud regions and surrounding cloud-free regions. The atmosphere surrounding organized cloud regions adjusts to its large radiational cooling at night through extra subsidence. This extra subsidence increases low-level convergence into adjacent cloud regions. During the day solar radiation reduces tropospheric radiation loss. Clear region subsidence warming and cloud region low-level convergence are substantially reduced.

For the diurnal variation of rainfall in Kerala the following factors can be taken as important: (1) radiational cooling of cloud tops. (ii) the land-sea breeze circulation (iii) convection triggered by orography (vi) summer low-level jet phenomenon. All these factors will have an influence on the diurnal rainfall variability. Each station variability becomes unique depending upon the contribution of individual factors and local topography.

Radiational cooling of cloud tops during the night changes the conditional instability of the atmosphere, which is conducive for cumulus convection in

early morning hours. Sea breeze during daytime affects the diurnal variation of rainfall giving a rainfall peak during evening hours. In the south-west monsoon season, the Low-Level jet is embedded in the mean monsoon flow and the wind increases very sharply with height in the boundary layer. The lower portion of the boundary layer will be heated due to increased ground heating in the afternoon hours and there will be turbulent exchange of higher momentum air of the Low Level Jet downwards and the lower boundary level winds will be stronger in the afternoon. The orography will give forced ascent to this wind and enhance the rainfall in evening hours. This is most pronounced for the stations on the sloping terrain of the Western Ghats. Land breeze effect on the diurnal variation is expected to be small.

6.4 Conclusion

In literature we find that diurnal variation of coastal stations of Trivandrum, Cochin and Mangalore (just north of Kerala) have been studied. Excepting for Trivandrum, the other two stations have a prominent early morning maximum for low and high rainfall spells. Our analysis show that Thikkodi a coastal station has a prominent 1st harmonic (24 hours) with maximum in the evening hours (~ 1800 hours). The first harmonic explains 77.6% for all the rain events put together. More study is needed using coastal rainfall data to resolve this difference.

A large number of stations have prominent 1st and 2nd harmonics (24-hour & 12-hour). Combination of these gives either a morning maximum or evening maximum in rainfall. Nearly ½ of the stations studied (45%) have very low amplitude for all the 4 harmonics and the diurnal curve for rainfall is a flat one.

Diurnal variation is a combination of the 4 or 5 important factors discussed in the earlier section. A combination of these gives the diurnal variation of any individual station. Since a majority of the stations have shown an afternoon/evening maximum it is inferred that prominent factors in diurnal variation in Kerala rainfall are:

- Diurnal variation of air temperature of lower levels.
- Downward momentum transport in the Low Level Jetstream that strengthens the low-level winds in the afternoon/evening, which together with orography increases rainfall in the evening.
- Effect of sea-breeze which strengthens the low level westerly flow during southwest monsoon season giving rainfall maximum during evening hours.

It is proposed that an east-west section with high density of continuously recording rain-gauge stations is maintained at a latitude where the orography is very prominent to study the diurnal variation in region with steep orography.

Chapter 7
Dynamic and Orographic Control on Rainfall

7.1 General

Kerala gets nearly 190cm of rainfall during the south-west monsoon season 1 June to 30 September. This is more than twice the monsoon rainfall of India. A good part of Kerala's rainfall is caused by the orography of the Western Ghat mountain ranges. Both convective (large cumulus and thunderstorm) and non-convective (nimbo-stratus) rain require vertical motion in the atmosphere and the slopes of the Western Ghats generate large vertical motion fields when winds impinge on them, particularly during the SW monsoon season with strong westerly winds. In addition to the orographic control there is a dynamic control by the Low Level Jetstream (LLJ) on the southwest monsoon rainfall of Kerala. When the LLJ axis is to the south of Kerala, cyclonic vorticity prevails over the state in the atmospheric boundary layer which enhances rainfall. When LLJ axis is to the north, the relative vorticity in the boundary layer becomes anticyclonic which suppresses rainfall activity. The orographic control is mainly decided by the strength of the low-level westerlies (zonal component of monsoon winds) as Western Ghats is oriented north-south and the steepness of the orography, the conditional instability (CAPE) in the atmosphere generally being favourable for deep convection on almost all days.

Computer modelling studies are needed to understand the role of orography in rainfall. Sarker (1967) made a two dimensional model study of the orographic rainfall along the Western Ghat section from Mumbai to Pune during south-west monsoon. He considered the mountain as a mechanical obstacle but offering no ground friction to the air flow (frictionless flow). Thus trees and forests and other forms of terrain friction are unimportant to his studies. Earth's rotation was also not considered. Even with such simplifications he obtained realistic variations of the rainfall along the slopes of the Western Ghats in that section showing the importance of the east-west configuration in terrain height (orography) of Western Ghats. Both the model and the observations show that the maximum rainfall is reached several kilometres west of the mountain peak.

Ascent of air caused by the mountain is seen to begin about 60 kms west of the mountain peak. Both in observations and model, rainfall decreases very fast to the east after reaching the peak rains near Lonavla. Results are shown in fig. 7.1

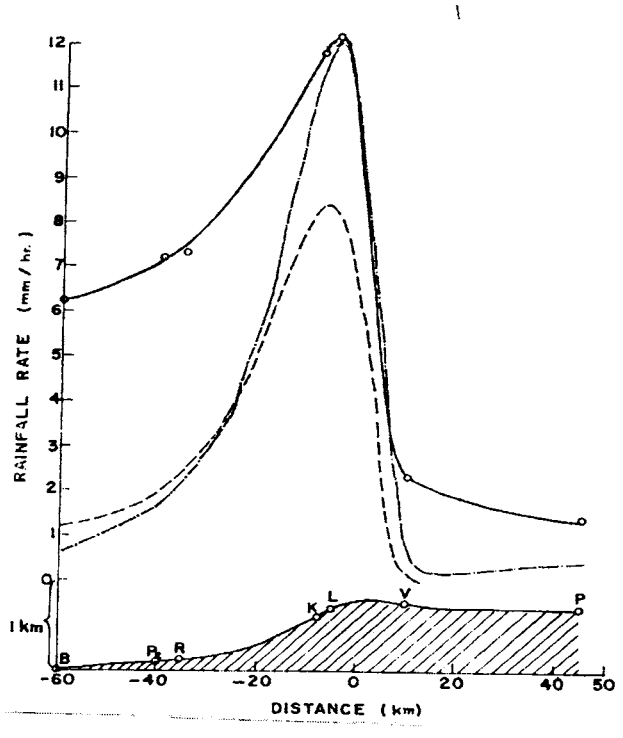

Fig. 7.1: Sarker's (1967) model of orography of Western Ghats. The solid line is the observed rainfall and the dashed lines are the simulated rain from two models.

A similar modelling study was made by Lariff Zubair (1999) for the orographic control of the SW monsoon rains in an east-west section through Colombo across the tall mountains in Sri Lanka whose peak Sita Eliya is at an altitude of more than 2000 metres. While the model rainfall intensity has a peak at a distance of 20 kms west from the crest of the mountain, the peak in the measured monsoon season rainfall is 30 kms to the west of the mountain crest. Figure 7.2(a, b) gives the contours of the terrain in Srilanka and those of the mean summer monsoon rainfall May to September. Fig. 7.3a gives the vertical section of the height contours along the section marked XX –XX in fig. 7.2a and the smoothed contours used in the modelling study. Fig. 7.3b below gives the variation along the section XX –XX of the May to September rainfall. Results of the rainfall simulation with the smoothed orography are given fig. 7.4.

Rainfall begins to increase where the terrain begins to rise and has reached a maximum where the terrain is at an altitude of about 500m. Where the terrain height is 1500m rainfall has already decreased to about half the peak rainfall. In the present study we have simulated the monsoon rainfall of Kerala using the PSU NCAR Mesoscale Model (MM5) for 3 days with the LLJ axis passing south of Kerala and 3 days with the LLJ axis north of Kerala. All these days are from a July month in 1995.

7.2 Spatial Distribution of Rainfall

Figure 7.5a gives the spatial distribution of the mean rainfall for July for the period 1901-1950, data taken from IMD publication described in Chapter-2 and fig. 7.5b the satellite measured contours. It can be seen that there are three pockets of large rainfall in July centred near 11.5^0N, 10^0N and 9.5^0N. Some of the stations in these regions with heavy July rainfall are Kuttiyadi, Vythiri, Neriamangalam, Munnar, and Peermade. There is a sharp decrease in rainfall on the lee side of the Ghats. Stations lying in the Palghat region receive low rainfall. Figure 7.6 (a&b) give the east-west cross section of rainfall and satellite measured height of the terrain at latitudes averaged for 10N –10.2N (Munnar section) and for 9.5N – 9.7N (Peermade section). Stations are marked with open circles. Fig. 7.6a gives the cross-section through 10-10.2N. There are 16 rainfall stations in this latitude belt. Neriamangalam, Munnar and Devikulam,(marked N,M and D respectively) which receive heavy rainfall during July, are located in this belt. In this cross-section the rainfall peak is reached before the sharp increase in orography begins and the peak is reached at a terrain height of about 30m itself (Neriamangalam) The rainfall maximum attained is about 40km away from the peak in terrain height of about 1830m.. There are 12 rainfall stations in the latitude belt 9.5N – 9.7N(fig.7.6b). The heavy rainfall station of Peermade (marked P) is located in this cross section. The peak in rainfall is about 15 km from the first peak in terrain (1000m) and about 40 km away from the highest peak (~1330m). The rainfall after reaching the peak decreases sharply to the east.

(a)

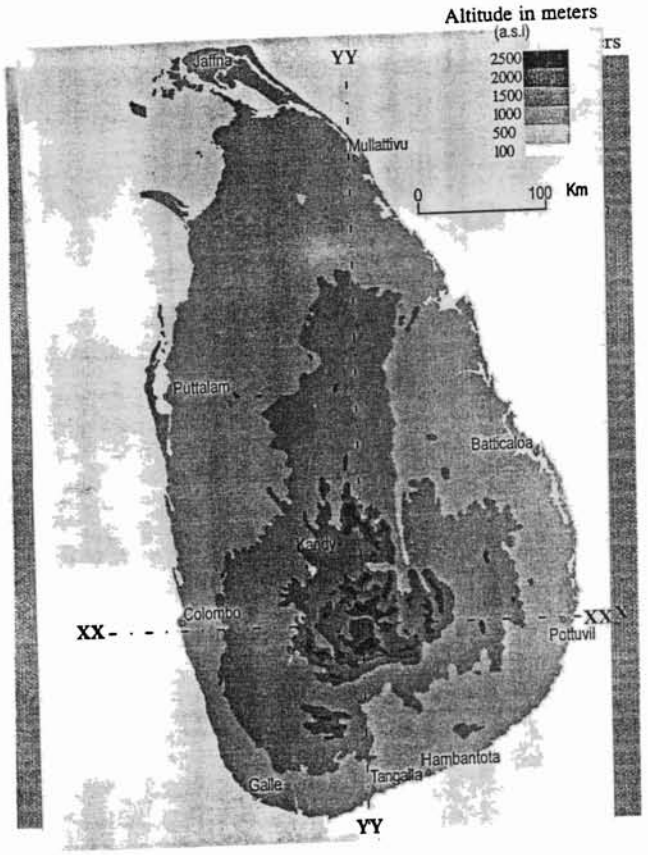

(b)

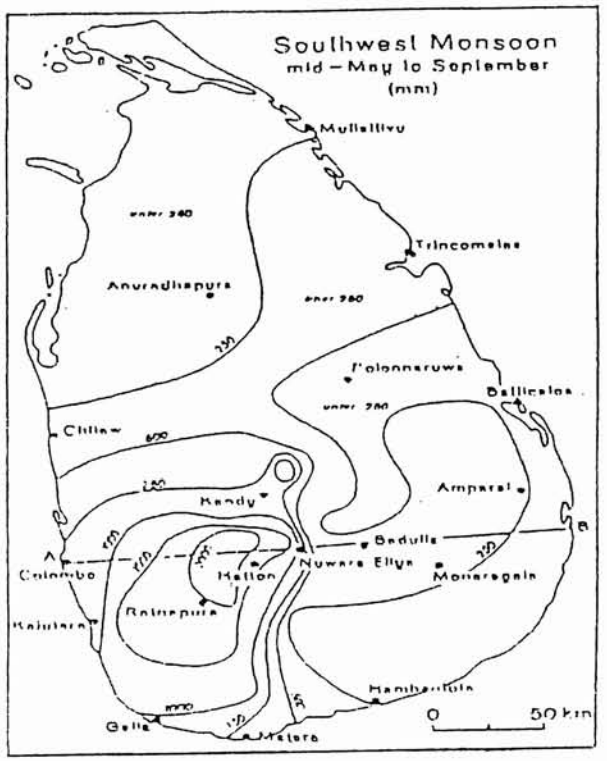

Figure 7.2: (a) Contours of the terrain in Srilanka (b) Contours of mean summer monsoon rainfall May to September.

As taken from Lariff (1999)

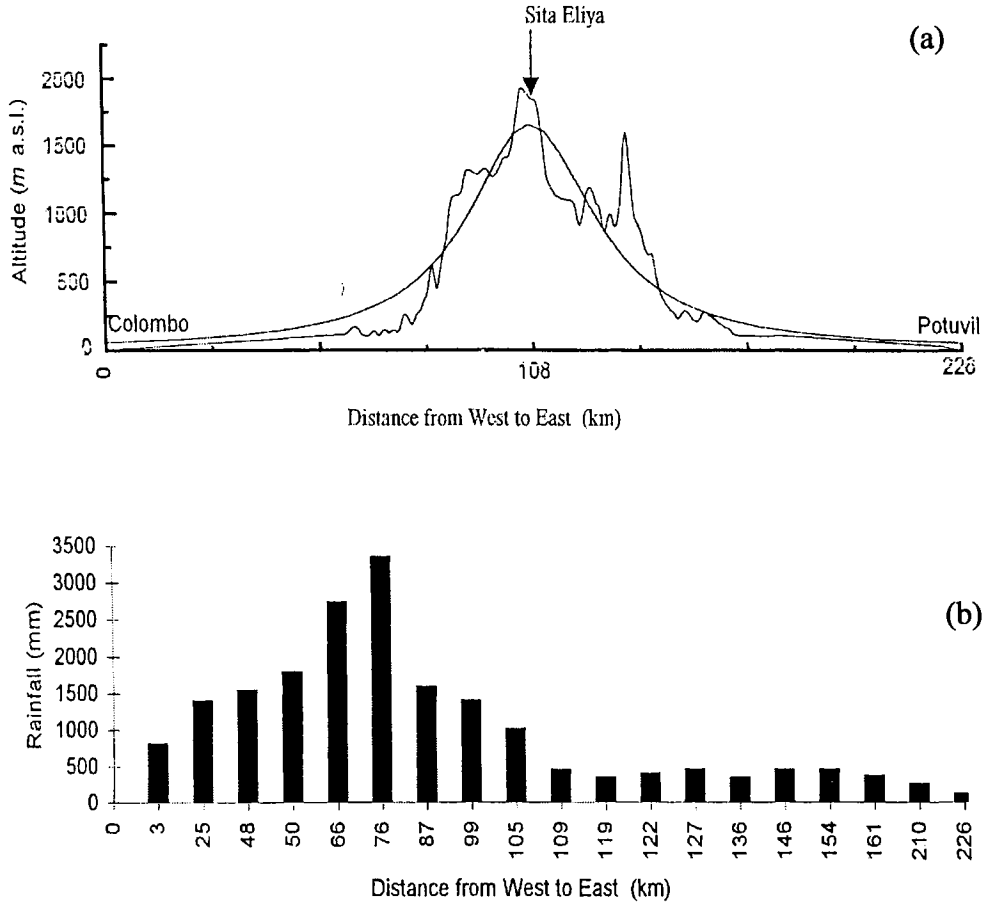

Fig. 7.3: (a) Vertical section of the height contours along the section marked XX –XX in fig. 7.2(a) and the smoothed contours used in the modelling study ; (b) Variation along the section XX-XX in fig. 7.2(a) of the May to September rainfall. As taken from Lariff (1999)

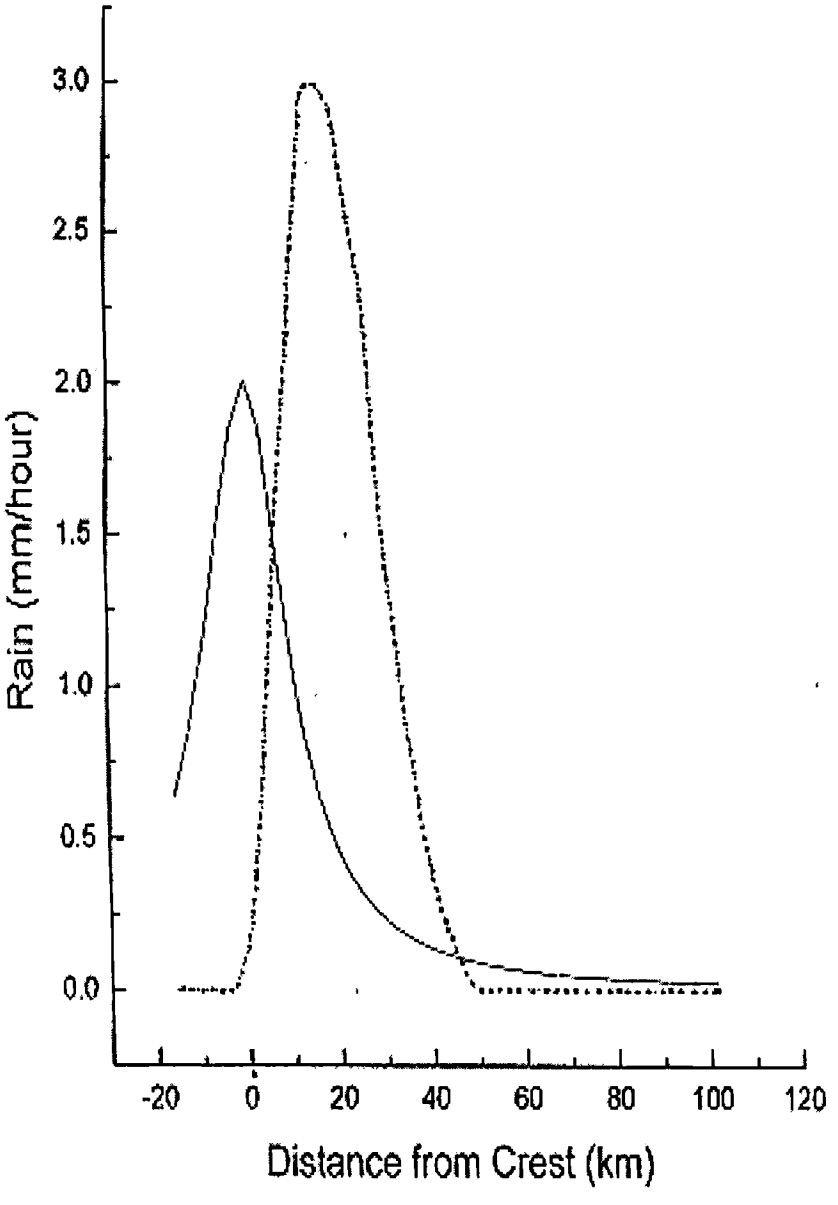

Fig. 7.4 : The rainfall simulation and the orography. The solid line is the terrain and the dashed line the simulated rainfall. The figure is taken from Lariff (1999)

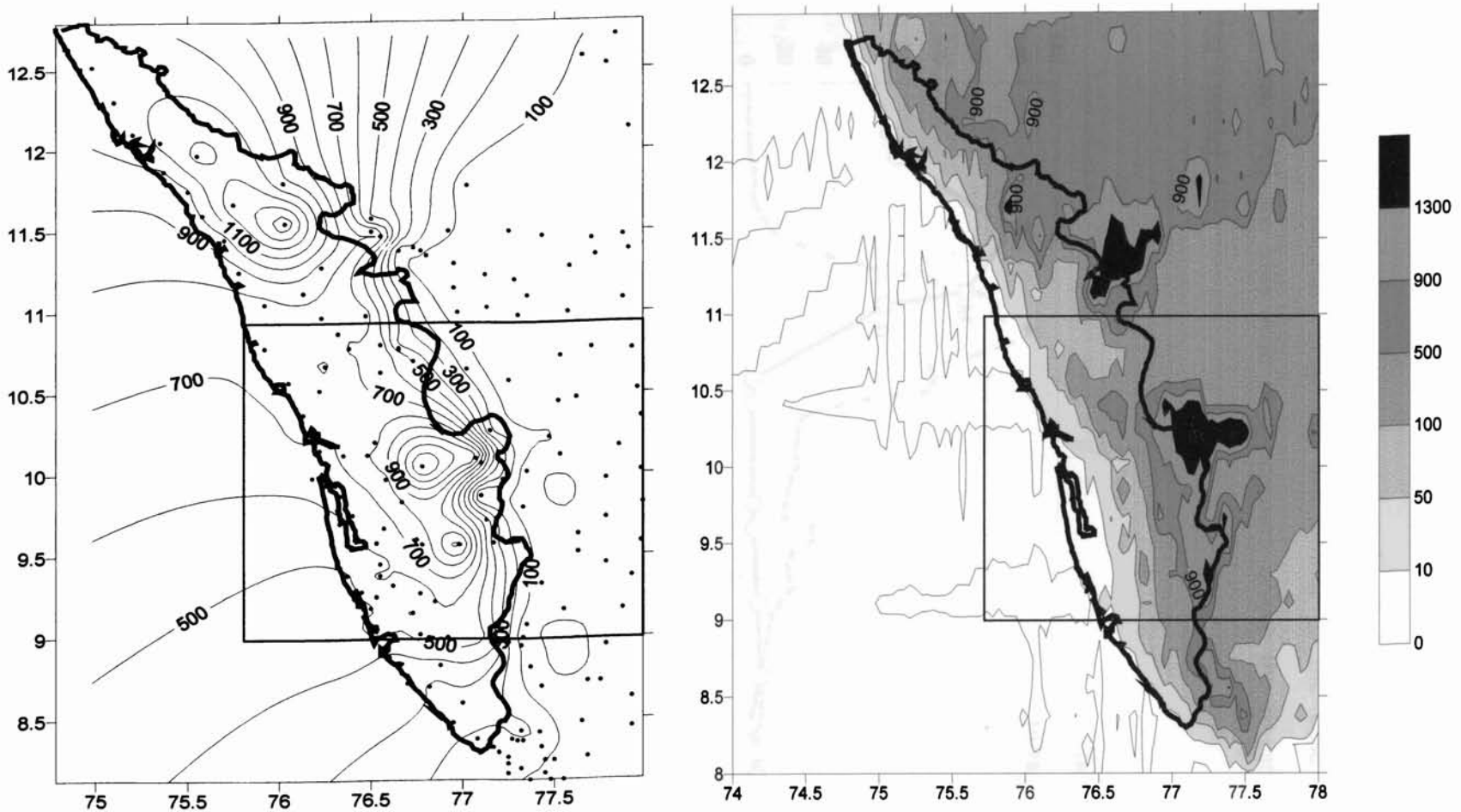

Fig.7.5 (a) Spatial distribution of the mean rainfall for July for the period 1901-1950.; (b) the satellite measured terrain of Kerala.

The rainfall variations across the mountains, in Munnar section (fig.7.6a) and in Peermade section (fig.7.6b) are similar to the case of Srilankan mountains. All are hills with oval contours unlike the linear mountain in Sarkar's model.

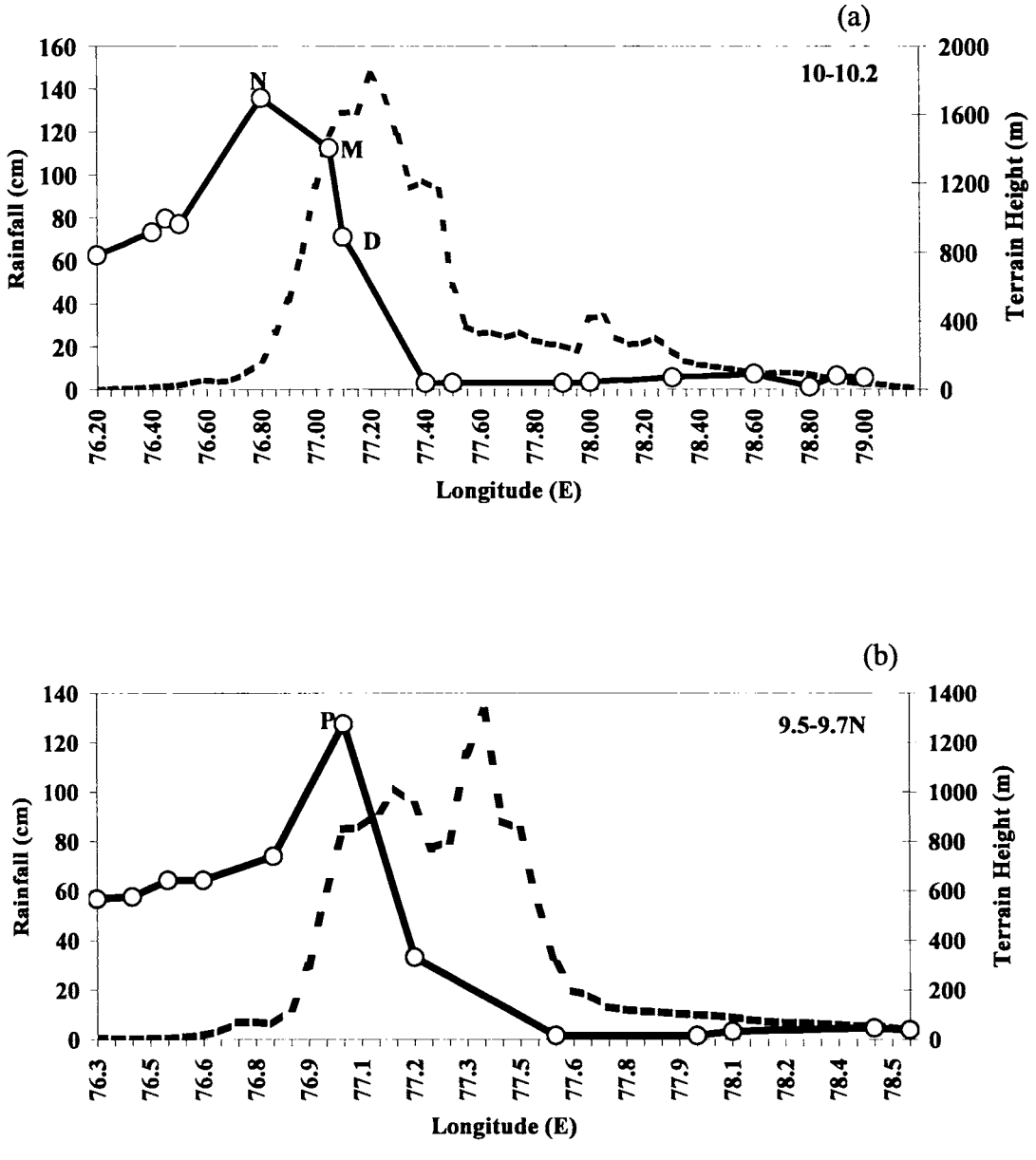

Fig. 7.6: Longitudinal cross section of rainfall and height of the terrain of latitude averaged for (a) 10-10.2^{0}N (b) 9.5 –9.7^{0}N. The stations are plotted as open circle.

7.3 MM5 simulation

The PSU/NCAR Mesoscale Model (MM5) is utilised to simulate the monsoon rainfall of Kerala. Details of model structure are described in Chapter 2. Input data, model domain, orography and physics options used for simulation are described in the following paragraphs.

7.3.1 Model Domain and Orography

We have selected three nested domains with grid resolutions 45 km, 15 km and 5 km for integration. The domain co-ordinates are *Domain 1*: 66-88E, 2-28N; *Domain 2:* 73.5 –79E, 8-12.5N *and Domain 3* : 75.8 – 78, 9-10.8N. These domains are shown in figure 7.7. Terrain height data with 10 min, 5 min and 2 min resolutions are used as input for these 3 domains. All these data are created from United States Geological Survey (USGS) elevation data at 30 sec resolution. Input for vegetation/Land-use is also taken from USGS. Overlapping parabolic interpolation with 2 pass smoother is used to construct mesoscale grid for orography and vegetation/Land-use data.

7.3.2 Physics options

Cumulus parameterization

We have used Grell scheme for cumulus parameterization. (Grell,1993; Grell et.al.1994). The scheme is a simplification of the Arakawa and Schubert (1974) scheme and is based on the rate of destabilization or quasi-equilibrium, simple single cloud scheme with updraft and downdraft fluxes and compensating motion determining heating/moistening profile. The convective instability is produced by the large scale (grid scale) and is dissipated by small scale (cumulus scale) on a time scale τ. There is a quasi-equilibrium between generation and dissipation of instability. The vertical distance between the lifted condensation level and the level of free convection is smaller that the threshold depth of 50mb. This scheme is chosen for the present study because it is most suited for grid sizes upto 5km as given by the designers of this scheme

(http://www.mmm.ucar.edu/mm5). Such a grid size is needed for studies of rainfall variations across mountains with steep orography. In this study only the convective rainfall obtained from the Mesoscale model is analysed in relation to orography.

PBL scheme

The MRF PBL or Hong-Pan PBL scheme is used for the boundary layer parameterization. This scheme is suitable for high-resolution in PBL. The height of the PBL is calculated using the Bulk Richardson number based on Troen and Mahart (1986) counter-gradient term and K profile in the well mixed PBL as implemented in the NCEP MRF model.

Moisture Scheme

Moisture scheme is Simple Ice (Dudhia, 1993). In this scheme cloud and rainwater fields are predicted explicitly with microphysical processes. Ice phase processes adds to above processes without adding memory. There is no supercooled water and immediate melting of snow below freezing level takes place. .

Radiative scheme

The radiation effects due to cloud are considered and are sophisticated enough to account for longwave and shortwave interaction (Cloud-radiation scheme).

The details are taken from the MM5 tutorial document. http://www.mmm.ucar.edu/mm5

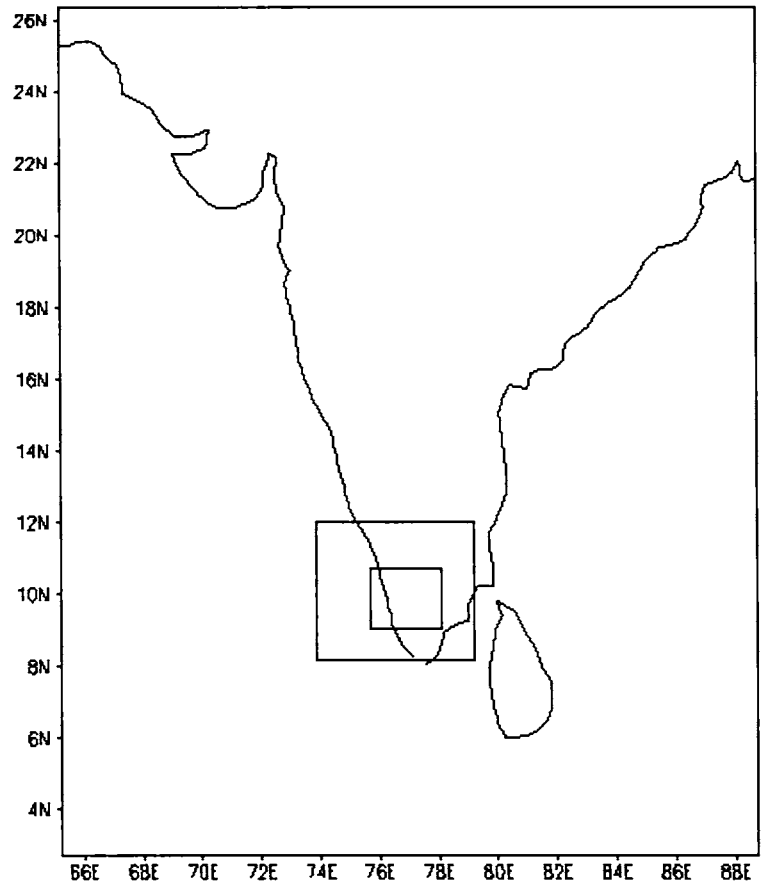

Fig. 7.7 The three nested domains chosen for the study.

7.4 Numerical Simulations

For the present study we have taken six cases of rainfall events during July 1995. 3 cases are with the LLJ axis just south of Kerala and 3 cases when the jet axis was north of Kerala. The input data used for the simulation is from NCEP/NCAR Reanalysis Project (NNRP). These data are on 2.5-2.5 degree latitude-longitude grid with 17 vertical levels. This data is interpolated by the MM5 model to the desired grid size for running the model. The simulation started 24 hours before the day of rainfall report (the rainfall reported on a day at 0300UT is for the period 0300UT of the previous day to 0300UT of that day) and model is run for the following 24 hours with time steps of 180 sec. The model output (convective rainfall) is taken every three hours. The integration has been performed with the model orography fig.7.10a.

Table 7.1 Observed Rainfall (mm) at 0300z for the previous 24 hours for south Kerala and the spell average for the six days selected for the study

Day And time	South Kerala rainfall (mm)	Spell average (mm)
9 July 1995 (03Z)	28.4	33.1
10 July 1995 (03Z)	27.5	
11 July 1995 (03Z)	43.5	
19 July 1995 (03Z)	7.2	10.9
20 July 1995 (03Z)	19.9	
21 July 1995 (03Z)	5.8	

Fig. 7.8 shows the wind at 850hPa for the 6 cases chosen for the study. For the three days (left panels) the LLJ axis is south of Kerala, and there is cyclonic vorticity north of the jet axis in the atmospheric boundary layer over Kerala. This will favour vertical upward motion and there is increased rainfall in Kerala as seen from Table 7.1. When the jet axis is north of Kerala (right panels), the anticyclonic vorticity in the boundary layer will suppress the rainfall in Kerala. The u-wind may be taken as the component normal to the Western Ghats and fig. 7.9 gives the variation of the mean u in a box (7.5-12.5N, 75-77.5E). It is seen that the strength of the u-wind is not much different in the two cases, but the rainfall values are drastically different as seen in the Table 7.1 showing the dynamic control by the low level jet.

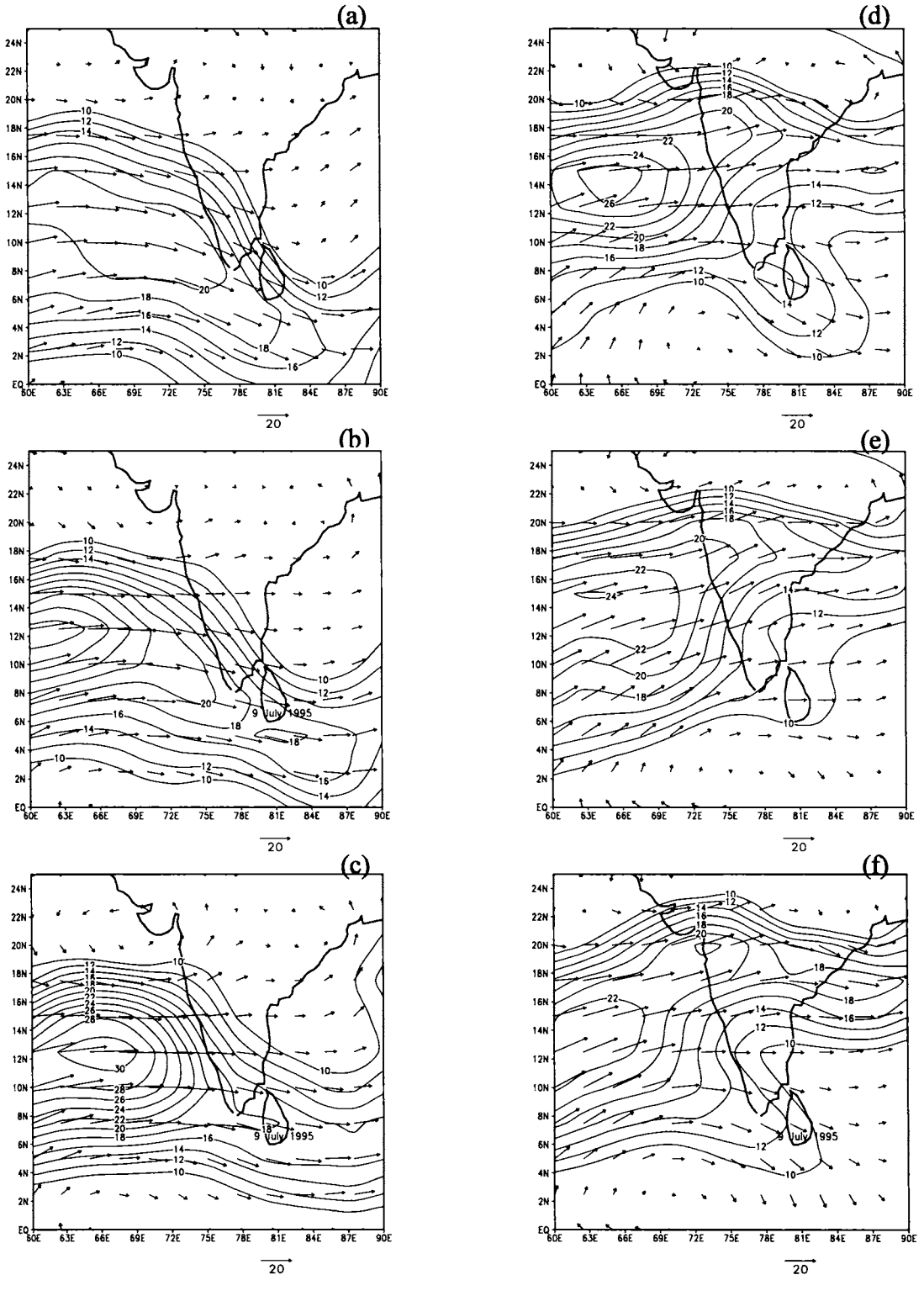

Fig. 7.8 : U-wind at 850hPa (1.5km) for 1200Z of (a) 8July 1995 (b)9 July 1995 (c) 10July 1995 (d) 18July 1995 (e) 19 July 1995 (f) 20 July 1995

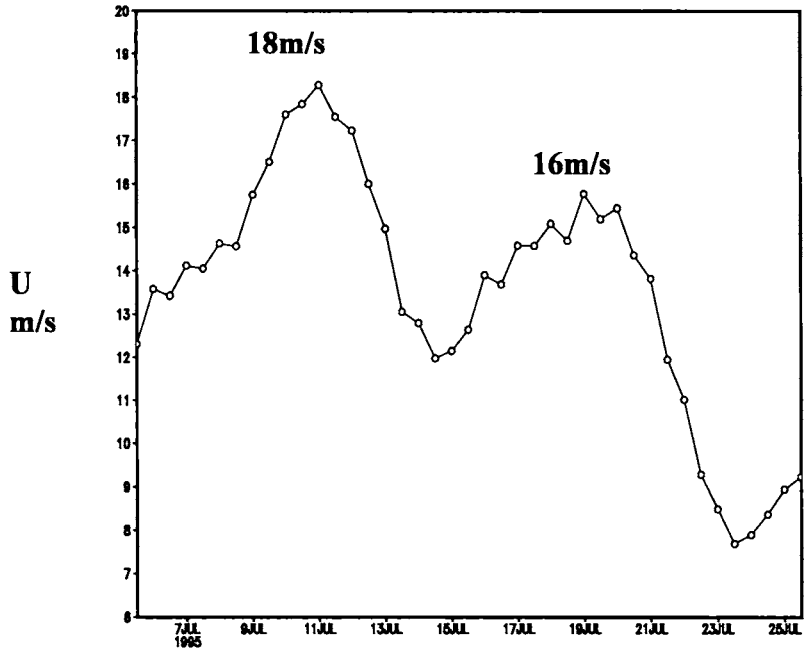

Fig. 7.9 : U- Wind (850hPa) averaged 7.5-12.5N,75 –77.5E

7.4.1 Case –I

The spatial distribution of convective rainfall obtained from the MM5 simulation for the inner domain for the 3days 9July, 10July and 11July of 1995 are given in fig.7.10(b-d). It is seen that the model has given high convective rainfall fairly well in these days with maximum rainfall of the order of 5cm/day, when the LLJ axis passed just south of Kerala. The 24-hour convective rainfall cross sections through Munnar and Peermade on these days are given in fig. 7.11(b-d) and fig.7.12 (b-d) respectively. In the latitude cross section 10–10.2N the rainfall has started to increase from 76.4E, much before the orography has started to increase and the maximum rainfall (peak) is attained at 76.9E which is about 25km away from the terrain peak. The peak rainfall values of 1.5, 5 and 4.5 cm/day on these days picked up by the model are large values compared to the simulation with LLJ axis to the north of Kerala. In the cross-section 9.5 – 9.7N the model simulation shows that the rainfall starts increasing form 76.4E

well before the slope in orography begins. However, the rainfall maximum is attained at 76.65E which is about 65km away from the terrain peak in the model. It should be noted that in the actual terrain as seen in (fig7.6b) there are peaks at 77.15E and 77.3E, whereas the model smoothens this and shows only one broad peak at ~77.25E. In actual observations the rainfall peak is about 15km from the 1st peak and 40 km away from the second peak.

The observed peaks in rainfall are subject to the availability of raingauge station data. In the Munnar cross section (fig. 7.6a) the observed rain peak is at Neriamangalam (marked N). If we have 2 stations in the large gap west of N and one station in the gap between N and M the observed profile would have been more realistic. Similar is the case with the Peermade section (fig. 7.6b).

7.4.2 Case –II

The spatial distribution of convective rainfall obtained from the MM5 simulation for the innermost domain for the three days 19 July, 20July and 21 July 1995 are given in fig.7.13(b-d). It is seen that the model has given low convective rainfall with maximum of the order of 1cm/day only with the Low Level Jetstream north of Kerala (as compared to 5cm of Case-I, showing the dynamic control by the Low Level Jetstream). The cross-sections of the 24-hour convective rainfall through Munnar and Peermade (fig.7.14(b-d) and 7.15 (b-d)) show peaks in relation to the model orography as in Case-I. It may be noted that sharp peaks are available in only few cases of these low rainfall simulations.

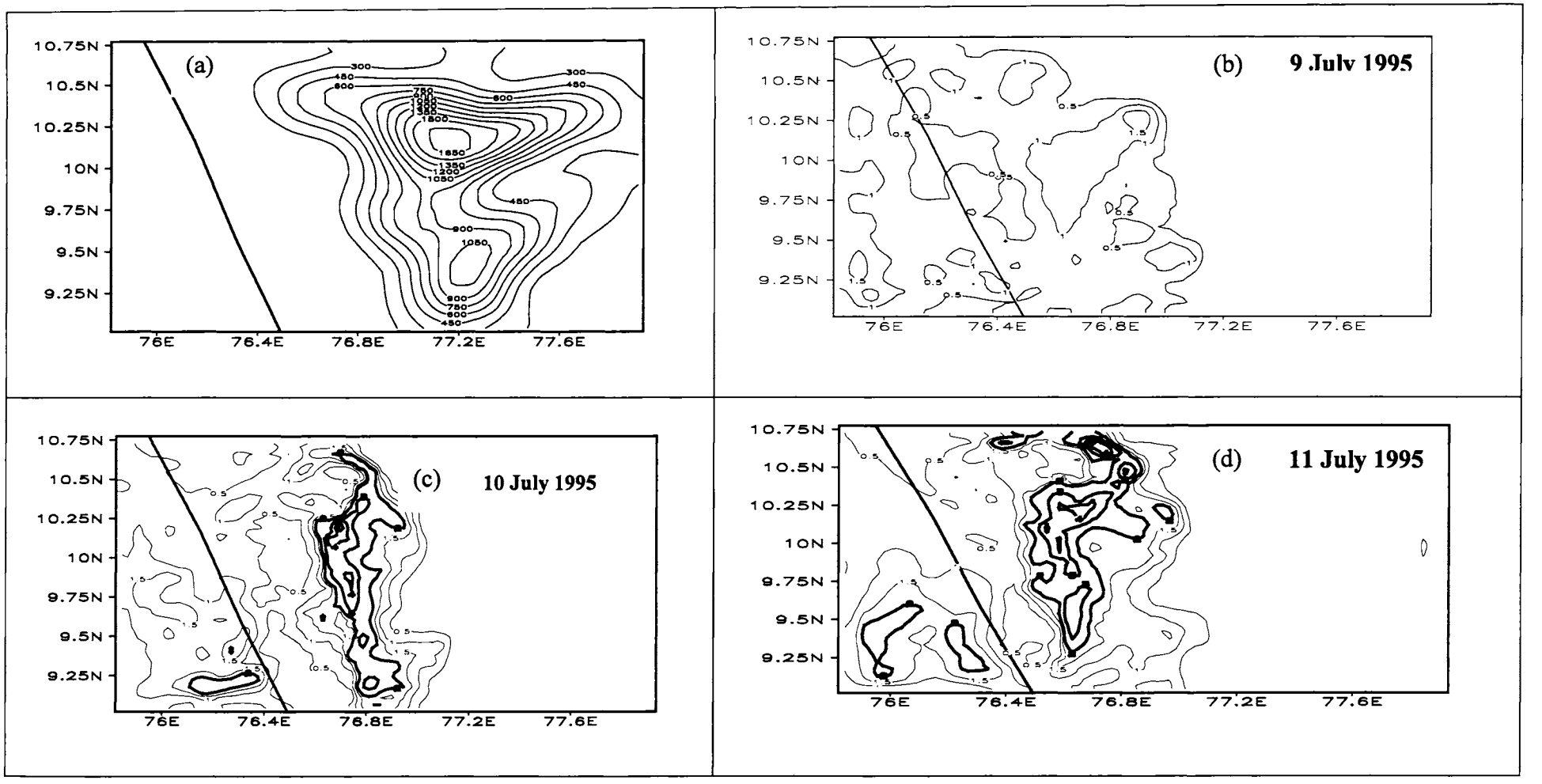

Fig.7.10 : (a) The terrain output of the innermost domain obtained from MM5 simulation. Spatial distribution of convective rainfall in the innermost domain on (b) 9th July 1995 (c) 10th July 1995 and (d) 11th July 1995.

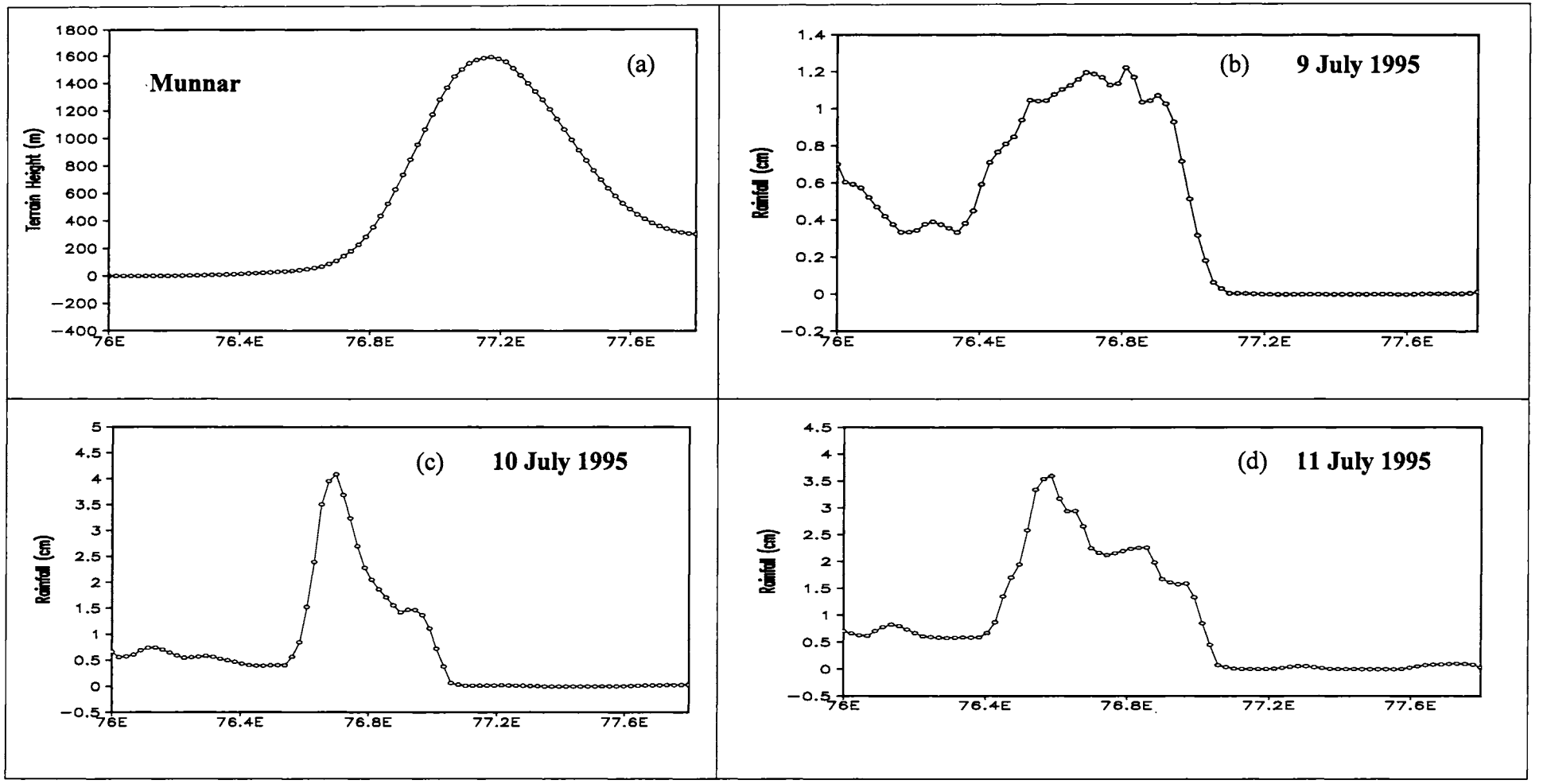

Fig.7.11 : (a) The terrain of the Munnar cross-section (averaged for 10-10.2N) obtained from MM5 simulation. Convective rainfall in this cross-section on (b) 9th July 1995 (c) 10th July 1995 and (d) 11th July 1995.

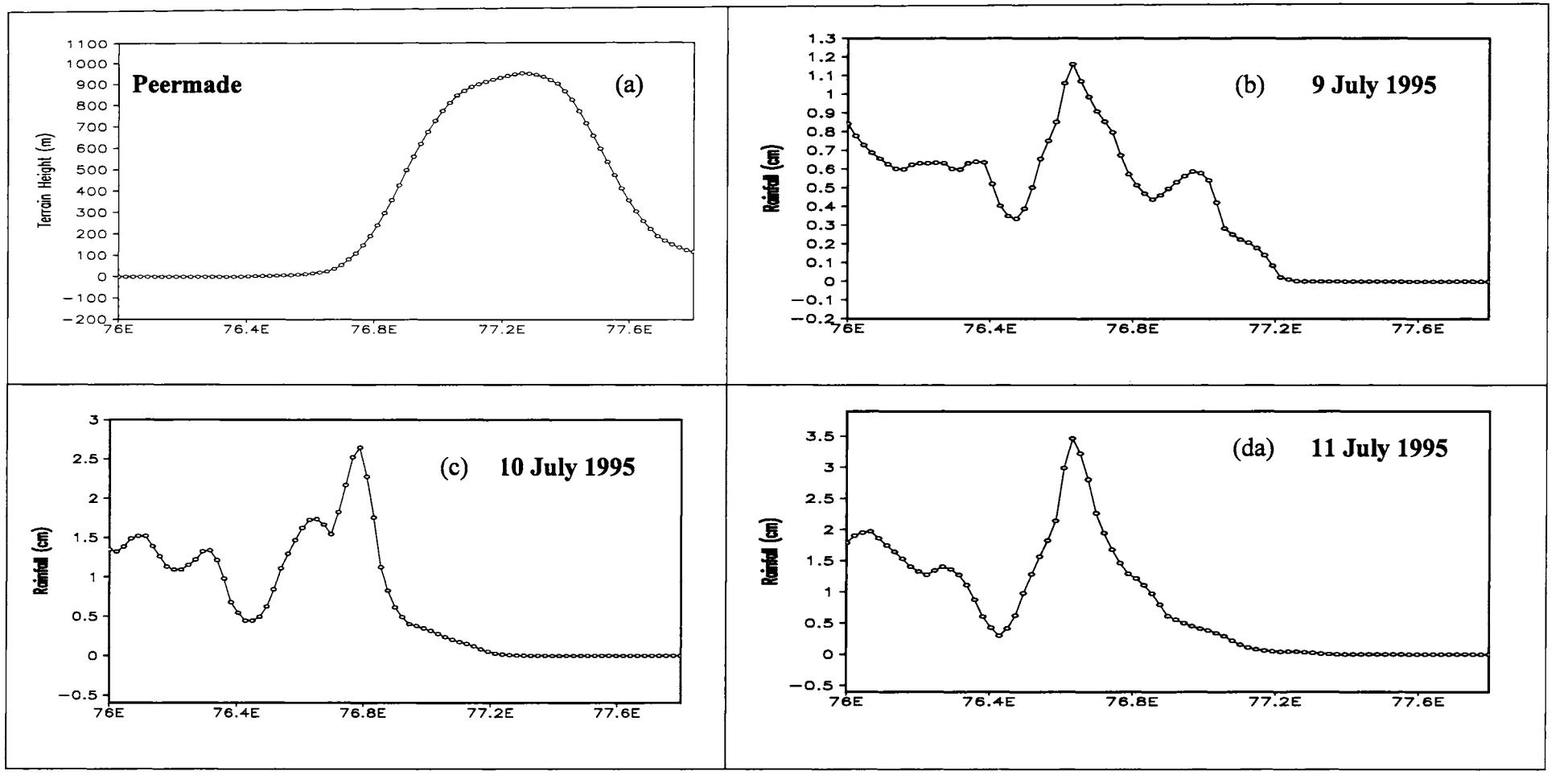

Fig.7.12 : (a) The terrain of the Peermade cross-section (averaged for 10-10.2N) obtained from MM5 simulation. Convective rainfall in this cross-section on (b) 9th July 1995 (c) 10th July 1995 and (d) 11th July 1995.

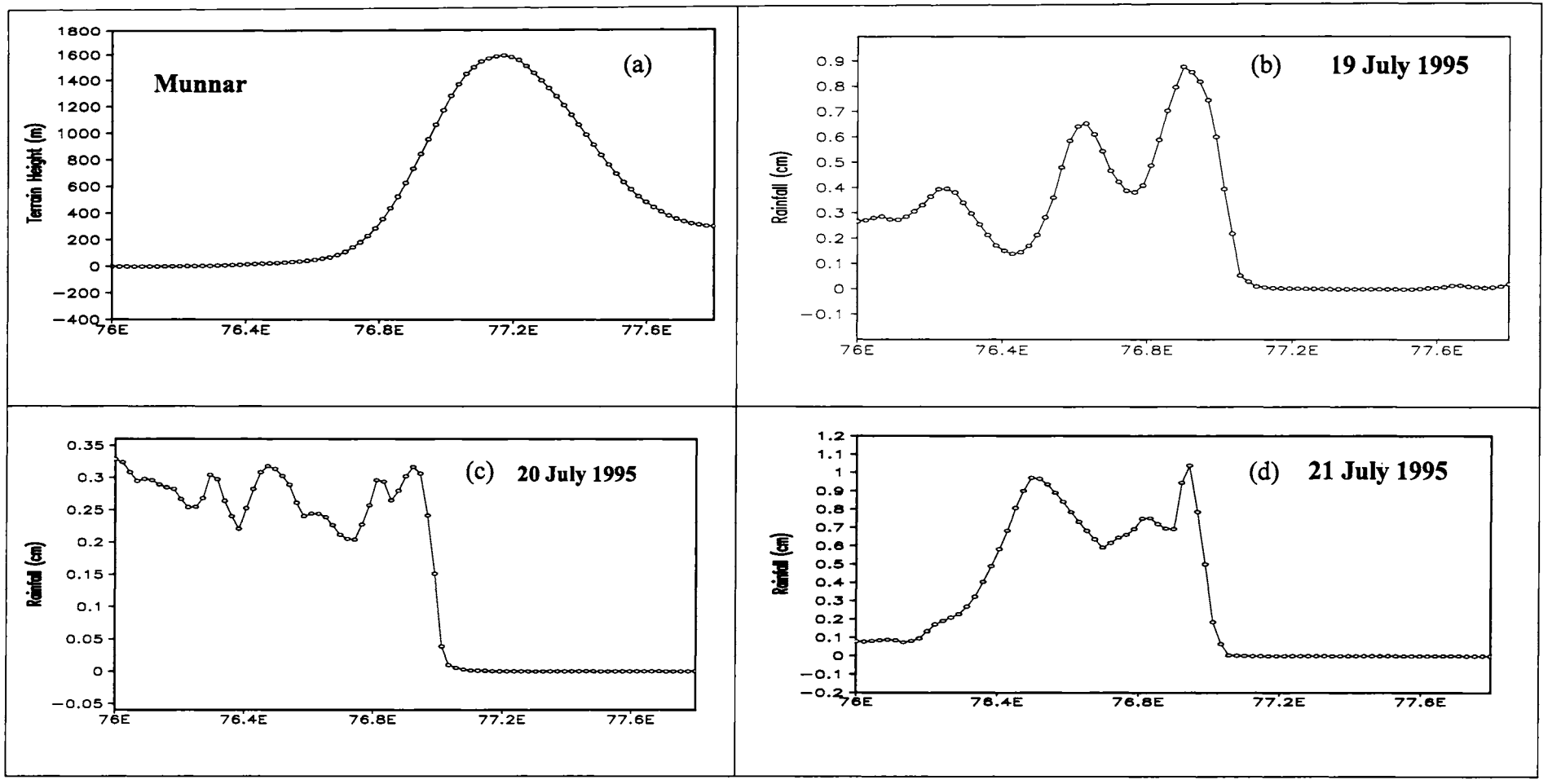

Fig.7.14 : (a) The terrain of the Munnar cross-section (averaged for 10-10.2N) obtained from MM5 simulation. Convective rainfall in the this cross-section on (b) 19th July 1995 (c) 20th July 1995 and (d) 21st July 1995.

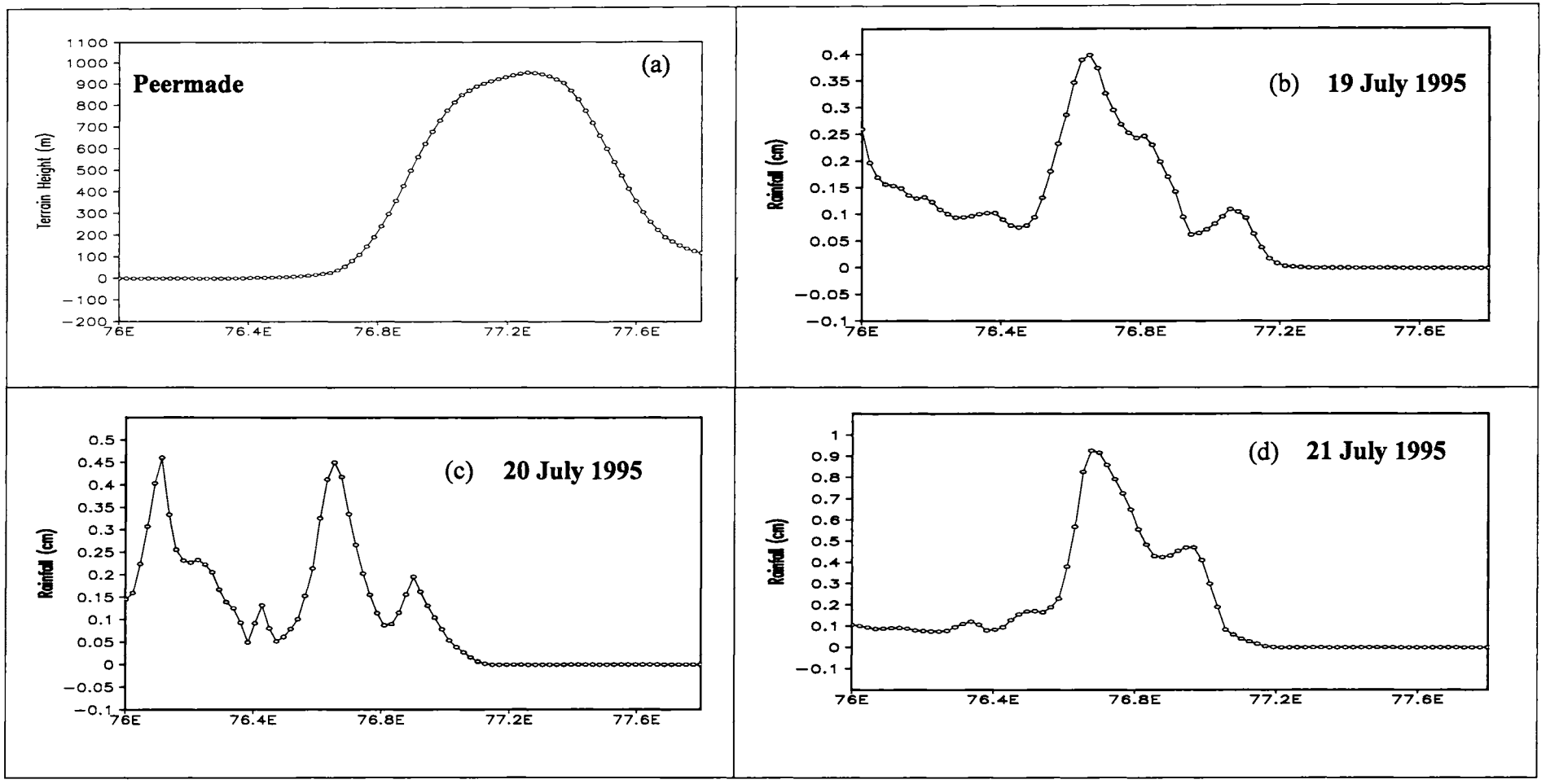

Fig.7.15 : (a) The terrain of the Peermade cross-section (averaged for 10-10.2N) obtained from MM5 simulation. Convective rainfall in this cross-section on (b) 19th July 1995 (c) 20th July 1995 and (d) 21st July 1995.

The innermost domain has a grid size of 5km only. Although the NCAR group has permitted the use of Grell scheme for convective parameterisation for grid sizes as low as 5km, it was tried to examine the variation of the convective rainfall with orography using larger grid size. Domain-2 in this simulation has grid size of 15km and the convective rainfall obtained over this domain was analysed with respect to the model orography. It is seen that the peak of the model's convective rainfall is about 40-60km west of the mountain peak as in the simulation with grid size of 5km, but the rainfall amounts were slightly less in the simulation with the larger grid size. However, the rainfall is much larger in the cases of LLJ axis south of Kerala compared to its position north of Kerala as in the simulation with grid size of 5km.

A few selected figures of the simulation using the grid size of 15km are shown. Fig.7.16(a,b) gives the spatial variation of rainfall for 11th July 1995 and 20 July 1995. Fig. 7.17 (a,b) gives the east-west section of the convective rainfall for the same days through Munnar section.

7.5 Conclusion

We have used Mesoscale Model MM5 to simulate the convective monsoon rainfall to understand the controls on the rainfall. Two factors control the rainfall of Kerala. One is a dynamic control by the Low Level Jet stream. The other is the orographic control. Using a Mesoscale model which has the orography of central Kerala hills (Anamalai and Cardamom hills) we have simulated the convective rainfall around these hills for three days with Low Level Jet axis just south of Kerala and three days with Low Level Jet axis just north of Kerala. These simulations bring out the controls both by LLJ and the orography.

It is seen that the peak of the models' convective rainfall is about 40-60km west of the mountain peak for the simulations with grid size of 5km and also with grid size 15km. The convective rainfall is much larger in the cases of

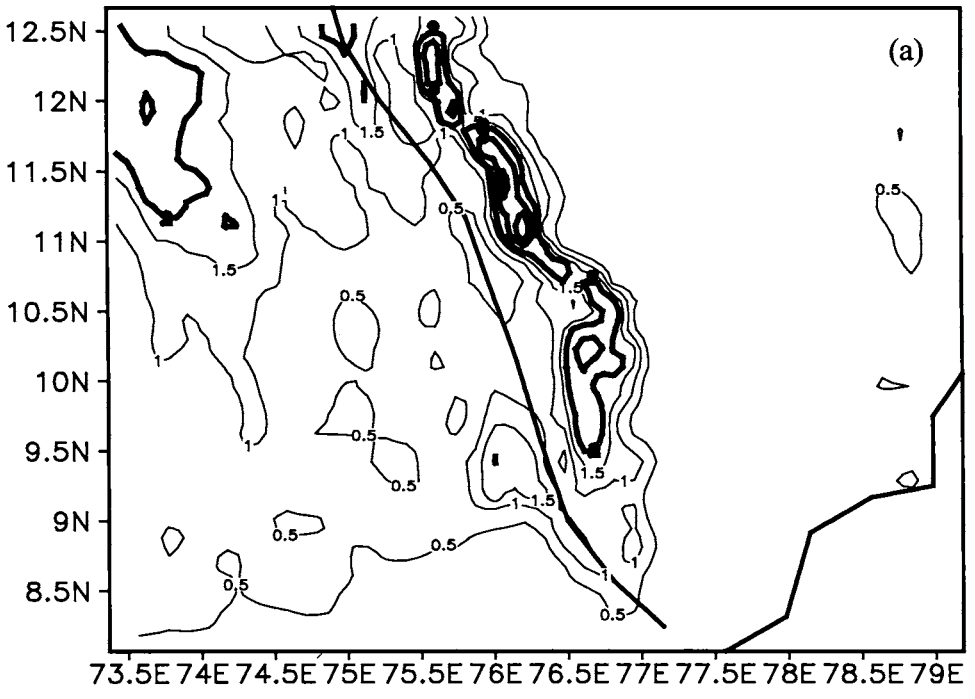

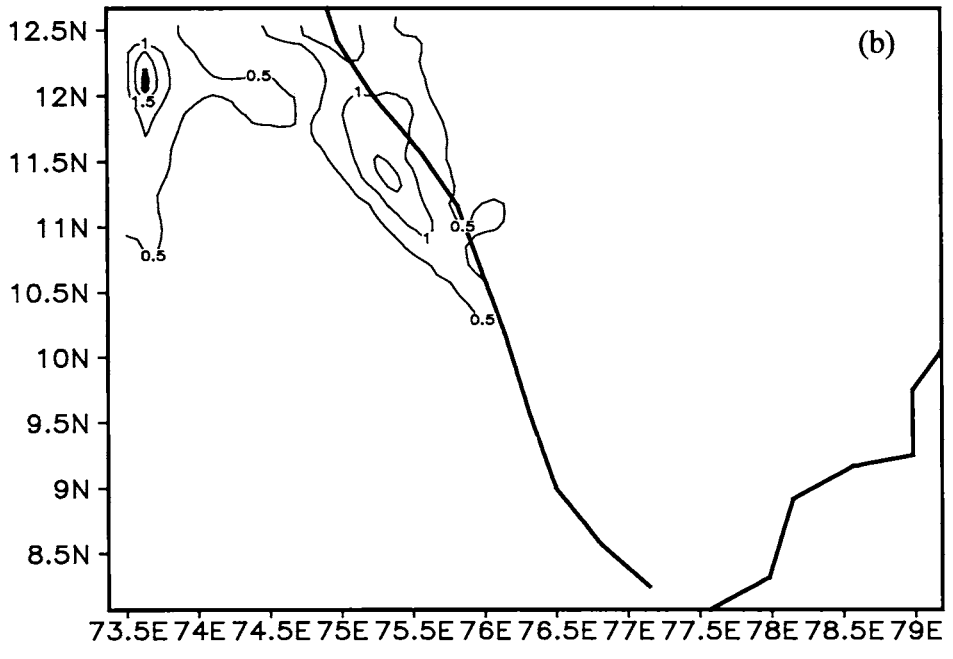

Fig. 7.16: Spatial distribution of convective rainfall in Domain-2 on (a) 11th July 1995 (b) (d) 20th July 1995

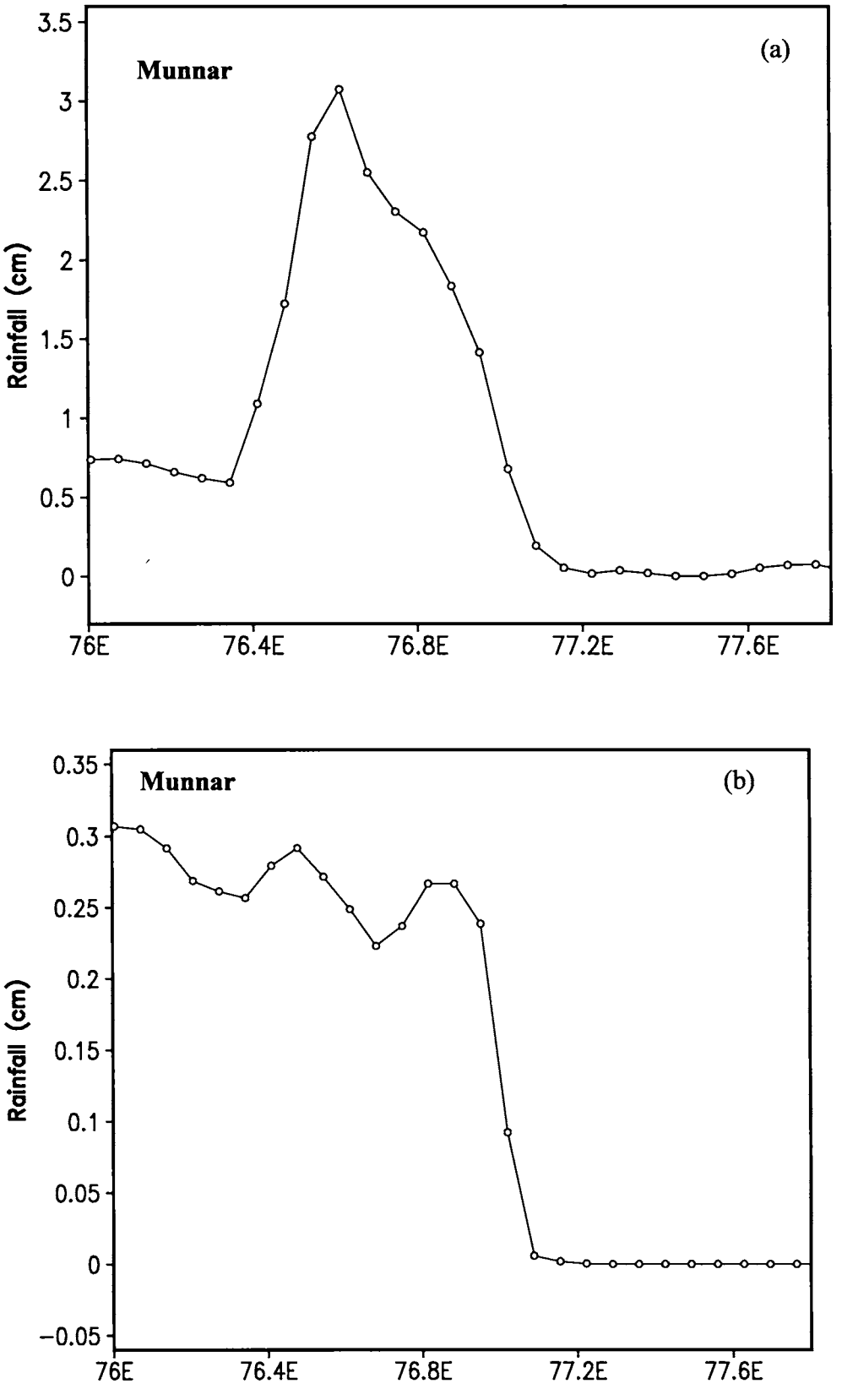

Fig. 7.17 : Convective rainfall in the Munnar cross-section from Domain-2 on (a) 11th July 1995 (b) 20th July 1995

LLJ axis south of Kerala than with LLJ axis north of Kerala for both the simulations with 5 and 15km grid sizes.

The observed peaks in rainfall are subject to the availability of rain-gauge stations. In the Munnar cross section the observed rain peak is at Nerianmangalam. If we have 2 stations in the large gap west of Neriamangalam and one station in the gap between Nerianmangalam and Munnar (see fig. 7.6) the observed rainfall profile would have been more realistic. Similar is the case with the Peermade section.

Chapter-8
Summary and Conclusions

8.1 Summary and Conclusions

Nature has bestowed Kerala with abundant rainfall. The state receives 286 cm of annual rainfall of which 68% is during the south-west monsoon season. There is however, large spatial and temporal variations in the rainfall distribution. It will be of great socio-economic importance if we learn to use the rainfall bounty to our greatest advantage. An investigation on the rainfall characteristics both on the spatial and temporal scales with emphasis on the influence of orography is done in this thesis. The results of such a study will help engineers and hydrologists to manage our rainfall resource in a proper manner.

This study focuses on south-west monsoon rainfall over Kerala and its variability both on the spatial and temporal scales. The thesis contains eight chapters. In the first chapter a very detailed literature review pertaining to the topic of research is presented. The chapter also includes the physiography of the state and general climatology with special emphasis on the rainfall climatology. Chapter-2 gives a detailed description of the data sets and the method of analysis used in the study. A detailed description of the MM5 model used is also given in this chapter.

Chapter- 3-is the study on the Intra Seasonal Variability of south-west monsoon rainfall. This is one of the main chapters of the thesis. Time series of the daily mean rainfall of south Kerala, north Kerala and whole India for the summer monsoon season of 95 years (1901-1995) have been analyzed to study the inter-annual variation of the period of the intra-seasonal oscillations in rainfall. Each data series has 128 days of daily rainfall data from 29th May to 3rd October. Intra Seasonal Oscillations (ISO) of periods 23,27,32,38,45,54 and 64 days were resolved using Wavelet Analysis and their statistical significance at levels 90%, 95% and 99% were determined.

It is found that for south Kerala out of the 95 years, 11 years had no significant ISO. Period-wise the remaining years clustered into two groups, the SHORT of periods 23,27 and 32 days and the LONG with a single period of 64 days. At 99% level of significance SHORT and LONG period ISO were found in 44 and 20 years respectively. Composites of LONG (SHORT) period ISO significant at 99% of the years 1965 to 1993 showed that the SST anomalies of the monsoon season are of the El Nino (La Nina) type in the tropical Pacific and Indian Oceans. It is seen that only in 4 years (7 years) during 1901-1995 all these three areas south Kerala, north Kerala and India as a whole have LONG (SHORT) periods significant at 99% level. In the remaining years the simple picture of Sikka-Gadgil cloud bands forming in low latitudes and moving across Kerala and India and being the dominant mechanism for modulating their rainfall at Intra Seasonal scales does not occur. The scenario is complicated by the synoptic disturbances that form during the monsoon in the 15^0N-25^0N latitude belt.

The interannual variability of whole Kerala summer monsoon rainfall and that of south and north Kerala rainfall is discussed in chapter-4 and compared to the variability of all India Summer Monsoon Rainfall (ISMR). The long-term mean of Kerala summer monsoon rainfall 1901-1996 is 195.5 cm and standard deviation is 37.6 cm. Kerala's monsoon rainfall has large interannual variability like ISMR. However, Kerala rainfall has no epochal variation unlike ISMR.Occurrences of two or more consecutive DRY years are seen in 1986,1987,1988,1989 and 1990 receiving rainfall less than ½ standard deviation of the long-term mean. The summer monsoon rainfall of Kerala shows a decreasing trend of 12.0% in 96 years. The decrease is seen more prominently in south Kerala rainfall with a decrease of 35.9 cm in 100 years which is 20.3% of the long-term mean. This decrease is comparable to the standard deviation of 36.1 cm. The long-term average of south Kerala is 176.2 cm. North Kerala receives an average rainfall of 223.6 cm and the standard deviation of the time

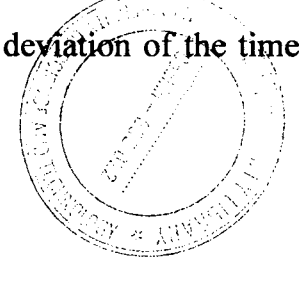

series is 44.8 cm. Even though there is considerable interannual variability in the summer monsoon rainfall of north Kerala the series does not exhibit a trend. During Active spells of monsoon rainfall in India, both south and north Kerala receive good rainfall and during the Break spells in India the rainfall in the state is very low. While, the strong monsoon days as defined by rainfall greater than or equal to 15 mm/day in south Kerala and greater than or equal to 20 mm/day in north Kerala does not exhibit any trend, the weak monsoon days during a monsoon season (rainfall less than or equal to 7.5 mm/day for both south and north Kerala) exhibits an increasing trend which is more prominent for south Kerala. However, this increasing trend is not statistically significant.

The relationship between antecedent global circulation parameters with monsoon rainfall of Kerala is studied in chapter-5 and an attempt has been made to develop a statistical model for long-range forecast of monsoon rainfall for the state. It is seen that although there is no close relationship between DRY/WET years and El Niño/La Nina events, the El Niño years are more likely to become DRY years than La Nina becoming WET. Southern Oscillation Index (SOI) of preceding September-November and concurrent March-May has significant negative correlations with summer monsoon rainfall of Kerala for the period 1977-2003. However, the relationship has large variation from epoch to epoch and hence cannot be used as a possible factor for long-range forecast of KSMR. The 500mb ridge position, which has a significant and large correlation with all India monsoon rainfall, is not correlated with KSMR.

An attempt to identify possible other factors for long-range forecast of Kerala Summer Monsoon Rainfall (KSMR) is made in this chapter. The factors that are associated with KSMR are (1) Low-level vorticity of May (2) Global surface air temperature of winter (average of January & February) (3) 200hPa meridional wind of May (4) 50hPa zonal wind (average of January & February) and all of them have significant correlation with the rainfall of Kerala. The multiple correlation coefficient of these factors with KSMR is 0.72 for the

period 1977-2003 and the estimated rainfall using this equation has a standard error of estimate of 22.9cm which is about 64% of the standard deviation of KSMR.

In chapter-6 we have studied the diurnal variation of south-west monsoon rainfall using hourly rainfall data of 33 stations mostly in central and north Kerala. In literature we find that diurnal variation of coastal stations of Trivandrum, Cochin and Mangalore (just north of Kerala) have been studied. Excepting for Trivandrum, the other two stations have a prominent early morning maximum for low and high daily rainfalls. Our analysis show that Thikkodi a coastal station has a prominent 1^{st} harmonic (24 hours) with maximum in the evening hours (~ 18 hours). The first harmonic explains 77.6% for all the rain events put together. More study is needed using coastal rainfall data to resolve this diffrence.

A large number of stations have prominent 1^{st} and 2^{nd} harmonics (diurnal & semi-diurnal). Combination of these give either a morning maximum or evening maximum in rainfall. Nearly half of the stations studied (45%) have very low amplitude for first 4 harmonics and the diurnal curve for rainfall is a flat one. Diurnal variation is a combination of the 3 or 4 important factors discussed in this cahpter. A combination of these gives the diurnal variation of any individual station. Since a majority of the stations have shown an afternoon/evening maximum it is inferred that the prominent factors in diurnal variation in Kerala rainfall are :

- Diurnal variation of air temperature of lower levels.
- Downward momentum transport in the Low Level Jetstream that strengthens the low-level winds in the afternoon/evening which together with orography increases rainfall then.

- Effect of sea-breeze which strengthens the low level westerly flow during southwest monsoon season giving rainfall maximum during afternoon/evening hours.

In chapter-7 we have used Mesoscale Model MM5 to simulate monsoon rainfall to understand the control on the rainfall by the orography of Western Ghats and the Low Level Jet Stream. Two major factors control the rainfall of Kerala. (1) Dynamic control by the Low Level Jet stream; (2) the orographic control. Using a mesoscale model which has the orography of central Kerala hills (Anamalai and Cardamom hills) we have simulated the convective rainfall around these hills for three days with Low Level Jet axis just south of Kerala and three days with Low Level Jet axis just north of Kerala. These simulations bring out the controls by LLJ and the orography.

8.2 Scope for future studies

It is seen from our study that the ISO of the monsoon season has large interannual variability, with some years having LONG period and other years having SHORT period ISO. We may do diagnostic and modelling studies to understand why some years have LONG period ISO and other years SHORT period ISO. Diurnal variation of several coastal stations may be studied as in this study Thikkodi has a prominent evening maximum not in agreement with the existing knowledge that coastal stations have a morning maximum. In this thesis four factors antecedent to monsoon having high and significant correlation with Kerala rainfall have been identified. We may explore possibility of identifying more such factors. It is seen that Western Ghats has a strong control on the east-west profile of monsoon rainfall. We may establish a closer network of observing stations along the latitudes of Munnar and Peermade to document the east-west variation in observed rainfall with orography.

REFERENCES

Ananthakrishnan, R. 1977: Some aspects of the monsoon circulation and monsoon rainfall. *Pure Appl. Geophys.*, **115**, 1209-1249

Ananthakrishnan R., Aralikatti, S.S., and Pathan, J.M., 1979a: Some features of the southwest monsoon rainfall along the west coast of India. . *Proc. Indian. Acad. Sci.* **88**, 177-199.

Ananthakrishnan R., and Pathan, J.M., 1971: Rainfall patterns over India and adjacent seas, *IITM Report*, Pune.

Ananthakrishnan R., Parthasarathy, B., and Pathan, J.M., 1979b : Meteorology of Kerala. *Contributions to Marine sciences*, 60-125.

Ananthakrishnan R., and Parthasarathy, B., 1984 : Indian rainfall in relation to the sunspot cycle: 1871-1978. *J. of Climatology*, **4**,149-169.

Ananthakrishnan R., and Soman M.K., 1988 : The onset of the southwest monsoon over Kerala : 1901-1980. *J. of Climatology*, **8**,283-296.

Anthes, R. A. and Warner, T. T., 1978: Development of hydrostatic model suitable for air pollution and other mesometeorological studies, *Mon. Weather Rev.*, **106**, 1045-1078.

Anu Simon and Mohankumar K., 2004: Spatial variability and rainfall characteristics of Kerala, Earth and Planetary Sciences, **113**, 211-222.

Anu Simon., Mohankumar K., And Joseph, P.V., 2003: SST-Indian Summer Monsoon relationship before and after 1976. Paper presented at SIVOM. International Seminar on Scale Interactions, held at Munnar, 6-10Oct. 2003.

Arakawa, A., and W.H. Schubert., 1974: Interaction of a cumulus cloud ensemble with the large-scale environment. Part I., *J. Atmos. Sci.*, **31**, 674-704.

Asnani G.C., 2001 : El Niño of 1997-1998 and Indian monsoon. *Mausam*, **52**, 57-66.

Atkinson, G.D., 1971: Forecaster's guide to tropical meteorology, Air Weather Service Tech. Rep. 240 (MAC), U.S. Air Force.

Bamzai, A.S., and Shukla, J., 1999: Relation between Eurasian snow cover, snow depth and the Indian summer monsoon : An observational study. *J. of Climate*, **10**, 3117-3132.

Banarjee A.K., and C.R.V. Raman., 1976: One hundred years of southwest monsoon rainfall over India. *Pre-published Sc. Report No. 76/(6), India. Meteor. Dept.* 7.

Banarjee, A.K., Sen, P.N., and C.R.V. Raman., 1978: On forecasting southwest monsoon rainfall over India with mid-tropospheric circulation anomaly of April. *Indian. J. Met. Hydrol. Geophy.* **29**, 425-431.

Bhalme, H.N. 1972: Trends and quasi-biennial oscillation in the series of cyclonic disturbances over the Indian region , *Ind. J. Meteor. Geophys.*, **23**, 335-340.

Bhalme, H.N., and Jadhav, S.K. 1984: The Southern Oscillation and its relation to the monsoon rainfall, *J.of Climatoloy.*, **4**, 509-520.

Bhalme, H.N., and Mooley, D.A. 1980: Large-scale droughts/floods and monsoon circulation, *Mon. Wea. Rev.*, **8**, 1197-1211.

Bhalme, H.N., Rahalker S.S., and Sikder, A.B. 1987: Tropical Quasi-Biennial Oscillation of the 10mb wind and Indian Monsoon Rainfall – implications for forecasting. *J. of Climatology.*, **7**, 345-353.

Bjerknes, J., 1969: Atmospheric teleconnection from the equatorial Pacific. *Mon. Wea. Rev.*, **97**,163.

Blackadar, A.K., 1957: Boundary layer wind maxima and their significance for the growth of nocturnal inversions. *Bull. Amer. Meteor. Soc.*, **38**, 283-290.

Blanford, H.P., 1886: Rainfall of India. *Mem. India Met. Dep.*, 3, 658.

Brier, G.W., and Simpson J.S., 1969: Tropical cloudiness and precipitation related to pressure and tidal variations. *Quart. J. Roy. Meteor. Soc.*, **95**, 120-147.

Brown, R.D. 2000. Northern hemisphere snow cover variability and change, 1915–97. *Journal of Climate* **13**:2339–2355.

Chandrasekar A and B N Goswami 1999: A Linear Model study of the Mid-Tropospheric Ridge and its Displacement, in *Advanced Technologies in Meteorology*, R K Gupta nd S J Reddy (eds), Tata McGraw Hill Publishing Co. New Delhi, 250-256.

Chang,C.P., and T.Li., 2000: A theory for tropical tropospheric biennial oscillation. J. Atmos.Sci., **57**,2209-2224.

Charney, J.G., and Shukal,J.,1981: Predictability of monsoons, in *Monsoon Dynamics* (edt. Lighhill, J and Peaarie, R.), Cambridge Univ. Press. USA.

Chowdhury, A., Mukhopadhay, R.K., and Ray, K.C., 1988: Low frequency oscillations in summer monsoon rainfall over India, *Mausam*, **39**, 375-382.

Cornejo-Garrido, A.G., and Stone, P.H., 1977: On the heat balance of the Walker circulation. *J. of Atm. Sci.*, **34**, 1155-1162.

Dai, A., 2001: Global precipitation and thunderstorm frequencies, Part II: Diurnal variations, *J.of Climate*, **14**, 1112-1128.

Dai, A., C. Deser., 1999: Diurnal and semi-diurnal variations in global surface wind and divergence fields. *Geo. Phy. Res.* **104**, 31109-31126.

De U.S, Lele R. R, Natu JC. 1998. Breaks in southwest monsoon. Pre-published Scientific Report, India Meteorological Department.

Derber, J. C., Parrish, D. F., and Lord, S. J., 1991: The new global operational analysis system at the National Meteorological Center, *Wea. Forcasting*, **6**, 538-547.

Dickson, R. R., 1984: Eurasian snow cover versus Indian monsoon rainfall - An extension of the Hahn-Shukla results. *J. Climate Appl. Meteor.*, **23**, 171-173.

Dudhia, J., 1993: A nonhydrostatic version of the Penn State/NCAR mesoscale model: Validation tests and simulation of an Atlantic cyclone and cold front, *Mon. Weather Rev.*, **121**, 1493-1513.

Ebdon, R. A., and Veryard, R.G., 1961: Fluctuations in equatorial stratospheric winds, *Nature*, **189**, 791.

Farge M. 1992: Wavelet transforms and their applications to turbulence. *Annu. Rev. Fluid Mech.*, **24:** 395-457.

Fasullo, J., 2004: A stratified diagnosis of Indian monsoon – Eurasian snow cover relationship. *J. of Climate*, **17**, 1110-1122.

Findlater, J., 1969: A major low-level air current near the Indian Ocean during the northern summer . *Quart. J. Roy. Meteor. Soc.*, **95**, 362-380

Flohn H, 1968: Contribution to a meteorology of the Tibetan Highlands, Atmos. Sci. Paper No. 130, Dept. of Atmos. Sci., Coloraado State University, Fort Collins, pp 120.

Gill, A.E., 1980: Some simple solutions for heat induced tropical circulation, *Quart. J. Roy. Meteor.*, **106**, 447-462.

Gowariker, V., Thapliyal, V., Sarker, R.P., Mandal, G.S., and Sikka, D.R., 1989: Parametric and power regression models : New approach to long range forcasting of monsoon rainfall in India. *Mausam,* **40**,115-122.

Gowariker, V., Thapliyal, V., Sarker, R.P., Mandal, S., Sen Roy, N., and Sikka, D.R., 1991: A power regression model for long range forecast of southwest monsoon rainfall over India. *Mausam,* **42**,125-130.

Gray, W.M., and Jacobson R.W., 1977: Diurnal variation of deep cumulus convection, *Mon. Wea. Rev.* , **105**, 1172-1188

Grell, G. A., 1993: Prognostic evaluation of assumptions used by cumulus parameterizations. *Mon. Wea. Rev.*, **121**, 764-787.

Grell, G., Dudhia, J., and Stauffer, D., 1994: A description of the fifth generation Penn State / NCAR Mesoscale Model. NCAR Tech. Note NCAR/ TN-390 TR, 117.

Gruber, A. and Krueger, A. F., The status of the NOAA outgoing longwave radiation data set, *Bull. Am. Meteorol. Soc.*, 65, 958-926, 1984.

Hackert, E.C., and Hasternath S., 1986: Mechanisms of Java rainfall anomalies. *Mon. Wea. Rev.*, **114**, 745-757.

Hahn, D.J., and Shukla, J., 1976: An apparent relationship between Eurasian snow cover and Indian monsoon rainfall. *J.Atmos. Sci.*, **33**, 2461-2462.

Harrison, D.E., 1984: On the appearance of sustained equatorial westerlies during the 1982 Pacific warm event. *Science*, **225**, 11099-1102.

Harrison, D.E., and Larkin, N., 1998: The ENSO surface temperature and wind signal : a near-global composite and time-series view, 1946-1995. *Rev. Geophys.* 36(3), 356-399.

Hartmann DL, Michelsen ML. 1989: Intraseasonal periodicities in Indian rainfall. *Journal of Atmospheric Sciences.* **46**: 2838-2862.

Hasternath, S., and Greischar, L., 1993: Changing predictability of Indian monsoon rainfall anomalies. *Proc. Indian Acad. Sci. (Earth Planet Sci.)*, **102**, 35-47.

Holton, J.R., 1968: The diurnal boundary layer wind oscillation above sloping terrain. *Tellus*, **19**,199-205.

Holton, J.R., 1988: A note on temperature propagation of the biennial oscillation, *J. Atmos. Sci.* **25**, 519-526.

Horrel, J.D., 1982: On the annual cycle of the tropical Pacific atmosphere. *J. of Atm. Sci.*, **37**, 1863-1878.

Hu, C.Y., and S.S. Hong, 1989: Diurnal variations of precipitation frequencies in the Taiwan area. *Meteor. Bull.*, **35**, 65-88.

Jagnnathan, P., and Bhalme H.N., 1973: Changes in the pattern of distribution of south-west monsoon rainfall over India associated with sunspots, *Mon. Wea. Rev.*, **101**, 691.

Jagannathan, P., and Parthasarathy, B., 1973: Trends and periodicities of rainfall over India. *Mon. Wea. Rev.*, **101**, 4, 371-375.

Joseph, P.V., 1976: Climate change in monsoon and cyclones 1891-1974. *Proc. Symp. Tropical Monsoons,* 378-387.

Joseph, P.V., 1978: Sub-tropical westerlies in relation to large-scale failure of Indian monsoon. *Indian J. Meteor. Geophys.*, **29**, 412-418.

Joseph. P.V., 1981: Ocean-atmosphere interaction on a seasonal scale over north Indian ocean and Indian monsoon rainfall and cyclone tracks – A preliminary study.. *Mausam*, **32**,237-246

Joseph. P.V., 1981: Meridional wind index for long range forecasting of Indian summer monsoon rainfall,. *Mausam*, **32**,31-34

Joseph. P.V., 1990: Monsoon variability in relation to equatorial trough activity over Indian and west Pacific oceans. *Mausam*, **41**,291-296.

Joseph, P.V., and Anu Simon, 2005: Weakening trend of the southwest monsoon current through peninsular India from 1950 to the present, Curr. Sci. **89**,4, 687-694.

Joseph P.V, Anu Simon, Venu G Nair, Aype Thomas., 2004: Intra Seasonal Oscillation (ISO) of South Kerala Rainfall During The Summer monsoons of 1901 to 1995. Earth and Planetary Sciences, **113**, 139-150.

Joseph P.V, Eischeid JK, Pyle RJ. 1994:. Interannual variability of the onset of Indian summer monsoon and its association with atmospheric features, El Nino and sea surface temperature anomalies. *J. Climate.* **7:** 81-105.

Joseph P.V., Mukhopadhyaya, R.K., Dixit, W.V., and Vaidya, D.V., 1981: Meridional wind index for long-range forecasting of Indian summer monsoon rainfall. *Mausam*, **32**,31-34.

Joseph, P.V. and Raman, P.L., 1966: Existence of Low Level westerly Jetstream over peninsular India during July. *Indian J. Meteor. Geophys.*, **17**, 407-410

Joseph. P.V., and Pillai, P.V., 1984: Air-sea interaction on a seasonal scale over north Indian ocean – Part 1: Interannual variations of sea surface temperature and Indian summer monsoon rainfall. *Mausam*, **35**,323-330.

Joseph, P.V. and Sijikumar, S., 2004: Intra Seasonal Variability of the Low Level Jetstream of the Asian Summer Monsoon, *J. Climate*, **17**, 1449-1458

Kalnay, E., Kanamitsu, M., Kistler, R., Collins, W., Deaven, D., Gandin, L., Iredell, M., Saha, S., White, G., Woollen, J., Zhu, Y., Leetmaa, A., Reynolds, R., Chelliah, M., Ebisuzaki, W., Higgins, W., Janowiak, J., Mo, K. C., Ropelewski, C., Wang, J., Jenne, R., and Joseph, D., 1996: The NCEP/NCAR 40-year reanalysis project, *Bull. Am. Meteorol. Soc.*, **77**, 437Œ471..

Keen, R.A., 1982: The role of cross-equatorial cyclone pairs in the southern oscillation. *Mon. Wea. Rev.*, **110**,1405-1416.

Kiladis GN, Diaz HF. 1989, Global climate anomalies associated with extremes in the southern oscillation, *J. of Climate.* **10**, 1069-1090.

Kraus, E.B., 1963: The diurnal precipitation change over the sea., *J. Atmos. Sci.,* **20,** 546-551.

Kripalani R.H, Singh S.V, and Arkin P.A., 1991, Sabade S.S., 2005, Large-scale features of rainfall and outgoing long-wave radiation over Indian and adjoining regions. Contributions to Atmospheric Physics, **64**, 159-168.

Kripalani, R. H., and Kulkarni, A., 1997: Of El Nino/La Nina on the Indian monsoon: A new perspective. *Weather,* **52**, 39-46

Kripalani, R. H., and Kulkarni, A., and Singh, S.V., 1997 : Association of the Indian summer monsoon with the Northern Hemisphere and mid-latitude circulation. *Int. J. Climatol.,* **17**,1055-1067.

Krishnakumar, K., Rajagopalan B., and Cane, M.A., 1999: On the weakening relationship between the Indian Monsoon and ENSO . *Science*, **284**, 2156-2159.

Krishnakumar, K., Soman, M.K., and Rupakumar, K., 1995: Seasonal forecasting of Indian summer monsoon rainfall. *Weather*, **50**, 449-467

Krishnamurthy V., and Goswami, B. N., 2000: Indian monsoon-ENSO relationship on interdecadal timescale, *J. Climate*, **4,** 579-595.

Krishnamurti TN. 1985: Summer Monsoon Experiment – A review. *Mon. Wea. Rev.* **113**: 1590-1626.

Krishnamurti T.N., and Balme, 1976: Oscillations of a monsoon system. Part I: Observational aspects. *J. Atmos. Sci.*, **33**, 1937-1954.

Krishnamurti T.N, Subrahmanyam D. 1982. The 30-50 day mode at 850 mb during MONEX. *Journal of Atmospheric Sciences.* **39:** 2088-2095.

Kumar K., Bajagopalan, B., and Cane, M.A., 1999: On the weakening relationship between Indian monsoon and ENSO, *Science*, **284**, 2156-2159.

Kumar Pradeep P.K., 1994: Physiographic features and changes in rainfall pattern of Kerala, 63. Cochin University of Science and Technology.

Lau, K.M., and Chan, P.H., 1983: Aspects of the 40-50 day oscillation during the northern summer as inferred from outgoing longwave radiation. *Mon. Wea. Rev.*, **114**, 1354-1367.

Lau K.M., and Chan P.H. 1985: Aspects of the 40-50 day oscillation during northern winter as inferred from OLR. *Mon. Weather Rev.* **113**: 1889-1909.

Lau K.M., and Chan P.H. 1986. Aspects of the 40-50 day oscillation during northern summer as inferred from OLR. *Mon. Weather Rev.* **114**: 1354-1367.

Lau, K.M., and Chan, P.H., 1986: Short-term planetary-scale interactions over the tropics and midlatitudes. Part I: Winter MONEX period. *Mon. Wea. Rev.*, **111**,1372-1388.

Lawrence DM, Webster PJ. 2001. Interannual Variations of the intraseasonal oscillation in the south Asian summer monsoon region. *Journal of Climate.* **14**: 2910-2922

Lettau, H., 1967: Small to large scale features of the boundary layer structure over mountain slopes. *Proc. Symp. Mountain Meteor.*, Dept. Atmos. Sci., Colorado State University, 221

Liebmann, B., and Hartman, D.L., 1982: Interannual variations of outgoing IR associated with tropical circulation changes during 1974-1978.. *J. of Atm. Sci.*, **39**, 1153-1162.

Lindzen R.S. and Sumant Nigam, 1987: On the role of sea surface temperature gradients in forcing low-level winds and convergence in the tropics. *J. of Atm. Sci.*, **44**, 2418-2436.

Lorenc AC. 1984. The evolution of planetary-scale 200 mb divergent flow during the FGGE year. *Quart.J. Roy. Meteor. Soc.,* **110**: 427-441.

Madden RA, Julian P.R. 1971: Detection of a 40-50 day oscillation in the zonal wind in the tropical Pacific. *Journal of Atmospheric Sciences.* **28**: 702-708.

Madden RA, Julian P.R. 1972. Description of global scale circulation cells in the tropics with a 40-50 day period. *Journal of Atmospheric Sciences.* **29**: 1109-1123.

Madden RA, Julian P.R. 1994: Observations of the 40-50 day tropical oscillation – A Review. *Mon. Weather Rev.* **122**: 814-837.

Marquardt, C., and B. Naujokat, 1997: An update of the equatorial QBO and its variability. 1st SPARC Gen. Assembly Melbourne Australia, WMO/TD-No. 814, Vol. 1, 87-90.

Matsuno, T., 1966: Quasi-geostrophic motions in the equatorial area, *J. Meteor. Soc. Japan.,* **44**, 25-43.

McBride, J.L., and Nicholls, N., 1993: Seasonal relationships between Australian rainfall and Southern Oscillation. *Mon. Wea. Rev.*, **111**, 1998-2004.

Meehl, G.A., 1987 : The annual cycle and interannual variability in the tropical Pacific and Indian ocean region.: Mon. Wea. Rev., **115**, 27-50.

Mooley, D.A., 1975: Vagaries of the Indian summer monsoon during the last 10 years. *Vayu Mandal*, **5**, 65-66.

Mooley, D.A., 1976: Worst summer monsoon failures over the Asiatic monsoon area. . *Indian. Nat. Sci,. Acad.* **54**, 34-43.

Mooley, D.A., and Paolino, D.A., 1988: A predictive monsoon signal in the surface level thermal field over India. *Mon. Wea. Rev.*, **116**, 339-352.

Mooley, D.A., Parthasarthy B., and Pant G.B., 1986: Relationship between all-India summer monsoon rainfall during 1871-1978. *Climate Change,* **6**, 287-301.

Mooley, D. A., Parthasarathy, B., Sontakke, N. A., and Munot A.A., 1981: Annual rain-water over India, its variability and impact on the economy. *J. Climatol*,,167-186.

Mooley, D and J. Shukla, 1987: Variability and forecasting of the summer monsoon rainfall over India., C.P. Chang and T. N Krishnamurti, Eds. *Monsoon Meteorology,* 26-59, Oxford Univ. Press

Morlet J. 1983. Sampling theory and wave propagation. *NATO, ASI Series FI, Springer.* 223-261.

Mukherjee, B.K., Indira, K., Reddy, R.S., and . Ramanmurti T.Y., Bh.V. 1985: Quasi-biennial oscillation in the stratospheric zonal wind and Indian monsoon, *Mon. Wea. Rev.*, **113**, 1421-1424.

Mukherjee, B.K., Reddy, R.S., Ramanmurti T.Y., Bh.V. 1979: High level warming and Indian summer monsoon, *Mon. Wea. Rev.*, **107**, 1581-1588.

Murakami T, Chen LX, Xie A, Shreshta. 1986: Eastward propagation of 30-60 day perturbations as revealed from outgoing longwave radiation data. *Journal of Atmospheric Sciences.* **42**: 1107-1122.

Naujokat, B., 1986: An update of the observed quasi-biennial oscillation of the stratospheric winds over the tropics. *J. Atmos. Sci.*,**43**,1873-1877.

Nicholls, N., 1988: El Niño –Southern Oscillation impact prediction. *Bull. Amer. Meteor. Soc.*, **69**, 173-176.

Oki, T., and Musaike K., 1994: Seasonal change of the diurnal cycle of precipitation over Japan and Malaysia, *J. Appl. Meteor.*, **33,** 1445-1463.

Pant, G.B. and Rupa Kumar, K., :1997. Climates of South Asia. John Wiley & Sons, Chichester, 320 pp.

Parrish, D. F. and Derber, J., 1992: The National Meteorological Center's spectral statistical interpolation analysis system, *Mon. Weather Rev.*, **120**, 1747-1763.

Parthasarathy, B., and Dhar, O.N., 1974: Secular variations of regional rainfall over India. *Quart. J. Roy. Met.Soc.*, **100**, 245-257.

Parthasarathy, B., Diaz, H.F., and Eischield J.K., 1988: Prediction of All India summer monsoon rainfall with r`egional and large-scale parameters. *J.Geophy.Res.*, **93**, 5341-5350.

Parthasarathy, B., Munot A.A., and Kothawale, D.R., 1994: All Indian monthly and seasonal rainfall series: 1871-1993. *Theor. Appl. Climatol*, **49**, 217-224.

Parthasarathy B., Munot A.A., Kothawale D.R., 1995. Monthly and seasonal rainfall series for all-India homogeneous regions and meteorological subdivisions : 1871-1994. Research Report No. RR-065, Indian Institute of Tropical Meteorology, Pune, 113pp.

Parthasarthy, B., and Mooley, D.A., 1978: Some features of a long homogenous series of Indian summer monsoon rainfall. *Mon. Wea. Rev.* **106**, 771-781.

Parthasarathy B., Pant G.B., 1984: The spatial and temporal relationships between the Indian summer monsoon rainfall and the Southern Oscillation. *Tellus*, **36A**, 269-277.

Parthasarthy, B., Rupakumar, K., and Deshpande V.R.,1991: Indian summer monsoon rainfall and 200-mbar meridional wind ndex: Application for long-range predication, *Int. J. Clim.*, **11**, 165-176.

Parthasarthy, B., Rupakumar, K., and Munot, A.A., 1991: Evidence of secular variations in Indian summer monsoon rainfall circulations relationships. *J. Climate*, **4**, 927-938.

Parthasarathy, B., RupaKumar, K and Munot, A. A. 1993 : Homogeneous Indian Monsoon Rainfall : variability and prediction. *Proc. Indian Acad. Sci. (Earth Planet. Sci.)* 121-155.

Parthasarthy, B., Sontakke, N.A., Munot, A.A. and Kothawale, D.R 1990: Vagaries of Indian monsoon rainfall and its relationships with regional/global circulations. *Mausam*, **41**, 301-308.

Parthasarthy, B., Sontakke, N.A., Munot, A.A. and Kothawale, D.R 1987: Droughts/floods in the summer monsoon season over different meteorological subdivisions of India for the period 1871-1984. *J. Climatol.*, **7**, 57-70.

Pathan, J.M., 1994: Diurnal variation of southwest monsoon rainfall at Indian stations. *Advances in Atmospheric Sciences*, **11**, 111-120.

Philander, S.G., 1981: The response of equatorial oceans to a relaxation of the trade winds. *J.Phys.Oceanoger,* 11,176-189.

Prasad, K.D., and S.V., Singh., 1991: Possibility of predicting Indian monsoon rainfall on reduced spatial and temporal scales. *Journal of Climate,* **11,** 1357–1361.

Quinn W.H. and Neal, V.,T., 1987, *El Nino occurrences over the past four and a half centuries*, Journal of Geophysical Research, **92**, 14449-14461.

Raja Rao, K.S., Lakhole, N.J., 1978: Quasi-biennial oscillation and summer southwest monsoon, *Ind. J. Met. Hydrol. Geophys.*, **29**, 403.

Rajan, C.K., Valsala, P., and Ananthakrishnan R. 1981: Some aspects of the rainfall of Kerala and adjoining areas. 1. southwest monsoon rainfall of Kerala. *Bull. Dept. Mar. Sci. Univ.* **2**, 65-102.

Rajeevan M., 2001: Prediction of Indian summer monsoon: Status, problems and prospects. *Curr. Sci.*, **81**, 1451-1457.

Rajeevan, M., Pai., D.S., Dikshit, S.K., and Kelkar, R.R., 2004: IMD's new operational models for long-range forcast of southwest monsoon rainfall over India and their verification for 2003. *Current Science*, **86**, 3, 422-431.

Rajeevan, M., Pai., D.S., Thapliyal, V., 1998: Spatial and temporal relationships between global and land surface air temperature anomalies and Indian summer monsoon rainfall.. *Meteorol Atmos. Phys.*, **66**, 157-171.

Ramage C.S., 1952: Diurnal variation of summer rainfall over east China, Korea and Japan. *J. Meteor.*, **9**, 83-86.

Ramage.C.S. 1971: *Monsoon Meteorology*, vol.**15** of International Geophysical Series, Academic Press, San Diego, Calif.

Ramage, C.S., Hori, H.M., 1981: Meteorological aspects of the El Nino. *Mon. Wea. Rev.*, **109**, 1827-1835.

Ramamurthy, K., 1969: Some aspects of 'break' in the Indian South west monsoon during July and August, India Meteorological Department, NewDelhi, Forecasting Manual, Part IV.18.3.

Ramanadham, R., Rao, P.V., and Pattanaik, J.K., 1973: Break in the Indian Summer Monsoon, Pure., *Appl. Geophy.*, **104**, 635-647.

Ramanathan, K.R., 1931: The structure of the sea breeze at Pune. *Ind. Met. Dept. Sci. Rep.*, **3**, 131-134.

Ramaswamy, C., 1976: Synoptic aspects of droughts in the Asiatic monsoon area. *Indian. Nat. Sci,. Acad.* **54**, 109-132.

Randall David A., 2004: An Introduction to the General Circulation of the Atmosphere, Course Outline. Dept. of Atmospheric Sciences, Colorado State University.

Rao, K.N., and Jagannathan, P., 1963: Climate changes in India. *Proc. Symp.on Changes in Climate*, Rome, UNESCO and WMO, 49-66.

Rao.Y.P., 1976: South West Monsoon India Meteorological Department, *Meteorological Monograph Synoptic Meteorology* **No. 1/ 1976**, Delhi, 367 pages.

Rasmusson E.M, Carpenter T.H. 1982. Variations in tropical sea surface temperature and surface wind fields associated with the Southern Oscillation/ El Nino. *Mon. Wea. Rev.* **110**: 354-384.

Rasmusson E.M, Carpenter T.H. 1983. The relationship between eastern equatorial Pacific sea surface temperatures and rainfall over India and Sri Lanka. *Mon. Wea. Rev.* **111:** 517-528

Reed R.J. and Rogers D.J., 1962: The circulation of the tropical stratosphere in the years 1954-1960, *J.Atm. Sci.* **19**,127.

Reihl, H., 1979: The trade wind inversion. *Climate and Weather in the tropics*.Academic Press, 611.

Rui H, Wang B. 1990. Development characteristics and dynamic structure of tropical intraseasonal convection anomalies. *Journal of Atmospheric Sciences.* **47**: 357-379.

Sahai, A.K., Grimm, A.M., Satyan, V., and Pant, G.B., 2002: Prospects of prediction of Indian summer monsoon rainfall using global SST anomalies. *IITM Research Report*, RR-093.

Sarachik, E.S., 1985: A simple theory for the vertical structure of the tropical atmosphere. *Pure Appl. Geophys.* **123**, 261-271.

Sarker, R.P., 1967: Some modifications in a dynamical model of orographic rainfall., *Mon. Wea. Rev.*, **95**, 673-683.

Shimoda, M.T., Okatani, and Saloum M., 1999: Diurnal variations of rainfall over Niger in the west Africa Sahel: A comparison between wet and drought years. *Int. J. Climatol.*, **19**, 81-94.

Shukla, J., and Mooley, D.A., 1987: Empirical Prediction of the summer monsoon rainfall over India. *Mon. Wea. Rev.*, **115**, 695-703.

Shukla, J., and Wallace, J.M., 1983: Numerical simulation of the atmospheric response to equatorial Pacific sea surface temperature anomalies. *J. Atm. Sci.***40**, 1613-1630.

Sikka, D.R., 1980: Some aspects of the large-scale fluctuations of summer monsoon rainfall over India in relation to fluctuations in planetary and regional scale circulation parameters. *Proc. Indian Acad. Sci. (Earth Planet Sci.),* **89**, 179-195

Sikka D.R, Sulocahna Gadgil. 1980. On the maximum cloud zone and the ITCZ over India longitude during the southwest monsoon. *Mon. Weather Rev.* **108**:1840-1853.

Singh S.V, Kripalani RH, Sikka DR. 1992. Interannual variability of the Madden – Julian oscillations in Indian summer monsoon rainfall. *Journal of Climate.* **5**: 973-978.

Soman M.K., Krishna Kumar and Nityanand Singh, 1988: Decreasing trend in the rainfall of Kerala, Current Science, **57**, 7-12.

Soman, M. K. and J. M. Slingo, 1997: Sensitivity of the Asian Summer Monsoon to aspects of the sea surface temperature anomalies in the tropical Pacific Ocean. *Q. J. R. Meteorol. Soc.*, **123**, 309-336.

Srinivasan, J., 2001: A simple Thermodynamic model for seasonal variation of monsoon rainfall. *Curr. Sci.*, 80,73-77.

Srinivasan, J., and Nanjundiah R.. S., 2002: The evolution of Indian summer monsoon in 1997 and 1983. *Meteorol. Atmos. Phys..*, **79**,243-257.

Stone, P.H., and Chervin, R.M., 1984: The influence of ocean temperature gradient and continentality on the Walker circulation. *Mon. Wea. Rev.*, **115**, 1524-1534..

Thapliyal, V., 1982: Stochastic dynamic model for long-range prediction of monsoon rainfall in peninsular India. *Mausam*, 33, 399-404.

Thapliyal, V., 1997: Preliminary and final long range forecasts for seasonal monsoon rainfall over India. *J. Arid. Environ.*, **36**, 385-403.

Thapliyal, V., and Kulshrestha, S.M.,.1992: recent models for long-range forecasting of southwest monsoon rainfall over India. *Mausam*, **43**, 239-248.

Thomas Aype, Anu Simon and Joepsh P.V., 2003: Monsoon rainfall droughts of India during 1987 and 2002 and their relation to the intra-seasonal oscillation. Paper presented at *SIVOM.* International Seminar on Scale Interactions, held at Munnar, 6-10Oct. 2003.

Torrence C, Compo PG. 1998. A practical guide to wavelet analysis. *Bulletin of the American Meteorological Society.* **79**:1, 61-78

Tourre YM, White WB. 1995. ENSO signals in global upper ocean temperature. *Journal of Physical Oceanography.* **25**: 1317-1330.

Tourre YM, White WB. 1997. Evolution of the ENSO signal over the Indo-Pacific domain. *Journal of Physical Oceanography.* 683-696.

Trenberth, K.E., 1976: Spatial and temporal variations of the Southern Oscillation. *Quart. J. Roy. Meteor.*, **12**, 639-653.

Trenberth KE. 1997. The definition of El Nino. *Bulletin of the American Meteorological Society.* **78**:12, 2771-2777.

Troen, I and L. Mahrt, 1986: A simple model of the atmospheric layer., *Boundary Layer Meteorology*, **37**, 129-148.

Verma, R.K., and Kamte, P.P : 1980 statistical technique for long-range forecasting of summer monsoon activity over India. Proceeding of Symposium on the Probabilistic and statistical methods in Weather forecasting, 8-12 Sept. 1980. World Meteorological Organization, Geneva, 303-307.

Verma, R.K., Subramaniam, K., and Dugam, S.S., 1985: Interannual and long-term variability of the summer monsoon rainfall and its possible lint with northern hemisphere surface air temperature. *Proc. Indian Acad. Sci. (Earth Planet Sci.),* **94**, 187-198.

Walker, G.T., 1910: On the meteorological evidence for supposed changes of climate in India. *Mem. India Meteor. Dept.* **21**, 1-21.

Wallace, J.M, 1975: Diurnal variations in precipitation and thunderstorm frequency over the conterminous United States. *Mon. Wea. Rev.*, **103,** 406-419.

Wang B, Rui H. 1990. Synoptic climatology of transient tropical intraseasonal convection anomalies: 1975-1985. *Meteorol. Atmmos. Phys.* **44**: 43-61.

Wang, B., 1995: Interdecadal changes in El Nino onset in the last four decades. *J. Climate*. **2**, 267-285.

Webster, P.J., 1972: Response of the tropical atmosphere to the local steady forcing, *Mon.Wea. Rev.*, **100**, 518-540.

Webster, P. J. and S. Yang, 1992 : Monsoon and ENSO: Selectively interactive systems *Q. J. R. Meteorol. Soc.*, **118**, 877-926.

Webster.P.J., 1987: The variable and interactive monsoons in *Monsoons* edited by J.S.Fein and P.L. Stephens, pp 269-330, Wiley and Sons New York.

Weickmann KM, Lussky GR, Kutzbach JE. 1985. Intraseasonal (30-60 day) fluctuations of outgoing longwave radiation and 250mb streamfunction during northern winter. *Mon. Wea. Rev.* **113**: 941-961.

Weickmann KM. 1983. Intraseasonal circulation and outgoing longwave radiation modes during Northern Hemisphere winter. *Mon. Wea. Rev.* **111:** 1838-1858.

Wyrtki,K., 1975: El Niño – The dynamic response of the equatorial Pacific Ocean to atmosphere forcing. *J.Phys.Oceanoger.*, **5**,575-584.

Yasunari Y. 1979. Cloudiness fluctuations associated with the northern hemisphere summer monsoon . *J. Met. Soc. Japan.*, **57**: 227-242.

Yasunari Y. 1980. A Quasi-stationary appearance of 30-40 day period in the cloudiness fluctuations during the summer monsoon over India. *J. Met Soc. Japan.* **58**: 225-229

Yasunari Y. 1981. Structure of an Indian summer monsoon system with around 40-day period. *J. Met Soc. Japan.* **59**: 336-354.

Zubair, Lariff., 1999: A dynamical model for orographic rainfall in Sri Lanka during southwest monsoon period ., Meteorology beyond 2000. Proc. of National symposium Tropmet-99, 16-19 Feb. 1999, 269-273.

FIGURE CAPTIONS

6.4 24-hour rainfall of Thikkodi along with the first harmonic, 1+2 harmonic (sum) and 1+2+3 harmonic (sum). The left panel is for total rainfall days and right panel for days with rainfall ≥5cm per day.

6.5 24-hour rainfall Kaithprem and Elanad with the first harmonic, 1+2 harmonic (sum) and 1+2+3 harmonic (sum). The left panel is for total rainfall days and right panel for days with rainfall ≥5cm per day.

6.6 24-hour rainfall Palapuzha and Vazhavatta with the first harmonic, 1+2 harmonic (sum) and 1+2+3 harmonic (sum). The left panel is for total rainfall days and right panel for days with rainfall ≥5cm per day.

6.7.1 24-hour rainfall of Cheruvanchery with the first harmonic, 1+2 harmonic (sum) and 1+2+3 harmonic (sum) for total rainfall days.

7.1 Sarker's (1967) model of orography of Western Ghats. The solid line is the observed rainfall and the dashed lines are the simulated rain from two models.

7.2 (a) Contours of the terrain in Srilanka (b) Contours of mean summer monsoon rainfall May to September.As taken from Lariff (1999)

7.3 (a) Vertical section of the height contours along the section marked XX – XX in fig. 7.2(a) and the smoothed contours used in the modelling study ; (b) Variation along the section XX-XX in fig. 7.2(a) of the May to September rainfall. As taken from Lariff (1999)

7.4 The rainfall simulation and the orography. The solid line is the terrain and the dashed line the simulated rainfall. The figure is taken from Lariff (1999)

7.5 (a) Spatial distribution of the mean rainfall for July for the period 1901-1950.; (b) the satellite measured terrain of Kerala

7.6 Longitudinal cross section of rainfall and height of the terrain of latitude averaged for (a) 10-10.2^{0}N (b) 9.5 –9.7^{0}N. The stations are plotted as open circle.

7.7 The three nested domains chosen for the study.

TABLE CAPTIONS

G9817

List of Publications, Papers presented in Seminars/Workshops and Courses attended

- ***Intra Seasonal Oscillation (ISO) of South Kerala Rainfall During The Summer monsoons of 1901 to 1995***. Joseph P.V, Anu Simon, Venu G Nair, **Aype Thomas.**, Earth and Planetary Sciences, **113**, 139-150, 2004.

- ***Monsoon rainfall droughts of India during 1987&2002.*** **Aype Thomas**, Anu Simon and Joseph P.V, (presented in Inter National Conference on 'Scale Interaction & Variability of Monsoon' 5-10 October 2003 at Munnar, Kerala.)

- ***Genesis of Monsoon Depressions triggered by Tropical Cyclones of Northwest Pacific Ocean.*** **Aype Thomas** and Anu Simon (paper presented in Iternational Symposium on Natural Hazards, 24-27 February, 2004, Hyderabad, INDIA).

- **Arabian Sea Monsoon Experiment (ARMEX), SK 179** in **Research Vessel 'Sagar Kanya'**18-07-2002 to 15-08-2002
  A project of Department of Ocean development

- **Refresher Course on Cloud Physics &Atmospheric Electricity,**
  8-5-2002 to 29-5-2002, Conducted by Department Of Atmospheric Sciences, Cochin University of Science and Technology Sponsored by University Grants Commission, New Delhi.

- **Refresher Course on Geophysical Fluid dynamics,**
  26-11-2002 to 18-12-2002, Conducted by Department Of Atmospheric Sciences, Cochin University of Science and Technology .Sponsored by University Grants Commission, New Delhi.

- **Refresher Course on Physics of the Atmosphere & Ocean,**
  1-12-2003 to 12-12-.2003, Conducted by Indian Institute Of Science Sponsored by Indian Academy of Sciences.